AD_____
(Leave blank)

Award Number:

DAMD17-01-1-0318

TITLE:

Immunotherapeutic Strategies in Breast Cancer:
Preclinical and Clinical Trials

PRINCIPAL INVESTIGATOR:
Sandra J. Gendler, PhD

CONTRACTING ORGANIZATION:
Mayo Clinic Scottsdale
Scottsdale, AZ 85259-5499

REPORT DATE:

September 2012

TYPE OF REPORT:

Final

PREPARED FOR: U.S. Army Medical Research and Materiel Command
Fort Detrick, Maryland 21702-5012

DISTRIBUTION STATEMENT: (Check one)

☒ Approved for public release; distribution unlimited

☐ Distribution limited to U.S. Government agencies only; report contains proprietary information

REPORT DOCUMENTATION PAGE

Form Approved
OMB No. 0704-0188

1. REPORT DATE *(DD-MM-YYYY)*	2. REPORT TYPE	3. DATES COVERED *(From - To)*
September 2012	Final	15 August 2001 – 14 August 2012

4. TITLE AND SUBTITLE
Immunotherapeutic Strategies in Breast Cancer:
Preclinical and Clinical Trials

5a. CONTRACT NUMBER

5b. GRANT NUMBER
DAMD17-01-1-0318

5c. PROGRAM ELEMENT NUMBER

6. AUTHOR(S)
Sandra J. Gendler, PhD

5d. PROJECT NUMBER

5e. TASK NUMBER

5f. WORK UNIT NUMBER

7. PERFORMING ORGANIZATION NAME(S) AND ADDRESS(ES)
Mayo Clinic Scottsdale
Scottsdale, AZ 85259-5499

8. PERFORMING ORGANIZATION REPORT NUMBER

9. SPONSORING / MONITORING AGENCY NAME(S) AND ADDRESS(ES)
U.S. Army Medical Research
and Material Command
Fort Detrick, MD 21702-5012

10. SPONSOR/MONITOR'S ACRONYM(S)

11. SPONSOR/MONITOR'S REPORT NUMBER(S)

12. DISTRIBUTION / AVAILABILITY STATEMENT
Approved for public release; distribution unlimited

13. SUPPLEMENTARY NOTES

14. ABSTRACT
This project is focused on novel tumor vaccines directed at MUC1 and other tumor antigens. Our specific aims are: 1)To assess the effectiveness of vaccines against MUC1 and other tumor antigens in the prevention and treatment of spontaneous breast carcinomas in mice; 2)To translate an effective vaccine strategy into a phase I clinical trial in patients with undetectable disease following standard therapy. We have tested five vaccines in the preclinical mouse models and all elicited a strong immune response. The vaccine using MUC1 class I binding peptides prevented MUC1-expressing tumor growth. We have designed the Phase I clinical trial using a peptide vaccine comprised of MUC1 and HER-2/neu MHC class I peptides and HER-2/neu MHC class II peptide with unmethylated CpG oligodeoxynucleotides and GM-CSF as adjuvants in breast cancer patients free of disease. Thirty-nine patients were enrolled. There was significant adjuvant-dependent sensitization to MUC1; a similar trend was observed for HER-2/neu. The combination vaccine of MUC1 and HER-2/neu peptides resulted in a high-frequency of immune responses with transient injection site reactions. Further studies for breast cancer are warranted.

15. SUBJECT TERMS
Immunotherapy, vaccine, MUC1, mucin, mouse model, tolerance

16. SECURITY CLASSIFICATION OF:			17. LIMITATION OF ABSTRACT	18. NUMBER OF PAGES	19a. NAME OF RESPONSIBLE PERSON
a. REPORT	b. ABSTRACT	c. THIS PAGE			USAMRMC
U	U	U	UU	175	19b. TELEPHONE NUMBER *(include area code)* (480) 301-7062

Standard Form 298 (Rev. 8-98)
Prescribed by ANSI Std. Z39.18

Table of Contents

INTRODUCTION

This project is focused on the development of novel tumor vaccines directed at MUC1, a transmembrane mucin that is aberrantly expressed in cancer. MUC1 is expressed on greater than 90% of breast cancers and often elicits cellular and humoral immune responses in humans. However, these responses are not sufficiently strong to eradicate tumors. MUC1 is a candidate peptide for novel immunotherapy strategies to strongly activate the immune system to eradicate tumors expressing these epitopes. This fact was recognized recently by the NCI's Special Translational Research Acceleration Project (STRAP) committee when it prioritized MUC1 for vaccine development based on a number of factors including therapeutic function, immunogenicity, oncogenicity, specificity, expression level, antigenic epitopes, and cellular localization of antigen (Cheever et al., Clin. Cancer Res. 2009; 15(17): 5323-37). In tumors, there is strong over expression of MUC1 on tumor cells and in circulation, expression is no longer restricted to the apical domain of cells, and glycosylation is altered, revealing immunodominant tumor-specific peptide sequences.

In our preclinical studies we have utilized mice that developed spontaneous mammary gland cancer that expresses MUC1. MUC1 transgenic mice (MUC1.Tg) were bred with mice carrying the MMTV-driven polyoma middle T antigen (MT) to create MMT mice. Mice transgenic for this protein develop B and T cell tolerance and are refractory to immunization with the protein encoded by the transgene. All mice are congenic on the C57BL/6 background to eliminate strain-specific modifier effects. In the MMT mice, mammary gland tumors are induced by the action of a potent tyrosine kinase activity associated with the polyoma virus middle T antigen driven by the mouse mammary tumor virus long terminal repeat (MMTV). Middle T specifically associates with and activates the tyrosine kinase activity of a number of c-src family members, eliciting tumors when a threshold level of gene product has been attained. This promoter is transcriptionally active throughout all stages of mammary gland development and results in widespread transformation of the mammary epithelium and the rapid production of multifocal mammary adenocarcinomas in 100% of the female mice. The MMT mouse expresses aberrantly glycosylated MUC1 in the mammary tumors and appears to be an appropriate model for human cancer. This preclinical mouse model enables us to study the effects of self-tolerance, immunity and auto-immunity to MUC1 as mammary tumors develop spontaneously.

The **hypothesis** of our study is that enhancing MUC1-specific immunity will result in anti-tumor immunity. We proposed to develop an optimal cancer vaccine using epithelial cell mucin MUC1 peptides or protein or MUC1-expressing tumors presented by DCs as immunogen. The optimal therapy was tested in a phase I clinical trial.

RESULTS (BODY)

Specific Aims:

Specific Aim 1: To assess the effectiveness of vaccine formulations against MUC1 and other tumor antigens in the prevention and treatment of spontaneous breast carcinomas in mice.

Our preclinical studies were completed at the end of year three and were described in the Annual Report for 2004.

All of the vaccine strategies elicited an immune response (1-8). Animals developed mature cytotoxic T cells (CTLs) which were lytic in vitro against MUC1-expressing tumor cells. Lytic activity was detected without further in vitro stimulation (2, 6-8). However, in most cases the spontaneous tumors progressed. The CTLs, while active outside of the environment of the

tumor, were tolerized and unreactive to MUC1 (a target antigen) in the vicinity of the tumor (1, 6-8). Tumors were found to exhibit several known escape mechanisms, such as the production of immunosuppressive factors such as Cox-2 and PGE_2 and down-modulation of MHC class I molecules on the cells (6-8). CTLs that were adoptively transferred into the tumor-bearing mice were used to follow the development of tolerance, which occurred within about three weeks following injection (7). Stimulation of co-stimulatory molecules, especially CD137, a member of the TNFR family, together with adoptive transfer of MUC1-specific T cells, resulted in significantly reduced tumor burden in the MMT mice. The CD137-stimulated CTLs appeared to remain lytic against the tumor in the tumor environment and tolerance/anergy was alleviated. CTLs recovered from the tumors were lytic against MUC1-expressing tumor cells (MMT tumor cells in culture, as well as B16.MUC1 cells) and they proliferated in response to DCs presenting MUC1 (7). A peptide vaccine was tested in MUC1.Tg mice using MUC1-expressing tumors injected subcutaneously. Two class I-binding peptides from MUC1 (APGSTAPPA and SAPDTRPA) from the MUC1 tandem repeat region and a class II helper peptide (TPPAYRPPNAPIL) were used together with CpG ODN and GM-CSF in Incomplete Freund's Adjuvant. The peptide vaccine inhibited the growth of MUC1-expressing tumor cells and elicited a strong immune response (9).

In preparation for the clinical trial of breast cancer patients, we investigated dendritic cell (DC) and T cell function in breast cancer patients prior to surgical tumor resection. We also investigated COX-2 expression and PGE_2 levels within the tumor milieu and in the circulation. We showed reduced functionality of T cells and dendritic cells (DC) in breast cancer patients (5). Analysis of T-helper type 1 and 2 cytokines revealed reduced levels of interferon gamma, tumor necrosis factor alpha, interleukin (IL)-12, and IL-2 and increased levels of IL-10 and IL-4. Dendritic cells from the breast cancer patients showed significantly reduced expression of the co-stimulatory molecules B7 and CD40 and decreased phagocytic ability. The levels of the immunosuppressive factors, COX-2 and PGE_2, were elevated in the cancer patients compared with normal controls (5). These results set the stage for our clinical trial enrollment of breast cancer patients from 3 months to 3 years post end of standard of care treatment in order to allow the tumor-induced immune suppression to resolve.

The papers (see appendix) describing the results are as follows:

1) Mukherjee, P., Ginardi, A.R., Madsen, C.S., Tinder, T. L., Jacobs, F., Parker, J., Agrawal, B., Longenecker, B.M., and Gendler, S.J. (2001) MUC1-specific CTLs are non-functional within a pancreatic tumor microenvironment. Glycoconjugate Journal 18:931-42. PMID 12820727.

2) Mukherjee, P., Madsen, C.S., Ginardi, A.R., Ginder, T.L., Jacobs, F., Parker, J., Agrawal, B., Longenecker, B.M., and Gendler, S.J. (2003) Mucin 1-specific immunotherapy in a mouse model of spontaneous breast cancer. Journal of Immunotherapy 26(1):47-62. PMID 12514429.

3) Xia, J., Tanaka, Y., Koido, S., Liu, C., Mukherjee, P., Gendler, S.J., and Gong, J. (2003) Prevention of spontaneous breast carcinoma by prophylactic vaccination with dendritic/tumor fusion cells. Journal of Immunology 170:1980-1986. PMID 12574367.

4) Chen, D., Xia, J., Tanaka, Y., Chen, H., Koido, S., Wernet, O., Mukherjee, P., Gendler, S.J., Kufe, D. and Gong, J. (2003) Immunotherapy of spontaneous mammary carcinoma with fusions of dendritic cells and mucin 1-positive carcinoma cells. Immunology 109:300-307. PMID 12757626. PMCID:PMC1782954.

5) Pockaj, B.A., Basu, G.D., Pathangey, L.B., Gray, R.J., Hernandez, J.L., Gendler, S.J. and Mukherjee, P. (2004) Reduced T cell function is related to COX-2 over-expression and PGE_2 secretion in patients with breast cancer. Annals of Surgical Oncology 11:328-339. PMID 14993030.

6) Basu, G.D., Pathangey, L.B., Tinder, T.L., LaGiola, M., Gendler, S.J. and Mukherjee, P. (2004) Cyclooxygenase-2 inhibitor induces apoptosis in breast cancer cells in an in vivo model of spontaneous metastatic breast cancer 2(11):632-642. PMID 15561779.

7) Mukherjee, P., Tinder, T.L., Basu, G.D., Pathangey, L.B., Chen, L. and Gendler, S.J. (2004) Therapeutic Efficacy of MUC1-Specific Cytotoxic T Lymphocytes and CD137 Co-Stimulation in a Spontaneous Breast Cancer Model. Breast Disease 20:53-63. PMID 15687707.

8) Basu, G.D., Pathangey, L.B., Tinder, T.L., Gendler, S.J. and Mukherjee, P. (2005) Mechanism underlying the growth inhibitory effects of COX-2 inhibitor in human breast cancer cells. Breast Cancer Research 7:R422-R435. PMID 15987447. PMCID:PMC1175053

9) Mukherjee, P., Pathangey, L.B., Bradley, J.B., Tinder, T.L., Basu, G.D., Akporiaye, E.T., and Gendler, S.J. (2007) MUC1-specific immune therapy generates a strong anti-tumor response in a MUC1-tolerant colon cancer model. Vaccine 25:1607-1618. PMID 17166639

Specific Aim 2: To translate the most effective vaccine strategies into phase I clinical trials in patients with high and low tumor burden.

Breast cancer continues to be a major cause of cancer death among women despite advances in surgery, chemotherapy, hormonal therapy, and radiation therapy (1). While surgery offers the possibility of cure, and adjuvant therapies reduce the risk of recurrence (2), breast cancer still recurs frequently despite adjuvant treatment. Distant recurrence of breast cancer after surgery is generally incurable. Novel adjuvant treatments that complement current chemotherapeutic and hormonal regimens are urgently needed to further reduce the frequency of breast cancer recurrence, and immunotherapeutic strategies such as vaccines offer this potential. Clinical trials using a peptide derived from the growth factor receptor HER-2/neu (HER2) have demonstrated a lower rate of breast cancer recurrence in vaccinated patients (3), and robust immune responses to HER2 are seen in patients with metastatic disease, as well as those defined as low HER2 expressors (4, 5). While HER2 is a promising vaccine antigen, a limitation to vaccines that target only HER2 is the variability in HER2 expression both among different tumors and within an individual tumor, providing a mechanism by which tumors might escape immune surveillance. One strategy to reduce the possibility of immune escape is to design vaccines using more than one antigen.

The MUC1 tumor antigen is an attractive and broadly applicable target antigen for vaccine approaches. MUC1 is a cell-associated mucin that is oncogenic and is overexpressed by many different tumor types, including over 90% of breast adenocarcinomas (6-8). Additionally, glycosylation on MUC1 is altered on tumor cells, leading to an antigen phenotype that is distinct from that on normal cells (9). Because of these and other properties, MUC1 was designated a high-priority cancer antigen by the National Cancer Institute (NCI) (10). To assess the immunogenicity of MUC1, HLA-A2-binding peptides from MUC1 were pulsed onto antigen

presenting cells (APC) and incubated with donor peripheral blood mononuclear cells (PBMC) (11). This elicited functionally active $CD8^+$ T cells recognizing MUC1-derived peptides in an HLA-A2-restricted fashion. Subsequently, several studies have demonstrated both safety and immune efficacy of vaccinating patients against MUC1-derived peptides (12-14). We and others have identified a peptide from the degenerate tandem repeat domain of MUC1 that binds HLA-A2 and elicits a robust response *in vitro* from healthy donor or patient $CD8^+$ T cells [(15), and our unpublished observations]; this peptide was selected for testing in this clinical trial of patients with resected breast cancer.

The use of immune adjuvants greatly enhances the ability of vaccines to elicit potent immune responses. Granulocyte-macrophage colony stimulating factor (GM-CSF) is a cytokine used clinically to augment myeloid cell recovery following chemotherapy (16); GM-CSF has also been studied as a vaccine adjuvant for metastatic melanoma patients and as an immunotherapeutic agent for resected high-risk melanoma patients (17-19). GM-CSF augments the generation and recruitment of dendritic cells and increases molecules associated with antigen presentation, thus augmenting presentation of vaccine peptides (20). Similarly, stimulation of APC through Toll-like receptor (TLR) ligation is a potent means of augmenting vaccine immunogenicity (21). DNA containing unmethylated cytosine-guanine (CpG) motifs has been shown to stimulate APC through TLR9 (22) and boosts vaccine efficacy in preclinical tumor vaccine models (23) and human cancer vaccines (24). We report here our study of the immunologic efficacy of GM-CSF and CpG as immune adjuvants with a multiple peptide vaccine.

We conducted a randomized study to assess the immunogenicity of a three-peptide vaccine comprised of an HLA-A2-binding peptide from HER2; a degenerate class II-binding peptide from HER2 that binds to diverse HLA-DR alleles, including HLA-DR1, HLA-DR4, HLA-DR52 and HLA-DR53 (25); and an HLA-A2-binding peptide from MUC1 combined with either GM-CSF (sargramostim), CpG (PF-3512676), or both. The rationale for use of an endogenous T helper epitope from HER2 was to promote induction of cognate $CD4^+$ T cells that could provide critical tumor-specific help intratumorally during the effector stage of tumor rejection (26).

METHODS

Eligibility and enrollment

This study enrolled women 18 years of age or older with histologically confirmed invasive breast cancer who had been surgically treated within 3 years of enrollment, who had completed adjuvant treatment with chemotherapy and/or radiation therapy, and who were without radiographic evidence of disease. Additional eligibility criteria included: MUC1 positive breast cancer by central pathology evaluation, HLA-A2-positive serotype, ECOG PS of 0-1, and adequate hematologic, renal and hepatic function. Concurrent adjuvant endocrine therapy with tamoxifen or an aromatase inhibitor was allowed. Exclusion criteria included active infection, known HIV positivity, hepatitis, an immune-compromising condition, another invasive malignancy within 5 years of enrollment, pregnancy or breast feeding.

All patients were treated at Mayo Clinic. Mayo Clinic obtained study approval from the institutional review board and filed assurances with the Department of Health and Human Services. Written, informed consent was required for enrollment.

Study treatment

All patients were vaccinated subcutaneously in a non-dissected lymph node region with a mixture of 1 mg of MUC1 peptide (STAPPVHNV); 1 mg of HER2 peptide 1 (ILHNGAYSL) and 1 mg HER2 peptide 2 (KVPIKWMALESILRRRF) suspended in 1.5 mL of Montanide ISA-51 (Seppic Inc., Fairfield, NJ). Peptides were produced by solid phase synthesis (Clinalfa, Torrence, CA) and were confirmed by an independent laboratory to have purities of 99.9% (MUC1), 99.4% (HER2 peptide 1), and 99.9% (HER2 peptide 2). The vaccine dose of 1 mg was based on a previous trial in which this dose was shown to be well-tolerated and induce peptide-specific $CD8^+$ T cells (14, 18). Forty-five patients (15 patients per immunization strategy) were to be randomized to receive the vaccine with 0.225 mg of GM-CSF (sargramostim, Bayer HealthCare Pharmaceuticals, Pittsburgh, PA; Arm A) or the vaccine with 2 mg CpG (Pf-3512676, sequence 5'-TCGTCGTTTTGTCGTTTTGTCGTT-3', Pfizer, New York, NY; Arm B) or vaccine with both 0.225 mg of GM-CSF and 2 mg CpG (Arm C) day 1 of a 28 day cycle for a maximum of 6 cycles. The 2 mg dose of CpG had been chosen based on a clinical trial using up to 3 mg CpG in the context of vaccine administration (27). The dose of CpG was lowered to 1 mg with implementation of Addendum 1.

Prior to registration, patients submitted a tumor specimen for central laboratory testing of MUC1 and HER2 expression and HLA serotyping. Only patients found to have MUC1 positive disease were allowed to register on this trial. Within 14 days of study registration, prior to each treatment cycle, 4 weeks after completion of treatment, and every 3 months thereafter until progression or a maximum of 2 years post-registration, patients underwent a complete physical exam, assessment of performance status, blood chemistries, toxicity assessments (CTCAE v. 3.0), and research blood draws for immunologic profiling. Disease status was radiographically evaluated at registration and per standard of care by the treating physician. Delayed type hypersensitivity (DTH) skin testing for mumps, candida, tetanus toxoid, and trichophyton was done prior to treatment and treatment cycle 6.

Treatment was discontinued if a patient developed a grade 2+ allergic reaction, autoimmune reaction, neurologic difficulties, or any grade 3+ adverse events. Treatment discontinuation for a grade 2 injection site reaction was added as part of Addendum 1.

Immunologic monitoring

Peripheral blood samples were obtained prior to the start of treatment, at the completion of cycles 2, 4, and 6 (approximately every two months) during study treatment, and then every three months until study completion. Blood was separated into plasma and peripheral blood mononuclear cells (PBMC) using a density gradient (Ficol-hypaque, Amersham, Uppsala, Sweden). Plasma samples were stored at -70 ºC, and PBMC were stored in liquid nitrogen. To reduce inter-assay variability, patient samples were batched and analyzed after study completion at a maximum of two years after randomization.

Quantification of antigen-specific $CD8^+$ T cells was performed by tetramer flow cytometry. Thawed PBMC were stained with FITC-conjugated antibody to CD8, PC5-conjugated antibodies to CD4, CD14 and CD19 (Becton-Dickinson, Franklin Lakes, NJ) and PE-conjugated HLA-A2/beta2-microglobulin tetramers (Beckman Coulter, Fullerton CA) containing peptides from HIV (negative control), MUC1 (STAPPVHNV), and HER2 (ILHNGAYSL). Samples were analyzed by flow-cytometry, and data were processed using CellQuest® software (Becton-Dickinson, Franklin Lakes, NJ). Gates were set on lymphocytes that were CD4, CD14 and CD19 (PC5)-negative. The percentage of antigen-specific CD8-positive cells was calculated as the difference in the percentage of CD8-positive cells stained with tetramer to the antigen of interest and the percentage of background staining with negative control tetramer. The threshold for detection of antigen-specific CD8+ T CELLS was 0.05% of CD8-positive T cells.

Quantitation of serum antibody concentrations was performed by ELISA using standard techniques. Briefly, 96-well plates were coated overnight with the following antigens: bovine serum albumin (negative control protein, 40 ng/ml, Denville Scientific, Metuchen, NJ), Cyclin D1 (negative control peptide, KISQAVHAAHAEINEAG, 40 ng/ml, Mayo Clinic Peptide Core Facility), tetanus toxoid (positive control protein for baseline antibody response, but negative control for change from pre-vaccine to post-vaccine, 100 ng/ml, Sigma-Aldrich, St. Louis, MO), $HER2_{883-899}$ (class II vaccine antigen, 40 ng/ml, Mayo Clinic Peptide Core Facility), $HER2_{676-1255}$ (larger peptide containing the 883-899 epitope, 40 ng/ml, Mayo Clinic Peptide Core Facility), HER2 protein (40 ng/ml Mayo Clinic Protein Core Facility), $HER2_{22-122}$ (distinct HER2 epitope from the vaccine peptide, 40 ng/ml, Abnova Corp., Taipei City, Taiwan), and the MUC1 peptide containing the tandem repeat and degenerate tandem repeat (APGSTAPPAHGVTSAPDTRPAP-GSTAPPVHNVTSAS, Mayo Clinic Peptide Core Facility). Plates were then washed and blocked with 1% bovine serum albumin (Denville Scientific). Patient plasma diluted 1:80 was added, and then washed. Horseradish peroxidase-conjugated goat anti-human IgG (Santa Cruz Biotech, Santa Cruz, CA) was used to detect antigen-specific IgG antibodies. TMB substrate (Becton Dickenson) and hydrochloric acid (Sigma-Aldrich) were used to produce and stop color change, respectively; this was quantitated by absorbance at 450 nm. Plasma samples were assayed in duplicate. Subjects were considered evaluable for antibody responses if pre-vaccination samples had coefficient of variation of 25% or less. Antigen responses were identified if any post-vaccination antibody concentration was greater than double the pre-vaccination concentration and had a coefficient of variation of 25% or less.

Statistical considerations

The study was designed to examine the safety profile and immunization efficacy of each immunization strategy. Fifteen patients were randomized to each strategy utilizing a computer application of the Pocock-Simon sequential allocation procedure (28) that was programmed to balance the marginal distributions of HER2-positivity between immunization strategies. The number and severity of all toxicities reported to be possibly, probably, or definitely related to treatment were reported using the NCI-CTC version 3.0 criteria. The immunologic parameters of primary interest were the number of peptide-specific T-cells and the antibody response.

The primary endpoints for considering whether an immunization strategy should be considered for further testing in this patient population were the MUC1 specific CD8+ T cells response rate and the HER2 specific CD8+ T cells response rate. A peptide specific immune response is defined as a 2-fold or greater increase in the percentage of antigen specific $CD8^+$ T cells at any post immunization evaluation from pre-immunization levels. A sample size of 15 patients per immunization strategy was chosen. If 11 or more of the 15 patients randomized to a given immunization strategy developed an immunologic response to either MUC1 and/or HER2 peptides, then we would be at least 95% confident that the true immunization response rate is at least 45%.

RESULTS

Study course

Between October 1, 2008 and July 1, 2010, 39 women were entered onto this trial. Two patients were found to be ineligible after starting immunization due to bone metastases at study entry (Arm A: 1 patient) and ocular melanoma within 5 years of registration (Arm C: 1 patient).

After the first 13 patients (Arm A-4 patients; Arm B-4 patients, and Arm C-5 patients) had been enrolled, grade 2 injection site reactions (ISRs) were first reported in 1 Arm A and 2 Arm C

patients during cycle 1; 2 Arm C patients during cycle 2; and in 2 Arm B patients during cycle 3. The trial protocol stipulated that grade 2 immunologic/allergic reactions, including ISRs, were considered DLT. (Since ISRs were transient and were not associated with systemic reactions, these will not be considered DLT for subsequent studies; however, for the purpose of this study, they are reported as DLT.) The trial was amended on May 19, 2009 to lower the dose of CpG to 1 mg for Arm B and Arm C. Patients enrolled after May 19, 2009 will be referred to as the post-Add1 patients. Enrollment to Arm B and Arm C closed early, as the pre-specified toxicity boundary was crossed. Enrollment to Arm B was closed on November 9, 2009, as one of the 5 post-Add1 patients developed a grade 3 ISR, and enrollment to Arm C was closed on February 3, 2010 as two of the 7 post-Add1 patients developed a grade 2 ISR. Enrollment to Arm A was closed on July 1, 2010 after Arm A met its accrual goal.

The patient and tumor characteristics of all 39 consented patients are presented in Table 1 by treatment arm.

Treatment course and toxicities

Arm A: GM-CSF suspended in Montanide ISA-51 as vaccine adjuvant

The median number of immunizations among the 16 patients randomized to Arm A was 6 (total: 84; range: 2-6). Moderate to severe toxicities (CAE grade ≥ 2) reported included: a grade 3 infection requiring hospitalization and 3 grade 2 ISRs. All patients have discontinued treatment. The reasons include: completion of all 6 immunizations (11 pts.); disease progression (1 pt.); intolerability (3 pts.) and refusal to complete last immunization (1 pt.). With a median follow-up of 2.0 years, 13 patients are alive without disease progression; 1 patient is alive with disease progression; and 2 patients have died due to disease progression (Table 2A).

Arm B: CpG suspended in Montanide ISA-51 as vaccine adjuvant

The median number of immunizations was 4 (total: 22; range: 1-6) among the 6 pre-Add1 patients and 6 (total: 20; range: 1-6) among the 5 post-Add1 patients randomized to Arm B. Moderate to severe toxicities (CAE grade ≥ 2) reported included: a grade 3 ISR (post-Add1 pt.) and 2 grade 2 ISRs (both pre-Add1 pts.). Two pre-Add1 patients discontinued treatment after one immunization on the recommendation of the study team, as safety issues with CpG were emerging. Other reasons for discontinuing treatment included: completion of all 6 immunizations (6 pts.); intolerability (1 pt.), and refusal (2 pt.). With a median follow-up of 2 years, all 11 patients are alive without disease progression (Table 2B).

Arm C: GM-CSF and CpG suspended in Montanide ISA-51 as vaccine adjuvant

The median number of immunizations was 3 (total: 18; range: 2-5) among the 5 pre-Add1 patients and 4 (total: 29; range: 1-6) among the 7 post-Add1 patients randomized to Arm C. Moderate to severe toxicities (CAE grade ≥ 2) reported included: 6 grade 2 ISRs (4 pre-Add pts.); 1 grade 2 bone pain (pre-Add1 pt.); 1 grade 2 fatigue (post-Add1 pt.); 1 grade 2 arthralgia (post-Add1 patient); and 2 grade 2 myalgia (post-Add1 patients). All 5 pre-Add1 patients discontinued treatment after 2, 3, 3, 5, and 5, immunizations respectively on the recommendation of the study team as safety issues with CpG were emerging. Other reasons for discontinuing treatment included: completion of all 6 immunizations (3 patients), intolerability (2 patients) and refusal (2 patients). With a median follow-up of 2.0 years, 11 patients are alive without disease progression, and 1 patient is alive with disease progression (Table 2C).

$CD8^+$ T cell responses to MUC1 and HER2

Of the 39 patients enrolled, 28 (Arm A: 11 patients; Arm B: 8 patients; Arm C: 9 patients) had blood draws taken prior to immunization and at least one time after randomization (after 2, 4, 6, 9 and/or 12 months on study). Peripheral blood mononuclear cells were isolated from the

blood and were used to determine the percentage of $CD8^+$ T cells binding the MUC1 tetramer (Figures 1A-C and Supplemental Figures 1 and 2) and the percentage of $CD8^+$ T cells binding the HER2 tetramer (Figures 2A-C and Supplemental Figures 1 and 2).

The rates of antigen-specific $CD8^+$ T cell responses were: 18.2% in Arm A; 75.0% in Arm B and 55.6% in Arm C for MUC1; and 18.2% in Arm A; 57.1% in Arm B and 44.4% in Arm C for HER2. Overall, the immunologic response rate to MUC1 and/or HER2 antigen was: 27.3% (95%CI: 6.0-61.0%) for Arm A; 87.5% (95%CI: 47.4-99.7%) for Arm B; and 67.3% (95%CI: 29.9-92.5%) for Arm C.

The rates of antigen specific $CD8^+$ T cells responses to HER2 (disregarding vaccine adjuvant) were similar between those with HER2-positive disease (n=6; 33.3%; 95%CI: 4.3-77.7%) and those with HER2-negative disease (n=21; 38.1%; 95%CI: 18.1-61.2%) (Table 2).

Also, the rates of antigen specific $CD8^+$ T cell responses to MUC1 and/or HER2 were similar between those who had pre-immunization DTH reactivity to tetanus toxoid and/or candida (n=19; 57.9%; 95%CI: 33.5-79.8%) and those who did not have pre-immunization DTH reactivity (n=9; 55.6%; 95%CI: 21.2-86.3%) (Table 2).

Antibody responses to HER2 and MUC1

Antibody responses (defined as a doubling of antigen-specific IgG from pre- to post-vaccination) to the negative control protein (bovine serum albumin) or peptide (Cyclin D1) were not detected, nor were responses seen against tetanus toxoid, MUC1 peptide, whole HER2 protein, or the $HER2_{22\text{-}122}$ or $HER2_{676\text{-}1255}$ peptides (data not shown). Antibody responses to $HER2_{883\text{-}899}$, the MHC class II-binding peptide used in the vaccine, were observed in 1/9 evaluable patients in Arm A, 5/10 patients in Arm B, and 3/6 patients in Arm C.

DISCUSSION

For an anti-cancer vaccine to generate effective immune responses that lead to eradication of residual disease, it must target prevalent antigens in a manner that produces an expansion of antigen-specific lymphocytes capable of killing antigen-bearing cells. Since effective responses to a single antigen frequently result in the outgrowth of antigen loss variants rather than tumor eradication, an ideal vaccine will generate responses to multiple tumor-associated antigens. By preventing immune tolerance, vaccine adjuvants that lead to immune activation can significantly augment the efficacy of cancer vaccines. We have developed a peptide vaccine for patients with resected breast cancer that combines three antigens from two cancer-associated proteins (MUC1 and HER2). In addition, we have used three preparations of immune adjuvants (GM-CSF, CpG, and combined GM-CSF and CpG) to assess which preparation results most frequently in expansion of antigen-specific $CD8^+$ T cells.

This report is the first describing immune responses to the MUC1 degenerate tandem repeat peptide STAPPVHNV. Responses to MUC1, defined as a doubling of MUC1-specific $CD8^+$ T cells from pre-vaccination levels or an increase MUC1-specific $CD8^+$ T cells to detectable levels, were seen in 13 of 28 (46.3%) patients. Of note, 25 patients had detectable levels of MUC1-specific T cells pre-vaccination, suggesting that MUC1 is a common antigen in the natural immune response to breast cancer.

TLRs represent an important family of innate immune modulators, and the recognition of this has led to the incorporation of TLR agonists into synthetic vaccines. Subjects in Arms B and C from our study received the TLR9 agonist CpG. The rate of antigen-specific $CD8^+$ T cell responses to MUC1 and/or HER2 with the immunization strategy which did not incorporate CpG

or GM-CSF (Arm A) was significantly lower than that of the strategy incorporating CpG (Arm B, difference B-A: 60.2%; 95% CI: 25.3 to 95.1%) and somewhat lower than the immunization strategy incorporating both CpG and GM-CSF (Arm C, difference C-A = 39.4%; 95% CI: -1.11 to 79.9). Also, the rate of antigen-specific $CD8^+$ T cell responses to MUC1 and/or HER2 with the immunization strategy did not appear to increase with the addition of GM-CSF to CpG (difference C-B = -20.8%; 95% CI: -59.2 to 17.6) Injection site skin reactions were more frequently seen in Arms B and C, but an increase in systemic adverse effects was not seen. Taken together, our data support incorporating TLR agonists into synthetic anti-cancer vaccines.

We assessed responses to the MHC class II-binding vaccine epitope by measuring antibody responses to the vaccine peptide ($HER2_{883-899}$), as well as to a larger peptide containing the vaccine epitope ($HER2_{676-1255}$) and the HER2 protein. Antibody responses to the vaccine epitope were identified in only 1 of 9 patients in the non-CpG-containing arm, but in 8 of 16 patients immunized with CpG-containing vaccines. This is concordant with the increased frequency of antigen-specific $CD8^+$ T cells seen in patients immunized with the CpG-containing vaccine. However, the peptide-directed antibody responses did not appreciably cross-react with the larger HER2 peptide or the whole HER2 protein, so it is unclear whether these responses directly provide relevant anti-tumor immunity.

The myeloid growth factor GM-CSF has been widely used in tumor vaccines. It has clearly demonstrated immune efficacy in mouse models of cancer (29). However, emerging evidence suggests that in humans, GM-CSF can have immunosuppressive as well as immunostimulatory effects (30). Our data suggest that the use of GM-CSF as a single vaccine adjuvant may be less effective in generating peptide-specific $CD8^+$ T cell responses to tumor antigens when compared with the TLR agonist CpG. Furthermore it did not appear that adding GM-CSF to CpG improved vaccine efficacy beyond that which could be obtained by the use of CpG alone.

Identifying those patients who will benefit most from vaccination requires assessment both of risk for tumor recurrence and likelihood of developing an immune response to vaccination. To assess whether any pre-vaccination parameters might predict vaccine immune responses, we tested DTH reactivity to a series of common antigens, hypothesizing that those patients demonstrating reactivity to at least one common antigen might be more likely to also respond to tumor antigen vaccination. However, the rate of antigen specific $CD8^+$ T cell responses to MUC1 and/or HER2 were similar between those who had pre-immunization DTH reactivity and those who did not have pre-immunization DTH reactivity. Thus, it appears that DTH reactivity to common antigens does not predict vaccine responsiveness. Similarly, pre-vaccine exposure to the HER2 antigen based on tumor overexpression did not lead to differences in vaccine responses to HER2. This is not surprising, given previous findings that suggested that HER2 low expressors had more robust immunologic responses than high expressors (5).

The use of a combination of MUC1 and HER2 peptides with the TLR agonist CpG results in a high-frequency of immune responses with ISR that subside with discontinuation of immunization. The immune modulator GM-CSF does not appear to provide additive benefit in immune efficacy. Further studies of MUC1 peptide-based vaccines for breast cancer are warranted.

REFERENCES

1. Pruthi S, Boughey JC, Brandt KR, Degnim AC, Dy GK, Goetz MP, et al. A multidisciplinary approach to the management of breast cancer, part 2: therapeutic considerations. Mayo Clin Proc. 2007;82:1131-40. PMID 17803883.
2. Slamon DJ, Romond EH, Perez EA. Advances in adjuvant therapy for breast cancer. Clin Adv Hematol Oncol. 2006;4:suppl 1, 4-9; discussion suppl 10; quiz 2 p following suppl
3. Peoples GE, Holmes JP, Hueman MT, Mittendorf EA, Amin A, Khoo S, et al. Combined clinical trial results of a HER2/neu (E75) vaccine for the prevention of recurrence in high-risk breast cancer patients: U.S. Military Cancer Institute Clinical Trials Group Study I-01 and I-02. Clin Cancer Res. 2008;14:797-803.
4. Disis ML, Wallace DR, Gooley TA, Dang Y, Slota M, Lu H, et al. Concurrent trastuzumab and HER2/neu-specific vaccination in patients with metastatic breast cancer. J Clin Oncol. 2009;27:4685-92.
5. Benavides LC, Gates JD, Carmichael MG, Patil R, Holmes JP, Hueman MT, et al. The impact of HER2/neu expression level on response to the E75 vaccine: from U.S. Military Cancer Institute Clinical Trials Group Study I-01 and I-02. Clinical cancer research : an official journal of the American Association for Cancer Research. 2009;15:2895-904.
6. Croce MV, Isla-Larrain MT, Rua CE, Rabassa ME, Gendler SJ, Segal-Eiras A. Patterns of MUC1 tissue expression defined by an anti-MUC1 cytoplasmic tail monoclonal antibody in breast cancer. J Histochem Cytochem. 2003;51:781-8.
7. Li Y, Liu D, Chen D, Kharbanda S, Kufe D. Human DF3/MUC1 carcinoma-associated protein functions as an oncogene. Oncogene. 2003;22:6107-10.
8. Schroeder JA, Masri AA, Adriance MC, Tessier JC, Kotlarczyk KL, Thompson MC, et al. MUC1 overexpression results in mammary gland tumorigenesis and prolonged alveolar differentiation. Oncogene. 2004;23:5739-47.
9. Gendler SJ. MUC1, the renaissance molecule. J Mammary Gland Biol Neoplasia. 2001;6:339-53.
10. Cheever MA, Allison JP, Ferris AS, Finn OJ, Hastings BM, Hecht TT, et al. The prioritization of cancer antigens: a national cancer institute pilot project for the acceleration of translational research. Clin Cancer Res. 2009;15:5323-37.
11. Agrawal B, Reddish MA, Longenecker BM. In vitro induction of MUC-1 peptide-specific type 1 T lymphocyte and cytotoxic T lymphocyte responses from healthy multiparous donors. J Immunol. 1996;157:2089-95.
12. Reddish M, MacLean GD, Koganty RR, Kan-Mitchell J, Jones V, Mitchell MS, et al. Anti-MUC1 class I restricted CTLs in metastatic breast cancer patients immunized with a synthetic MUC1 peptide. Int J Cancer. 1998;76:817-23.
13. Lepisto AJ, Moser AJ, Zeh H, Lee K, Bartlett D, McKolanis JR, et al. A phase I/II study of a MUC1 peptide pulsed autologous dendritic cell vaccine as adjuvant therapy in patients with resected pancreatic and biliary tumors. Cancer Ther. 2008;6:955-64.
14. Ramanathan RK, Lee KM, McKolanis J, Hitbold E, Schraut W, Moser AJ, et al. Phase I study of a MUC1 vaccine composed of different doses of MUC1 peptide with SB-AS2 adjuvant in resected and locally advanced pancreatic cancer. Cancer Immunol Immunother. 2005;54:254-64.
15. Brossart P, Heinrich KS, Stuhler G, Behnke L, Reichardt VL, Stevanovic S, et al. Identification of HLA-A2-restricted T-cell epitopes derived from the MUC1 tumor antigen for broadly applicable vaccine therapies. Blood. 1999;93:4309-17.
16. Crawford J, Althaus B, Armitage J, Balducci L, Bennett C, Blayney DW, et al. Myeloid growth factors. Clinical practice guidelines in oncology. J Natl Compr Canc Netw. 2007;5:188-202.
17. Fagerberg J. Granulocyte-macrophage colony-stimulating factor as an adjuvant in tumor immunotherapy. Med Oncol. 1996;13:155-60.

18. Block MS, Suman VJ, Nevala WK, Kottschade LA, Creagan ET, Kaur JS, et al. Pilot study of granulocyte-macrophage colony-stimulating factor and interleukin-2 as immune adjuvants for a melanoma peptide vaccine. Melanoma Res. 2011;21:438-45.
19. Spitler LE, Weber RW, Allen RE, Meyer J, Cruickshank S, Garbe E, et al. Recombinant human granulocyte-macrophage colony-stimulating factor (GM-CSF, sargramostim) administered for 3 years as adjuvant therapy of stages II(T4), III, and IV melanoma. J Immunother. 2009;32:632-7.
20. Carlsson T, Struve J. Granulocyte-macrophage colony-stimulating factor given as an adjuvant to persons not responding to hepatitis B vaccine [letter]. Infection. 1997;25:129.
21. Tormo D, Ferrer A, Bosch P, Gaffal E, Basner-Tschakarjan E, Wenzel J, et al. Therapeutic efficacy of antigen-specific vaccination and toll-like receptor stimulation against established transplanted and autochthonous melanoma in mice. Cancer Res. 2006;66:5427-35.
22. Takeda K, Kaisho T, Akira S. Toll-like receptors. Annu Rev Immunol. 2003;21:335-76.
23. Davila E, Celis E. Repeated administration of cytosine-phosphorothiolated guanine-containing oligonucleotides together with peptide/protein immunization results in enhanced CTL responses with anti-tumor activity. Journal of Immunology. 2000;165:539-47.
24. Haining WN, Davies J, Kanzler H, Drury L, Brenn T, Evans J, et al. CpG oligodeoxynucleotides alter lymphocyte and dendritic cell trafficking in humans. Clinical cancer research : an official journal of the American Association for Cancer Research. 2008;14:5626-34.
25. Kobayashi H, Wood M, Song Y, Appella E, Celis E. Defining promiscuous MHC class II helper T-cell epitopes for the HER2/neu tumor antigen. Cancer Res. 2000;60:5228-36.
26. Wang LX, Shu S, Plautz GE. Host lymphodepletion augments T cell adoptive immunotherapy through enhanced intratumoral proliferation of effector cells. Cancer Res. 2005;65:9547-54.
27. Cooper CL, Davis HL, Morris ML, Efler SM, Adhami MA, Krieg AM, et al. CPG 7909, an immunostimulatory TLR9 agonist oligodeoxynucleotide, as adjuvant to Engerix-B HBV vaccine in healthy adults: a double-blind phase I/II study. J Clin Immunol. 2004;24:693-701.
28. Pocock SJ, Simon R. Sequential treatment assignment with balancing for prognostic factors in the controlled clinical trial. Biometrics. 1975;31:103-15.
29. Dranoff G, Jaffee E, Lazenby A, Golumbek P, Levitsky H, Brose K, et al. Vaccination with irradiated tumor cells engineered to secrete murine granulocyte-macrophage colony-stimulating factor stimulates potent, specific, and long-lasting anti-tumor immunity. Proc Natl Acad Sci U S A. 1993;90:3539-43.
30. Parmiani G, Castelli C, Pilla L, Santinami M, Colombo MP, Rivoltini L. Opposite immune functions of GM-CSF administered as vaccine adjuvant in cancer patients. Ann Oncol. 2007;18:226-32.

TABLES

Table 1. Patient and Tumor Characteristics

	Arm A n=16	Arm B n=11	Arm C n=12
Median age (range)	53 (35-75)	58 (42-86)	55 (32-69)
Group pre-Addendum 1 post-Addendum 1	 6 (37.5%) 10 (62.5%)	 6 (54.6%) 5 (45.5%)	 5 (41.7%) 7 (58.3%)
Estrogen receptor positive negative	 11(68.8%) 5 (31.3%)	 8 (72.7%) 3 (27.3%)	 8 (66.7%) 4 (33.3%)
Her2 expression positive negative	 4 (25.0%) 12 (75.0%)	 3 (27.3%) 8 (72.7%)	 3 (25.0%) 9 (75.0%)
Extent of surgery mastectomy lumpectomy	 12 (75.0%) 4 (25.0%)	 5 (45.5%) 6 (54.6%)	 8 (66.7%) 4 (33.3%)
Axillary lymph nodes negative positive not reviewed	 2 (12.5%) 10 (62.5%) 4 (25.0%)	 2 (18.2%) 3 (27.3%) 6 (54.6%)	 10 (83.3%) 2 (16.7%)
Adjuvant therapy chemotherapy radiation therapy	 15 (93.8%) 12 (75.0%)	 10 (90.9%) 5 (45.5%)	 12 (100%) 11 (91.7%)
DTH testing candida positive tetanus positive	 1 (6.3%) 9 (53.6%)	 3 (27.3%) 7 (63.6%)	 4 (33.3%) 8 (66.7%)
Concurrent mediations NSAIDS ACE inhibitors Steroids Thyroid hormones beta blockers	 8 (50.0%) 1 (6.3%) 1 (6.3%) 3 (18.8%) 3 (18.8%)	 3 (27.3%) 2 (18.2%) 1 (9.1%) 2 (18.2%) 4 (36.4%)	 5 (41.7%) 0 0 3 (25.0%) 0
Signs/Symptoms grade 2 fatigue grade 2 rash grade 2 joint pain	 1 (6.3%) 1 (6.3%) 0	 1 (9.1%) 0 1 (9.1%)	 0 0 0

Table 2. Clinical Course

ID	DTH positivity pre-vaccination[a]	HER2 positive disease[b]	Pre-vac MUC1	Pre-vac HER2	number of vaccinations; off treatment reason	toxicities reported	MUC1 response[c]	Her2 response[c]	progression-free survival (days)	survival[d]
Arm A: Vaccine emulsified in Montanide ISA-51 and GM-CSF										
A01	tetanus	yes	0.06	0.47	6 – complete	none	no	no	245+	592+
A02	tetanus & candida	yes	not done	not done	2 - toxicity	none	------	------	731+	731+
A03	neither	no	<0.05	<0.05	6 - complete	cyc 1: grade 2 ISR[e]	yes	yes	259+	721+
A04	neither	no	0.09	0.26	6 - complete	none	yes	no	313+	696+
A05	neither	no	0.45	<0.05	3 - progression	none	no	no	progression in liver and bone on day 129	died day 135
A06	neither	no	0.79	<0.05	6 - complete	none	no	no	232+	731+
A07	tetanus	no	0.30	0.25	6 -complete	none	no	no	441+	731+
A08	tetanus	no	1.02	0.36	6 -complete	cyc 3: grade 2 bone pain	no	no	649+	731+
A09	tetanus	no	not done	not done	3-toxicity	cyc 3: grade 2 ISR	------	------	progression in nodes, bone, and retroperitoneum: day 141	died day 394
A10	neither	yes	0.45	0.24	6 - complete	none	------	------	180+	330+
A11	tetanus	yes	0.45	0.53	6 - complete	none	no	no	630+	731+
A12	tetanus	no	0.58	0.56	5 - toxicity	cyc 5: grade 2 ISR	no	no	144+	743+
A13	neither	no	not done	not done	6 - complete	none	------	------	183+	632+
A14[f]	tetanus	no	0.54	0.18	6 - complete	cyc 1: grade 2 ISR	no	yes	progression in bone: day 411	731+
A15	neither	no	0.49	0.56	5 - refusal	none	no	no	198+	731+
A16	tetanus	no	not done	not done	6 – complete	none	------	------	168+	682+

Table 2. Clinical Course (continued)

ID	DTH positivity pre-vaccination[a]	HER2 positive disease[b]	Pre-vac MUC1	Pre-vac HER2	number of vaccinations; off treatment reason	toxicities reported	MUC1 response[c]	Her2 response[c]	progression-free survival (days)	survival[d]
Arm B: Vaccine emulsified in Montanide ISA-51 and CpG										
B01 pre	tetanus /candida	yes	<0.05	0.29	1 - study rec	none	yes	no	484+	731+
B02 pre	tetanus /candida	no	0.26	0.49	1 - study rec	none	yes	no	29+	731+
B03 pre	candida	no	0.33	<0.05	6 - complete	none	yes	yes	339+	731+
B04 pre	tetanus	no	0.08	<0.05	6 - complete	cyc 2: grade 2 ISR	yes	yes	247+	731+
B05 pre	tetanus	no	0.09	<0.05	6 - complete	cyc 2: grade 2 ISR	yes	yes	242+	731+
B06 pre	tetanus	no	not done	not done	2 - refusal	none	------	------	134+	499+
B07 post	neither	no	0.27	0.14	6 - complete	none	no	no	233+	731+
B08 post	tetanus	no	not done	not done	1 - toxicity	cyc 1: grade 3 ISR	------	------	731+	731+
B09 post	tetanus	yes	0.65	0.25	6 - complete	none	no	yes	476+	731+
B10 post	neither	yes	not done	not done	1 - refusal	none	------	------	622+	622+
B11 post	neither	no	0.56	not done	6 - complete	none	yes	------	484+	708+

Table 2. Clinical Course (continued)

ID	DTH positivity pre-vaccination[a]	HER2 positive disease[b]	pre-vac percentage of MUC-1 CD8-positive cells	pre-vac percentage of HER2 CD8-positive cells	number of vaccinations; off treatment reason	toxicities reported	MUC1 response[c]	Her2 response[c]	progression-free survival (days)	survival[d]
Arm C: Vaccine emulsified in Montanide ISA-51, GM-CSF, and CpG										
C1 pre	tetanus	no	0.08	0.05	3 - study rec	none	yes	yes	progression in liver: day 600	731+
C2 pre	tetanus /candida	yes	0.22	0.14	2 - study rec	cyc 2: grade 2 bone pain & ISR	yes	yes	494+	731+
C3 pre	tetanus /candida	no	< 0.05	< 0.05	5 - study rec	cyc 1: grade 2 ISR	no	no	731+	731+
C4 pre[g]	neither	no	0.18	< 0.05	5 - ineligible	cyc 2: grade 2 ISR	yes	no	234+	234+
C5 pre	tetanus /candida	no	0.05	< 0.05	3 - study rec	cyc 1: grade 2 ISR	yes	yes	457+	731+
C6 pre	tetanus	no	0.28	0.22	4 - toxicity	cyc 3: myalgia cyc 4: grade 2 ISR	no	yes	631+	727+
C7 post	neither	no	not done	not done	3 - refusal	none	------	------	565+	565+
C8 post	neither	yes	0.09	0.89	6 - complete	cyc 2: grade 2 joint pain & myalgia	yes	no	614+	713+
C9 post	tetanus	no	0.97	0.33	1 - toxicity	cyc 1: grade 2 ISR & rash desquamation	no	no	352+	640+
C10 post	neither	no	not done	not done	3 - refusal	none	------	------	85+	85+
C11 post	tetanus	yes	0.60	0.58	6 - complete	none	------	------	661+	731+
C12 post	tetanus /candida	no	1.04	0.14	6 - complete	cyc 2: grade 2 fatigue	no	no	160+	160+

a: candida or tetanus reactivity ≥ 10 mm
b: either HER2 gene amplification or HER2 expression 3+ by IHC using local laboratory findings
c: peptide-specific response defined as 2 fold or more increase in the percentage of peptide specific $CD8^+$ T cells from pre-immunization level or an increase to detectable levels (i.e. ≥ 0.5%) if pre-immunization levels were below the lower limit of detection
d: per protocol, maximum length of follow-up post registration is 2 years.
e: injection site reaction
f: ineligible due to bone mets at time of registration.
g: ineligible had an ocular melanoma within 5 years of registration.

KEY RESEARCH ACCOMPLISHMENTS

- The preclinical research was completed and described in the annual reports for years 3 and 4. The summary from year 4 is provided in this final report.
- Among the 39 patients enrolled, two patients were found to be ineligible due to prior cancer and bone metastases.
- Arm A met the accrual goal. Arms B and C closed early as the pre-specified toxicity safety boundary was crossed.
- Arm A: With a median follow-up of 2 years, 13 patients are alive without disease progression; 1 patient is alive with disease progression; 2 patients have died due to disease progression (Table 2A)
- Arm B: With a median follow-up of 2 years, all 11 patients are alive without disease progression (Table 2B)
- Arm C: With a median follow-up of 2 years, 11 patients are alive without disease progression and 1 patient is alive with disease progression (Table 2C)
- There was significant adjuvant-dependent sensitization to MUC1; a similar trend was observed for HER2/neu.
- Arm B (CpG) was significantly better than Arm A (GM-CSF) ($p=0.02$, Fisher's exact 2-tailed test)
- Combined arms with CpG (Arms B, C) were significantly better than no CpG (Arm A) ($p=0.03$).
- Arm B (CpG only) was significantly better than combined Arms with GM-CSF (Arms A, C) ($p=0.04$).
- For $HER2^+$ tetramers, a similar trend was observed.
- Antibody responses to $HER2_{883-899}$, the MHC class II-binding peptide used in the vaccine, were observed in 1/9 evaluable patients in Arm A, 5/10 patients in Arm B, and 3/6 patients in Arm C.
- There were no consistent changes observed in cytokine levels or percentages of $CD4^+$, $CD8^+$ or myeloid cell populations.

REPORTABLE OUTCOMES

- Manuscripts Published

1) Mukherjee, P., Ginardi, A.R., Madsen, C.S., Tinder, T. L., Jacobs, F., Parker, J., Agrawal, B., Longenecker, B.M., and Gendler, S.J. (2001) MUC1-specific CTLs are non-functional within a pancreatic tumor microenvironment. Glycoconjugate Journal 18:931-42. PMID 12820727.

2) Mukherjee, P., Madsen, C.S., Ginardi, A.R., Ginder, T.L., Jacobs, F., Parker, J., Agrawal, B., Longenecker, B.M., and Gendler, S.J. (2003) Mucin 1-specific immunotherapy in a mouse model of spontaneous breast cancer. Journal of Immunotherapy 26(1):47-62. PMID 12514429.

3) Xia, J., Tanaka, Y., Koido, S., Liu, C., Mukherjee, P., Gendler, S.J., and Gong, J. (2003) Prevention of spontaneous breast carcinoma by prophylactic vaccination with dendritic/tumor fusion cells. Journal of Immunology 170:1980-1986. PMID 12574367.

4) Chen, D., Xia, J., Tanaka, Y., Chen, H., Koido, S., Wernet, O., Mukherjee, P., Gendler, S.J., Kufe, D. and Gong, J. (2003) Immunotherapy of spontaneous mammary carcinoma with fusions of dendritic cells and mucin 1-positive carcinoma cells. Immunology 109:300-307. PMID 12757626. PMCID:PMC1782954.

5) Pockaj, B.A., Basu, G.D., Pathangey, L.B., Gray, R.J., Hernandez, J.L., Gendler, S.J. and Mukherjee, P. (2004) Reduced T cell function is related to COX-2 over-expression and PGE_2 secretion in patients with breast cancer. Annals of Surgical Oncology 11:328-339. PMID 14993030.

6) Basu, G.D., Pathangey, L.B., Tinder, T.L., LaGiola, M., Gendler, S.J. and Mukherjee, P. (2004) Cyclooxygenase-2 inhibitor induces apoptosis in breast cancer cells in an in vivo model of spontaneous metastatic breast cancer 2(11):632-642. PMID 15561779.

7) Mukherjee, P., Tinder, T.L., Basu, G.D., Pathangey, L.B., Chen, L. and Gendler, S.J. (2004) Therapeutic Efficacy of MUC1-Specific Cytotoxic T Lymphocytes and CD137 Co-Stimulation in a Spontaneous Breast Cancer Model. Breast Disease 20:53-63. PMID 15687707.

8) Basu, G.D., Pathangey, L.B., Tinder, T.L., Gendler, S.J. and Mukherjee, P. (2005) Mechanism underlying the growth inhibitory effects of COX-2 inhibitor in human breast cancer cells. Breast Cancer Research 7:R422-R435. PMID 15987447. PMCID:PMC1175053

9) Mukherjee, P., Pathangey, L.B., Bradley, J.B., Tinder, T.L., Basu, G.D., Akporiaye, E.T., and Gendler, S.J. (2007) MUC1-specific immune therapy generates a strong anti-tumor response in a MUC1-tolerant colon cancer model. Vaccine 25:1607-1618. PMID 17166639

10) Block, M.S., Suman, V.J., Markovic, S.N., Northfelt, D.W., Mukherjee, P., McCullough, A.E., Pockaj, B.A., Nevala, W.K., Madsen, C.S., Erskine, C.L., Knutson, K.L., Perez, E.A., Hobday, T.J., Ingle, J.N. and Gendler, S.J. CD8+ T cell responses elicited by MUC1/HER2/neu peptide-based vaccines for early breast cancer, manuscript under revision.

- Posters

Gendler, S.J., Mukherjee, P., Basu, G.D., Tinder, T.L., Madsen, C.S., Ginardi, A.R. Immunotherapeutic Strategies in a Mouse Model of Spontaneous Breast Cancer, Era of Hope, 2002 Department of Defense Breast Cancer Research program Meeting, 2002.

Mukherjee, P., Tinder, T.L., Ginardi, A.R., Gendler, S.J. DC-tumor cell fusion vaccine tested in preclinical mouse model of spontaneous breast cancer. Proceedings American Association for Cancer Research Annual Meeting 2001 March; 42:24.

Mukherjee, P., Ginardi, A.R., Tinder, T.L., Madsen, C.S., and Gendler, S.J. Adoptively transferred MUC1-specific CTL home to lymph node and tumors in a spontaneous mouse model of mammary gland cancer. Proceedings of the American Association for Cancer Research 43:976 (#4835), 2002.

Basu. G.D., Mukherjee, P., Bradley, J., Madsen, C.S., Pathangey, L., Croft, M., and Gendler, S.J. Immunization with OX40 antibody in a spontaneous model of breast cancer. Keystone Symposium: Mechanisms of Immunologic Tolerance and Its Breakdown, 2002.

Mukherjee, P., Basu, G.D., Pathangey, L.B., Pockaj, B.A., Gendler, S.J., Mukherjee, P. The cyclo-oxgenase 2-selective inhibitor, celecoxib, mediates growth inhibition in breast cancer cell lines via diverse pathways. Cancer Epidemiol. Biomarkers Prev. 12(11 Part 2):1298s, Nov.2003

Mukherjee, P., Pockaj, B.A., Basu, G.D., Pathangey, L.B., Tinder, T.L., Ginardi, A.R., and Gendler, S.J. COX-2 induced PGE_2 synthesis is involved in down regulation of immune cell function in patients with breast cancer. Maricopa Integrated Health System and Mayo Clinic Scottsdale 2003 Academic Excellence Day, May 14, 2003.

Basu, G.D., Mukherjee, P., Bradley, J., Madsen, C.S., Pathangey, L.B., Croft, M., and Gendler, S.J. Immunization with OX40 antibody in a spontaneous model of breast cancer. Maricopa Integrated Health System and Mayo Clinic Scottsdale 2003 Academic Excellence Day, May 14, 2003.

Mukherjee, P., Tinder, T.L., Basu, G.D., Pathangey, L.B., Chen, L., and Gendler, S.J. Therapeutic efficacy of MUC1-specific cytotoxic T lymphocytes and CD137 co-stimulation in a spontaneous mammary cancer model. International Society for Biological Therapy of Cancer, Nov. 2004 (Abstract and platform presentation) 27(6):S45

Mukherjee, P., Basu, G.D., Pathangey, L., Tinder, T., Madsen, C., Chen, L., Markovic, S.N., and Gendler, S.J. Vaccine Strategies for Breast Cancer, Women;s Cancers 2006: Merging Science and Care, Mayo Clinic Cancer Center, September 2005.

Gendler, S.J., Block, M.S., Markovic, S.N., Nevala, W.K., Northfelt, D.W., McCullough, A.E., Pockaj, B.A., Ingle, J. N., Fitch, T.R., Perez, E.A., Madsen, C.S., Cohen, P.A., Mukherjee, P., Suman, V.J. MUC1/HER-2/neu Peptide-Based Immunotherapeutic Vaccine Clinical Trial for Breast Adenocarcinoma. Era of Hope Poster 3rd August 2011 in Orlando, Florida and a platform talk was given on 5th August 2011.

Invited speaker presentation entitled “MUC1: From Bench to Bedside and Back” at Mucins in Health and Disease, 12th International Workshop of Carcinoma-Associated Mucins, to be presented 27th – 31st July 2013.

- Funding Received
  NIH/NCI P50 CA116201 (Ingle) 2005-2010
  Project 3 (Principal Investigator project 3), 15%
  Preclinical and Clinical Studies of MUC1 Glycopeptide Strategies in Breast Cancer

- Experience/training supported by this award
  Dr. Pinku Mukherjee
  Dr. G.D. Basu
  A.R. Ginardi
  T.L. Tinder
  J.B. Bradley
  L.B. Pathangey
  C.S. Madsen
  Dr. S.N. Markovic
  Dr. M.S. Block
  Dr. D.W. Northfelt

Time Table of Protocol Development

- Clinical protocol concept approved by Mayo Clinic Cancer Center 12-11-03
- Completed Mayo Clinic Cancer Center Peer Review process 5-4-04
- List of recommendations by FDA (pre IND conference) 4-21-04
- Peptides synthesized and vialed by ClinAlfa® for use in this clinical trial:
  1. Her2/neu (435-443)
  2. Her2/neu (883-899)
  3. MUC1 (950-958)
- Completion of IND documentation and submission to FDA on December 17, 2004.
- FDA approval (IND # 12155)
- Mayo IRB approval April 22, 2005 (IRB 782-05)
- Submission to DOD HSRRB on May 11, 2005
- Submission to FDA of the revised 1572 and Investigator's Brochure on September 15, 2005
- Submission to Mayo IRB of amendment, which excludes prisoners from the study population and reduces the number of personnel involved in the study (September 12, 2005)
- Submission of revision to HSRRB on February 10, 2006 (response to request for revisions from 14 December 2005 HSRRB meeting)
- Submission of revision to HSRRB on May 18, 2006
- Submission of final documents to the Mayo IRB August 30, 2006
- Final approval Mayo IRB December 15, 2006
- Final approval DoD HSRRB (Log Number A-10856) January 26, 2007
- CpG-7909 adjuvant to be supplied by Pfizer as PF3512676 for this clinical trial.
- Submission of revised clinical protocol to Mayo IRB, HSRRB and IND (July, August 2007)
- Final Mayo IRB approval August 2, 2007
- Extension of "performance period" by 24 months to 14 September 2009
- Approval from DOD HRPO on June 9, 2008
- Clinical Trial was activated August 28, 2008.
- Clinical Trial was closed from 2/24/09 to 5/19/09 due to toxicitiy at injection sites. The amount of CpG ODN adjuvant was reduced from 2 mg to 1 mg (Addendeum 1) and the trial was reopened.

- Enrollment has been completed and the trial was closed June 30, 2010. Thirty-nine patients out of the anticipated 45 patients (87%) were enrolled. Two of the arms (B and C) were closed prematurely (June 30, 2010) due to dose limiting toxicities (injection site reaction toxicity > CTC grade 2).

CONCLUSIONS

The trial opened August 28, 2008 and it has accrued 39 patients by June 30, 2010, when it was permanently closed to enrollment. Accrual was met for Arm A. Arms B and C were closed after accrual of 11 and 12 patients, respectively. Arm B was temporarily closed on November 4, 2009 and was permanently closed on June 30th, 2010 due to dose limiting toxicity of the regimen (injection site reactions toxicity > CTC grade 2). Arm C was temporarily closed on February 23, 2009 and then permanently closed June 30th, 2010 for intolerability of regimen. As of September 13, 2011, enrolled patients are under observation and follow-up.

Among the 39 eligible patients enrolled, one patient (Arm A) developed tumor progression and died. The remaining 37 patients are alive without disease progression with a median follow-up time of 2 years (range 5 months to 2.8 years). Arm A met the accrual goal. Arms B and C closed early as the pre-specified toxicity safety boundary was crossed. It is important to note that CTC criteria did not previously separate injection site reaction from allergic reaction. Under the new guidelines, we could have completed accrual. When a relevant autoantigen is introduced, the CpG toxicity observed was greater than previously reported. Higher toxicity may be due to efficacy of the immune response. Feasibility studies need to be developed to achieve tolerability at the same time that effective immunization is achieved.

There was significant adjuvant-dependent sensitization to MUC1; a similar trend was observed for HER2/neu (see figure below). Arm B (CpG) was significantly better than Arm A (GM-CSF) (p=0.02, Fisher's exact 2-tailed test). Combined Arms with CpG (Arms B,C) were significantly better than no CpG (Arm A) (p=0.03). Arm B (CpG only) was significantly better than combined Arms with GM-CSF (Arms A,C) (p=0.04). For HER 2^+ tetramers, a similar trend was observed. GM-CSF did not appear to be as effective an adjuvant as CpG. In contrast to the results with tetramers, there were no consistent changes observed in cytokine levels or percentages of $CD4^+$, $CD8^+$ or myeloid cell populations. Antibody responses (defined as a doubling of antigen-specific IgG from pre- to post-vaccination) to the negative control proteins or MUC1 were not seen. Antibody responses to HER2883-899, the MHC class II-binding peptide used in the vaccine, were observed in 1/9 evaluable patients in Arm A, 5/10 patients in Arm B, and 3/6 patients in Arm C.

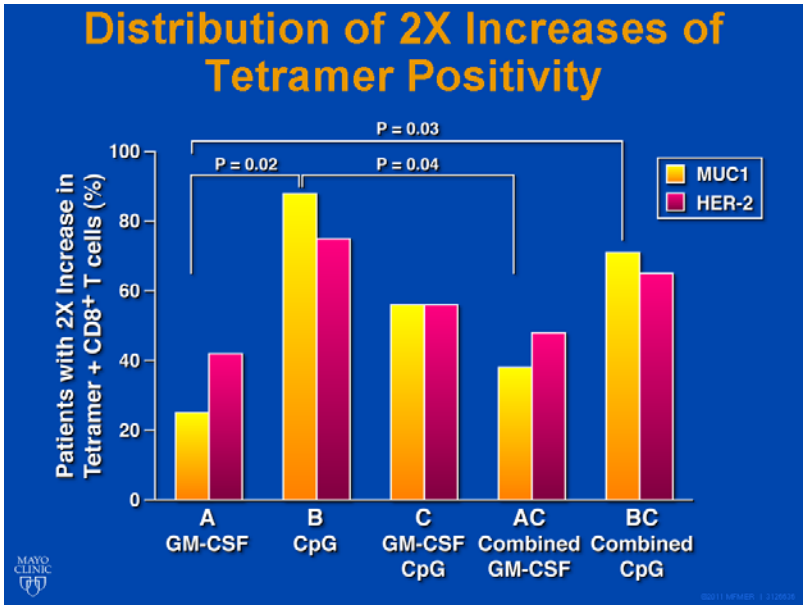

Figure Legend

Serial PBMC samples were obtained. Immunophenotyping of PBMC and tetramer quantification of antigen-specific CD8+ T cells were performed using standard flow cytometry techniques.

Although these studies and the clinical trial took a number of years to complete, the trial was not outdated when it eventually opened. All three peptides elicited strong responses, both cellular and humoral. Breast cancer patients were eager to enroll in the vaccine study; the treatment was not particularly toxic (other than transient inflammatory responses). A concern is that the CpG adjuvant has been taken off the market by Pfizer, which purchased from Coley the rights for the use of CpG in cancer. CpG is a powerful adjuvant, both in mice and in humans as this work showed. Fortunately, there are bioactive compounds under investigation such as VentiRx 2337, a toll-like receptor 8 agonist.

Plans are underway to utilize the same peptide vaccine with the adjuvant GM-CSF in a neoadjuvant trial for breast cancer patients with ductal carcinoma in situ (DCIS). The proposal will be submitted to the NCI Cancer Prevention Network in the autumn of 2013. The overall objective is to determine the safety and immunization efficacy of the MUC1 and HER2/neu peptide vaccine using GM-CSF as an immune adjuvant suspended in Montanide ISA-51 for patients with newly diagnosed DCIS. The secondary goals are to determine pathologic change in tumor from pre- to post-neoadjuvant vaccine, determine changes in tumor microenvironment, determine change in imaging characteristics, and determine immune responses.

Appendices:

1. Mukherjee, P., Ginardi, A.R., Madsen, C.S., Tinder, T. L., Jacobs, F., Parker, J., Agrawal, B., Longenecker, B.M., and Gendler, S.J. (2001) MUC1-specific CTLs are non-functional within a pancreatic tumor microenvironment. Glycoconjugate Journal 18:931-42. PMID 12820727.

2. Mukherjee, P., Madsen, C.S., Ginardi, A.R., Ginder, T.L., Jacobs, F., Parker, J., Agrawal, B., Longenecker, B.M., and Gendler, S.J. (2003) Mucin 1-specific immunotherapy in a mouse model of spontaneous breast cancer. Journal of Immunotherapy 26(1):47-62. PMID 12514429.

3. Xia, J., Tanaka, Y., Koido, S., Liu, C., Mukherjee, P., Gendler, S.J., and Gong, J. (2003) Prevention of spontaneous breast carcinoma by prophylactic vaccination with dendritic/tumor fusion cells. Journal of Immunology 170:1980-1986. PMID 12574367.

4. Chen, D., Xia, J., Tanaka, Y., Chen, H., Koido, S., Wernet, O., Mukherjee, P., Gendler, S.J., Kufe, D. and Gong, J. (2003) Immunotherapy of spontaneous mammary carcinoma with fusions of dendritic cells and mucin 1-positive carcinoma cells. Immunology 109:300-307. PMID 12757626. PMCID:PMC1782954.

5. Pockaj, B.A., Basu, G.D., Pathangey, L.B., Gray, R.J., Hernandez, J.L., Gendler, S.J. and Mukherjee, P. (2004) Reduced T cell function is related to COX-2 over-expression and PGE_2 secretion in patients with breast cancer. Annals of Surgical Oncology 11:328-339. PMID 14993030.

6. Basu, G.D., Pathangey, L.B., Tinder, T.L., LaGiola, M., Gendler, S.J. and Mukherjee, P. (2004) Cyclooxygenase-2 inhibitor induces apoptosis in breast cancer cells in an in vivo model of spontaneous metastatic breast cancer 2(11):632-642. PMID 15561779.

7. Mukherjee, P., Tinder, T.L., Basu, G.D., Pathangey, L.B., Chen, L. and Gendler, S.J. (2004) Therapeutic Efficacy of MUC1-Specific Cytotoxic T Lymphocytes and CD137 Co-Stimulation in a Spontaneous Breast Cancer Model. Breast Disease 20:53-63. PMID 15687707.

8. Basu, G.D., Pathangey, L.B., Tinder, T.L., Gendler, S.J. and Mukherjee, P. (2005) Mechanism underlying the growth inhibitory effects of COX-2 inhibitor in human breast cancer cells. Breast Cancer Research 7:R422-R435. PMID 15987447. PMCID:PMC1175053

9. Mukherjee, P., Pathangey, L.B., Bradley, J.B., Tinder, T.L., Basu, G.D., Akporiaye, E.T., and Gendler, S.J. (2007) MUC1-specific immune therapy generates a strong anti-tumor response in a MUC1-tolerant colon cancer model. Vaccine 25:1607-1618. PMID 17166639.

10. Clinical Trial MCO338: MUC1/HER-2/neu Peptide Based Immunotherapeutic Vaccines for Breast Adenocarcinomas

Glycoconjugate Journal 18, 931–942, 2001

MUC1-specific CTLs are non-functional within a pancreatic tumor microenvironment

Pinku Mukherjee[1], Amelia R. Ginardi[1], Cathy S. Madsen[1], Teresa L. Tinder[1], Fred Jacobs[2], Joanne Parker[2], Babita Agrawal[2], B. Michael Longenecker[2] and Sandra J. Gendler[1]*

[1] *Department of Biochemistry and Molecular Biology, Mayo Clinic Scottsdale, Scottsdale, AZ 85259 USA,*
[2] *Biomira, Inc., Edmonton, Canada*

Pancreatic cancer is a highly aggressive, treatment refractory disease and is the fourth leading cause of death in the United States. In humans, 90% of pancreatic adenocarcinomas over-express altered forms of a tumor-associated antigen, MUC1 (an epithelial mucin glycoprotein), which is a target for immunotherapy. Using a clinically relevant mouse model of pancreas cancer that demonstrates peripheral and central tolerance to human MUC1 and develops spontaneous tumors of the pancreas, we have previously reported the presence of functionally active, low affinity, MUC1-specific precursor cytotoxic T cells (pCTLs). Hypothesis for this study is that MUC1-based immunization may enhance the low level MUC1-specific immunity that may lead to an effective anti-tumor response. Data demonstrate that MUC1 peptide-based immunization elicits mature MUC1-specific CTLs in the peripheral lymphoid organs. The mature CTLs secrete IFN-γ and are cytolytic against MUC1-expressing tumor cells *in vitro*. However, active CTLs that infiltrate the pancreas tumor microenvironment become cytolytically anergic and are tolerized to MUC1 antigen, allowing the tumor to grow. We demonstrate that the CTL tolerance could be reversed at least *in vitro* with the use of anti-CD40 co-stimulation. The pancreas tumor cells secrete immunosuppressive cytokines, including IL-10 and TGF-ß that are partly responsible for the down-regulation of CTL activity. In addition, they down-regulate their MHC class I molecules to avoid immune recognition. $CD4^+CD25^+$ T regulatory cells, which secrete IL-10, were also found in the tumor environment. Together these data indicate the use of several immune evasion mechanisms by tumor cells to evade CTL killing. Thus altering the tumor microenvironment to make it more conducive to CTL killing may be key in developing a successful anti-cancer immunotherapy.

Keywords: **CTL, antigens/peptides/epitopes, tolerance, tumor immunity, transgenic models**

Abbreviations: **APC: Antigen presenting cell; CTL: cytotoxic T lymphocytes; DC: dendritic cell; MET: MUC1-expressing pancreatic tumor mouse model; MUC1: human mucin 1; Muc1: mouse mucin 1; MUC1.Tg: MUC1 transgenic; TAA: tumor associated antigen; TILs: tumor infiltrating lymphocytes; TR: tandem repeat.**

Introduction

The 5-year survival of patients with adenocarcinoma of the pancreas remains low at only 4%. In 2000, an estimated 28,300 patients were diagnosed with pancreatic cancer in the United States. Metastatic pancreatic cancer is uniformly fatal because no effective chemotherapy is available. Despite progress in the treatment of cancer with surgery, radiotherapy and chemotherapy, only minimal advances have been made in improving survival rates in patients with pancreatic cancer. The National Cancer Institute has therefore designated research on pancreatic cancer as high priority. Along with research focused on the nature of cells that become transformed in the pancreas and the molecules involved in the process of transformation and metastasis, alternative treatment strategies must be addressed. Cancer immunotherapy is an attractive, non-toxic treatment that should enable the activation of the immune system to attack a developing or metastasizing tumor. Development of preclinical models of spontaneous pancreatic cancer that resemble human cancer is key to progress in this area. One of the major goals of such a therapy is to generate cytotoxic T lymphocytes (CTLs) and memory T lymphocytes directed against tumor associated antigens (TAA), which eventually lead to long lasting anti-tumor immunity. Some of the most promising TAA for immune targeting are conventional cellular proteins that are expressed on both normal and transformed cells, and one such candidate is MUC1.

*To whom correspondence should be addressed: Sandra J. Gendler, Mayo Clinic Scottsdale, S.C. Johnson Medical Research Center, 13400 East Shea Boulevard, Scottsdale, AZ 85259. Tel.: 480-301-7062; Fax: 480-301-7017; E-mail: gendler.sandra@mayo.edu

Although MUC1 is a self-molecule that is normally expressed on epithelial cells lining ducts and glands at low levels, it is a target for immunotherapy because MUC1 is significantly altered in expression during tumorigenesis. There is a large increase in the amount of MUC1 expressed on cells and in circulation. Its distribution is no longer restricted to the apical surface of the ducts and glands, but it is found throughout the tumor mass and on the surface of tumor cells. Most importantly, the glycosylation is altered. Oligosaccharides are shorter and fewer in number, revealing immunodominant peptide sequences that on normal cell surfaces would be sequestered by glycosylation. In 2000, cancers including pancreatic cancer that express MUC1 accounted for about 72% of new cases and for 66% of the deaths [1]. These observations have prompted clinical vaccination trials aimed at boosting the weak anti-MUC1 immune responses to therapeutic levels.

Human clinical testing should ideally be preceded by extensive animal model studies to show that the concepts can be translated into efficacious therapy for cancer. Until recently, the mouse has not been a suitable preclinical model for testing MUC1-specific immune responses as human MUC1 sequence differs substantially from that of mouse Muc1 and is strongly antigenic in the mouse. In this project, we have utilized a human MUC1 transgenic mouse model (MUC1.Tg) that expresses human MUC1 as a self-molecule. Because the transgene is driven under its own promoter, MUC1 is not over-expressed but is expressed in normal levels, in a tissue specific manner. Mice transgenic for human MUC1 develop B and T cell tolerance and are refractory to immunization with the protein encoded by the transgene [2]. We have crossed the MUC1.Tg mice with mice that carry the first 127 amino acids of the SV40 large T-antigen driven by the elastase promoter. These mice are designated MET and develop spontaneous MUC1-expressing tumors of the pancreas [3]. This experimental model represents an improved model system for evaluating the efficacy of anti-MUC1 vaccine formulations *in vivo* within the context of existing tolerance mechanisms. As previously described, these mice exhibit acinar cell dysplasia at birth, which progresses to microadenomas and single or multiple acinar cell carcinomas. We have previously shown that non-immunized MET mice develop low affinity precursor MUC1-specific CTLs (pCTLs) i.e. the CTLs were cytotoxic only when primed *in vitro* with MUC1 antigen or MUC1 TR peptide at 10^{-6} M for several days. Although these CTLs have minimal effect on the spontaneously growing pancreatic tumors, they were efficient in eradicating injected MUC1 expressing tumors when adoptively transferred [3,4].

In this study, we tested a vaccine formulation comprised of liposomal-MUC1 tandem repeat lipopeptide (L-MUC1-TR) along with liposomal IL-2 (L-IL-2) with the goal of enhancing the already existing MUC1-specific immunity. We compared the immune responses that developed during treatment and at time of sacrifice in the MET mice. Survival and tumor burden were used as end points for determining the effectiveness of the treatment strategy. Data from this study show that MUC1-specific immunization resulted in mature CTLs and that adoptively transferred functional CTLs were rendered non-responsive within the tumor microenvironment, thus interrupting an anti-tumor response. Immunization results in a MUC1-specific CTL response that became tolerized within the growing tumor. Tolerance may be defined as accumulation of antigen-specific T cells, which are hypo-responsive and may have been induced within a non-inflammatory and immunosuppressive tumor micro-environment.

Results

Characterization of immunized MET mice

Tumor burden in immunized MET mice

We immunized mice with L-MUC1-TR ± L-IL-2. A schematic representation of the immunization protocol is illustrated in Figure 1. The first two immunizations administered to young (3 and 5 week old) MET mice utilized syngeneic dendritic cells (DC) loaded with liposomal MUC1 to induce strong immunity as young mice respond well to an antigen when presented in context of DC without the induction of tolerance [5]. From week 7 onwards, mice were given L-MUC1-TR reconstituted in PBS (s.c.) and subsequently boosted with the same formulation every two weeks. L-IL-2 was administered (i.p.) every two weeks to the appropriate groups. Tumor burden was evaluated only at

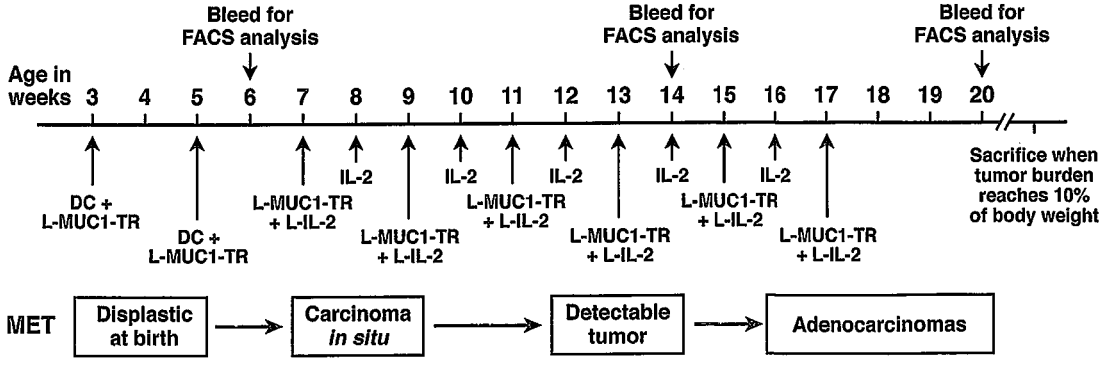

Figure 1. Schematic representation of immunotherapy strategy in MET mice.

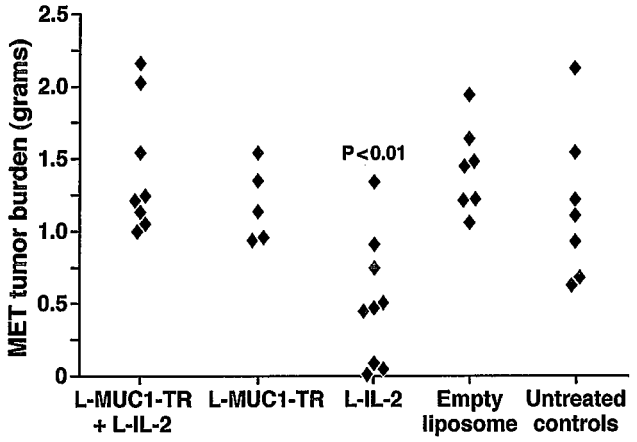

Figure 2. MUC1-specific immunization did not alter pancreatic tumor weight in MET mice, although L-IL-2 treatment had a beneficial effect. At time of necropsy, pancreatic tumors from immunized MET mice were weighed and compared to pancreatic tumor weights from untreated MET mice. No significant differences were observed between untreated control mice and mice immunized with L-MUC1-TR + L-IL-2, L-MUC1-TR, or empty liposome. Significantly lower pancreatic tumor burden (in grams) was observed in L-IL-2 treated mice as compared to untreated control mice ($p < 0.01$). *P* values are from the pair-wise contrasts from a one-way ANOVA model. Individual mice data are shown ($n = 6$ to 9 mice/group).

time of sacrifice, when mice had become morbid and showed weight loss. As tumors are internal and not palpable, tumor progression cannot be readily monitored. Our data demonstrate that treatment with L-IL-2 alone showed significant reduction in tumor burden when compared to untreated controls (Figure 2). All other treatment groups failed to have an effect on tumor burden. No effects on survival or metastasis were observed (data not shown).

T cell immune response in immunized MET mice

The immunization strategy was successful in eliciting strong T cell responses as measured by intracellular cytokine staining and by ^{51}Cr-release assay. We evaluated (a) intracellular IFN-γ expression in T cells and (b) T cells recognizing H-2D^b MUC1 tetramer from peripheral blood lymphocytes (PBL) at 6, 10, and 14 weeks post immunization. MHC class I H-2D^b tetramers containing MUC1 TR APGSTAPPA peptide were used in this experiment. T cells from PBLs were stained with 0.1 mgs/ml MUC1-tetramer directly conjugated to phycoerythrin (PE) for 1 hour on ice, counterstained with fluorescein (FITC)-conjugated anti-CD4 and CD8 antibody for 15 minutes on ice and analyzed by two-color flow cytometry. All treatment groups in immunized mice showed increased numbers of T cells expressing intracellular IFN-γ by 10–14 weeks of age as compared to untreated control or mice treated with empty liposomes (Figure 3A, *p* values shown in the figures). Similarly, we observed an increase in T cells reactive with H-2D^b/MUC1 tetramer in immunized mice as compared to

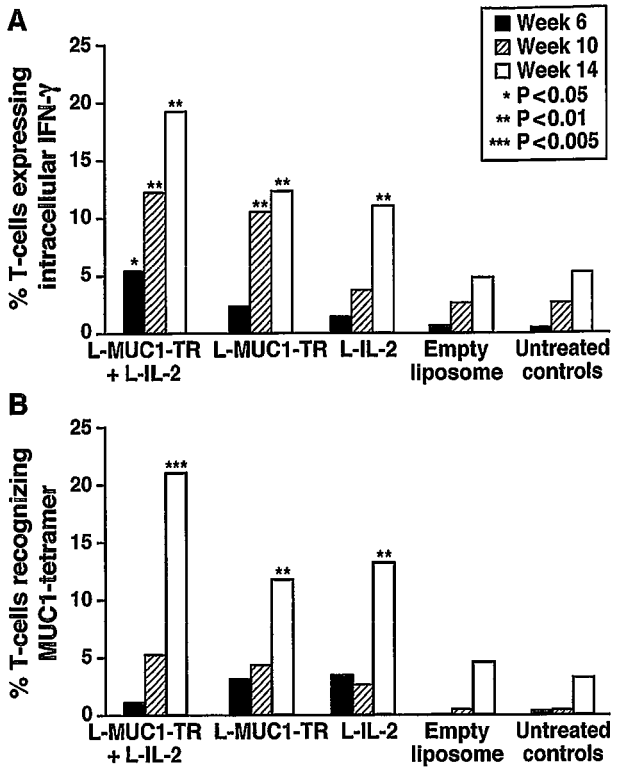

Figure 3. MUC1-specific immunization elicits (A) IFN-γ expressing T cells and (B) T cells that recognize MUC1/D^b tetramer in MET mice. At weeks 6, 10 and 14 post immunization and at necropsy, PBLs were analyzed for presence of T cells expressing IFN-γ and T cells recognizing MUC1/D^b tetramer. (A), Compared to untreated controls only mice in L-MUC1-TR + L-IL-2 treated group showed significant increase in percent of IFN-γ expressing T cells as early as 6 weeks post immunization ($^*p < 0.05$). By 10 weeks post immunization, mice in L-MUC1-TR + L-IL-2 and L-MUC1 TR group showed significant increase in this cell type as compared to untreated controls ($^{**}p < 0.01$). By 14 weeks post immunization, percent T cells expressing IFN-γ increased even more in the L-MUC1-TR + L-IL-2 treated mice ($^{**}p < 0.01$), whereas it stayed the same in L-MUC1-TR treated mice ($^{**}p < 0.01$). At this time, L-IL-2 treated mice also showed significant increase in IFN-γ expressing T cells ($^{**}p < 0.01$) as compared to untreated control mice. (B) Mice in all treatment groups showed no significant increase in percent T cells recognizing MUC1/D^b tetramer at 6 or 10 weeks post immunization as compared to untreated controls. By 14 weeks, mice in all treatment groups except empty liposome group showed increase in percent T cells recognizing MUC1/D^b tetramer ($^{***}p < 0.005$ for L-MUC1 TR + L-IL-2 treated group; $^{**}p < 0.01$ for L-MUC1-TR alone and L-IL-2 alone treated groups). Average of $n = 6$ mice/group is shown. *P* values are from the pair-wise contrasts from a one-way ANOVA model. *indicates comparison of untreated controls versus treatment groups.

control groups (Figure 3B, *p* values shown in the figures). MUC1-specific T cells arise naturally in MET mice as tumors develop [3], thus an increase in IFN-γ-expressing T cells and MUC1 tetramer$^+$ T cells are observed at 14 week time point in untreated and empty liposome treated MET mice.

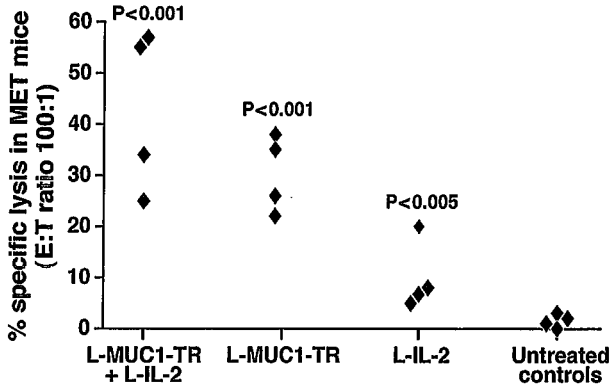

Figure 4. MUC1-specific immunization elicits mature MUC1-specific CTLs in immunized MET mice. CTL activity was determined by a standardized 8 hr ^{51}Cr-release assay using B16 melanoma cells transfected with full-length human MUC1 transgene as targets and splenic T cells from immunized mice with no *in vitro* stimulation with L-MUC1-TR or cytokines. Specific lysis was calculated according to the following formula: (experimental CPM-spontaneous CPM/maximum CPM-spontaneous CPM) × 100. (A) MET mice in all treatment groups showed significant increase in percent of MUC1-specific mature CTL as compared to untreated mice ($p < 0.001$ for L-MUC1-TR + L-IL-2 treated mice and L-MUC1-TR treated mice; $p < 0.005$ for L-IL-2 treated mice). We were unable to do the CTL assay for mice in the empty liposome treatment group. *Indicates comparison of untreated controls versus treatment groups.

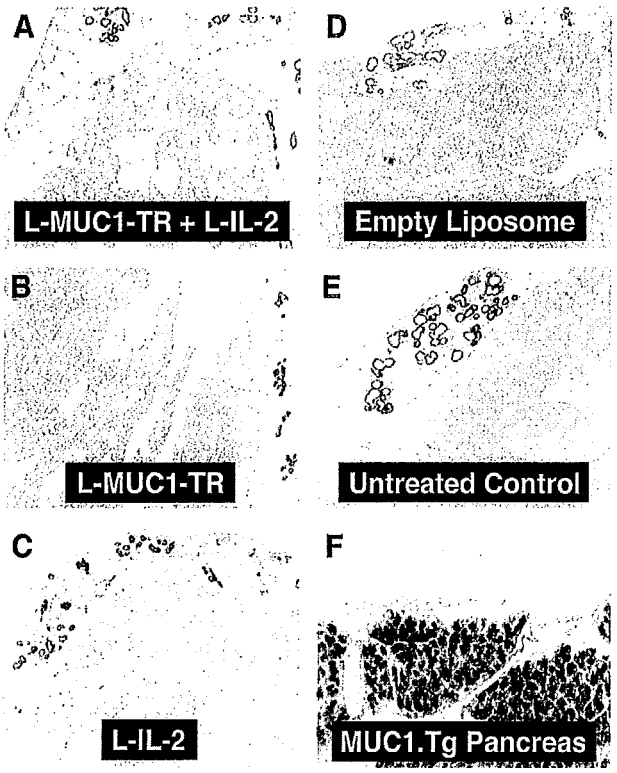

Figure 5. MUC1 expression is significantly reduced in solid undifferentiated tumor sections from MET mice as compared to normal pancreas of MUC1.Tg mice. At time of sacrifice, methacarn fixed and paraffin-embedded sections of tumors from MET mice and normal pancreas from MUC1.Tg mice were stained with B27.29 monoclonal antibody, reactive with MUC1 TR. (A) L-MUC1-TR and L-IL-2 treated tumor; (B) L-MUC1-TR treated; (C) L-IL-2 treated tumor; (D) empty liposome treated tumor; (E) untreated tumor; and (F) pancreas of MUC1.Tg mice. Images were captured at 200X magnification. The large moderately differentiated tumor does not stain for MUC1; however, the more differentiated portions of the pancreas surrounding the tumor stains strongly with the antibody, as does the pancreas from a MUC1.Tg mouse.

However, the levels are significantly higher in MET mice immunized with L-MUC1-TR and L-IL-2. Data suggest that immunization with L-MUC1-TR elicited MUC1-specific T cells that release IFN-γ and persist in MET mice with high tumor burden.

Mature cytotoxic T cells develop in immunized MET mice

Mature CTLs were observed in L-MUC1-TR + L-IL-2 (4/4 mice) and L-MUC1-TR (4/4 mice) groups but only 1 out of 4 L-IL-2 treated mouse had 20% lytic activity (Figure 4). These CTLs expressed intracellular IFN-γ and were reactive with H-2D^b/MUC1 tetramer (data not shown). Since L-IL-2 alone had a positive effect on MET tumor burden but failed to reproducibly elicit mature MUC1-specific CTLs, we suggest that the beneficial effect of L-IL-2 treatment may be attributed to stimulation of other TAA-specific CTLs that have yet to be identified *in vitro*. To determine specificity of the CTL to MUC1 antigen, B16.neo transfected cells were used as control target cells with lysis of <5% (data not shown).

MUC1 expression decreases in immunized MET mice

A plausible explanation for the failure of MUC1-specific immunization to reduce MET could be that the MUC1-specific CTLs are indeed eradicating MUC1-expressing tumor cells but what eventually grows out are the MUC1 non-expressing tumor cells. To evaluate this, we stained MET tumor sections from immunized and unimmunized MET mice and compared it to normal pancreas. Normal pancreas from MUC1.Tg mice stains very strongly for MUC1 with Mab. B27.29. This antibody is known to react well with highly glycosylated MUC1, in contrast to most other MUC1-specific antibodies [6]. However, solid moderately differentiated tumor sections from treated or untreated MET mice stained very weakly for MUC1 with the same antibody (Figure 5A–E). These results suggest that the naturally occurring MUC1-specific CTLs that exist in the untreated MET mice [3] may be capable of destroying the MUC1$^+$ cells in the tumors and that the tumors grow without MUC1. However, an alternative explanation could be that the tumors antigenically modulate MUC1 antigen by causing changes in glycosylation of MUC1 and therefore evade recognition by MUC1-specific antibodies and CTL.

Table 1. Surface expression of MHC class I molecule on tumor cells decreases as tumors progress in MET mice. Flow cytometric analysis demonstrating percent cells positive for pancytokeratin and MHC class I molecule (H2-D^b/K^b)

Tumor age	*MET*
6 week	35.25 ± 5.1
12 week	15.04 ± 4.1
18 week	3.07 ± 1.0

MHC class I expression decreases in MET mice as tumors progress

A well characterized mechanism by which tumor cells evade CTL killing is by downregulation of MHC class I molecule on their surface. In Table 1, we show that in MET tumors, H2-D^b and K^b positive cells are significantly decreased. In the MET mice, the percent cells that are double positive for pancytokeratin and MHC class I are >30% in 6 week old tumor and decrease to <20% in 12 week old tumor and <5% in 18 week old tumor.

MET tumors release a bioactive form of TGF-ß that down regulates CTL lytic activity

Tumors utilize several mechanisms to escape immune recognition and/or killing. Another such mechanism is the release of immunosuppressive factors such as TGF-ß that are capable of hindering T cell signaling and down regulating their function. We have previously shown that MET tumors express high levels of TGF-ß as detected by immunohistochemistry [3], which does not distinguish between active or latent forms of the protein. We now present data represented in Figure 6A that MET tumor cells grown in culture release an active form of TGF-ß that can inhibit proliferation of Mv1Lu, a mink lung epithelial cell line. Surprisingly, the supernatant from MET tumor cells was as effective in inhibiting MylLu cell proliferation as the standard rHuTGF-ß. Thus, tumors may utilize this mechanism to down regulate CTL activity *in vivo* and escape immune intervention. When MUC1-specific CTLs (1×10^7 cells/ml) were cultured in the presence of supernatant from MET tumor cells for 24 hours, CTL lytic function against B16.MUC1 tumor target was significantly reduced in a dose dependent fashion (Figure 6B). Data presented in Figure 6A clearly demonstrates that MET-derived supernatant contains immunosuppressive factors including TGF-ß that can down-regulate CTL function. CTL clones remained viable and were not apoptotic as determined by trypan blue exclusion and Annexin V staining, post incubation with MET tumor-derived supernatant (data not shown).

Adoptively transferred MUC1-specific CTL clone became tolerized within the pancreas tumor

Mature CTL were observed *in vitro* (Figure 4), from peripheral tissues of MET mice with high tumor burden. These CTLs were

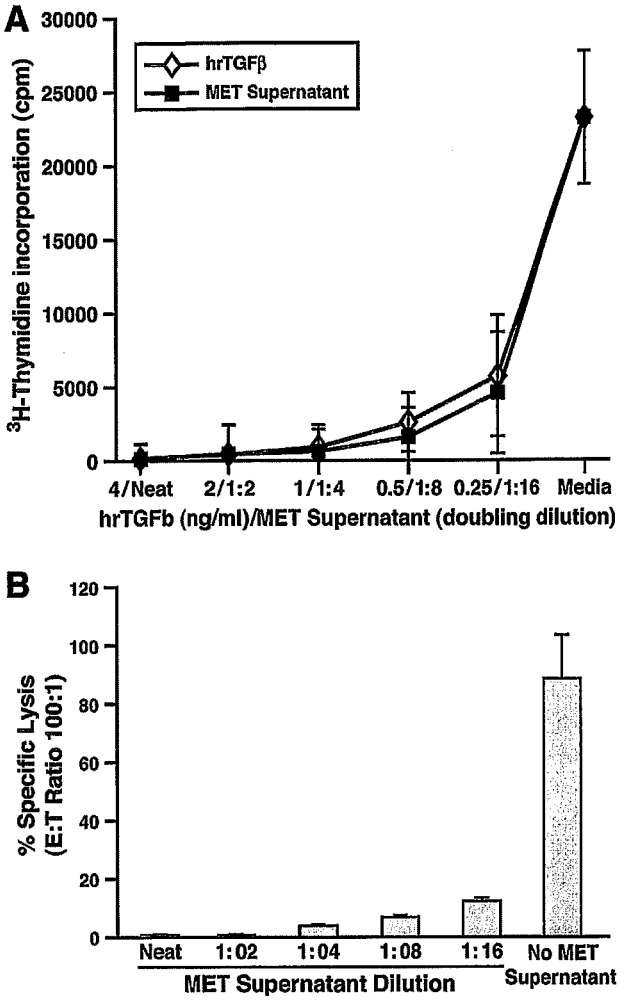

Figure 6. (A) Bioactive form of TGF-ß is secreted by MET tumor cells in culture. Supernatant derived from MET tumor cell culture was tested in a growth inhibition assay with MvlLu cells that are sensitive to TGF-ß inhibition. rHuTGF-ß in DMEM + Nutridoma serum supplement were used as standard (4, 2, 1, 0.5, 0.25, and 0.125 ngs/ml) and serial dilution of the activated supernatant was used as the test sample (neat to 1:16) MvlLu cells were prepared by resuspending at a concentration of 5×10^5 cells/ml in DMEM + Nutridoma serum supplement (no FBS). 100 uls (5×10^4 cells) of cells were added to wells containing the standard rHuTGF-ß or the supernatants. Cells were cultured for 24 h at 37°C in a 10% CO_2 incubator and 1 μCi of ^{3}H-thymidine was added to each well 16 h prior to harvesting. Data are presented as ^{3}H-thymidine incorporation in cpms. All assays were run in triplicate. (B) Supernatant derived from MET tumor cells inhibits cytolytic activity of MUC1-specific CTL. CTLs at 1×10^7 cells/ml in 100 uls were cultured with 100 uls of MET tumor cell supernatant (neat to 1:16 dilution) for 24 hours in a 96 well tissue culture plate. Cells were washed twice prior to being analyzed for lytic activity in a standard ^{51}Cr-release assay at an effector:target (E:T) ratio of 100:1 with the target cells being B16.MUC1 tumors. Titration of E:T ratio was observed in every ^{51}Cr-release CTL experiment, only E:T ratio of 100:1 is presented. Data is presented as % specific lysis.

not effective against the growing pancreatic tumor *in vivo*. To determine the fate of CTL within the growing tumor *in vivo*, we infused 12 week old MET mice with highly cytolytic MUC1-specific clonal CTLs, which were $CD8^+$ T cells expressing specific T cell receptor $V\beta5.1/2^+$ (Figure 7A, left panel). At time of infusion, MET mice have approximately 0.1–0.3 grams of tumor [3]. Two weeks post CTL infusion, pancreatic tumors were removed, tumor infiltrated lymphocytes (TILs) isolated, and percent cells that were double positive for CD8 and $V\beta5.1/2$ determined by flow cytometry (Figure 7A, central panel). As controls, pancreas tumor from MET mice that did not receive CTL infusion was used (Figure 7A, right panel). These control mice did not have T cells that were double positive for CD8 and $V\beta5.1/2$, indicating that the infused CTL enter the pancreas tumor and persist in the tumor for at least 2 weeks. We choose to take TILs at 2 weeks post infusion because in a model of mammary gland cancer, using CFSE (an *in vivo* tracking dye)-labeled CTL we observed that adoptively transferred CTL home to the lymph node and tumor site by 2 days post infusion and are no longer detectable by 21 days (unpublished data). We wanted to determine if the CTLs isolated from MET tumors were tolerant to MUC1 antigen. Tolerance is defined by accumulation of antigen-specific T cells, which are hypo-responsive to the antigen and are cytolytically inactive. We clearly show that the CTLs no longer proliferate to MUC1 antigen presented by syngeneic DC (Figure 7B) nor are they capable of lysing MUC1-expressing tumor cells *in vitro* (Figure 7C). Adding co-stimulatory factors such as anti-CD40 *in vitro* during T cell proliferation assay can reverse the T cell tolerance such that CTLs isolated from TILs can now proliferate to MUC1 antigen (Figure 7B). Anti-CD40 treatment completely restored CTL proliferation, whereas less effect was observed with murine IL-2 (Figure 7B). Isotype control antibodies did not restore proliferation (data not shown). Thus, we were able to demonstrate that, although functionally active CTLs were generated within the periphery of immunized mice, prolonged contact with tumor cells within the tumor environment makes them non-functional. Further analysis of the TIL population revealed the presence of T regulatory or suppressor cells that are defined by $CD4^+CD25^+$ surface markers. These $CD4^+CD25^+$ T cells were sorted, cultured for 24 hours at

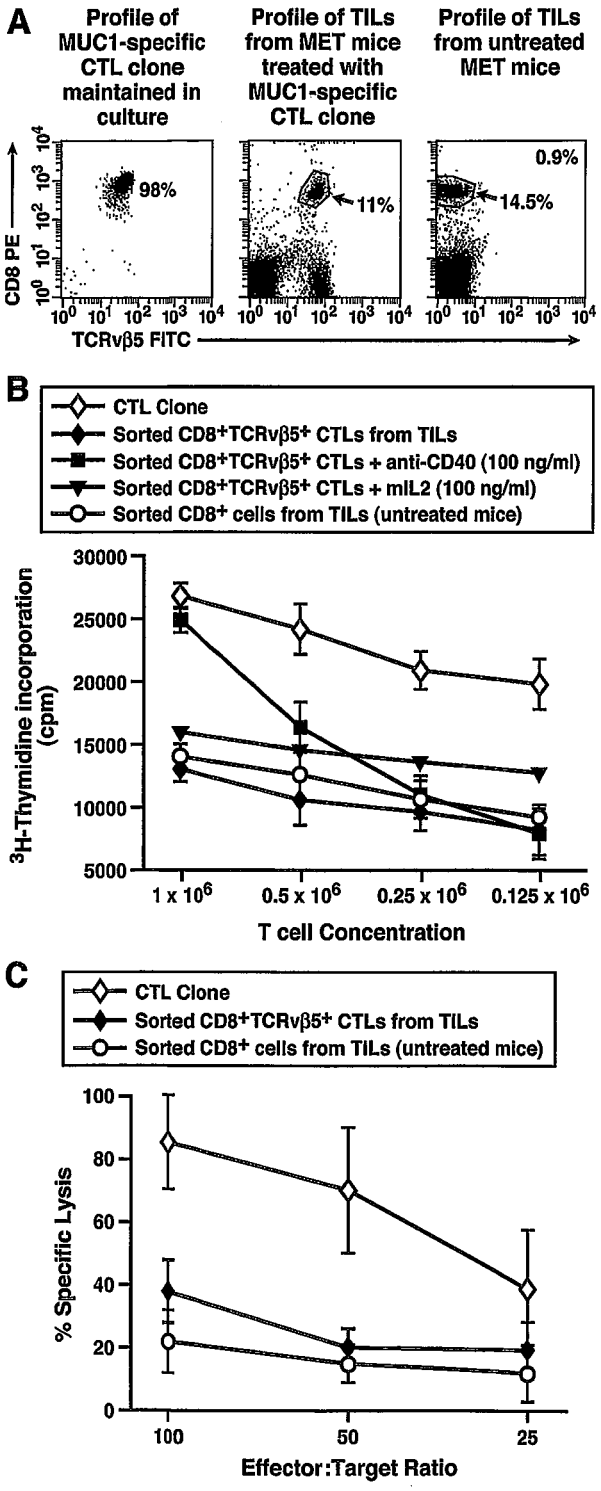

Figure 7. Adoptively transferred CTL become tolerant to MUC1 and are cytolytically inactive after encounter with MET tumor cells. TILs were isolated from tumors of MET mice that received adoptively transferred MUC1-specific CTL clone ($CD8^+/Vb5^+$ cells). (A) The $V\beta5^+/CD8^+$ cells were sorted 15 days post infusion from MET tumors (represented in the central panel). As a positive control, the CTL clone maintained *in vitro* was used (represented in the left panel) and as a negative control, $CD8^+$ T cells were sorted from TILs isolated from tumors of age matched MET mice that were not injected with the CTL clone (represented in the right panel). A box drawn around the cell population represents the sorted cells. CTL-infused MET mice have 11% of their TILs as $CD8^+V\beta5^+$ whereas control mice have 0.9% of their TILs double positive for CD8 and Vß5. Sorted cells were between 90–95% pure. Data representative of one mouse data is shown. The sorted cells were further analyzed for either proliferation in response to DCs pulsed with MUC1 peptide ± anti-CD40 or murine IL-2 (B) or cytotoxic activity against MUC1-expressing B16 melanoma target tumor cells (C). Three CTL-infused MET mice and 3 control MET mice were studied.

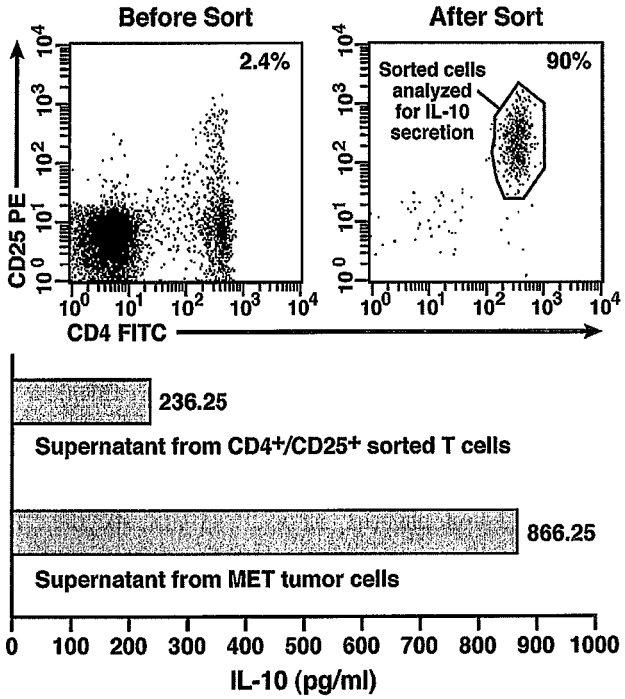

Figure 8. $CD4^+CD25^+$ double positive T regulatory cells were present in MET tumor infiltrate. (A) Unsorted TILs from MET tumors were phenotyped for presence of $CD4^+CD25^+$ double positive cell population and sorted by flow cytometry. Box with the arrow represents sorted population (2.4% of the total MET TIL population was $CD4^+CD25^+$). Sorted cells were 90% pure $CD4^+CD25^+$ T cells. (B) These T regulatory cells were cultured *in vitro* for 24 hours at 1×10^6 cells/ml and analyzed for IL-10 secretion by specific ELISA. MET tumor cell supernatant was also analyzed for IL-10 secretion in the same assay. IL-10 was present in both supernatant derived from T regulatory cells and MET tumor cells, although levels are much higher in the MET tumor supernatant.

37°C in complete DMEM media, supernatant collected and analyzed for IL-10 release. Figure 8 demonstrates that these immunoregulatory cells indeed secrete the immunosuppressive cytokine IL-10, which is known to cause CD8 and CD4 anergy [7,8]. Supernatant from MET tumor cells were also analyzed for presence of IL-10 in the same assay and showed moderate levels of IL-10 (Figure 8).

Discussion

In human cancer patients, the functional status of vaccine-induced, tumor antigen-specific CTL has been questioned due to its inability to inhibit tumor growth [9,10]. In addition, correlation between precursor CTL (pCTL) frequency and clinical outcome could not be established [8,9]. Stimulation of the pCTL with tumor-specific antigen can induce IFN-γ secretion *in vitro*, suggesting that the CTL retain antigen responsiveness [11] and should be capable of lysing tumor cells. However, recently it has been shown that IFN-γ expression may not be the optimal functional parameter to best describe the potential of effector cells [12]. Researchers have used perforin levels in the CTL as a marker for active CTL and combined that with levels of expression of CD27 (a marker for naïve T cells) and CD45RA (marker for effector T cells) to determine the maturation status of the CTL [12–15]. Despite the use of these markers, the standard immune monitoring post immunotherapy is still defined by (a) CTL effector function determined by IFN-γ secretion and ^{51}Cr-release assay and (b) phenotypic analysis determined by Ag-specific tetramer staining. We compared the immune responses that developed during treatment and at time of sacrifice. Our data demonstrate that MUC1-specific immunization elicits MUC1-tetramer reactive CTL that are functionally lytic *in vitro* and express intracellular IFN-γ, but fail to eradicate the spontaneous pancreatic tumors, which is what is observed in human studies. Similar phenomena have been shown in another spontaneous tumor model, the HER-2/neu transgenic mice that develop spontaneous focal mammary carcinomas and demonstrate immunological tolerance to the neu antigen. These mice also were able to elicit neu-specific T cells following neu-specific vaccination but were not protected from the developing mammary tumors [16,17].

Several tumor evasion mechanisms may be employed by the growing pancreas tumor to avoid recognition and killing by functional CTLs. In our previous work, we established that the tumor cells are heterogeneous in nature and can modulate expression of MUC1-epitopes as well as fas ligand epitopes and express high levels of TGF-ß, an immunosuppressive cytokine [3]. In the present study, we demonstrate that cytolytically active CTL become inactive when cultured in the presence of MET tumor cell supernatant (Figure 6B) and that the MET tumor cells secrete a bioactive form of TGF-ß that may be one of the factors responsible for down-regulation of CTL activity (Figure 6A). Other factors secreted by MET cells include IL-10 (Figure 8). Preliminary data showed that treatment of MET mice with neutralizing antibody to TGF-ß did not result in tumor regression (data not shown) suggesting a role for other factors in immune evasion. In addition to immunosuppressive factors released by MET tumor cells *in vitro*, MET tumor cells down-regulate their MHC class I molecule (Table 1) *in vivo* as tumors progress, thus avoiding recognition by class I-restricted $CD8^+$ CTL. We also found immune regulatory T cells that secrete IL-10 in the pancreas tumor microenvironment and may further contribute to the induction of CTL tolerance and/or anergy (Figure 8). These regulatory T cells can inhibit proliferation and function of other T cells and are major players in induction of CD4 and CD8 T cell tolerance [18–22]. Thus, taken together our data suggest that a combination of factors may be employed by the MET tumor cells to evade CTL killing as well as down-regulate CTL function.

It is reported in the literature that CTLs that are detectable in the peripheral lymphoid organs but that do not migrate to the site of the tumor in sufficient numbers may not be active

in destroying the tumor target tissue [23]. Therefore, the fundamental question remains whether the MUC1-specific CTLs in the MET mice infiltrate the pancreas tumor bed and remain active within the solid tumor. To determine the fate of these MUC1-specific CTLs within the growing pancreas tumor, we adoptively transferred functionally active CTLs into MET mice *in vivo* and observed that the CTLs do infiltrate the tumor bed and after an initial period of proliferation, become tolerized to MUC1 antigen and are rendered cytolytically inactive (Figure 7A). This strongly indicates that exposure of CTL to the tumor microenvironment can down-regulate their proliferation and function. Maintenance of the activated state of CTLs is one of the major requirements for effective cancer immunotherapy. This activated state is strongly influenced by inflammatory stimuli as well as the action of $CD4^+$ T helper (Th) cells. Th and CTLs must recognize antigens presented on the same antigen presenting cell (APC) [24,25] and the interaction of Th and APC is sufficient to convert the APC to a state that allows priming and maintenance of CTL. Our data show that treatment with L-IL-2 alone leads to lower tumor burden but not eradication of spontaneous tumors in MET mice (Figure 5). One possibility is that the L-IL-2 may activate the natural killer cells that recognize MHC class I-negative tumor cells. Another possibility is that exogenous L-IL-2 can activate the naturally occurring low affinity MUC1-specific or other TAA-specific CTLs that already exist in the tumor bearing mice and make them effective against the tumor. On the other hand, treatment with MUC1 peptide and liposomes may cause over-activation and induce tolerance of the T cells that ultimately leads to inactivation of effector T cells such that anti-tumor response is interrupted. This result points us to the direction of providing necessary and effective help for the CTL to overcome immunization-induced tolerance or tumor-induced inactivation. In recent years, there is growing evidence that cross-linking of co-stimulatory molecules such as CD40 expressed on APC and CD40L expressed on Th cells as well as OX40 expressed on activated Th cells and OX40L expressed on APC can reverse established T cell tolerance. Both of these molecules are members of the TNF receptor family and signaling through these molecules promotes helper T cell expansion and restores normal functionality of the tumor-specific cytotoxic T cells. Previous data in the literature highlight the potent co-stimulatory capacity of OX40 and CD40, which make them targets for therapeutic intervention in cancer [26–31]. In Figure 7B, we demonstrate that the down-regulation of CTL proliferation (post exposure to MET tumors *in vivo*) to MUC1 peptide-pulsed DC was completely restored by cross-linking CD40 co-stimulatory molecules with specific antibody *in vitro*. Addition of murine IL-2 to these cultures had a beneficial effect although not as significant as treatment with CD40 antibodies. These experiments were conducted *in vitro* and similar experiments are being repeated *in vivo* to determine if an anti-tumor response could be achieved in MET mice with these antibodies and whether CTL activity can be maintained in the presence of the growing pancreas tumor.

The possibility that MUC1-specific CTL can eradicate $MUC1^+$ cells, allowing outgrowth of MUC1 non-expressing cells in the tumor cannot be ignored. In Figure 5, we observed negligible MUC1 staining in pancreatic tumor sections from MET mice as compared to normal pancreas and as compared to dysplastic acinar cell carcinoma or microadenomas [3]. However, considering that the CTLs become tolerized within the tumor microenvironment, it is highly unlikely that the CTLs were active against $MUC1^+$ tumor cells, especially because there was no difference between immunized versus non-immunized MET tumor sections, whereas highly lytic CTLs were detected in immunized MET mice as compared to non-immunized controls. Thus, once again it argues for the possibility of antigenic modulation of MUC1 in which the glycosylation status of MUC1 is altered, thereby hindering antibody reactivity as well as CTL recognition.

In summary, our data suggest that the MUC1-specific CTLs are cytolytically active and are capable of eradicating injectable $MUC1^+$ tumor cells *in vitro* and *in vivo* but that the tumor microenvironment is non-conducive to CTL proliferation and killing. The tumor cells utilize a combination of immune-evasion mechanisms both to down-regulate CTL function and avoid recognition. We also suggest that secondary immunization with antibodies to co-stimulatory molecules such as CD40 may be a useful therapeutic strategy that may provide necessary help to control induction of CTL tolerance and maintain its lytic activity, thus leading to an anti-tumor response. The MET mice appropriately mimic the human situation and serve as an excellent model system in which to study the mechanisms that are involved in inactivation of CTL function as well as to study tolerance versus immunity post vaccination. The tumors arise in an appropriate tissue background and hormonal and stromal milieu as well as in the context of a viable immune system. Future studies utilizing this mouse model may facilitate the design of appropriate immunotherapeutic strategies as well as immune monitoring parameters that may correlate with clinical outcome.

Materials and methods

Mouse model MET

MUC1.Tg mice are bred with oncogene-expressing mice that spontaneously develop tumors of the pancreas and are designated as MET [3]. MUC1.Tg mice were developed in our laboratory [2]. ET mice were obtained as a kind gift from Dr. Judith M. Tevethia (University of Pennsylvania, Hershey, PA) [32]. All mice are congenic on C57BL/6 background at backcross ≥ 10 [33]. All mice were bred and maintained in specific pathogen free conditions in the Mayo Clinic Scottsdale Natalie Schafer Transgenic Animal Facility. All experimental procedures were conducted according to IACUC guidelines.

PCR screening

PCR was used to routinely identify MUC1 and ET positive mice in the colony. PCR was carried out as previously described [2,32]. The primer pairs for MUC1.Tg are 5′-CTTGCCAGCCATAGCACCAAG-3′ (bp. 745 to 765) and 5′-CTCCACGTCGTGGACATTGATG-3′ (bp. 1086 to 1065). Primer pairs for ET are 5′-GCTCCTTTAACCCACCTG-3′ (bp. 4055 to 4072) and 5′-CCAACCTATGGAACTGATGAATG-3′ (bp. 4546 to 4568). The amplification program for MUC1 consisted of one cycle of 5 min at 95°C and 40 cycles of 30 sec at 95°C, 1 min at 61°C, and 30 sec at 72°C followed by one cycle of 10 min at 72°C. The amplification for ET PCR reaction is as above with the exception of annealing temperature of 52°C. The PCR product of each reaction was analyzed by size fractionation through a 1% agarose gel. Amplification of MUC1 resulted in approximately a 500 bp fragment, and of ET in a 491 bp fragment.

Cell lines

B16 melanoma cells transfected with either full-length human MUC1 gene (B16.MUC1) or neomycin resistance gene (B16.neo) were used as targets for CTL assays. These cell lines were originally provided by Dr. Tony Hollingsworth (Eppley Cancer Center, University of Nebraska). B16.MUC1 and B16.neo were maintained in DMEM media with 10% FBS, immglutamax, penicillin (50 units/ml) and streptomycin (50 ugs/ml), supplemented with 300 ugs/ml G418. One day prior to conducting the ^{51}Cr-release assay, cells were treated with 5 ngs/ml IFN-γ (Pharmingen, San Diego, CA). Cells were routinely tested by flow cytometry for the presence of MUC1 and MHC class I. MvlLu cells, a mink lung epithelial cell line, was a kind gift from Dr. E. Akporiaye (University of Arizona, Tucson, AZ). These cells were maintained in DMEM supplemented with 10% FBS, 1 mM glutamax, penicillin (50 units/ml) and streptomycin (50 ugs/ml). FGK 45.5 hybridoma cell supernatant (ATCC, Rockville, MD) was used as a source of CD40 antibody. These cell lines were maintained in the Immunology Core at Mayo Clinic Scottsdale and supernatant immunoglobulins were purified and protein concentration was determined prior to use.

Analysis of MET tumors

The entire pancreas was dissected free of fat and lymph nodes, fixed in methacarn followed by 70% ethanol, air-dried and weighed. Tumor weights plotted represent individual animal data at time of sacrifice. Mice were carefully observed for signs of ill-health, including lethargy, abdominal distention, failure to eat or drink, marked weight loss, and hunched posture.

Immunohistochemistry

Tumors were obtained from control and immunized MET mice at time of sacrifice. Tumors were fixed in methacarn followed by 70% ethanol, paraffin embedded, and sectioned for immunohistochemical analysis. MUC1 antibodies used were B27.29, a mouse monoclonal antibody with epitopes in the tandem repeat extracellular domain of MUC1 [34]. B27.29 is specific for human MUC1 and does not cross react with mouse Muc1. HRP-conjugated B27.29 was obtained from Biomira, Inc., Edmonton, Canada. Antibody staining was blocked with the appropriate peptide.

Adoptive transfer of MUC1-specific CTL and isolation of tumor infiltrated lymphocytes (TILs)

At 12 weeks of age, MET mice received tail vein injection of MUC1-specific CTL clone (2×10^7 cells/mouse/150 uls). MET CTL clonal cells were CD8$^+$ T cells that expressed TCR-Vß5.1/2. Fifteen days post injection, TILs were isolated from MET tumors by manually dissociating the tumor mass with a sterile scalpel, followed by dissociation in 0.5 mM EDTA for 1 hour in a 37°C incubator with constant shaking. Dissociated cells were passed through a nylon sieve and then separated by Ficoll-Hypague (density: 1.077 ± 0.001 g/ml, Invitrogen Corp., Carlsbad, CA) gradient centrifugation. The buffy coat was removed, washed and counted for further analysis. CD8$^+$Vß5.1/2$^+$ from experimental MET TILs and CD8$^+$ CTL from control MET TILs were isolated by sorting using FACs Vantage (BD instruments, San Diego, CA). Sorted cells were further analyzed for their proliferative capacity to MUC1 TR antigen and cytolytic activity against MUC1-expressing tumor cells. Other sorts from TILs included T cells that were double-positive for CD4$^+$CD25$^+$.

T cell proliferation in response to MUC1 TR peptide

Sorted cells from CTL-infused and control MET mice (various concentrations as illustrated in Figure 7B) were cultured for 5 days in the presence of irradiated dendritic cell (1×10^5/ml) pulsed with 10 μgs/ml MUC1 TR peptide (TAPPAHGVTSAPDTRPAPGSTAPP). MUC1-specific CTL clone was used as a positive control and DC without TILs was used as the negative control. Proliferation was determined by measuring ^{3}H-thymidine incorporation using the beta plate counter (Packard Instruments, Perkin Elmer LifeSciences, Boston MA). In some experiments, anti-CD40 or mouse IL-2 (Pharmingen, San Diego, CA) were added to the co-culture at 100 ngs/ml concentration. Isotype control antibodies at the same concentration were used as negative controls in these assays (data not shown).

CTL assays

Determination of mature CTL activity was performed using a standard ^{51}Cr-release method with no *in vitro* peptide stimulation. Splenocytes from immunized and unimmunized MET mice were harvested by passing through a nylon mesh followed by lysis of red blood cells using Pharmlyze (0.45% ammonium chloride solution purchased from Pharmingen (San

Diego, CA)). Splenocytes or TILs isolated from MET tumors were used as effector cells. The target cell line, B16.MUC1, expressed high levels of MUC1 as determined by flow cytometric analysis using antibodies to the MUC1 conjugated to FITC (Pharmingen, San Diego, CA). For better presentation of MUC1 antigen, B16.MUC1 target cells were treated with 5 ngs/ml IFN-γ one day prior to the assay to up regulate MHC class I surface expression. Specific ^{51}Cr-release was calculated according to the following formula: (experimental CPM-spontaneous release CPM/maximum release CPM-spontaneous release CPM) $\times$ 100. Spontaneous release in all experiments was less than 15% of maximum release. In some experiments, B16.neo transfected cells were used as control target cells with lysis of <5% (data not shown). In some experiments sorted CTLs from CTL-infused and control MET mice were used as effector cells.

Flow cytometry and cell sorting

Single cells from peripheral blood lymphocytes (PBLs) collected from immunized and unimmunized MET mice at various times post immunization were analyzed by two color immunofluorescence for intracellular IFN-γ expression. Intracellular cytokine levels were determined after cells were treated with brefeldin-A [also called Golgi-Stop (Pharmingen)] according to the manufacturer's recommendation (4 uls/1.2 $\times$ 10^7 cells/6 mls for 3 h at 37°C prior to staining). Cells were surface labeled with CD4 and CD8 antibodies conjugated to FITC prior to permeabilizing with the Pharmingen permeabilization kit (Cat # 554722, containing 0.005% saponin and 4% formaldehyde) and staining with anti-IFN-γ conjugated to PE. Tumor cells from freshly dissociated MET tumors were stained with fluorescently labeled anti-pan-cytokeratin (FITC) and anti-MHC class I H2-D^b and H2-K^b (PE). All fluorescently labeled antibodies were purchased from Pharmingen except anti-pan-cytokeratin, clone C-11, purchased from Sigma, St. Louis, MO. Flow cytometric analysis was done on Beckton Dickinson FACscan using the Cell Quest program. TILs isolated from MET tumors were surface labeled with CD25 conjugated to PE and CD4 conjugated to FITC. $CD4^+/CD25^+$ double positive T cell population was isolated by cell sorting using FACs Vantage (BD Instruments).

IL-10 ELISA

$CD4^+/CD25^+$ double positive T cells were cultured for 24 h in DMEM complete media at concentration of 1–2 $\times$ 10^6/ml. Supernatant was assessed for the presence of IL-10 using a murine IL-10 ELISA kit purchased from Biosource (Caramillo, CA). MET tumor cell supernatant was also analyzed for IL-10.

Mv1Lu cell growth inhibition assay

The growth inhibition assay was performed as described [38]. First, latent TGF-ß in supernatant from confluent MET tumor cell culture was activated by adjusting the pH to below 3 with 12 M HCl and incubating at RT for 1 h. The supernatant was then neutralized to pH 7 with 10 M NaOH. rHuTGF-ß was purchased from R&D Systems (Minneapolis, MN) and standard was prepared in DMEM + Nutridoma serum supplement. rHuTGF-ß was prepared at 8 ngs/ml stock solution and serially diluted 1:2 to obtain standards of 4, 2, 1, 0.5, 0.25, and 0.125 ngs/ml. Serial dilution of the activated supernatant was also prepared from neat to 1:16 and 100 uls added to each well of a 96 well plate. Mv1Lu cells were prepared by resuspending at a concentration of 5 $\times$ 10^5 cells/ml in DMEM + Nutridoma serum supplement (no FBS). 100 uls (5 $\times$ 10^4 cells) were added to wells containing the standard rHuTGF-ß or the supernatants. Cells were cultured for 24 h at 37°C in a 10% CO_2 incubator. 1 μCi of ^{3}H-thymidine was added to each well and incubated for 16 h. Cells were harvested and incorporated radioactivity was measured using a beta plate counter. All assays were run in triplicate.

MUC1-tetramer staining

MHC class I H-$2D^b$ tetramers containing MUC1 TR APGSTAPPA peptide were created by Dr. Larry Pease at Mayo Clinic Rochester. PBLs were stained with 0.1 mgs/ml MUC1-tetramer (directly conjugated to phycoerythrin) for 1 hour on ice. To confirm specificity, a H-$2D^b$ tetramer containing an irrelevant peptide was used as control ($VP2_{121-130}$). The cells were then stained for 15 minutes with CD8 and CD4 antibodies conjugated to FITC prior to analyzing by two-color flow cytometry. Flow cytometric analysis was done on Beckton Dickinson FACscan using the Cell Quest program.

Preparation of dendritic cell-pulsed liposomal MUC1 TR lipopeptide

DCs were derived from C57BL/6 bone marrow cells according to the method described [35]. Briefly, bone marrow cells were flushed from tibia and femur and red blood cells were lysed with ammonium chloride. Cells were cultured in DMEM with 10% fetal bovine serum, 1% glutamax, 50 U/ml penicillin, 50 ugs/ml streptomycin (DMEM complete medium), supplemented with 10 U/ml murine GM-CSF (Pharmingen) and 10 U/ml murine IL-4 (Pharmingen). On day 7, adherent cells were fed with fresh DMEM complete media supplemented with GM-CSF and IL-4 at the same concentration. Between days 10 and 14, we obtained approximately 85 to 90% cells that showed DC phenotype by flow cytometry. DC were fed with MUC1 TR lipopeptide that were enclosed in liposomes according to the method provided by Biomira, Inc. [36]. Briefly, 2 mls of the liposomal MUC1 TR formulation was fed to 200 $\times$ 10^6 DC in a total volume of 20 mls, 24 hours prior to injection. Mice were injected i.p. with 1 $\times$ 10^6 MUC1 TR pulsed DC per mouse in 200 ul volume. For T cell proliferation assays, DCs were pulsed with naked 25 mer MUC1 TR peptide at 10 ngs/ml.

Vaccination strategy

The vaccine formulation consisted of a lipid derivative of a 25 mer MUC1 TR peptide STAPPAHGVTSAPDTR-PAPGSTAPP) which was incorporated into liposomes along with Lipid A as adjuvant. The vaccine was supplied as a sterile powder formulated at Biomira, Inc. (Edmonton, AB, Canada) by a proprietary method. Upon reconstitution with sterile saline for injection, it contained 400 ug/ml of MUC1 lipopeptide, 200 ug/ml of Lipid A (Avanti Polar Lipids, Inc. Alabaster, AL, USA) and 20 mg/ml of carrier lipids in multilamellar vesicles with a mean particle size of 2–3 μm. For the preparation of pulsed dendritic cells, particle size of the vaccine was reduced to <200 nm by ultrasonication. Randomized preclinical trials were performed in MET mice starting at 3 weeks of age.

Five arms in the study include: (i) liposomal MUC1 TR lipopeptide (L-MUC1-TR) (200 ugs/mouse/250 uls s.c.) + L-IL-2 (20,000 Units/mouse/100 uls i.p.), (ii) L-MUC1-TR, (iii) L-IL-2 [37], (iv) empty liposomes, and (v) no treatment. We compared the immune responses that developed during treatment and used survival and tumor burden as the endpoints for determining the clinical effectiveness of the vaccine. A schematic of the immunization protocol is shown in Figure 1.

Statistical analysis

P values are from the one-way ANOVA *F* test for comparing the treatment groups simultaneously and from the pair-wise contrasts from a one way ANOVA model.

Acknowledgments

We would like to acknowledge the following people for their contributions to this project: Biomira, Inc. (Edmonton, Canada) for generously providing MUC1 TR lipopeptides, Dr. Larry Pease for providing the MUC1 tetramers, Dr. Judith Tevethia for kindly providing the original breeding stock of the ET mice, Dr. E. Akporiaye for kindly providing the Mv1Lu cells, Marv Ruona for the preparation of figures, Carol Williams for assistance with preparation and submission of the manuscript, and Suresh Savarirayan and the animal care technicians for excellent animal care.

This work was funded by the Mayo Comprehensive Cancer Center (NCI CA15083), the Mayo Foundation, The Susan G. Komen Breast Cancer Foundation (PM), DOD Breast Cancer Research Program DAMD17-01-1-0318 (SJG) and Biomira Inc., Edmonton, Canada.

References

1 Greenlee RT, Murray T, Bolden S, Wingo PA, Cancer statistics, *CA Cancer J* **50**, 7–33 (2000).
2 Rowse GJ, Tempero RM, VanLith ML, Hollingsworth MA, Gendler SJ, Tolerance and immunity to MUC1 in a human MUC1 transgenic murine model, *Cancer Res* **58**, 315–21 (1998).
3 Mukherjee P, Ginardi AR, Madsen CS, Sterner CJ, Adriance MC, Tevethia MJ, Gendler SJ, Mice with spontaneous pancreatic cancer naturally develop MUC1-specific CTLs that eradicate tumors when adoptively transferred, *J Immunol* **165**, 3451–60 (2000).
4 Mukherjee P, Ginardi AR, Tinder TL, Sterner CJ, Gendler SJ, MUC1-specific CTLs eradicate tumors when adoptively transferred *in vivo*, *Clin Can Res* **7**, 848s–55s (2001).
5 Ridge JP, Fuchs EJ, Matzinger P, Neonatal tolerance revisited: Turning on newborn T cells with dendritic cells, *Science* **271**, 1723–6 (1996).
6 Sikut R, Sikut A, Zhang K, Baeckstrom D, Hansson GC, Reactivity of antibodies with highly glycosylated MUC1 mucins from colon carcinoma cells and bile, In *Tumor Biology*, edited by Rye PD, Price MR (S. Karger Medical and Scientific Publishers, 1998), pp. 122–6.
7 Papac RJ, Spontaneous regression of cancer, *Cancer Treat Rev* **22**, 395–423 (1996).
8 Rosenberg SA, Yang JC, Schwartzentruber DJ, Hwu P, Marincola FM, Topalian SL, Restifo NP, Dudley ME, Schwarz SL, Spiess PJ, et al., Immunologic and therapeutic evaluation of a synthetic peptide vaccine for the treatment of patients with metastatic melanoma, *Nat Med* **4**, 321–7 (1998).
9 Lee KH, Wang E, Nielsen MB, Wunderlich J, Migueles S, Connors M, Steinberg SM, Rosenberg SA, Marincola FM, Increased vaccine-specific T cell frequency after peptide-based vaccination correlates with increased susceptibility to *in vitro* stimulation but does not lead to tumor regression, *J Immunol* **163**, 6292–300 (1999).
10 Marchand M, Weynants P, Rankin E, Arienti F, Belli F, Parmiani G, Cascinelli N, Bourlond A, Vanwijck R, Humblet Y, et al., Tumor regression responses in melanoma patients treated with a peptide encoded by gene MAGE-3, *Int J Cancer* **63**, 883–5 (1995).
11 Monsurro V, Nielsen MB, Perez-Diez A, Dudley ME, Wang E, Rosenberg SA, Marincola FM, Kinetics of TCR use in response to repeated epitope-specific immunization, *J Immunol* **166**, 5817–25 (2001).
12 Appay V, Nixon DF, Donahoe SM, Gillespie GM, Dong T, King A, Ogg GS, Spiegel HM, Conlon C, Spina CA, et al., HIV-specific CD8(+) T cells produce antiviral cytokines but are impaired in cytolytic function, *J Exp Med* **192**, 63–75 (2000).
13 Gamadia LE, Rentenaar RJ, Baars PA, Remmerswaal EB, Surachno S, Weel JF, Toebes M, Schumacher TN, ten Berge IJ, van Lier RA, Differentiation of cytomegalovirus-specific CD8(+) T cells in healthy and immunosuppressed virus carriers, *Blood* **98**, 754–61 (2001).
14 Hamann D, Kostense S, Wolthers KC, Otto SA, Baars PA, Miedema F, van Lier RA, Evidence that human CD8+CD45RA+CD27-cells are induced by antigen and evolve through extensive rounds of division, *Int Immunol* **11**, 1027–33 (1999).
15 Nagai M, Kubota R, Greten TF, Schneck JP, Leist TP, Jacobson S, Increased activated human T cell lymphotropic virus type I (HTLV-1) Tax11-19-specific memory and effector CD8+ cells in patients with HTLV-I-associated myelopathy/tropical spastic paraparesis: Correlation with HTLV-I provirus load, *J Infect Dis* **183**, 197–205 (2001).
16 Reilly RT, Gottlieb MB, Ercolini AM, Machiels JP, Kane CE, Okoye FI, Muller WJ, Dixon KH, Jaffee EM, HER-2/neu is a

tumor rejection target in tolerized HER-2/neu transgenic mice, *Cancer Res* **60**, 3569–76 (2000).
17 Reilly RT, Machiels JP, Emens LA, Ercolini AM, Okoye FI, Lei RY, Weintraub D, Jaffee EM, The collaboration of both humoral and cellular HER-2/neu-targeted immune responses is required for the complete eradication of HER-2/neu-expressing tumors, *Cancer Res* **61**, 880–3 (2001).
18 Nukina M, Mochida Y, Sakaguchi S, Sakaguchi G, Purification of Clostridium botulinum type G progenitor toxin, *Zentralbl Bakteriol Mikrobiol Hyg [A]* **268**, 220–7 (1988).
19 Papiernik M, de Moraes ML, Pontoux C, Vasseur F, Penit C, Regulatory CD4 T cells: Expression of IL-2R alpha chain, resistance to clonal deletion and IL-2 dependency, *Int Immunol* **10**, 371–8 (1998).
20 Read S, Mauze S, Asseman C, Bean A, Coffman R, Powrie F, CD38+CD45RB(low) CD4+ T cells: A population of T cells with immune regulatory activities *in vitro*, *Eur J Immunol* **28**, 3435–47 (1998).
21 Smith H, Sakamoto Y, Kasai K, Tung KS, Effector and regulatory cells in autoimmune oophoritis elicited by neonatal thymectomy, *J Immunol* **147**, 2928–33 (1991).
22 Suri-Payer E, Amar AZ, Thornton AM, Shevach EM, CD4+CD25+ T cells inhibit both the induction and effector function of autoreactive T cells and represent a unique lineage of immunoregulatory cells, *J Immunol* **160**, 1212–8 (1998).
23 van Stipdonk MJ, Lemmens EE, Schoenberger SP, Naive CTLs require a single brief period of antigenic stimulation for clonal expansion and differentiation, *Nat Immunol* **2**, 423–9 (2001).
24 Bennett SR, Carbone FR, Karamalis F, Miller JF, Heath WR, Induction of a CD8+ cytotoxic T lymphocyte response by cross-priming requires cognate CD4+ T cell help, *J Exp Med* **186**, 65–70 (1997).
25 Husmann LA, Bevan MJ, Cooperation between helper T cells and cytotoxic T lymphocyte precursors, *Ann NY Acad Sci* **532**, 158–69 (1988).
26 Akiba H, Oshima H, Takeda K, Atsuta M, Nakano H, Nakajima A, Nohara C, Yagita H, Okumura K, CD28-independent costimulation of T cells by OX40 ligand and CD70 on activated B cells, *J Immunol* **162**, 7058–66 (1999).
27 Bansal-Pakala P, Jember AG, Croft M, Signaling through OX40 (CD134) breaks peripheral T-cell tolerance, *Nat Med* **7**, 907–12 (2001).
28 Bennett SR, Carbone FR, Karamalis F, Flavell RA, Miller JF, Heath WR, Help for cytotoxic-T-cell responses is mediated by CD40 signalling, *Nature* **393**, 478–80 (1998).
29 Gramaglia I, Jember A, Pippig SD, Weinberg AD, Killeen N, Croft M, The OX40 costimulatory receptor determines the development of CD4 memory by regulating primary clonal expansion, *J Immunol* **165**, 3043–50 (2000).
30 Gramaglia I, Weinberg AD, Lemon M, Croft M, Ox-40 ligand: A potent costimulatory molecule for sustaining primary CD4 T cell responses, *J Immunol* **161**, 6510–7 (1998).
31 Maxwell JR, Weinberg A, Prell RA, Vella AT, Danger and OX40 receptor signaling synergize to enhance memory T cell survival by inhibiting peripheral deletion, *J Immunol* **164**, 107–12 (2000).
32 Tevethia MJ, Bonneau RH, Griffith JW, Mylin L, A simian virus 40 large T-antigen segment containing amino acids 1 to 127 and expressed under the control of the rat elastase-1 promoter produces pancreatic acinar carcinomas in transgenic mice, *J Virol* **71**, 8157–66 (1997).
33 Silver LM, Laboratory mice, In *Mouse Genetics Concepts and Applications* (Oxford University Press, 1995), pp. 32–61.
34 Price MR, Rye PD, Petrakou E, Murray A, Brady K, Imai S, Haga S, Kiyozuka Y, Schol D, Meulenbroek MF, et al., Summary report on the ISOBM TD-4 Workshop: Analysis of 56 monoclonal antibodies against the MUC1 mucin (San Diego, California, 1996) *Tumour Biol* **19**, 1–20 (1998).
35 Inaba K, Inaba M, Romani N, Aya H, Deguchi M, Ikehara S, Muramatsu S, Steinman RM, Generation of large numbers of dendritic cells from mouse bone marrow cultures supplemented with granulocyte/macrophage colony-stimulating factor, *J Exp Med* **176**, 1693–702 (1992).
36 Guan HH, Budzynski W, Koganty RR, Krantz MJ, Reddish MA, Rogers JA, Longenecker BM, Samuel J, Liposomal formulations of synthetic MUC1 peptides: Effects of encapsulation versus surface display of peptides on immune responses, *Bioconjug Chem* **9**, 451–8 (1998).
37 Boni LT, Batenjany MM, Neville ME, Guo Y, Xu L, Wu F, Mason JT, Robb RJ, Popescu MC, Interleukin-2-induced small unilamellar vesicle coalescence, *Biochim Biophys Acta* **1514**, 127–38 (2001).
38 Maeda H, Tsuru S, Shiraishi A, Improvement of macrophage dysfunction by administration of anti-transforming growth factor-beta antibody in EL4-bearing hosts, *Jpn J Cancer Res* **85**, 1137–43 (1994).

Received 19 July 2002; revised 19 August 2002;
accepted 30 August 2002

Journal of Immunotherapy
26(1):47–62 © 2003 Lippincott Williams & Wilkins, Inc., Philadelphia

Mucin 1-Specific Immunotherapy in a Mouse Model of Spontaneous Breast Cancer

*Pinku Mukherjee, *Cathy S. Madsen, *Amelia R. Ginardi, *Teresa L. Tinder, †Fred Jacobs, †Joanne Parker, †‡Babita Agrawal, †B. Michael Longenecker, and *Sandra J. Gendler

**Department of Biochemistry and Molecular Biology, Mayo Clinic Scottsdale, Scottsdale, Arizona, U.S.A.; †Biomira, Incorporated, Edmonton; ‡Current address: University of Alberta, Department of Surgery, Alberta, Canada.*

Summary: Human mucin 1 (MUC1) is an epithelial mucin glycoprotein that is overexpressed in 90% of all adenocarcinomas including breast, lung, pancreas, prostate, stomach, colon, and ovary. MUC1 is a target for immune intervention, because, in patients with solid adenocarcinomas, low-level cellular and humoral immune responses to MUC1 have been observed, which are not sufficiently strong to eradicate the growing tumor. The hypothesis for this study is that enhancing MUC1-specific immunity will result in antitumor immunity. To test this, the authors have developed a clinically relevant breast cancer model that demonstrates peripheral and central tolerance to MUC1 and develops spontaneous tumors of the mammary gland. In these mice, the authors tested a vaccine formulation comprised of liposomal-MUC1 lipopeptide and human recombinant interleukin-2. Results indicate that when compared with untreated mice, immunized mice develop T cells that express intracellular IFN-γ, are reactive with MHC class I H-2D^b/MUC1 tetramer, and are cytotoxic against MUC1-expressing tumor cells in vitro. The presence of MUC1-specific CTL did not translate into a clinical response as measured by time of tumor onset, tumor burden, and survival. The authors demonstrate that some of the immune-evasion mechanisms used by the tumor cells include downregulation of MHC-class I molecule, expression of TGF-β2, and decrease in IFN-γ -expressing effector T cells as tumors progress. Finally, utilizing an injectable breast cancer model, the authors show that targeting a single tumor antigen may not be an effective antitumor treatment, but that immunization with dendritic cells fed with whole tumor lysate is effective in breaking tolerance and protecting mice from subsequent tumor challenge. A physiologically relevant spontaneous breast cancer model has been developed to test improved immunotherapeutic approaches. **Key Words:** Immune evasion mechanisms—MUC1-specific cytotoxic T lymphocytes—Spontaneous mouse models of cancer—Tolerance—Transgenic mice.

Human cancers frequently express abnormal or altered self-proteins that are potentially immunogenic and trigger immune recognition. Low-level humoral and cellular immune responses to several antigens, including mucin 1 (MUC1), HER2/neu, p53, and PSA, are present in a significant proportion of patients with early and late stage cancer. It is important to determine how to obtain an effective immune response, since the native immune responses fail to eradicate tumors. In this study, human MUC1 is the tumor antigen of choice, as it is widely expressed on most solid adenocarcinomas. Although MUC1 is a self-molecule that is normally expressed on epithelial cells lining ducts and glands at low levels, it is a target for immunotherapy because it is significantly altered in expression during tumorigenesis. There is a

Received March 26, 2002; accepted September 17, 2002.
Address correspondence and reprint requests to Sandra J. Gendler, Mayo Clinic Scottsdale, S.C. Johnson Medical Research Center, 13400 East Shea Boulevard, Scottsdale, AZ 85259, U.S.A.; e-mail: gendler.sandra@mayo.edu

B16.MUC1 as target cells. In some experiments, B16.neo cells were used as control target cells.

Flow Cytometry

Single cells from peripheral blood lymphocytes (PBLs) collected from immunized and nonimmunized MMT mice at various times after immunization were analyzed by two-color flow cytometry for lymphocyte activation markers and intracellular cytokines. This included early and late surface activation markers, CD69 and CD25 (IL2-R) on $CD4^+$ and $CD8^+$ T cells. Intracellular cytokine levels were determined after cells were treated with brefeldin-A (Golgi-Stop; Pharmingen) according to the manufacturer's recommendation (4 μL/1.2 × 10^7 cells/6 mL for 3 hours at 37°C before staining). Cells were surface labeled with CD4, CD8, or CD11c antibodies before permeabilizing with the Pharmingen permeabilization kit (Cat #554722, containing 0.005% saponin and 4% formaldehyde) and staining for intracellular IFN-γ, IL-2, IL-4, IL-5, IL-10, or IL-12. Tumor cells from freshly dissociated MMT tumors were stained with fluorescently labeled antipan-cytokeratin and anti-MHC class I $H\text{-}2D^b$ and $H\text{-}2K^b$. All fluorescently labeled antibodies were purchased from Pharmingen except for antipan-cytokeratin, clone C-11, purchased from Sigma (St. Louis, MO, U.S.A.). Flow cytometric analysis was done on Beckton Dickinson FACscan using the Cell Quest program.

MUC1-Tetramer Staining

MHC class I $H\text{-}2D^b$ tetramers containing MUC1 TR peptide APGSTAPPA were created by Dr. Larry Pease at Mayo Clinic Rochester. PBLs were stained with 0.1 mg/mL $H\text{-}2D^b$/MUC1 tetramer (directly conjugated to phycoerythrin) for 1 hour on ice. To confirm specificity, an $H\text{-}2D^b$ tetramer containing an irrelevant peptide was used as control ($VP2_{121-130}$). The cells were then stained with CD8 and CD4 antibodies conjugated to FITC for 15 minutes before being analyzed by two-color flow cytometry.

Preparation of Dendritic Cell-Pulsed Liposomal MUC1 TR Lipopeptide

Dendritic cells were derived from C57BL/6 bone marrow cells according to the method described (18). Briefly, bone marrow cells were flushed from tibia, and femur and red blood cells were lysed with ammonium chloride. Cells (1 × 10^6/mL) were cultured in DMEM with 10% FBS, 1% glutamax, 50 U/mL penicillin, 50 μg/mL streptomycin (DMEM complete medium), supplemented with 10 ng/mL murine GM-CSF (Pharmingen) and 10 ng/mL murine IL-4 (Pharmingen). At day 7, nonadherent cells were removed, washed, resuspended (1 × 10^6/mL) in fresh DMEM complete media supplemented with 5 ng/mL GM-CSF. Adherent cells were re-fed fresh DMEM complete media supplemented with 5 ng/mL GM-CSF. Between days 10 and 13, we obtained approximately 70–75% cells that showed DC phenotype by flow cytometry. DC were fed with MUC1 TR lipopeptide that was enclosed in liposomes according to the method provided by Biomira, Inc. (19). Briefly, 2 mL of the liposomal MUC1 TR formulation was fed to 200 × 10^6 DC in a total volume of 20 mL, 1 day before injection. Mice were injected i.p. with 1 × 10^6 MUC1 TR pulsed DC per mouse in 200 μL volume. The first two immunizations at weeks 3 and 5 consisted of DC-fed liposomal MUC1 formulation. Thereafter, mice were immunized with liposomal MUC1 vaccine in PBS.

Vaccination Strategy

The vaccine formulation consisted of a lipid derivative of a 25mer MUC1 TR peptide (STAPPAHGVTSAPDTRPAPGSTAPP), which was incorporated into liposomes along with Lipid A as adjuvant. The vaccine was supplied as a sterile powder formulated at Biomira, Inc. by a proprietary method. Upon reconstitution with sterile saline for injection, it contained 400 μg/mL of MUC1 lipopeptide, 200 μg/ml of Lipid A (Avanti Polar Lipids, Inc., Alabaster, AL, U.S.A.) and 20 mg/mL of carrier lipids in multilamellar vesicles with a mean particle size of 2 to 3 μm. For the preparation of pulsed DC, particle size of the vaccine was reduced to < 200 nm by ultrasonication. Randomized preclinical trials were performed in MMT mice starting at 3 weeks of age.

Treatment Arms Include

Treatment arms include (a) liposomal MUC1 TR lipopeptide (L-MUC1-TR) (200 μg/mouse/250 μL s.c.) + L-IL-2 (20,000 U/mouse/100 μL i.p.), (b) L-MUC1-TR, (c) L-IL-2 (20), (d) empty liposomes, and (e) no treatment. We compared the immune responses that developed during treatment and used tumor onset, tumor burden, and survival as the endpoints for determining the clinical effectiveness of the vaccine. A schematic of the immunization protocol is shown in Figure 1.

Dendritic Cells Pulsed with C57mg.MUC1 Tumor Lysate

DCs were prepared as described above. Lysates from C57mg.MUC1 cells were made in tissue lysis buffer con-

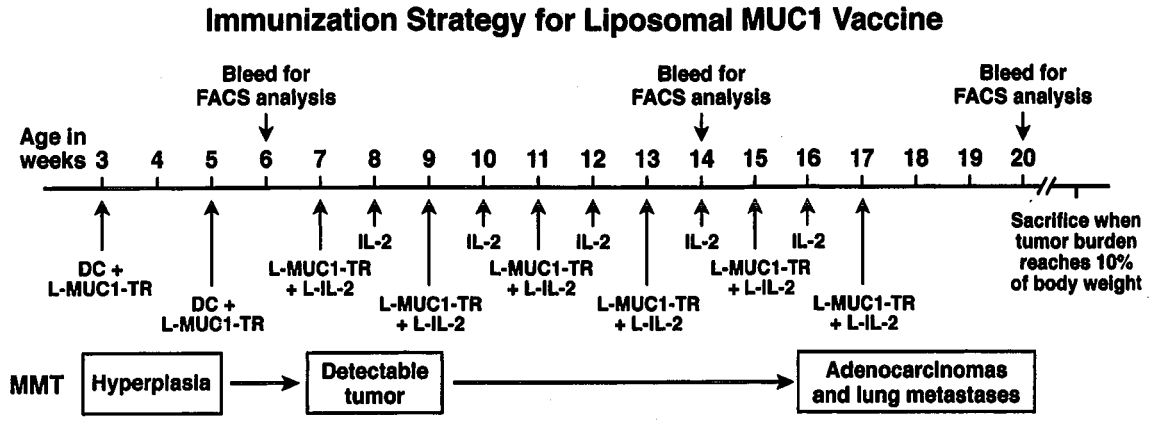

FIG. 1. Schematic representation of immunotherapy strategy in MMT mice.

taining 20 mmol/L Hepes, 0.15 mol/L NaCl, and 1% Triton X-100. Cells were sonicated using a Branson Sonifier 450 (VWR Scientific) at 20% duty cycle setting with three pulses of 10 seconds each. Immature 7-days-old DC were pulsed with 20 ng/mL of the tumor lysate for 1 day and then matured with 5 ng/mL TNF-α (Pharmingen) for 1 day. MUC1.Tg mice received two intradermal injections, 2 weeks apart of tumor lysate-pulsed DC at 1×10^7 DC per mouse. One week after the last injection, mice were challenged with 2×10^6 C57mg.MUC1 tumor cells (subcutaneously).

Statistical Analysis

p values are from the one-way ANOVA *F* test for comparing the treatment groups simultaneously and from the pairwise contrasts from a one-way ANOVA model. p values for lung metastasis are from the Pearson χ^2 statistic and from Kruskal-Wallis test.

RESULTS

MMT Mice Develop Spontaneous Mammary Gland Cancer and Lung Metastases

MUC1.Tg mice were bred with mice carrying the MMTV-driven polyoma middle T antigen (MT) to create MMT mice. Prior to generating the double transgenics, the MTag mice had been backcrossed 10 generations onto C57BL/6 mice, making them congenic (12). In the MMT mice, mammary gland tumors are induced by the action of a potent tyrosine kinase activity associated with

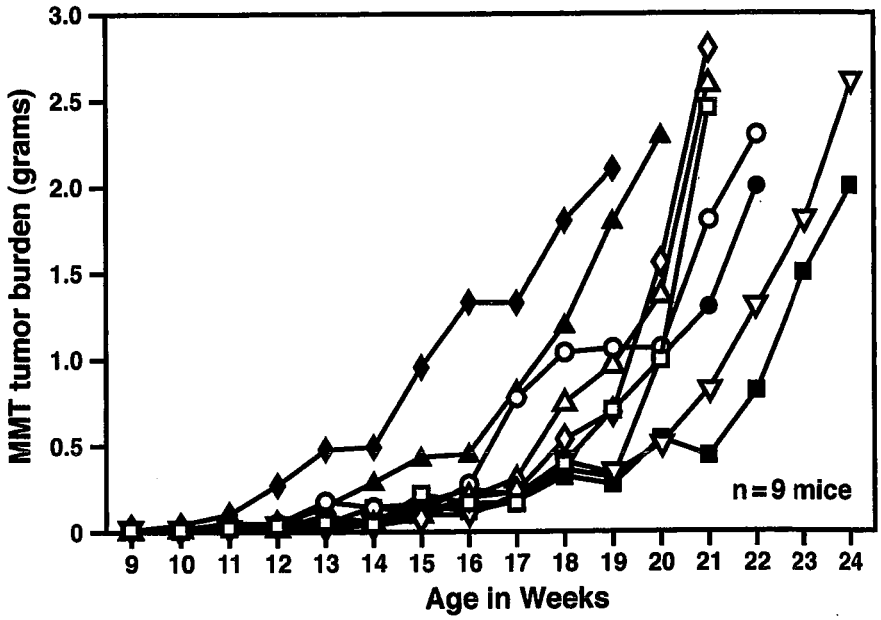

FIG. 2. Tumor growth curve in MMT mice as a function of age. Tumor burden was determined by palpation beginning at 8–9 weeks of age and calculated by the formula: gm = (Length × Width^2) × 0.5. Most mice develop palpable tumors by 10–11 weeks. Tumors reach 10% of mouse body weight between 20 and 24 weeks at which point mice are killed. Data for individual mice are shown (n = 9 mice).

the polyoma virus middle T antigen driven by the mouse mammary tumor virus long terminal repeat (MMTV) (11). Middle T specifically associates with and activates the tyrosine kinase activity of a number of c-src family members, eliciting tumors when a threshold level of gene product has been attained. This promoter is transcriptionally active throughout all stages of mammary gland development and results in widespread transformation of the mammary epithelium and the rapid production of multifocal mammary adenocarcinomas. Hyperplastic alveolar nodules (HANs) can be detected by whole mount as early as 21 days and palpable mammary gland tumors are detectable from approximately 49 days onwards. Tumor progression is quite rapid, reaching 10% of body weight by approximately 20 to 24 weeks (Fig. 2). 100% of the female MMT mice get tumors. Tumors arise with synchronous kinetics and are highly fibrotic with dense connective tissue separating individual nests of tumor cells, a pathology that closely resembles scirrhous carcinomas of the human breast (21). These mice exhibit metastasis in the lungs (30 of 49 MMT mice tested or 60%) and micro-metastasis in the bone marrow by 4 months of age. After the observation that epithelial cells were present in several of the 20- to 24-week-old MMT-derived bone marrow cultures, we examined if bone marrow micro-metastasis was occurring in these mice. Bone marrow metastasis was determined by staining bone marrow cells from MUC1.Tg mice and MMT mice with pan-cytokeratin and MUC1, markers commonly used to detect epithelial tumor cells. Cells positive for both markers were determined by two-color flow cytometry as well as by confocal microscopy and represent micro-metastasis (Figs. 3A and B). By flow cytometry, 3 to 4% of bone marrow cells were positive for both pan-cytokeratin and MUC1. It is important to note that mortality in patients with breast cancer is directly associated with lung and bone metastasis. The MMT mouse appears to be an appropriate model for human cancer and allows us to study the effects of self-tolerance, immunity, and autoimmunity to MUC1 as mammary tumors develop spontaneously.

Tumor Burden and Lung Metastasis in Immunized MMT Mice

We immunized mice with L-MUC1-TR ± L-IL-2. The first two immunizations administered to young (3- and 5-week-old) MMT mice used syngeneic DC loaded with

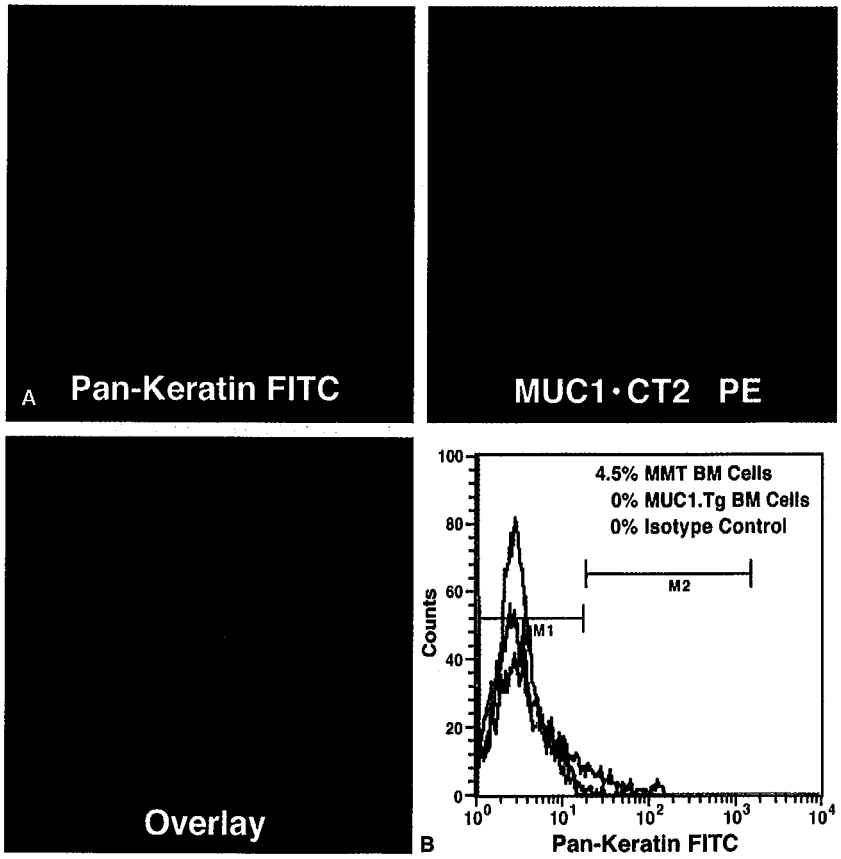

FIG. 3. Bone marrow metastasis is detected in MMT mice. **(A)** Confocal microscopy showing bone marrow cells from MMT mice positive for pan-cytokeratin (green) and MUC1 (red). Colocalization is shown in yellow. For MUC1 staining, a hamster monoclonal antibody, CT2 is used. **(B)** Representative histogram for two-color flow cytometric analysis of bone marrow cells derived from 22-week-old MMT mouse. The histogram represents percent cells stained positive for pan-cytokeratin that were gated on $MUC1^+$ cells. Two controls include bone marrow cells from age matched MUC1.Tg mice and isotype IgG.

liposomal MUC1 to induce strong immunity as young mice respond well to an antigen when presented in context of DC without the induction of tolerance (22). From week 7 onwards, mice were given L-MUC1-TR reconstituted in PBS (s.c.) and subsequently boosted with the same formulation every 2 weeks. L-IL-2 was administered (i.p.) every 2 weeks to the appropriate groups. Although no significant differences were observed in the onset and progression of the MMT tumors with immunization (Fig. 4A), by 18 weeks of age there was significant decrease ($p < 0.05$ to $p < 0.005$) in tumor burden between immunized and control MMT mice (Fig. 4B). To our surprise, empty liposomes elicited a similar response suggesting that the lipid A in the formulation may have an effect on the tumor. However, by 20 to 24 weeks, no significant differences in tumor burden between immunized and control mice were observed (Fig. 4A). Interestingly, we observed that treatment with L-IL-2 alone had significantly lower numbers of lung metastasis than mice in all other treatment groups and in untreated control mice (Fig. 4C). Incidence of metastasis was also lower in mice treated with L-IL-2 as compared with other treatment groups and untreated MMT mice (44% versus 64% in untreated MMT) (Table 1). These results did not reach significance due to low animal numbers. All mice were killed when tumors reached 10% of body weight, and, therefore, difference in survival was not observed. Because MUC1 is expressed on normal cells, we routinely examined mice for signs of autoimmunity after immunization. We monitored weight loss, food intake, general health, hunched back, and histopathology of various MUC1-expressing organs. No signs of autoimmunity were evident in our study group (data not shown).

MUC1 Expression in MMT Tumors

Tumor sections from 6-, 12-, and 21-week-old nonimmunized MMT mice show strong heterogeneous expression of MUC1 as tumors progress (Fig. 5). Paraffin embedded tumor sections from 6-, 12-, and 21-week-old MMT mice were stained with two antibodies, one recognizing the CT of MUC1 (CT2) and the other recognizing the TR epitope of MUC1 (B27.29). CT2 antibody recognizes mouse and human CT of MUC1. It is a monoclonal antibody (Mab) raised in Armenian hamster and thus gives very little background when used to stain tissues from mice. Mammary tumors showed moderate expression of human MUC1, using Mab. B27.29, which reacts only with the human MUC1 and not with mouse

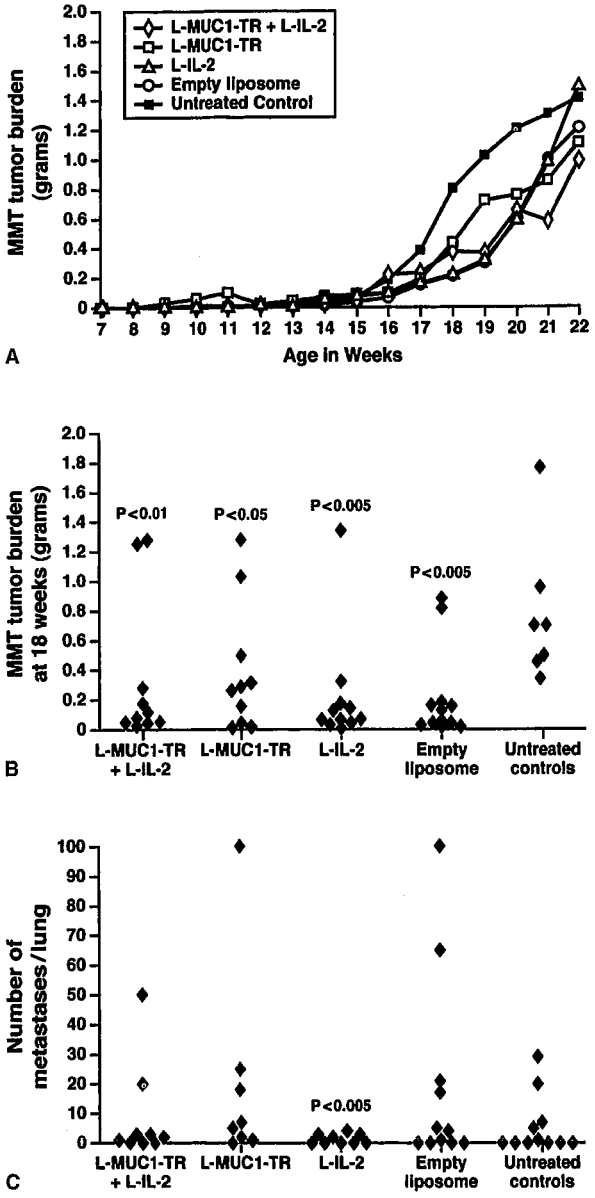

FIG. 4. (A) MUC1-specific immunization did not alter tumor burden in MMT mice. Tumor growth of immunized MMT mice versus untreated MMT mice. Tumor burden was determined by palpation beginning at 6–8 weeks and calculated by the formula: gm = (Length × Width^2) × 0.5. No significant difference was observed in mice immunized with MUC1 TR + L-IL-2 as compared with untreated control mice (n = 6–9 mice/group). (B) Tumor burden was lower in immunized MMT mice at 18 weeks of age. In treatment groups, tumor burden at 18 weeks was significantly lower as compared with untreated control mice. Individual mouse data are shown. p values are derived from the pairwise contrasts from a one-way ANOVA model. (C) L-IL-2 treatment reduces lung metastasis in MMT mice. The presence of pulmonary metastases was determined by counting gross morphologic disease using low power microscopy. Number of metastatic lesions counted in the lungs was significantly lower in mice treated with L-IL-2 as compared with other treatment groups and untreated control mice. Individual mouse data are shown (n = 8 to 11 mice/group). p values were from the Pearson χ^2 statistic and from Kruskal-Wallis test.

TABLE 1. *Percentage of MMT mice with lung metastasis*

Treatment	Number	%
L-MUC1 TR + L-IL-2	6/9	66
L-MUC1 TR	7/8	87
L-IL-2	4/9	44
No treatment	8/12	64

Pulmonary metastases was determined by counting gross morphologic disease using low power microscopy. The authors determined how many mice developed lung metastasis.

Muc1 (23). MUC1 was expressed throughout the cytoplasm and around the cells in a pattern similar to that observed in human breast carcinomas. Western blots of tumor lysates using B27.29 for detection showed protein expression (data not shown). Thus, mammary gland tumors that occurred spontaneously in the MMT mice expressed the transgene protein MUC1 in a manner similar to humans. Any alteration in MUC1 expression will be important in the immunologic recognition and presentation of the antigen. Immunization did not alter the MUC1 expression in the MMT tumors (data not shown).

Native Immune Responses Developing in MMT Mice as Tumors Progress

We have determined the native cellular and humoral immune responses in the nonimmunized MMT mice as tumors progressed. MMT mice were bled at 6, 14, and 21 weeks of age and PBLs were examined for T cells expressing early and late activation markers (CD69 and CD25), DC ($CD11c^+$ cells) expressing B7 costimulatory receptors, T cells and DC expressing intracellular cytokines such as IFN-γ, IL-2, IL-4, IL-5, IL-10, and IL-12. We also examined PBLs for presence of T cells recognizing $H\text{-}2D^b$/MUC1 tetramer. The results are tabulated in Table 2. Increases were observed in some of the markers (IL-2R and intracellular IL-4 and IL-12) at the 14-week time point but the difference was not statistically significantly and was no longer observed at 21 weeks. $CD11c^+$ and $B7^+$ cells were significantly lower at 21 weeks when the tumor burden was high as compared with 6 and 14 weeks, which may indicate a defect in the antigen presenting cells during tumor progression. Thus our data clearly show that no significant alterations in

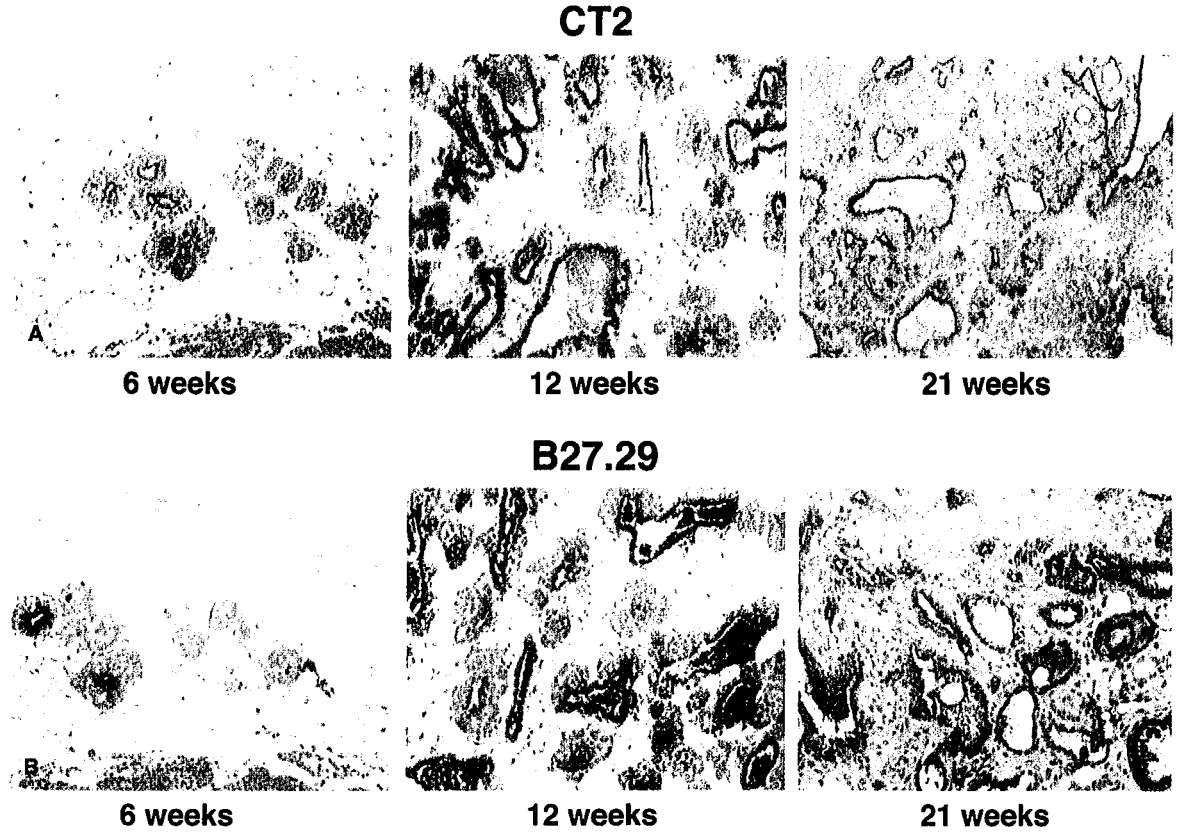

FIG. 5. MUC1 expression increases as tumors develop in MMT mice. Methacarn fixed and paraffin-embedded sections of mammary gland tumors from 6-, 12-, and 21-week-old MMT mice were stained with **(A)** CT2, reactive with MUC1 cytoplasmic tail and **(B)** B27.29, reactive with MUC1 TR. Specific staining was observed on lumenal surface of mammary epithelial cells and staining pattern is similar to that seen in humans. Staining with these antibodies showed increase in MUC1 expression as tumors developed (original magnification ×200).

TABLE 2. *Immunophenotype of lymphocytes as tumors progress in MMT mice*

Markers	6-week MMT	14-week MMT	21-week MMT
IL-2R	1.58	3.28	0.28
CD69	0.75	0.30	0.17
IL-2	1.03	1.29	0.20
IFN-γ	0.50	0.73	0.38
IL-4	0.56	7.67	2.31
IL-5	0.16	2.61	2.28
IL-10	0.24	0.43	0.42
IL-12	0.26	6.43	2.69
B7	4.50	7.70	1.30*
CD11c	11.20	12.30	5.50*
MUC1-Tetramer	0.31	1.32	0.19

We have determined expression of early and late activation markers (CD69 and IL-2R) on T cells, as well as levels of intracellular cytokines produced by T cells (IFN-γ, IL-2, IL-4, IL-5, and IL-10) and dendritic cell (IL-12). The numbers represent percent positive cells stained with the specific antibody and analyzed by flow cytometry. Increases were observed in some of the markers (IL-2R and intracellular IL-4 and IL-12) at the 14-week time point that declined by 21 weeks but the difference was not statistically significantly. $CD11c^+$ and $B7^+$ cells were significantly lower at 21 weeks (when the tumor burden was high) as compared with 6 and 14 weeks. Average of n = 6 mice/group is shown. P values are from the pair-wise contrasts from a one-way ANOVA model.

*$p < 0.05$.

Th1 or Th2 immune phenotype occurs in MMT mice as tumors progressed. Presence of naturally occurring precursor CTL activity against MUC1 in 6-, 9-, 12-, 15-, 18-, and 21-week-old MMT mice was also tested and the data are presented in Figure 6. We were unable to detect precursor CTL activity in splenocytes at any time during tumor progression. With regards to humoral immune response, circulating antibody to MUC1 was undetectable by specific ELISA at any time during tumor progression (data not shown). These data taken together clearly indicate that naturally occurring cellular or humoral immune responses in nonimmunized MMT mice were nondetectable, which is in sharp contrast to the results reported previously for a similar model of pancreas cancer (3).

T Cell Immune Response in Immunized MMT Mice

Immunization elicited mature MUC1-specific CTL that were cytotoxic against B16.MUC1 tumor cells in vitro (Fig. 6). To determine MUC1 specificity, B16 cells transfected with vector alone (B16.neo) were routinely used as control tumor target and lysis of < 5% was observed making the CTL specific for MUC1 (data not shown). Both MHC-restricted and nonrestricted MUC1-specific CTL have been reported in the literature for human cancer (1,24); however, in MMT mice, we only detect restricted CTL. It is possible that these mice do possess unrestricted CTL but these CTLs may be difficult to detect in vitro and therefore have never been

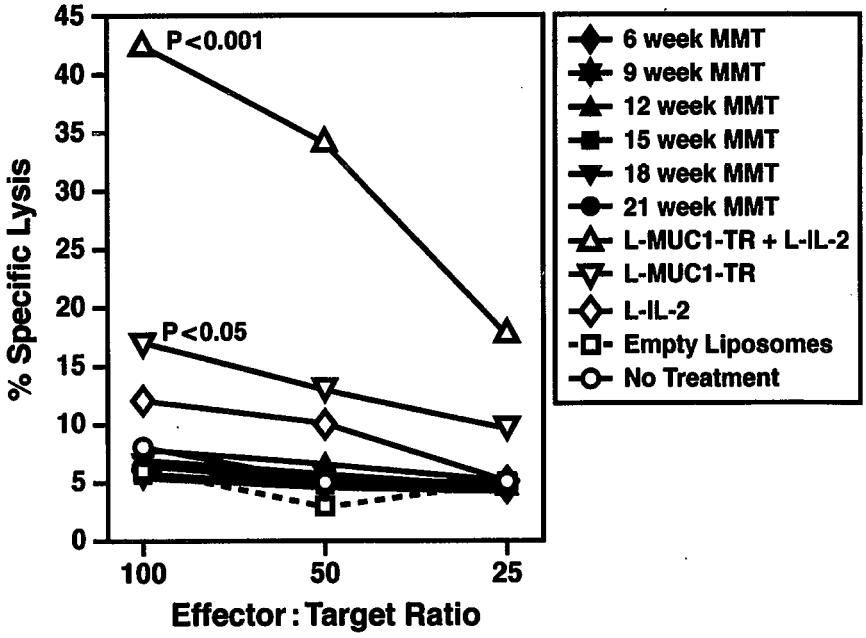

FIG. 6. Immunized MMT mice develop MUC1-specific CTLs. CTL activity in 6-, 9-, 12-, 15-, 18-, and 21-week-old untreated MMT mice was determined by a standardized 8-hour ^{51}Cr-release assay using B16 melanoma cells transfected with human MUC1 as target cells. Splenic T cells from MMT mice were used as effector cells. In immunized mice, CTL activity was determined at time of sacrifice when tumors reached 10% of body weight. The effector cells were not stimulated in vitro with MUC1-TR or cytokines. In untreated mice, no CTL activity was detected at any age. MMT mice in all treatment groups showed increase in MUC1-specific CTL with most lysis detected in mice immunized with L-MUC1-TR + L-IL-2. (*$p < 0.001$) as compared with untreated control. L-MUC1-TR immunization alone gave significantly higher CTL activity as compared with empty liposome group and untreated controls ($p < 0.05$). Specific lysis was calculated according to the formula: (experimental CPM − spontaneous CPM/maximum CPM − spontaneous CPM) × 100. Average of n = 6 mice/group is shown. p values are from the pairwise contrasts from a one-way ANOVA model. *Indicates comparison of untreated controls versus treatment groups.

reported previously in mice (25–28). Although the CTLs were cytotoxic in vitro, they had no effect on the growing tumor cells in vivo in MMT mice. This was determined by immunohistochemistry of MMT tumor sections in which MUC1-expressing tumor cells remained unchanged with immunization, suggesting that the MUC1-specific CTLs were not cytotoxic against the tumor cells in vivo (data not shown). To evaluate the T cell responses during immunization and as the tumors progressed, immunized and nonimmunized MMT mice were tail-bled at 6, 14, and 20 weeks, PBLs were isolated and tested for presence of a) T cells expressing intracellular IFN-γ and b) T cells recognizing H-2D^b/MUC1 tetramer. All treatment groups in immunized MMT mice showed increased numbers of T cells expressing intracellular IFN-γ by 10 to 14 weeks of age as compared with untreated control mice (Fig. 7A, p values shown in the figures). By 20 weeks of age, there was a decrease in these cell numbers suggesting that repeated immunization with MUC1 TR peptide or high tumor burden may affect T cell effector function. This observation correlates well with the decrease in tumor burden at 18 weeks in immunized mice, which does not last at 21 weeks (Fig. 4B). Similarly, T cells reactive with H-2D^b/MUC1 tetramer increased by 14 weeks in immunized MMT mice but no further increase was observed at 20 weeks (Fig. 7B), p values shown in the figures). Although some increase in percent T cells recognizing MUC1-tetramer was observed in the empty liposome treated mice versus untreated controls, significantly higher percent was observed in mice treated with L-MUC1-TR alone or with L-MUC1-TR + L-IL-2 ($p < 0.01$ and $p < 0.05$, respectively) versus empty liposome group. The increase in empty liposome group suggests that the lipid A present in the liposomal vaccine formulation may be sufficiently immunogenic in eliciting an anti-MUC1 response, albeit

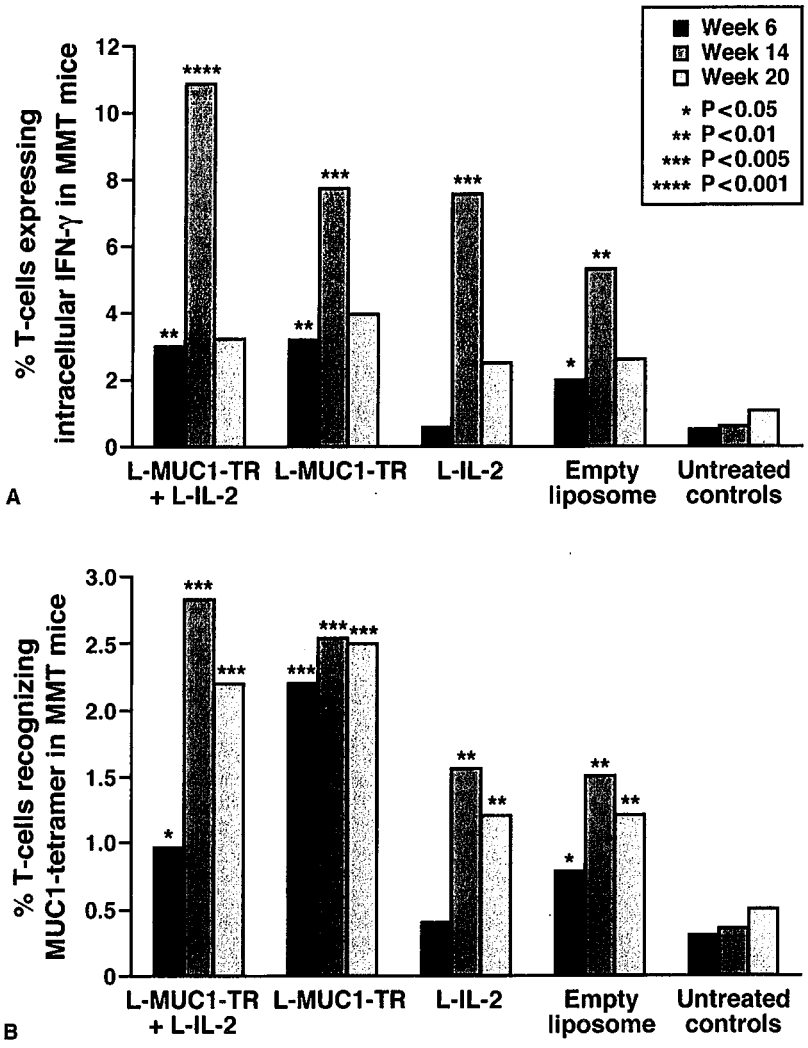

FIG. 7. MUC1-specific immunization elicits **(A)** T cells expressing IFN-γ and **(B)** T cells that recognize H-2D^b/MUC1 tetramer. At 6, 14, and 20 weeks after immunization, PBLs were analyzed for presence of T cells expressing IFN-γ and T cells recognizing H-2D^b/MUC1 tetramer. **(A)** Six weeks after immunization, mice in all treatment groups showed an increased percent of T cells expressing IFN-γ (**$p < 0.01$ for L-MUC1-TR groups). No difference in L-IL-2 treated group was observed at 6 weeks, as L-IL-2 treatment only begins at week 7. By 14 weeks after immunization, these T cells further increased. By 20 weeks after immunization, these cells decreased and were at levels similar to that observed at 6 weeks after immunization. At 14 weeks, percent T cells expressing intracellular IFN-γ was significantly higher ($p < 0.06$) in the L-MUC1-TR treated and L-IL-2 treated groups as compared with mice treated with empty liposome. Much higher significance ($p < 0.005$) was observed between L-MUC1-TR + L-IL-2 treated group versus empty liposome group. *Indicates comparison of untreated controls versus treatment groups. **(B)** Compared with untreated controls, mice in all treatment groups showed significant increase in percent T cells recognizing H-2D^b/MUC1 tetramer as early as 6 weeks after immunization. By 14–20 weeks after immunization, treated mice showed higher percent of circulating T cells recognizing H-2D^b/MUC1 tetramer. At all time points, percent T cells recognizing MUC1-tetramer was significantly higher ($p < 0.01$) in the L-MUC1-TR treated group as compared with mice treated with empty liposome. Significant difference ($p < 0.01$) was also observed between the L-MUC1-TR + L-IL-2 treated group versus empty liposome group at 14- and 20-week time points but not at the 6-week time point. No significant difference was observed between L-IL-2 treated group versus empty liposome group. *Indicates comparison of untreated controls versus treatment groups. Average of n = 6 mice/group is shown. p values are from the pairwise contrasts from a one-way ANOVA model.

not as strong as the vaccine formulation containing MUC1. Furthermore, the response seen with the empty liposome group did not translate into MUC1-specific CTL response (Fig. 6) nor did it correlate with elevated serum MUC1 levels in Figure 8A.

MUC1 Serum Levels in Immunized MMT Mice

As tumors progressed in the MMT mice, MUC1 serum levels increased only slightly as compared with age matched MUC1.Tg mice with maximum reaching to 1,500–2,500 U/mL of serum at 20 weeks of age. In age matched female MUC1.Tg mice, serum MUC1 levels ranged from 500 to 1,200 U/mL, which is likely to depend upon their estrous cycle status (data not shown). The low levels of circulating MUC1 may explain the lack of an immune response to MUC1 in nonimmunized MMT mice (Fig. 6 and Table 2). Immunization, however, significantly increased the serum MUC1 levels compared with untreated MMT mice (Fig. 8A), which corresponded directly to the increased CTL activity in these mice. These results suggested that high levels of circulating tumor antigen, MUC1, may activate MUC1-specific CTL that are capable of specifically lysing MUC1-expressing tumor cells in vitro (Fig. 6). We also detected low levels of circulating antibodies to MUC1 in

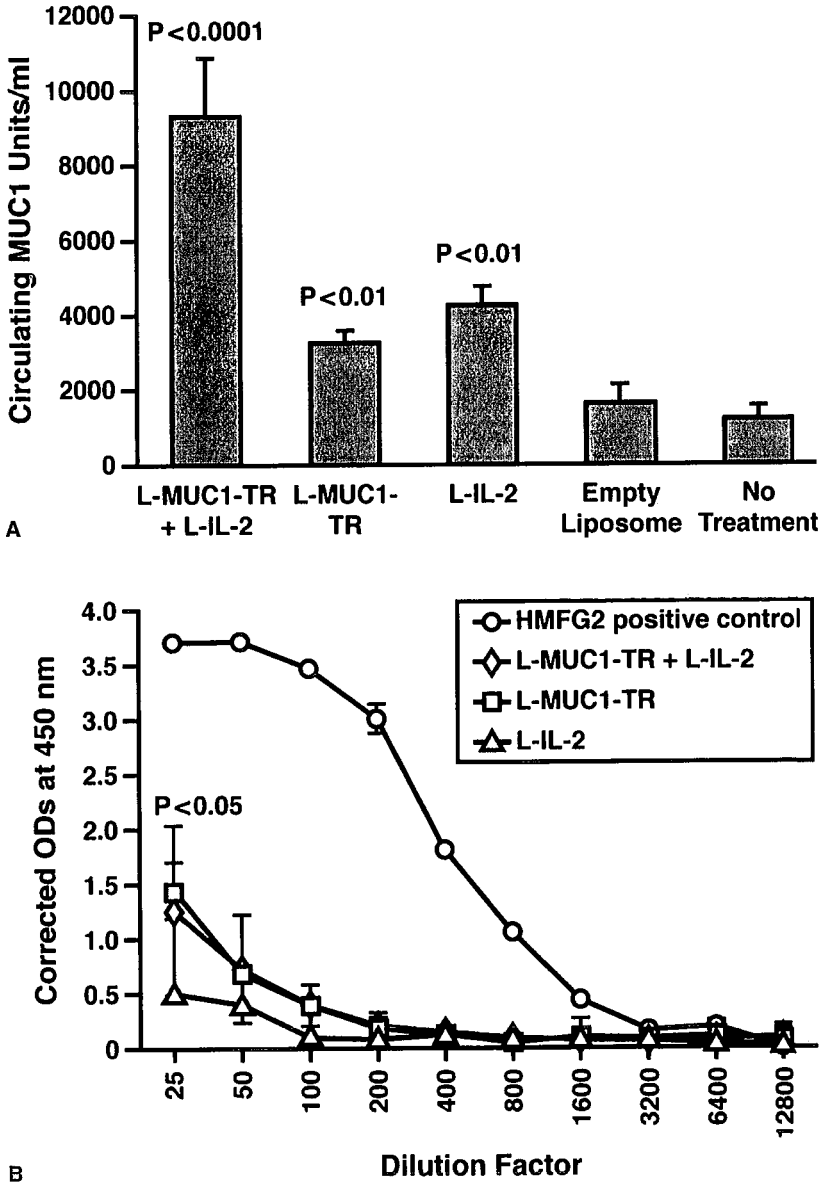

FIG. 8. Circulating MUC1 and anti-MUC1 levels in serum of immunized MMT mice. **(A)** Circulating MUC1 levels increase significantly with MUC1-specific immunization as well as with IL-2 treatment. **(B)** Low levels of MUC1 antibodies were detected in MMT mice immunized with MUC1 TR containing vaccine formulation. IL-2 treatment did not elicit MUC1-specific antibodies. Average of n = 6 mice/group is shown. p values are from the pairwise contrasts from a one-way ANOVA model. *Indicates comparison of untreated controls versus treatment groups.

the L-MUC1-TR + IL-2 treated mice (Fig. 8B) suggesting that immunization and the high level of circulating tumor associated MUC1 has changed the antigenic profile and elicited a low level humoral response to MUC1. Antibodies reactive with MUC1 have been reported in a small number of humans with breast cancer (29,30). Although a humoral response is often dismissed as being ineffective against solid tumors, it is still important that the response in the MMT mice once again parallels that in humans.

MHC Class I Expression in MMT Mice as Tumors Progress

Since the MUC1-specific CTLs have minimal effect in vivo, we postulated that the growing MMT tumor cells evaded immune recognition. We evaluated one of the well-characterized mechanisms by which tumor cells evade CTL killing, downregulation of their surface MHC class I molecules. We observed by two-color flow cytometry that percent cells positive for MHC class I and pan-cytokeratin are approximately 13% in 6-week-old MMT tumor mice which steadily decreases to <2% in 18-week-old tumor mice (Table 3) and that immunization was unable to upregulate these levels.

MMT Tumors Express TGF-ß

Another effective way a tumor cell evades T cell killing is to render the effector T cells nonfunctional by releasing immunosuppressive factors. One such factor is TGF-β that is capable of hindering T cell signaling and down regulating their function. We tested whether mammary tumors from MMT mice express TGF-ß by specific immuno-histochemical staining and demonstrate that MMT tumors express TGF-ß as early as 6 weeks of age and that the expression increases as the tumors progress (Fig. 9). MUC1-specific immunizations did not alter the expression of TGF-ß, suggesting that the tumors may be utilizing this mechanism to downregulate T cell activity in vivo and escape immune intervention. This phenomenon is also evident from the decrease in the numbers of IFN-γ expressing T cells (Fig. 7A) as tumor burden increases.

TABLE 3. *MHC class I expression on tumor cells*

Tumor age (wk)	MHC I expression
6	12.5 ± 2.0
12	4.1 ± 0.89
18	1.5 ± 0.5

Surface expression of MHC class I molecule on tumor cells decreases as tumors progress in MMT mice. FACs analysis demonstrating percent cells positive for pancytokeratin and MHC class I molecule ($H\text{-}2D^b/K^b$). n = 5 MMT mice.

Tumor Lysate Pulsed DC were Effective in Breaking Tolerance and Preventing Tumor Formation in MUC1.Tg Mice

Another plausible explanation for the failure of MUC1-specific immunization to eradicate MMT tumors is the utilization of a single tumor antigen as immune target. Recent findings suggest that tumor lysate-fed DC generate tumor-specific proliferative cytokine release and cytolytic reactivities in vitro as well as effectively prime mice to reject subsequent lethal challenges with viable parental tumor cells (31,32). Using an injectable tumor model, we show that MUC1.Tg mice immunized with DC pulsed with lysates prepared from C57mg.MUC1 cells were completely protected from subsequent challenge with C57mg.MUC1 tumor cells (Fig. 10). These results are promising, as we were able to break tolerance in the MUC1.Tg mice and protect them against tumor challenge. However, the challenge is to achieve these results in our spontaneous model, which is physiologically more appropriate and, to a large extent, mimics the human situation.

DISCUSSION

We describe a mouse model of spontaneous breast cancer that appropriately mimics human cancer and is an excellent model for testing novel immunotherapeutic strategies. Some important features of this model are the reproducible development of spontaneous mammary gland tumors, the occurrence of invasion and metastasis, the presence of an intact immune system, and the presence of a targetable and stable tumor antigen, MUC1. Most importantly, the tumor models resemble human cancer with regards to progression through various development stages of cancer and sensitivity to hormonal and stromal alterations. A recent study has established that MTag-induced hyperplasias, like early proliferative lesions seen in human breast, are heterogeneous with respect to their malignant potential. The study further establishes that MTag gene expression alone is insufficient to induce tumors and that additional events are required for tumorigenesis and metastasis (33).

In the MMT mice, as in humans, the mammary gland develops after birth, tumors are multifocal, grow rapidly, and are histologically homogeneous, highly fibrotic with dense connective tissue separating individual nests of cells. Tumors occur in a reasonable time frame to allow

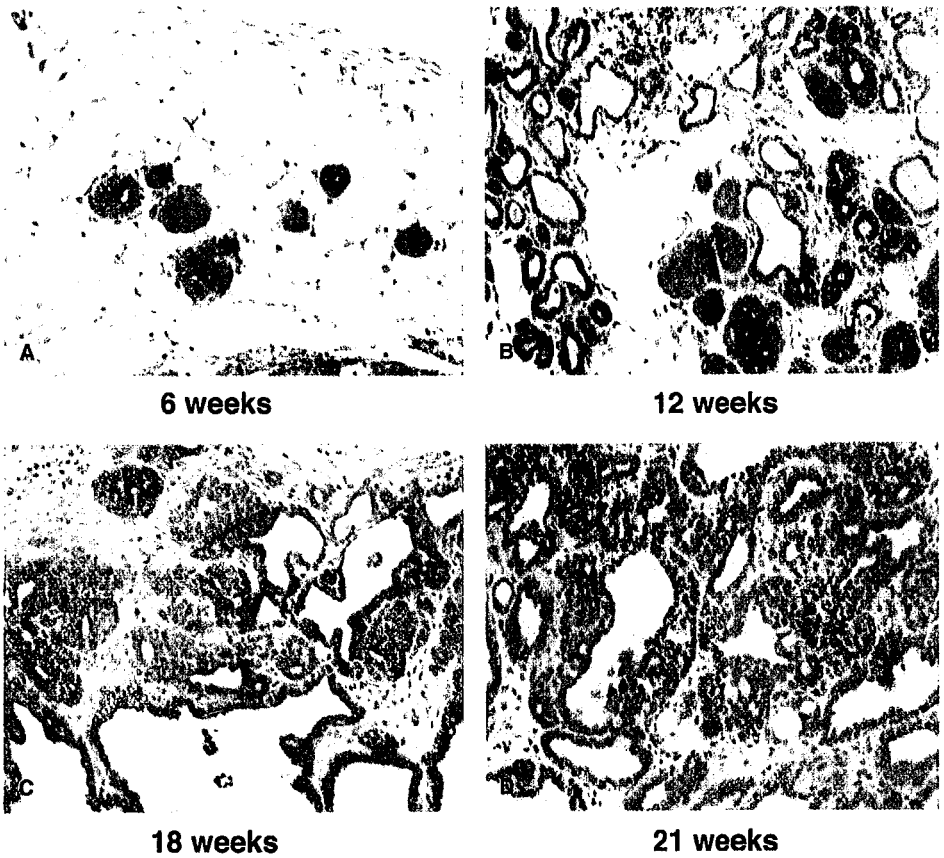

FIG. 9. Tumors from MMT mice express TGF-β as early as 6 weeks of age, which increases with time. Methacarn fixed and paraffin-embedded sections of mammary gland tumors from 6-, 12-, 18-, and 21-week-old MMT mice were stained with antibody to TGF-β2. MMT tumor at **(A)** 6 weeks, **(B)** 12 weeks, **(C)** 18 weeks, and **(D)** 21 weeks of age (original magnification ×200).

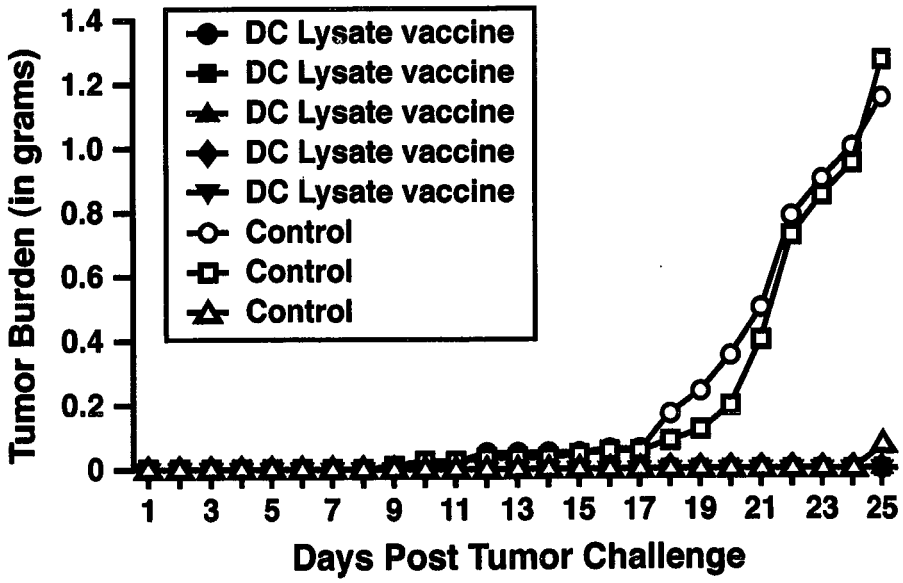

FIG. 10. Tumor progression in MUC1.Tg mice immunized with tumor lysate-pulsed dendritic cells (DC). MUC1.Tg mice received two intradermal injections, 2 weeks apart, of C57mg.MUC1 tumor lysate-pulsed DC at 1×10^7 DC per mouse. One week after the last injection, mice were challenged with 2×10^6 C57mg.MUC1 tumor cells (subcutaneously). All five immunized mice were protected from tumor challenge, while all three control mice developed tumors. One control mouse had delayed tumor growth.

for prevention as well as therapeutic studies. Mammary tumors, which can be followed by palpation, are useful for therapeutic studies, as tumor location alleviates the need to sacrifice the animal to determine clinical response and is optimal for prevention therapies, as the tumors develop after birth, and immunizations could precede tumor development. MUC1 is overexpressed in these tumors and immunization with a MUC1-specific vaccine significantly increases MUC1 serum levels and elicits a MUC1-specific cellular and a humoral immune response. Similar to humans, these immune responses do not translate into an antitumor response suggesting that a) the tumor cells successfully evade the immune effector cells using a variety of mechanisms, and b) targeting a single tumor antigen may not be effective. Similar to our study, recent studies showed that the HER-2/neu transgenic mice that are immunologically tolerant to the neu antigen and develop spontaneous unifocal mammary carcinomas, developed neu-specific T cells after vaccination. However, the neu-specific effector T cells were unable to protect these mice from the developing breast tumors (34,35).

MMTV-driven polyoma middle T antigen affects almost every cell in the mammary gland, and the entire mammary tree is burdened with tumors, which may be too aggressive for the immune effector cells to act effectively. We have previously shown by adoptive transfer that MUC1-specific CTL developed in vitro can eradicate less aggressive, transplantable $MUC1^+$ tumors (4). Whether these CTLs gain access into the growing tumor mass was tested by adoptively transferring carboxyfluorescein succinimidyl ester-labeled MUC1-specific CTL into tumor-MMT mice. Preliminary data suggest that CTLs can enter the tumor mass and multiply for up to 14 days, after which they are undetectable in the tumor mass (unpublished data).

Many reports have suggested that progressing tumors in patients with cancer have elaborate means of escaping an apparently effective MHC class I restricted immune response (36,37). Other investigators have found that the CTL response occurs too late to be effective against the tumors (38). Tumors evade host immunity at both the induction and effector phases. Because immunized MMT mice have developed MUC1-specific CTL responses, these spontaneously arising mammary gland tumors must have evaded the existing CTL. We have shown that the immunosuppressive factor, TGF-β2 is expressed by MMT tumor cells and may be a factor responsible for rendering the CTLs cytolytically anergic (Fig. 9). It has been shown previously that TGF-β may alter TCR subcomponent composition and downregulate CD3ζ, γ, δ, but not CD3ϵ, thereby reducing T cell signaling and CTL responses against tumor cells, and reducing TGF-β2 expression reverses this effect (39). However, including TGF-β2 antibody treatment in our vaccination strategy did not lead to effective antitumor response in the MMT mice (unpublished data), suggesting that multiple immune evasion mechanisms may be used by the tumors to avoid immune destruction. We have demonstrated that the MMT tumor cells may avoid immune recognition by down-regulating MHC class I expression (Table 3). It has been recently shown that functionally active inhibitory receptors that impart negative signals have been found on T cells. One such inhibitory receptor, CD94-NKG2A, can induce cytolytic anergy in CTLs specific for polyomavirus induced tumors (40). Since the tumors in the MMT mice are induced by the polyomavirus middle T antigen, it is likely that a similar mechanism is occurring these mice. In our preliminary data, we observe that the tumor-infiltrated lymphocytes isolated from MMT tumors do not proliferate in response to MUC1 antigen nor are they cytolytic against MUC1-expressing tumor cells in vitro, suggesting that the effector T cells may be tolerant to the antigen or may be anergic (unpublished data). Further experiments need to be conducted to confirm these results.

The beneficial effect of IL-2 treatment may be attributed to stimulation of other tumor antigen-specific CTLs that may exist in these mice, but have never been identified in vitro. Analyzing some of the other known tumor antigen-specific CTLs may provide us with better answers and these studies are under way. We show that immunotherapy that targets multiple tumor antigens elicits an effective antitumor response, albeit in an injectable tumor model (Fig. 10). Similar studies are under way in the MMT mice.

Finally, targeting a single tumor antigen, such as MUC1, may lead to activation-induced tolerance and anergy of CTLs in vivo, which eventually results in inactivation of the effector T cells and interruption of an antitumor response. A defining feature for a tolerant T cell is its hyporesponsiveness to antigen when compared with either a naïve or a primed T cell, and experiments are under way to evaluate if MUC1-specific immunization leads to T cell tolerance. This phenomenon of antigen-specific CTL tolerance after peptide immunization is not new and has been reported by several investigators (38,41,42). Thus, immunotherapy must be effective in breaking the existing tolerance. Recent studies have highlighted the role of two costimulatory molecules, OX40 expressed on activated T helper cells and CD40 expressed on antigen presenting cells, as targets for therapeutic intervention in cancer. Both molecules belong to the tumor necrosis factor receptor family and are

implicated in preventing tolerance induction as well as reversing established tolerance observed during anticancer immunotherapy (43,44). These studies indicate that ligation of these costimulatory molecules with specific antibodies may be a useful strategy for enhancing T cell unresponsiveness to anticancer vaccination (45).

As is frequently observed with human immunotherapy clinical trials, there is a poor correlation between the ability to induce an in vitro cellular T cell response and a clinical response (46,47). The MMT model appropriately mimics the human condition and is an excellent model for testing therapy in a setting relevant to the treatment of patients with cancer as well as for prevention and delineation of the mechanisms of tolerance, immunity, and autoimmunity. This study has only touched upon some of the major issues that are critical for designing suitable immune therapies for cancer. Future immunizations in MMT mice will target multiple antigens and costimulatory molecules.

Acknowledgment: The authors acknowledge Biomira, Inc. (Edmonton, Canada) for generously providing MUC1 TR lipopeptides and liposomal IL-2, Dr. Larry Pease for providing the H-2D^b/MUC1 tetramers, Dr. W.J. Muller for kindly providing the original breeding stock of the MT mice, Barbara Reid for technical support, Marv Ruona for the preparation of figures, Carol Williams for assistance with preparation and submission of the manuscript, and Suresh Savarirayan and the animal care technicians for excellent animal care. Supported by the Mayo Comprehensive Cancer Center (NCI CA15083), The Mayo Foundation, The Susan G. Komen Breast Cancer Foundation #99–3159 (PM), DOD Breast Cancer Research Program DAMD17–01–1-0318 (SJG), and Biomira Inc., Edmonton, Canada.

REFERENCES

1. Barnd DL, Lan MS, Metzgar RS, et al. Specific, major histocompatibility complex-unrestricted recognition of tumor-associated mucins by human cytotoxic T cells. *Proc Natl Acad Sci U S A* 1989;86:7159–63.
2. Ioannides CG, Fisk B, Jerome KR, et al. Cytotoxic T cells from ovarian malignant tumors can recognize polymorphic epithelial mucin core peptides. *J Immunol* 1993;151:3693–703.
3. Mukherjee P, Ginardi AR, Madsen CS, et al. Mice with spontaneous pancreatic cancer naturally develop MUC1-specific CTLs that eradicate tumors when adoptively transferred. *J Immunol* 2000;165:3451–60.
4. Mukherjee P, Ginardi AR, Tinder TL, et al. MUC1-specific CTLs eradicate tumors when adoptively transferred in vivo. *Clin Can Res* 2001;7:848–55s.
5. Greenlee RT, Murray T, Bolden S, et al. Cancer statistics, 2000. *CA Cancer J* 2000 50:7–33.
6. Wang J, Saffold S, Cao X, et al. Eliciting T cell immunity against poorly immunogenic tumors by immunization with dendritic cell-tumor fusion vaccines. *J Immunol* 1998;161:5516–24.
7. Gong J, Nikrui N, Chen D, et al. Fusions of human ovarian carcinoma cells with autologous or allogeneic dendritic cells induce antitumor immunity. *J Immunol* 2000;165:1705–11.
8. Tanaka Y, Koido S, Chen D, et al. Vaccination with allogeneic dendritic cells fused to carcinoma cells induces antitumor immunity in MUC1 transgenic mice. *Clin Immunol* 2001;101:192–200.
9. Gong J, Koido S, Chen D, et al. Immunization against murine multiple myeloma with fusions of dendritic and plasmacytoma cells is potentiated by interleukin 12. *Blood* 2002;99:2512–7.
10. Rowse GJ, Tempero RM, VanLith ML, et al. Tolerance and immunity to MUC1 in a human MUC1 transgenic murine model. *Cancer Res* 1998;58:315–21.
11. Guy CT, Cardiff RD, Muller WJ. Induction of mammary tumors by expression of polyomavirus middle T oncogene: a transgenic mouse model for metastatic disease. *Mol Cell Biol* 1992;12: 954–61.
12. Silver LM. *Mouse Genetics Concepts and Applications* Oxford: Oxford University Press, 1995:32–61.
13. Tevethia MJ, Bonneau RH, Griffith JW, et al. A simian virus 40 large T-antigen segment containing amino acids 1 to 127 and expressed under the control of the rat elastase-1 promoter produces pancreatic acinar carcinomas in transgenic mice. *J Virol* 1997;71: 8157–66.
14. Simpson-Herrerns L, Lloyd HH. Kinetic parameters and growth curves for experimental tumor systems. *Cancer Chemother Rep* 1970;54:143–74.
15. Schroeder JA, Thompson MC, Gardner MM, et al. Transgenic MUC1 interacts with EGFR and correlates with MAP kinase activation in the mouse mammary gland. *J Biol Chem* 2001;276: 13057–64.
16. Price MR, Rye PD, Petrakou E, et al. Summary report on the ISOBM TD-4 Workshop: analysis of 56 monoclonal antibodies against the MUC1 mucin. San Diego, Calif., November 17–23, 1996. *Tumor Biol* 1998;19:1–20.
17. Reddish MA, MacLean GD, Poppema S, et al. Pre-immunotherapy serum CA27.29 (MUC-1) mucin level and CD69+ lymphocytes correlate with effects of Theratope sialyl-Tn-KLH cancer vaccine in active specific immunotherapy. *Cancer Immunol Immunother* 1996;42:303–9.
18. Inaba K, Inaba M, Romani N, et al. Generation of large numbers of dendritic cells from mouse bone marrow cultures supplemented with granulocyte/macrophage colony-stimulating factor. *J Exp Med* 1992;176:1693–702.
19. Guan HH, Budzynski W, Koganty RR, et al. Liposomal formulations of synthetic MUC1 peptides: effects of encapsulation versus surface display of peptides on immune responses. *Bioconjug Chem* 1998;9:451–8.
20. Boni LT, Batenjany MM, Neville ME, et al. Interleukin-2-induced small unilamellar vesicle coalescence. *Biochim Biophys Acta* 2001; 1514:127–38.
21. Cardiff RD, Muller WJ. Transgenic mouse models of mammary tumorigenesis. *Cancer Surv* 1993;16:97–113.
22. Ridge JP, Fuchs EJ, Matzinger P. Neonatal tolerance revisited: turning on newborn T cells with dendritic cells. *Science* 1996;271: 1723–6.
23. Sikut R, Sikut A, Zhang K, et al. *Tumor Biology* In: Rye PD, Price MR, eds. S. Karger Medical and Scientific Publishers, 1998:122–6.
24. Domenech N, Henderson RA, Finn OJ. Identification of an HLA-A11-restricted epitope from the tandem repeat domain of the epithelial tumor antigen mucin. *J Immunol* 1995;155:4766–74.
25. Apostolopoulos V, Xing PX, McKenzie IF. Murine immune response to cells transfected with human MUC1: immunization with cellular and synthetic antigens. *Cancer Res* 1994;54:5186–93.
26. Apostolopoulos V, Karanikas V, Haurum JS, et al. Induction of HLA-A2-restricted CTLs to the mucin 1 human breast cancer antigen. *J Immunol* 1997;159:5211–8.
27. Acres B, Apostolopoulos V, Balloul JM, et al. MUC1-specific immune responses in human MUC1 transgenic mice immunized with various human MUC1 vaccines. *Cancer Immunol Immunother* 2000;48:588–94.
28. Pietersz GA, Li W, Osinski C, et al. Definition of MHC-restricted

CTL epitopes from non-variable number of tandem repeat sequence of MUC1. *Vaccine* 2000;18:2059–71.
29. Rughetti A, Turchi V, Ghetti CA, et al. Human B-cell immune response to the polymorphic epithelial mucin. *Cancer Res* 1993; 53:2457–9.
30. Kotera Y, Fontenot JD, Pecher G, et al. Humoral immunity against a tandem repeat epitope of human mucin MUC-1 in sera from breast, pancreatic, and colon cancer patients. *Cancer Res* 1994;54: 2856–60.
31. Fields RC, Shimizu K, Mule JJ. Murine dendritic cells pulsed with whole tumor lysates mediate potent antitumor immune responses in vitro and in vivo. *Proc Natl Acad Sci U S A* 1998;95:9482–7.
32. Schnurr M, Galambos P, Scholz C, et al. Tumor cell lysate-pulsed human dendritic cells induce a T-cell response against pancreatic carcinoma cells: an in vitro model for the assessment of tumor vaccines. *Cancer Res* 2001;61:6445–50.
33. Maglione JE, Moghanaki D, Young LJ, et al. Transgenic Polyoma middle-T mice model premalignant mammary disease. *Cancer Res* 2001;61:8298–305.
34. Reilly RT, Gottlieb MB, Ercolini AM, et al. HER-2/neu is a tumor rejection target in tolerized HER-2/neu transgenic mice. *Cancer Res* 2000;60:3569–76.
35. Reilly RT, Machiels JP, Emens LA, et al. The collaboration of both humoral and cellular HER-2/neu-targeted immune responses is required for the complete eradication of HER-2/neu- expressing tumors. *Cancer Res* 2001;61:880–3.
36. Garrido F, Ruiz-Cabello F, Cabrera T, et al. Implications for immunosurveillance of altered HLA class I phenotypes in human tumors. *Immunol Today* 1997;18:89–95.
37. Hicklin DJ, Marincola FM, Ferrone S. HLA class I antigen down-regulation in human cancers: T-cell immunotherapy revives an old story. *Mol Med Today* 1999;5:178–86.
38. Toes RE, Blom RJ, Offringa R, et al. Enhanced tumor outgrowth after peptide vaccination. Functional deletion of tumor-specific CTL induced by peptide vaccination can lead to the inability to reject tumors. *J Immunol* 1996;156:3911–8.
39. Pawelec G, Zeuthen J, Kiessling R. Escape from host-antitumor immunity. *Crit Rev Oncog* 1997;8:111–41.
40. Welsh RM, Stepp SE, Szomolanyi-Tsuda E, et al. Tumor viral escape from inhibited T cells. *Nat Immunol* 2002;3:112–4.
41. Diehl L, Den Boer AT, van der Voort EI, et al. The role of CD40 in peripheral T cell tolerance and immunity. *J Mol Med* 2000;78: 363–71.
42. Toes RE, Offringa R, Blom RJ, et al. Peptide vaccination can lead to enhanced tumor growth through specific T-cell tolerance induction. *Proc Natl Acad Sci U S A* 1996;93:7855–60.
43. Bansal-Pakala P, Jember AG, Croft M. Signaling through OX40 (CD134) breaks peripheral T-cell tolerance. *Nat Med* 2001;7: 907–12.
44. Diehl L, den Boer AT, Schoenberger SP, et al. CD40 activation in vivo overcomes peptide-induced peripheral cytotoxic T-lymphocyte tolerance and augments anti-tumor vaccine efficacy. *Nat Med* 1999;5:774–9.
45. Sotomayor EM, Borrello I, Tubb E, et al. Conversion of tumor-specific $CD4^+$ T-cell tolerance to T-cell priming through in vivo ligation of CD40. *Nat Med* 1999;5:780–7.
46. Gilboa E. The makings of a tumor rejection antigen. *Immunity* 1999;11:263–70.
47. Houghton AN. Cancer antigens: immune recognition of self and altered self. *J Exp Med* 1994;180:1–4.

Prevention of Spontaneous Breast Carcinoma by Prophylactic Vaccination with Dendritic/Tumor Fusion Cells

Jianchuan Xia, Yasuhiro Tanaka, Shigeo Koido, Chunlei Liu, Pinku Mukherjee, Sandra J. Gendler and Jianlin Gong

J Immunol 2003; 170:1980-1986; ;
http://www.jimmunol.org/content/170/4/1980

The Journal of Immunology is published twice each month by
The American Association of Immunologists, Inc.,
9650 Rockville Pike, Bethesda, MD 20814-3994.

Print ISSN: 0022-1767 Online ISSN: 1550-6606.

Prevention of Spontaneous Breast Carcinoma by Prophylactic Vaccination with Dendritic/Tumor Fusion Cells[1]

Jianchuan Xia,*† Yasuhiro Tanaka,* Shigeo Koido,* Chunlei Liu,*† Pinku Mukherjee,‡ Sandra J. Gendler,‡ and Jianlin Gong[2]*†§

Genetically modified mice with spontaneous development of mammary carcinoma provide a powerful tool to study the efficacy of tumor vaccines, since they mimic breast cancer development in humans. We used a transgenic murine model expressing polyomavirus middle T oncogene and mucin 1 tumor-associated Ag to determine the preventive effect of a dendritic/tumor fusion cell vaccine. The MMT (a transgenic murine model) mice developed mammary carcinoma between the ages of 65–108 days with 100% penetrance. No spontaneous CTL were detected. However, prophylactic vaccination of MMT mice with dendritic/tumor fusion cells induced polyclonal CTL activity against spontaneous mammary carcinoma cells and rendered 57–61% of the mice free of the disease at the end of experiment (180 days). Furthermore, the level of CTL activity was maintained with multiple vaccinations. The antitumor immunity induced by vaccination with dendritic/tumor fusion cells reacted differently to injected tumor cells and autochthonous tumor. Whereas the injected tumor cells were rejected, the autochthonous tumor evaded the attack and was allowed to grow. Collectively these results indicate that prophylactic vaccination with dendritic/tumor fusion cells confers sufficient antitumor immunity to counter the tumorigenesis of potent oncogenic products. The findings in the present study are highly relevant to cancers in humans. ***The Journal of Immunology*****, 2003, 170: 1980–1986.**

Genetic predisposition plays a major role in breast cancer development. The identification of oncogenes and tumor suppressor genes associated with cancer development provides an opportunity for immunologic manipulation to target these gene products, so that the onset of cancer development will be inhibited. Ideally, these studies should be conducted in animal models that mimic human cancer development. Although the transplantable tumor models have been the primary screening tools for cancer vaccine development, they do not fit this criterion, since the tumor in these models grows very quickly without the multiple stages of cancer development found in human cancers.

The advent of genetically engineered mice with a targeted gene mutation that mimics the gene alteration in human cancers provides a powerful tool to study the efficacy of vaccines. One of the transgenic murine models (MMT) developed by us (P. Mukherjee and S. Gendler, unpublished observation) expresses the polyomavirus middle T (PyMT)[3] oncogene under the transcriptional control of the mouse mammary tumor virus promoter long terminal repeats (1) and the human mucin 1 (MUC1) in a tissue-specific fashion (2). Although PyMT Ag is not associated with carcinogenesis in humans, it binds signal transduction proteins such as the c-Src family (3–5), phosphatidylinositol 3′-kinase (6), Ras (7, 8), and c-Myc (9–12). These proteins are altered in human cancers. The association with and activation of the tyrosine kinase activity of these signal transduction proteins by PyMT Ag promote cell growth and/or survival and result in widespread transformation of the mammary epithelia and rapid production of multifocal mammary adenocarcinomas in 100% of female mice (1, 13). The majority of the mice develop metastases in the lungs (1).

MUC1 is a high m.w. glycoprotein that is overexpressed in human breast cancers (14, 15). Aberrant glycosylation of the MUC1 core in breast carcinoma cells results in the generation of distinct epitopes not found in normal tissues (16, 17). Studies have demonstrated that these cryptic epitopes are recognized by CTL in patients with breast carcinoma (18, 19) and in animal models (20–23). Taken together, these findings suggest that the MUC1 Ag may represent an appropriate target for immunotherapy of breast carcinomas.

In the present study we vaccinate MMT mice at varying time points of tumor development with dendritic cells (DC) fused with spontaneous mammary carcinoma cells (FC/MMT). We show that vaccination of MMT mice with fusion cells in the early stage of tumorigenesis induces immunity that is sufficient to block or delay tumor development. This inhibition of tumor development is associated with the induction of polyclonal CTL and Ag-specific Ab. These results indicate that prophylactic vaccination with fusion cells elicits sufficient immune response to counter the tumorigenesis of potent oncogenic products.

Materials and Methods

Mice

Female C57BL/6 mice, 6–8 wk old, were purchased from Taconic Farms (Germantown, NY). The transgenic mice include 1) MT mice expressing polyomavirus middle T (PyMT) oncogene driven by the mouse mammary tumor virus long terminal repeat and developing spontaneous mammary carcinoma (1), 2) MUC1 transgenic mice (MUC1.Tg) expressing MUC1 Ag in a tissue-specific fashion similar to that in humans (2), and 3) MMT

*Dana-Farber Cancer Institute, Harvard Medical School, Boston, MA 02115; †Boston University School of Medicine, Boston, MA 02118; ‡Mayo Clinic, Scottsdale, AZ 85259; and §Beth Israel Deaconess Medical Center, Harvard Medical School, Boston, MA 02115

Received for publication September 6, 2002. Accepted for publication December 12, 2002.

The costs of publication of this article were defrayed in part by the payment of page charges. This article must therefore be hereby marked *advertisement* in accordance with 18 U.S.C. Section 1734 solely to indicate this fact.

[1] This work was supported by National Cancer Institute Grant R01CA87057, U.S. Department of Defense Breast Cancer Research programs (Grant 990344), and The Susan G. Komen Breast Cancer Foundation (Grant 9825).

[2] Address correspondence and reprint requests to Dr. Jianlin Gong, Department of Medicine, Boston University School of Medicine, 88 East Newton Street, Boston, MA 02118. E-mail address: jgong@medicine.bu.edu

[3] Abbreviations used in this paper: PyMT, polyomavirus middle T; DC, dendritic cell; FC/MT, DC fused with MT tumor cells; FC/MMT, DC fused with spontaneous mammary carcinoma cells; MUC1, mucin 1.

0022-1767/03/$02.00

mice expressing PyMT and human MUC1 double transgenes and developing spontaneous mammary carcinoma. MT mice were generated by breeding the female wild-type C57BL/6 strain with male MT mice. MMT mice were generated by crossing the female C57BL/6 strain of MUC1.Tg mice with male MT mice. All mice are congenic on the C57/BL6 background more than 10 generations. The mice were selected for expression of the PyMT oncogene and/or MUC1 by PCR (2, 24). Only female mice either positive for MT (MT mice) or MT/MUC1 double transgenes (MMT mice) were used for the experiments. The mice were maintained in microisolator cages under specific pathogen-free conditions.

PCR

The mice were examined for MUC1 and MT gene expression with PCR analysis. Ten-microgram aliquots of tail and mammary tumor tissue were digested with proteinase K, and DNA was extracted using the DNeasy Tissue Kit (Qiagen, Valencia, CA). PCR was conducted in a total volume of 50 μl in PerkinElmer Gene Amp tubes (Norwalk, CT) with the following reagents: 5 μl of 10× PCR buffer including 15 mM $MgCl_2$, 0.02% formamide, 0.2 mM dNTP, 100 nM 5′-CTTGCCAGCCATAGCACCAAG-3′ (bp 745–765) forward primer, and 100 nM 5′-CTCCACGTCGTGGACATTGATG-3′ (bp 1086–1065) reverse primer for the MUC1 gene; 100 nM 5′-AGTCACTGC TACTGCACCCAG-3′ (bp 282–302) and 100 nM 5′-CTCTCCTCAGTTC CTCGCTCC-3′ (bp 817–837) primer for the MT gene; 1.25 U of *Taq* polymerase; 2 μl of tail DNA (~500 ng), and reagent quality H_2O. The amplification program consisted of one cycle of 10 min at 94°C and 40 cycles of 30 s each at 94, 61, and 72°C. The PCR product of each reaction was analyzed by size fraction through a 1% agarose gel. Amplification of MUC1-positive DNA resulted in a 500-bp fragment (2), and amplification of MT-positive DNA resulted in a 491-bp fragment (24).

Cell culture and fusion

DC were obtained from bone marrow culture of C57BL/6 mice as described previously (25). Mammary carcinoma cells were isolated from MMT or MT mice. Briefly, spontaneous mammary tumors removed from female MMT or MT mice were teased into single cells. The tumor cells were cultured in RPMI 1640 medium supplemented with 10% heat-inactivated FCS, 2 mM L-glutamine, 10 U/ml penicillin, and 100 μg/ml streptomycin. After overnight culture, the nonadherent and dead cells were removed, and fresh medium was added. On days 2–3 of culture, the viability and phenotype of mammary carcinoma cells were checked. DC and mammary carcinoma cells were collected from the above primary cultures and placed in tubes at a 10:1 ratio. Fusion was conducted with 50% polyethylene glycol in Dulbecco's PBS without Ca^{2+} or Mg^{2+} at pH 7.4 (26, 27). DC were fused with MT tumor cells (FC/MT, MUC1-negative) or MMT tumor cells (FC/MMT, MUC1-positive). The percentage of fused cells was checked by cell surface Ag expression.

FACS analysis

The phenotypes of DC, MMT carcinoma cells, and FC/MMT cells were analyzed by flow cytometry. The cells were washed with PBS and incubated with FITC-conjugated-mAb and HMPV (anti-MUC1; BD PharMingen, San Diego, CA) for 30 min on ice. After washing twice with PBS, PE-conjugated mAb M5/114 (anti-MHC class II; BD PharMingen) or CD86 (anti-B7; BD PharMingen) was added for another 30 min on ice. Cells were washed, fixed, and analyzed by FACScan (BD Biosciences, Bedford, MA). In some experiments the fused cells were selected by FITC-HMPV (anti-MUC1) and PE-M5/114 (anti-MHC II) double-colored fluorescence cell sorting using MoFlo (Cytomation, Fort Collins, CO) with Summit version 3.0 analysis software.

Vaccination

Groups of MT or MMT mice were vaccinated s.c. with 5×10^5 FC/MT or FC/MMT cells (irradiated with 30 Gy) at the age of 15 days or younger or at 16–30 days. Vaccination was repeated monthly four additional times. The control groups consisted of mice immunized with irradiated MMT or MT tumor cells, DC mixed with tumor cells, or DC alone or mice injected with PBS. The mice were followed for up to 180 days. Mammary tissue was palpated twice a week before tumor development and every other day after the appearance of tumor. Progressively growing mass was regarded as tumor and was measured by calipers in two perpendicular diameters. The mice were sacrificed if the tumor was >2 cm. The mice were cared for according to institutional animal care and use committee guidelines.

Histologic and immunohistochemical staining

Groups of MT or MMT mice were sacrificed at varying ages. The mammary glands were harvested and fixed in 2% paraformaldehyde. Sections (5 μm) were prepared, stained with H&E, and examined under microscopy. To determine MUC1 expression in MMT mammary tissue, the section was also stained with anti-MUC1 mAb (BD PharMingen) for 30 min at room temperature and then subjected to indirect immunoperoxidase staining using the Vectastain ABC kit (Vector Laboratories, Burlingame, CA).

Humoral immune response

Sera were obtained from MMT mice immunized with 5×10^5 FC/MMT cells. Serum from MMT mice injected with PBS was used as control. Microtiter plates were precoated overnight at 4°C with 100 μl/well of MUC1 Ag (50 U/ml in PBS, pH 7.4). MUC1 Ag was purified from the ZR75 human breast cancer cell line (28). Each well was washed three times with PBS/Tween (0.05% Tween 20, v/v) and blocked with 120 μl/well 5% horse serum in PBS for 1 h at room temperature. After washing, 4-fold dilutions of mouse serum were added to each well for 2 h. The plates were washed and incubated with sheep anti-mouse IgG conjugated to HRP (Amersham Pharmacia Biotech, Piscataway, NJ). Ab complexes were detected by development with *o*-phenylenediamine (Sigma-Aldrich, St. Louis, MO) and measured with an ELISA microplate Autoreader EL310 at OD 490 nm.

Chromium-51 cytotoxicity assay

Splenocytes were isolated from MT or MMT mice immunized with 5×10^5 FC/MT or FC/MMT cells by Ficoll separation. Splenocytes from nonvaccinated MT or MMT mice were used as controls. The target cells (MT and MMT tumor cells or MC38 and MC38/MUC1 carcinoma cell lines) were prelabeled with chromium 51 for 1 h at 37°C and added to the wells of 96-well, V-bottom plates with T cells (effector) for 5 h at 37°C. The supernatants were assayed for chromium-51 release in a gamma counter, and CTL activity was determined at the indicated E:T cell ratios. The percentage of specific chromium-51 release was determined by the following equation: percent specific release = [(experimental − spontaneous)/(maximum − spontaneous)] × 100.

Tumor cell challenge

Groups of MMT mice at the age of 38, 65, or 92 days were vaccinated three times with 5×10^5 FC/MMT at 7-day intervals. Five days after the third vaccination, the mice were challenged s.c. in the flank near the base of tail with mammary carcinoma cells isolated from MMT. As controls, littermates were injected with PBS and then challenged with mammary carcinoma cells. The mice were followed for up to 30 days after inoculation of tumor cells. Tumor growth was checked and measured daily using calipers.

Statistical analysis

Statistical significance was analyzed using χ^2 and Student's *t* tests.

Results

Characterization of MMT mice

The MMT mice were generated by crossing female C57BL/6 strain of MUC1.Tg with male MT mice that expressed PyMT oncogene. PCR was used to detect the bitransgenes. Amplification of MUC1- and MT-positive DNA resulted in 500- and 491-bp fragments, respectively. Whereas the MT gene occurred in tail and mammary tissues from MMT and MT mice, the MUC1 gene was present only in samples from MMT mice (Fig. 1*A*). To determine tumorigenesis, groups of MMT and MT mice were sacrificed at multiple time points, and mammary tissue was collected. Histologic examination revealed that MMT and MT mice developed mammary carcinoma in roughly three stages that arose sequentially over the lifetime of the mouse. Normal mammary glands expressed MUC1, yet were morphologically asymptomatic until 3 wk of age. Focal hyperplasia, beginning to appear in the fourth week, evolved into mammary intraepithelial neoplasms, carcinoma in situ, and finally diffuse invasive tumors (Fig. 1*B*). The mammary tumors in MMT and MT mice consisted of glandular adenocarcinoma with some variation. Most tumors were sclerotic, with dense connective tissue stroma separating the tumor cells. Cribriform and solid tumors were also observed. Immunohistologic examination demonstrated MUC1 expression in mammary tissue and/or tumors from MMT, but not MT, mice. Whereas MUC1 was detected on the apical surface of epithelial cells lining

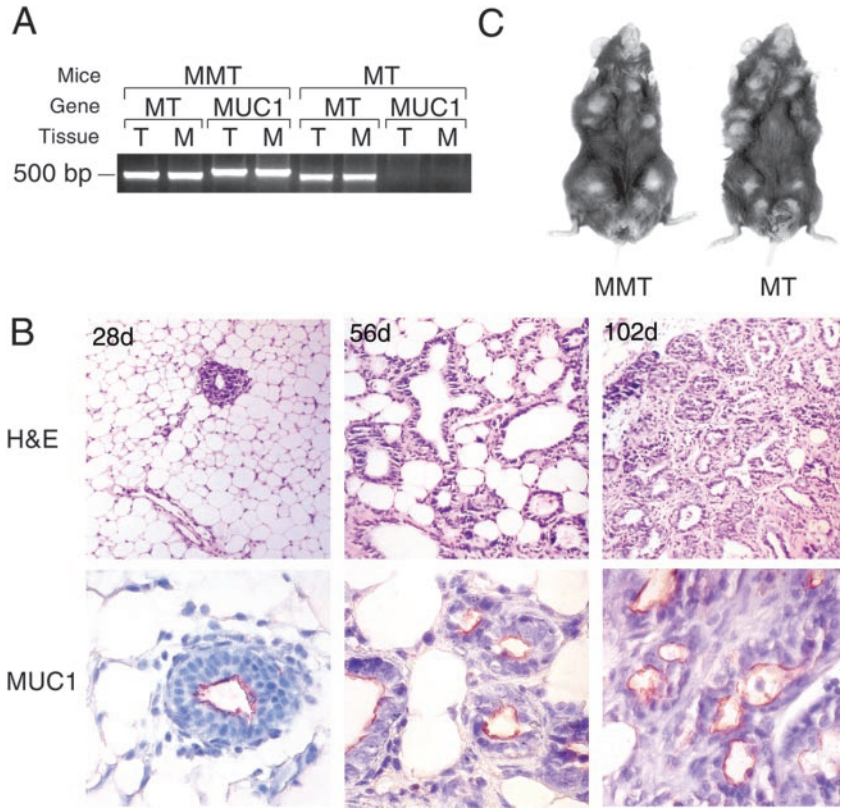

FIGURE 1. Development of spontaneous carcinoma in MMT and MT mice. *A*, PCR analysis for MT genes and MUC1 in tail tissue (T) and mammary tumor (M) of MMT and MT mice. Amplification of MUC1-positive DNA results in a 500-bp fragment, and amplification of MT-positive DNA results in a 491-bp fragment. *B*, Histologic examination with H&E staining of spontaneous mammary tumor in MMT mice at different ages (magnification, ×10). Immunohistochemical staining with anti-MUC1 mAb to detect MUC1 expression in mammary tissue or tumor (magnification, ×40). *C*, Development of multiple mammary carcinomas in MMT and MT mice by the age of 102 days.

the lumen in mammary tissue, strong MUC1 staining was found throughout mammary tumor cells (Fig. 1*B*).

The tumor incidence data indicate that the mammary tumors could be palpated when the mice were ~65 days old. Approximately half the mice developed mammary tumors at 80–90 days. Almost all the tumors were multiple, with synchronous kinetics in MT and MMT mice (Fig. 1*C*). The tumors progressed very rapidly, and the mice became moribund and were sacrificed 3–4 wk after the appearance of mammary carcinoma.

Collectively, these findings indicate that the expression of PyMT oncogene results in transformation of mammary epithelia and rapid production of mammary carcinomas in MT and MMT mice. More important, multiple stages of tumor development, similar to those in human cancers, are observed. Thus, MMT mice provide a better model for studies of tumorigenesis and vaccine development. The consistent expression of MUC1 in mammary carcinomas represents a potential target for immunotherapy and a marker for measuring the immune response.

Generation of DC/spontaneous mammary carcinoma fusion cells

To develop a DC/tumor fusion cell vaccine, spontaneous mammary carcinoma cells were isolated from MMT and MT mice. The tumor cells were cultured in vitro for 2 days and fused with syngeneic DC generated from wild-type mice. To assess the formation of fusion cells, two-colored flow cytometry was used. Whereas MUC1 was detected in the mammary carcinomas of MMT tumor, and MHC class II and costimulatory molecules were detected in DC, fusion of DC with mammary carcinoma cells from MMT mice (FC/MMT) resulted in dual expression of MUC1 and MHC class II or MUC1 and costimulatory molecules (Fig. 2). In contrast, there was no MUC1 expression on DC or fusion of DC with mammary carcinoma cells from MT mice (FC/MT; data not shown). These results indicate that fusion of DC with spontaneous mammary carcinomas results in the expression of tumor Ags in the context of costimulatory signals and MHC molecules.

Prevention of mammary carcinomas in MMT and MT mice by fusion cell vaccination

Previous data indicate that immunization of mice with FC/MUC1 induces antitumor immune responses that provide protection against the challenge of MUC1-positive tumor cells (26, 29). However, we do not know whether prophylactic vaccination with fusion cells can block the development of mammary carcinomas in a genetically altered model prone to breast cancer. To address this issue, two groups of MMT mice were immunized with FC/MMT. The vaccination was commenced in the first group of mice at the age of 15 days or younger and in the second group of mice at the age of 16–30 days. The immunization was repeated four times at

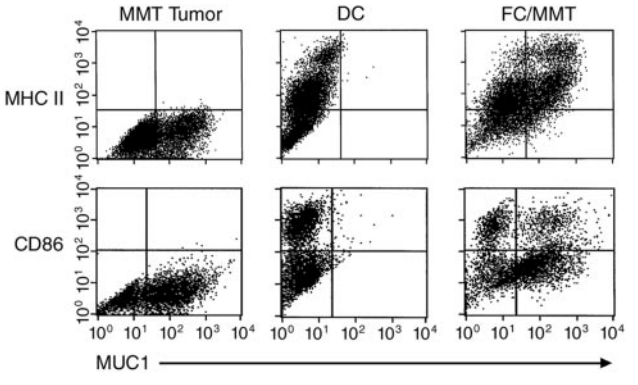

FIGURE 2. Phenotype of FC/MMT fusion cells. Expression of MUC1 and MHC class II or CD86 on FC/MMT determined by two-color flow cytometric analysis.

monthly intervals. All MMT mice treated with irradiated MMT tumor cells, DC mixed with tumor cells, DC alone, or PBS developed mammary carcinomas between the age of 65–108 days and were usually sacrificed after becoming moribund around 90–120 days (Fig. 3*A*). In contrast, immunization with FC/MMT fusion cells rendered 57–61% of the mice free of disease at the end of the experiment (180 days). It appears that the group with earlier vaccination faired better, with 61% protection (<15 days old; $n = 18$) compared with 57% protection in groups vaccinated at the age of 16–30 days ($n = 42$). The percentage of tumor-free mice from both groups is statistically significant compared with those of the control groups ($p = 0.001$). However, there is no statistically significant difference between the two experimental groups ($p = 0.5$; Fig. 3*A*). A similar trend, yet less positive results, were obtained in MT mice. Vaccination with FC/MT provided 41% protection for the mice with earlier vaccination and 33% protection for mice with later vaccination (Fig. 3*B*). Histologic examination of mammary tissue from vaccinated MMT mice at the end of the experiment revealed no tumor formation (Fig. 3*C*). These results indicate that prophylactic vaccination with DC/tumor fusion cells induces potent antitumor immunity to prevent or delay the development of mammary tumors in genetically altered mice prone to breast cancer.

Polyclonal CTL induced by vaccination with FC/MMT fusion cells

To define in part the basis of antitumor immunity induced by vaccination with FC/MMT, we measured CTL activity against syngeneic mammary carcinoma cells at varying time points in groups of different ages. Fig. 4*A* shows increased CTL activity against MMT mammary carcinoma cells after vaccination. The CTL activity was elevated after the second vaccination and peaked after the third and fourth vaccinations. It appears that the age of the mice had little impact on the CTL activity. In contrast, there was little, if any, CTL activity in nonvaccinated mice, regardless of whether they were tumor-bearing. A similar trend of CTL activity was found with splenocytes from immunized MT mice (Fig. 4*B*). Moreover, the CTL from immunized MMT mice lysed not only the MMT tumor cells from which the fusion cells were constructed, but also the syngeneic MC38/MUC1 carcinoma and MT tumor cells (Fig. 4, *C* and *D*), indicating that polyclonal CTL were induced. These results indicate that there are no spontaneous CTL in naive MMT and MT mice and that vaccination with FC/MMT or FC/MT induces polyclonal CTL against the relevant tumor cells with shared tumor Ags.

Induction of anti-MUC1 humoral response in MMT mice vaccinated with FC/MMT fusion cells

To determine the level of MUC1-specific Ab, MMT mice were vaccinated s.c. with 5×10^5 FC/MMT. The vaccination was repeated three additional times at monthly intervals. Nonvaccinated MMT mice were used as controls. The sera from MMT mice vaccinated with FC/MMT at different ages were collected at multiple time points and analyzed for the presence of anti-MUC1 Ab by ELISA. Vaccination with FC/MMT induced an anti-MUC1 humoral response in MMT mice. The level of anti-MUC1 Ab increased after the third and fourth vaccinations (Fig. 5*A*). However,

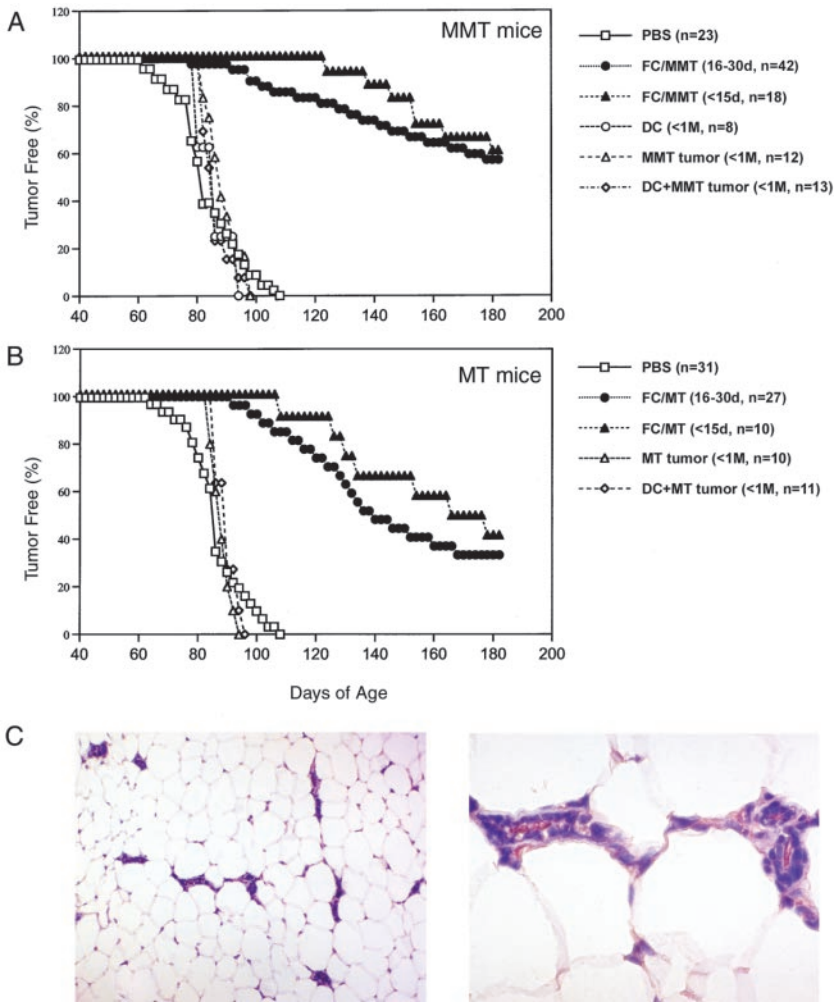

FIGURE 3. Prevention of spontaneous mammary tumor in vaccinated MMT and MT mice. *A*, Female MMT mice were vaccinated s.c. with 5×10^5 FC/MMT fusion cells at the base of tail at the age of 15 days or younger (▲) or at 16–30 days (●). Vaccination was repeated four times at monthly intervals. Mice <1 mo old were injected with irradiated MMT tumor cells (△), DC mixed with MMT tumor cells (◇), DC alone (○), or PBS (□) as controls. *B*, Female MT mice were vaccinated s.c. with 5×10^5 FC/MT fusion cells at the age of 15 days or younger (▲) or at 16–30 days (●). Vaccination was repeated four times at monthly intervals. Mice <1 mo old were injected with irradiated MT tumor cells (△), DC mixed with MT tumor cells (◇), or PBS (□) as controls. The mice were followed for up to 180 days, at which time the number of mice free of tumor was determined. *C*, Photomicrograph of immunohistochemical stained sections of mammary tissue removed from a vaccinated MMT mouse at the age of 180 days (*left panel*, ×10; *right panel*, ×40).

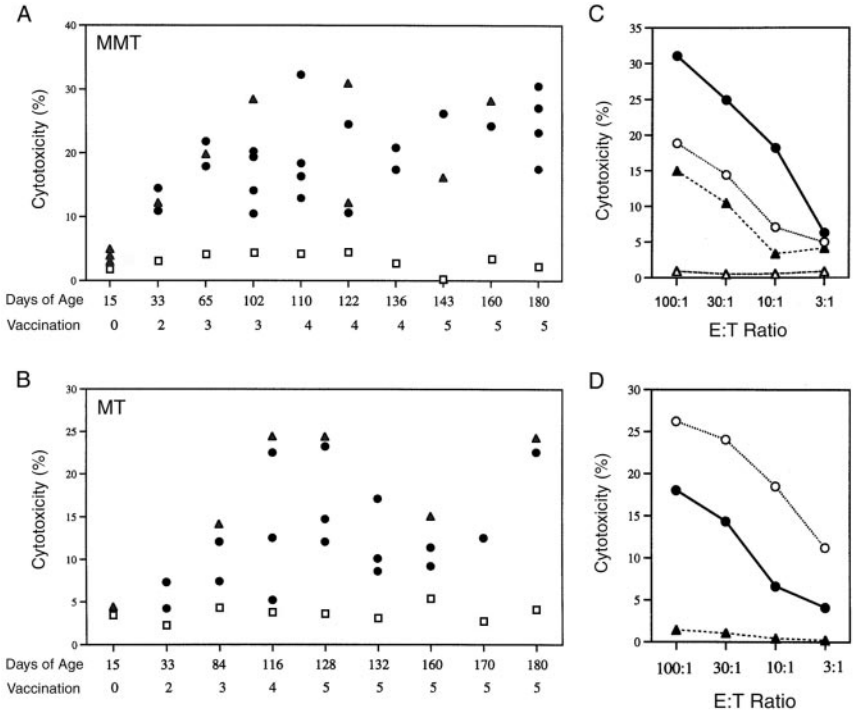

FIGURE 4. Antitumor response induced by FC/MMT and FC/MT fusion cell vaccination. *A* and *B*, Dot plot illustration of CTL activity induced by vaccination with fusion cells in MMT and MT mice. *A*, Splenocytes isolated from MMT mice at various ages that had been vaccinated at different times with 5×10^5 FC/MMT were incubated with MMT spontaneous mammary tumor cells at a 100:1 ratio. Each dot represents CTL activity in an MMT mouse at the indicated age and number of vaccinations. CTL activity was determined in splenocytes from MMT mice vaccinated with FC/MMT at the age of <15 days (▲) or at 16–30 days (●) or injected with PBS (□). *B*, Splenocytes isolated from MT mice at various ages vaccinated at different times with 5×10^5 FC/MT were incubated with MT spontaneous mammary tumor cells at a 100:1 ratio (●). CTL activity was determined in splenocytes from MT mice vaccinated with FC/MT at the age of <15 days (▲) or at 16–30 days (●) or injected with PBS (□). *C* and *D*, Specificity of CTL from immunized mice. Splenocytes isolated from MMT mice vaccinated with FC/MMT (*C*) and MT mice vaccinated with FC/MT (*D*) were incubated with MC38/MUC1 (▲), MC38 (△), and spontaneous mammary tumor cells from MMT mice (●) and MT mice (○) at the indicated E:T cell ratio. CTL activity was determined by the standard ^{51}Cr release assay.

a low level of anti-MUC1 Ab was detected in nonvaccinated MMT mice (Fig. 5*B*). In contrast, there was no anti-MUC1 Ab in MT mice immunized with FC/MT (Fig. 5, *A* and *B*). These results indicate that immunization with FC/MUC1 is associated with the production of anti-MUC1 Ab in MMT mice.

Rejection of challenge MMT mammary carcinoma cells in vaccinated MMT mice

Our previous data demonstrate that prophylactic vaccination with fusion cells rendered more than half the mice free of tumors for up to 180 days. Yet the remaining mice still developed tumors, although their appearance was delayed (Fig. 3). One possibility is that the host CTL are exhausted or have developed tolerance/ignorance. To explore this possibility we determined the existence of antitumor immunity by challenging MMT mice vaccinated at various ages with MMT mammary carcinoma cells. Three colonies of mice were vaccinated with FC/MMT. The vaccination was commenced in mice at the ages of 38, 65, and 96 days ($n = 4$/group). The vaccination was repeated three times at weekly intervals. Five days after the last vaccination, the mice were challenged s.c. with 5×10^5 MMT tumor cells in the flank near the base of tail. There was no tumor growth in the challenge sites of all vaccinated MMT mice regardless of age (Fig. 6, *A–C*). In contrast, all nonvaccinated littermates ($n = 4$/group) developed MMT tumor at the challenge sites (Fig. 6, *A–C*). The group of MMT mice vaccinated at the age of 65 days rejected the challenge tumor, but developed spontaneous mammary carcinoma, although its appearance was delayed (Fig. 6*B*). These results indicate a differential immune response to injected and autochthonous tumors. Moreover, even though mammary tumors had already been palpated in the group of mice at the age of 96 days when vaccination was initiated, the tumor-bearing mice were still able to mount an effective antitumor immune response against the injected MMT tumor (Fig. 6*C*). Antitumor immunity is induced in MMT mice regardless of age and presence of tumor at the time of vaccination. The CTL (Fig. 4) are functional in response to the tumor cell challenge; however, they fail to inhibit or eliminate autochthonous tumors. Taken together, these results indicate that fundamental differences exist in the immune response against challenge or autochthonous tumors.

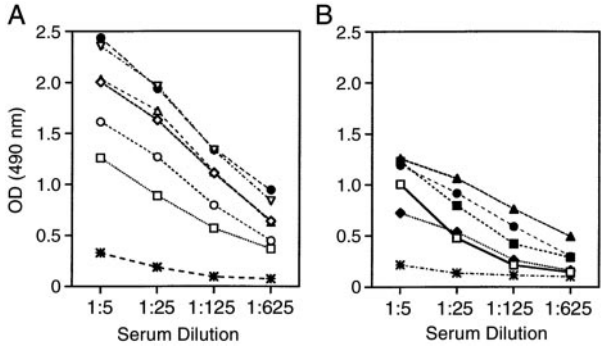

FIGURE 5. Humoral response induced by vaccination with FC/MMT in MMT mice. Sera were collected from vaccinated MMT mice at various ages ($n = 3$ in each group). Anti-MUC1 Ab was detected by ELISA assay. *A*, Anti-MUC1 Ab detected in FC/MMT-vaccinated MMT mice at the age of 36 (□), 65 (○), 102 (◇), 111 (△), 160 (▽), and 182 (●) days. *B*, MUC1-specific Ab from nonvaccinated MMT mice at the age of 46 (□), 110 (♦), 120 (■), 132 (▲), and 142 (●) days. Sera from MT mice (*) were assayed as control.

Discussion

DC/tumor fusion cells have induced potent antitumor immunity in a variety of models (26, 29–32). However, this is the first time that such a study has been conducted in a genetically modified model of spontaneous breast cancer. The use of genetically modified mice (MMT) offers several advantages over the transplantable tumor models: 1) the mice carry genetic alterations that interfere with signal transduction in a manner similar to that in human breast cancers; 2) the mammary carcinoma develops in multiple stages, as does human cancer; 3) the tumor develops in a competent immune system; 4) the mammary carcinoma progresses much more slowly than transplanted tumor, thus giving the host sufficient time

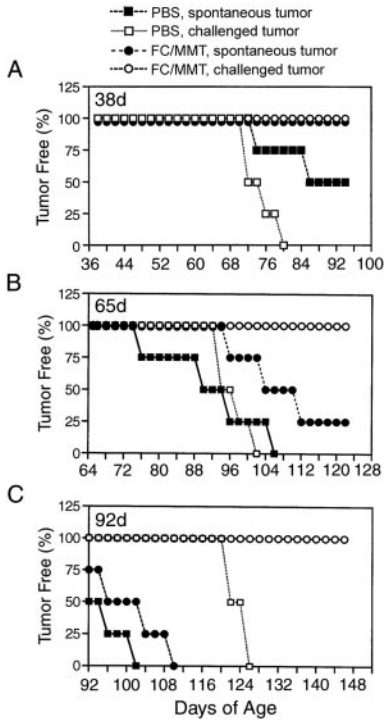

FIGURE 6. Rejection of injected mammary carcinoma cells in vaccinated MMT mice. MMT mice at different ages were vaccinated three times s.c. with 5×10^5 FC/MMT. Five days after the third vaccination, the mice were challenged s.c. with 5×10^5 MMT tumor cells in the flank near the base of the tail. The mice were followed for 30 days. Growth of spontaneous mammary tumor from mice vaccinated with FC/MMT (●) or from their littermates injected with PBS (■) and growth of injected MMT tumor from vaccinated mice (○) or from their littermates vaccinated with PBS (□) were determined. *A*, Percentage of tumor-free mice when vaccination was commenced at the age of 38 days. *B*, Percentage of tumor-free mice when vaccination commenced at the age of 65 days. *C*, Percentage of tumor-free mice when vaccination commenced at the age of 92 days.

to mount an effective immune response; 5) 100% of the mice develop mammary tumors within a reasonable time, making this a reliable tumor model; and 6) the expression of MUC1 provides a useful target for immunotherapy as well as a marker for measuring the immune response.

The present study demonstrates that vaccination with DC/tumor fusion cells confers sufficient antitumor immunity to block or delay mammary tumor development in a genetically altered model prone to breast cancer. The advantage of using DC/tumor fusion cells are 3-fold. First, the fusion cells are capable of expressing the whole repertoire of tumor Ags from an individual tumor. Thus, tumor-specific polyclonal CTLs are induced. Second, the fusion cells express the tumor Ags in the context of costimulatory signals and MHC class I and II molecules. Therefore, both arms of cell-mediated immunity are activated, and the immune response is greatly enhanced (27). Third, fusion cells are capable of processing and presenting tumor Ag, including those that are unidentified, thus circumventing the necessity of defining the tumor Ags. The findings that prophylactic use of DC/tumor fusion cells blocks or delays the development of spontaneous mammary tumor in the present study further support the idea that DC/tumor fusion cells may represent a promising alternative in the prevention and treatment of breast cancer.

One commonly shared tumor Ag is MUC1, which is expressed in 72% of cancers (33). MUC1 has been recognized as a multifunctional protein that plays a role in the protection and lubrication of mucous membrane, signal transduction, and modulation of the immune system (34). MUC1 is not required for mammary carcinogenesis in MMT mice. However, our study shows that vaccination with FC/MMT provides better protection than that with FC/MT (Fig. 3, *A* and *B*). These results indicate that MUC1 is an immunogenic Ag capable of eliciting immune response to reject MUC1-positive tumors when properly presented.

MUC1 is a tumor-associated Ag expressed in a variety of normal tissues. Theoretically, the anti-MUC1 immune response can be detrimental to the healthy organs expressing MUC1. However, we failed to observe any autoimmune disease in animal studies. Vaccinated MMT mice have been followed for >1 yr. They have survived in a healthy state without manifestation of any autoimmune disease (our unpublished observations). The difference in the expression of MUC1 between cancer and normal tissue may be attributed to the differential response. The spontaneous mammary cancer overexpressed MUC1 diffusely (Fig. 1). In contrast, MUC1 expression in mammary tissue was limited to the apical surface of the epithelium facing the lumen, which is not accessible to the immune system. The MUC1 expressed by cancer cells is also underglycosylated, thus exposing the protein core. The unmasking of the core protein may reveal the peptide epitopes that are recognized by CTL (22). Collectively, these results suggest that MUC1 is a preferred target for a cancer vaccine.

Vaccination leads to life-long protection against infectious disease. However, tumor Ag elicits an immune response of only a short duration. To determine whether CTL can be induced and then maintained, we vaccinated the MMT and MT mice multiple times at monthly intervals. A comparable level of CTL was demonstrated in multiply vaccinated mice, indicating the CTL are maintained. Furthermore, these CTL are functional and reject injected tumor cells in vivo. We have also shown the induction of competent antitumor immunity regardless of tumor burden by the host, indicating that tumor burden in mice may not be translated into systemic immune suppression. However, we failed to detect MUC1-specific CTL in tumor-bearing naive MMT mice. The lack of spontaneous MUC1-specific CTL may be attributed to the fact that tumor cells are not professional APC. The differences in spontaneous tumor models may also dictate whether spontaneous CTL are induced. No naturally occurring MUC1-specific CTL have been found in tumor-bearing MMT mice (P. Mukherjee and S. J. Gendler, unpublished observations).

The goal of vaccine development has been to prevent the disease; thus, its use is prophylactic. Most studies for tumor vaccine are focused on the treatment of tumors. Few studies have been conducted for prophylactic use, partly due to the lack of suitable tumor models. In the present study the prophylactic use of FC/MMT fusion cell vaccine rendered 57–61% mice free of mammary tumors at the end of the experiment. The result raises hope that a tumor vaccine can be developed to prevent the disease in populations with a high risk of breast cancer. Our results also indicate that 40% of the mice still develop mammary carcinoma, although its inception is delayed. Several mechanisms may contribute to this situation. Tumor cells are known to evade the immune system by down-regulation of tumor Ag/MHC molecules (35, 36), by Ag presentation in the absence of costimulatory molecules (37, 38), or by the development of tolerance and/or anergy of T cells (39). Our data, however, suggest that differential immune response by the host to injected and autochthonous tumor may be responsible for the development of spontaneous mammary carcinomas in our model. The vaccinated mice reject the transplanted mammary tumor cells, thus indicating the existence of functionally competent CTL; yet they still develop autochthonous

mammary tumors. It appears that the autochthonous tumor is ignored by the CTL. Of particular interest, such ignoring develops late in tumor development, since the CTL or antitumor immunity induced by the vaccination with fusion cells in all the mice is effective in delaying the development of mammary tumor. These results contradict the findings by Rovero et al. (40). In their report immunization with DNA vaccine against rat Her-2/neu p185 rendered six BALB/c mice expressing the Her-2/neu oncogene free of spontaneous mammary tumors, whereas three of the mice developed challenge tumors. We attribute the discrepancy to differences in the animal models used, the potency of oncogenes, the vaccines, and the vaccination regimens. It remains to be investigated whether the autochthonous tumor develops a shield to escape attack by CTL and/or whether the CTL have lost the ability to kill tumor cells. Alternatively, stimulation by the oncogene product may be too powerful to be inhibited in the long term, since PyMT is a potent oncogene (1, 41). Nevertheless, the finding that vaccination with fusion cells doubles the latency period of mammary carcinoma in a model expressing such a potent oncogene is encouraging. Our next goal is to improve the long term efficacy of the vaccine.

References

1. Guy, C. T., R. D. Cardiff, and W. J. Muller. 1992. Induction of mammary tumors by expression of polyomavirus middle T oncogene: a transgenic mouse model for metastatic disease. *Mol. Cell. Biol. 12:954.*
2. Rowse, G. J., R. M. Tempero, M. L. VanLith, M. A. Hollingsworth, and S. J. Gendler. 1998. Tolerance and immunity to MUC1 in a human MUC1 transgenic murine model. *Cancer Res. 58:315.*
3. Courtneidge, S. A., and A. E. Smith. 1983. Polyoma virus transforming protein associates with the product of the c-src cellular gene. *Nature 303:435.*
4. Guy, C. T., S. K. Muthuswamy, R. D. Cardiff, P. Soriano, and W. J. Muller. 1994. Activation of the c-Src tyrosine kinase is required for the induction of mammary tumors in transgenic mice. *Genes Dev. 8:23.*
5. Kornbluth, S., M. Sudol, and H. Hanafusa. 1987. Association of the polyomavirus middle-T antigen with c-yes protein. *Nature 325:171.*
6. Webster, M. A., J. N. Hutchinson, M. J. Rauh, S. K. Muthuswamy, M. Anton, C. G. Tortorice, R. D. Cardiff, F. L. Graham, J. A. Hassell, and W. J. Muller. 1998. Requirement for both Shc and phosphatidylinositol 3′ kinase signaling pathways in polyomavirus middle T-mediated mammary tumorigenesis. *Mol. Cell Biol. 18:2344.*
7. Jelinek, M. A., and J. A. Hassell. 1992. Reversion of middle T antigen-transformed Rat-2 cells by Krev-1: implications for the role of p21c-ras in polyomavirus-mediated transformation. *Oncogene 7:1687.*
8. Dankort, D. L., and W. J. Muller. 2000. Signal transduction in mammary tumorigenesis: a transgenic perspective. *Oncogene 19:1038.*
9. D'Cruz, C. M., E. J. Gunther, R. B. Boxer, J. L. Hartman, L. Sintasath, S. E. Moody, J. D. Cox, S. I. Ha, G. K. Belka, A. Golant, et al. 2001. c-MYC induces mammary tumorigenesis by means of a preferred pathway involving spontaneous Kras2 mutations. *Nat. Med. 7:235.*
10. Nass, S. J., and R. B. Dickson. 1997. Defining a role for c-Myc in breast tumorigenesis. *Breast Cancer Res. Treat. 44:1.*
11. Dawe, C. J., R. Freund, G. Mandel, K. Ballmer-Hofer, D. A. Talmage, and T. L. Benjamin. 1987. Variations in polyoma virus genotype in relation to tumor induction in mice: characterization of wild type strains with widely differing tumor profiles. *Am. J. Pathol. 127:243.*
12. Blackshear, P. E. 2001. Genetically engineered rodent models of mammary gland carcinogenesis: an overview. *Toxicol. Pathol. 29:105.*
13. Cardiff, R. D., and W. J. Muller. 1993. Transgenic mouse models of mammary tumorigenesis. *Cancer Surv. 16:97.*
14. Hayes, D. F., V. R. Zurawski, Jr., and D. W. Kufe. 1986. Comparison of circulating CA15–3 and carcinoembryonic antigen levels in patients with breast cancer. *J. Clin. Oncol. 4:1542.*
15. Zotter, S., P. C. Hageman, A. Lossnitzer, M. J. Mooi, and J. Hilgers. 1988. Tissue and Tumor distribution of human polymorphic epithelial mucin. *Cancer Rev. 11/12:55.*
16. Burchell, J., S. Gendler, J. Taylor-Papadimitriou, A. Girling, A. Lewis, R. Millis, and D. Lamport. 1987. Development and characterization of breast cancer reactive monoclonal antibodies directed to the core protein of the human milk mucin. *Cancer Res. 47:5476.*
17. Girling, A., J. Bartkova, J. Burchell, S. Gendler, C. Gillett, and J. Taylor-Papadimitriou. 1989. A core protein epitope of the polymorphic epithelial mucin detected by the monoclonal antibody SM-3 is selectively exposed in a range of primary carcinomas. *Int. J. Cancer 43:1072.*
18. Jerome, K. R., D. L. Barnd, K. M. Bendt, C. M. Boyer, J. Taylor-Papadimitriou, I. F. McKenzie, R. C. Bast, Jr., and O. J. Finn. 1991. Cytotoxic T-lymphocytes derived from patients with breast adenocarcinoma recognize an epitope present on the protein core of a mucin molecule preferentially expressed by malignant cells. *Cancer Res. 51:2908.*
19. Reddish, M., G. D. MacLean, R. R. Koganty, J. Kan-Mitchell, V. Jones, M. S. Mitchell, and B. M. Longenecker. 1998. Anti-MUC1 class I restricted CTLs in metastatic breast cancer patients immunized with a synthetic MUC1 peptide. *Int. J. Cancer 76:817.*
20. Mukherjee, P., A. R. Ginardi, C. S. Madsen, C. J. Sterner, M. C. Adriance, M. J. Tevethia, and S. J. Gendler. 2000. Mice with spontaneous pancreatic cancer naturally develop MUC-1-specific CTLs that eradicate tumors when adoptively transferred. *J. Immunol. 165:3451.*
21. Morikane, K., R. Tempero, C. L. Sivinski, S. Kitajima, S. J. Gendler, and M. A. Hollingsworth. 2001. Influence of organ site and tumor cell type on MUC1-specific tumor immunity. *Int. Immunol. 13:233.*
22. Mukherjee, P., A. R. Ginardi, T. L. Tinder, C. J. Sterner, and S. J. Gendler. 2001. MUC1-specific cytotoxic T lymphocytes eradicate tumors when adoptively transferred in vivo. *Clin. Cancer Res. 7:848.s.*
23. Schell, T. D., J. D. Lippolis, and S. S. Tevethia. 2001. Cytotoxic T lymphocytes from HLA-A2.1 transgenic mice define a potential human epitope from simian virus 40 large T antigen. *Cancer Res. 61:873.*
24. Ritland, S. R., G. J. Rowse, Y. Chang, and S. J. Gendler. 1997. Loss of heterozygosity analysis in primary mammary tumors and lung metastases of MMTV-MTAg and MMTV-neu transgenic mice. *Cancer Res. 57:3520.*
25. Inaba, K., M. Inaba, N. Romani, H. Aya, M. Deguchi, S. Ikehara, S. Muramatsu, and R. M. Steinman. 1992. Generation of large numbers of dendritic cells from mouse bone marrow cultures supplemented with granulocyte/macrophage colony-stimulating factor. *J. Exp. Med. 176:1693.*
26. Gong, J., D. Chen, M. Kashiwaba, and D. Kufe. 1997. Induction of antitumor activity by immunization with fusions of dendritic and carcinoma cells. *Nat. Med. 3:558.*
27. Koido, S., Y. Tanaka, D. Chen, D. Kufe, and J. Gong. 2002. The kinetics of in vivo priming of CD4 and CD8 T cells by dendritic/tumor fusion cells in MUC1-transgenic mice. *J. Immunol. 168:2111.*
28. Sekine, H., T. Ohno, and D. W. Kufe. 1985. Purification and characterization of a high molecular weight glycoprotein detectable in human milk and breast carcinomas. *J. Immunol. 135:3610.*
29. Gong, J., D. Chen, M. Kashiwaba, Y. Li, L. Chen, H. Takeuchi, H. Qu, G. J. Rowse, S. J. Gendler, and D. Kufe. 1998. Reversal of tolerance to human MUC1 antigen in MUC1 transgenic mice immunized with fusions of dendritic and carcinoma cells. *Proc. Natl. Acad. Sci. USA 95:6279.*
30. Wang, J., S. Saffold, X. Cao, J. Krauss, and W. Chen. 1998. Eliciting T cell immunity against poorly immunogenic tumors by immunization with dendritic cell-tumor fusion vaccines. *J. Immunol. 161:5516.*
31. Lespagnard, L., P. Mettens, A. M. Verheyden, N. Tasiaux, K. Thielemans, S. van Meirvenne, A. Geldhof, P. De Baetselier, J. Urbain, O. Leo, et al. 1998. Dendritic cells fused with mastocytoma cells elicit therapeutic antitumor immunity. *Int. J. Cancer 76:250.*
32. Lindner, M., and V. Schirrmacher. 2002. Tumour cell-dendritic cell fusion for cancer immunotherapy: comparison of therapeutic efficiency of polyethylen-glycol versus electro-fusion protocols. *Eur. J. Clin. Invest. 32:207.*
33. Greenlee, R. T., T. Murray, S. Bolden, and P. A. Wingo. 2000. Cancer statistics, 2000. *CA Cancer J. Clin. 50:7.*
34. Gendler, S. J. 2001. MUC1, the renaissance molecule. *J. Mammary Gland. Biol. Neoplasia 6:339.*
35. Cohen, E. P., and T. S. Kim. 1994. Neoplastic cells that express low levels of MHC class I determinants escape host immunity. *Semin. Cancer Biol. 5:419.*
36. Lollini, P. L., G. Nicoletti, L. Landuzzi, C. De Giovanni, I. Rossi, E. Di Carlo, P. Musiani, W. J. Muller, and P. Nanni. 1998. Down regulation of major histocompatibility complex class I expression in mammary carcinoma of HER-2/neu transgenic mice. *Int. J. Cancer 77:937.*
37. Townsend, S. E., and J. P. Allison. 1993. Tumor rejection after direct costimulation of $CD8^+$ T cells by B7-transfected melanoma cells. *Science 259:368.*
38. Huang, A. Y., A. T. Bruce, D. M. Pardoll, and H. I. Levitsky. 1996. Does B7–1 expression confer antigen-presenting cell capacity to tumors in vivo? *J. Exp. Med. 183:769.*
39. Speiser, D. E., R. Miranda, A. Zakarian, M. F. Bachmann, K. McKall-Faienza, B. Odermatt, D. Hanahan, R. M. Zinkernagel, and P. S. Ohashi. 1997. Self antigens expressed by solid tumors do not efficiently stimulate naive or activated T cells: implications for immunotherapy. *J. Exp. Med. 186:645.*
40. Rovero, S., A. Amici, E. D. Carlo, R. Bei, P. Nanni, E. Quaglino, P. Porcedda, K. Boggio, A. Smorlesi, P. L. Lollini, et al. 2000. DNA vaccination against rat her-2/Neu p185 more effectively inhibits carcinogenesis than transplantable carcinomas in transgenic BALB/c mice. *J. Immunol. 165:5133.*
41. Jakubczak, J. L., G. Merlino, J. E. French, W. J. Muller, B. Paul, S. Adhya, and S. Garges. 1996. Analysis of genetic instability during mammary tumor progression using a novel selection-based assay for in vivo mutations in a bacteriophage λ transgene target. *Proc. Natl. Acad. Sci. USA 93:9073.*

Immunology 2003 **109** 300–307

Immunotherapy of spontaneous mammary carcinoma with fusions of dendritic cells and mucin 1-positive carcinoma cells

DONGSHU CHEN,* JIANCHUAN XIA,*† YASUHIRO TANAKA,* HONGSONG CHEN,* SHIGEO KOIDO,* OLIVER WERNET,* PINKU MUKHERJEE,‡ SANDRA J. GENDLER,‡ DONALD KUFE* & JIANLIN GONG*†§

**Dana–Farber Cancer Institute, Harvard Medical School, Boston, MA, †Boston University School of Medicine, Boston, MA, ‡Samuel C. Johnson Medical Research Building, Mayo Clinic, Scottsdale, AZ, and §Beth Israel Deaconess Medical Center, Harvard Medical School, Boston, MA, USA*

SUMMARY

The tumour-associated antigen mucin 1 (MUC1) is a multifunctional protein involved in protection of mucous membranes, signal transduction, and modulation of the immune system. More than 70% of cancers overexpress MUC1, making MUC1 a potential target for immunotherapy. In the present study, MUC1 transgenic mice were crossed with syngeneic strains that express the polyomavirus middle-T oncogene (PyMT) driven by the mouse mammary tumour virus promoter long-terminal repeat (MMTV-LTR). The resultant breed (MMT mice) developed spontaneous MUC1-expressing mammary carcinomas with 100% penetrance at 8–15 weeks of age. As found in human breast cancer, the mammary carcinoma in MMT mice arose in multiple stages. Immunization with fusions of dendritic cells and MUC1-positive tumour cells (FC/MUC1) induced MUC1-specific immune responses that blocked or delayed the development of spontaneous breast carcinomas. In contrast, there was no delay of tumour development in MMT mice immunized with irradiated MC38/MUC1 tumour cells. The efficacy of fusion cells was closely correlated with the timing of initial immunization. Immunization with FC/MUC1 initiated in MMT mice at <1, 1–2 and 2–3 months of age rendered 33, 5 and 0% of mice free of tumour, respectively, up to 6 months. Whereas mice immunized in the later stage of tumour development succumbed to their disease, immunization resulted in control of tumour progression and prolongation of life. These results indicate that immunization with FC/MUC1 can generate an anti-MUC1 response that is sufficient to delay the development of spontaneous mammary carcinomas and control tumour progression in MMT mice.

INTRODUCTION

Active specific immunotherapy is an approach used to elicit and boost immune effector mechanisms to achieve an augmented antitumour response.[1–3] T-cell-mediated immunity directed against tumour antigens has been documented in animal models and patients with breast carcinomas.[4–7] These responses, however, are often ineffective in eradicating the tumour. The activation and boosting of the host's immune surveillance against antigens selective for or overexpressed in breast carcinomas represent a potentially useful antitumour strategy. One such tumour antigen is mucin 1 (MUC1). MUC1 is a high-molecular-weight glycoprotein that is overexpressed in human breast cancers.[8] Aberrant glycosylation of MUC1 in breast carcinoma cells results in the generation of distinct epitopes not found in normal tissues.[9,10] Studies have demonstrated that these cryptic epitopes are recognized by cytotoxic T lymphocytes (CTLs) in patients with breast carcinomas[5,11] and in animal models.[12–15] These findings suggest that the MUC1 antigen may represent a target for immunotherapy of breast cancer.

Effective antigen presentation is the key to an efficacious tumour vaccine. Dendritic cells (DCs) have been identified as the most potent antigen-presenting cells.[16–18] Fusions of DCs with carcinoma cells have proved to be effective in the induction of antitumour immunity. Vaccination with fusions of murine tumour cells and syngeneic DCs has been shown to eliminate established tumour metastases in wild-type and MUC1 transgenic (MUC1.Tg) mice. These studies were conducted in

Received 4 November 2002; revised 26 February 2003; accepted 25 March 2003.

Correspondence: Dr Jianlin Gong, Department of Medicine, Boston University School of Medicine, 88 East Newton Street, Boston, MA 02118, USA. E-mail: jgong@medicine.bu.edu

murine models of transplanted tumour cells. The injected tumours usually grow quickly and the host immune system, while potentially competent, does not have sufficient time to generate an effective antitumour response. Furthermore, these models are not appropriate for cancer prevention studies because the tumours lack the premalignant or early lesions that are the critical stage at which the host must mount an effective immune response. We have produced a transgenic murine model (MMT) that expresses the polyomavirus middle-T (PyMT) oncogene under control of the mouse mammary tumour virus promoter long-terminal repeat (MMTV-LTR)[19] and develops spontaneous mammary carcinomas. The spontaneous mammary tumours also express the MUC1 tumour-associated antigen.[15] One advantage of this model is that tumours develop from normal cells in their natural tissue microenvironment with a viable immune system and progress through multiple stages found in human cancer.[19–21]

In the present study, MMT mice were immunized with fusions of DCs and MUC1-positive tumour cells (FC/MUC1) to determine the effectiveness of cancer prevention and treatment in a murine model relevant to human cancers. We demonstrate that immunization with FC/MUC1 induces specific anti-MUC1 immunity that delays the development of spontaneous breast carcinomas and controls the progression of tumours in MMT mice. These results indicate that MUC1 is a potent immunogenic antigen capable of inducing an immune response and tumour rejection.

MATERIALS AND METHODS

Mice

Female C57BL/6 mice, 6 to 8 weeks old, were purchased from Taconic (Germantown, NY). The transgenic mice included: (i) MT mice expressing the polyomavirus middle-T oncogene driven by the mouse mammary tumour virus (MMTV) long-terminal repeat (LTR) that develop spontaneous mammary carcinomas,[19] (ii) MUC1 transgenic mice (MUC1.Tg) expressing the human MUC1 antigen in a tissue-specific fashion similar to that in humans,[22] and (iii) MMT mice that express the PyMT and the MUC1 antigen and develop spontaneous mammary carcinomas.[15] The MT mice were generated by breeding the female wild-type C57BL/6 strain with male MT mice. The MMT mice were generated by crossing the female C57BL/6 strain of MUC1.Tg mice with male MT mice. All mice were congenic on the C57BL/6 background at $N > 10$. The mice were selected for the expression of the PyMT oncogene and/or MUC1 using the polymerase chain reaction (PCR).[22,23] Only female mice positive for either MT (MT mice) or MT/MUC1 double transgenes (MMT mice) were used for the experiments. The mice were maintained in microisolator cages under specific pathogen-free conditions.

Cell culture and fusion

Murine MC38 adenocarcinoma cells (C57BL/6) were stably transfected with a MUC1 cDNA (MC38/MUC1).[24] Cells were maintained in Dulbecco's modification of Eagle's medium (DMEM) supplemented with 10% heat-inactivated fetal calf serum (FCS), 2 mM L-glutamine, 100 U/ml penicillin and 100 μg/ml streptomycin. DCs were obtained from bone marrow cultures of C57BL/6 mice.[25] The methods of DC generation and fusion with MC38 or MC38/MUC1 tumour cells in the presence of 50% polyethylene glycol have been described.[26] Briefly, DC and MC38/MUC1 cells were collected, washed twice in serum-free medium, and counted. DCs were mixed with MC38/MUC1 cells in a 10 : 1 ratio. The fusion process was carried out with 50% polyethylene glycol (PEG) in prewarmed Dulbecco's phosphate-buffered saline (PBS) without Ca^{2+} or Mg^{2+} at pH 7·4. After washing twice, the fused cells were plated in 24-well culture plates for 5 days. Then the cells were plated in six-well culture plates in complete RPMI 1640 medium supplemented with 20 ng/ml recombinant murine GM-CSF (Sigma Chemical Co., St. Louis, MO). By day 5 of culture, the unfused tumour cells had become firmly attached to the tissue culture flask, while the fused cells could be dislodged by gentle pipetting. The latter were then collected and analysed by flow cytometry for antigen expression.

PCR

The mice were examined for MUC1 and MT genes by PCR analysis. Ten-μg aliquots of tail and mammary tumour tissue were digested with proteinase K. DNA was extracted using the Dneasy™ Tissue Kit (QIAGEN, Valencia, CA). PCR was carried out in a total volume of 50 μl in Perkin-Elmer Gene Amp tubes (Perkin-Elmer, Norwalk, CT) with the following reagents: 5 μl 10 × PCR buffer including 15 mM $MgCl_2$; 0·02% formamide; 0·2 mM dNTPs; 100 nM 5′-CTTGCCAGCCATAGCACCAAG-3′ (bp 745–765) forward primer, and 100 nM 5′-CTCCACGTCGTGGACATTGATG-3′ (bp 1086–1065) reverse primer for the MUC1 gene; 100 nM 5′-AGTCACTGCTACTGCACCCAG-3′ (bp 282–302), and 100 nM 5′-CTCTCCTCAGTTCCTCGCTCC-3′ (bp 817–837) primers for the MT gene; 1·25 units of Taq polymerase; 2 μl of tail DNA (approximately 500 ng) and reagent quality H_2O. The amplification programme consisted of one cycle for 10 min at 94° and 40 cycles of 30 s each at 94°, 61° and 72°. The PCR product of each reaction was analysed by size fractionation in a 1% agarose gel. Amplification of MUC1-positive DNA resulted in a 500-bp fragment[22] and that of MT-positive DNA in a 491-bp fragment.[23]

Immunoblotting

Mammary carcinomas from MT or MMT mice were harvested, rapidly frozen in liquid nitrogen and stored at −80° until use. The samples were lysed in a solution containing 0·05 M sodium chloride, 0·02 M Tris, pH 7·4, 100 μg/ml leupeptin, 50 μg/ml aprotinin and 1% NP-40. Equivalent amounts of protein were separated in 5% SDS-polyacrylamide gels and transferred to nitrocellulose membranes. The membranes were stained with Ponceau S, photographed, blocked in 5% non-fat dry milk in PBS + 0·05% Tween 20 and probed with anti-MUC1 mAb (DF-3) for 1 hr at 25°. Membranes were incubated with horseradish proxidase (HRP)-conjugated rabbit anti-mouse antibody (Amersham, Pharmacia Biotech, Piscataway, NJ) for 1 hr at 25°. The antigen–antibody complexes were visualized by Electro Chemiluminescence (ECL, Amersham).

Histological and immunohistochemical staining

Groups of MT or MMT mice were killed at various ages (from 3 weeks to 6 months). Mammary tissue or tumour was

harvested and fixed in 2% paraformaldehyde. Sections (5 μm) were cut and stained with hematoxylin and eosin (H&E). For detecting MUC1 expression, sections were stained with anti-MUC1 mAb (DF3) for 30 min at room temperature and then subjected to indirect immunoperoxidase staining using the Vectastain ABC kit (Vector Laboratories, Burlingame, CA).

Flow cytometry

DC, FC/MUC1 and MC38/MUC1 carcinoma cells were double stained with fluorescein-isothiocyanate (FITC)-conjugated-mAb HMPV (anti-MUC1, BD Pharmingen, San Diego, CA) for 30 min on ice. After washing twice with PBS, the phycoerythrin (PE)-conjugated mAb M5/114 (anti-MHC class II, BD Pharmingen) was added for another 30 min on ice. Splenocytes were purified by passage through nylon wool and stained with the following antibodies: anti-CD4 (H129·19), anti-CD8 (53-6·7), anti-NK1·1 (PK136), anti-αβ TCR (H57-597) and anti-γδ TCR (GL3) (BD Pharmingen) for 30 min on ice. The cells were washed with PBS and incubated with FITC-conjugated anti-rat, mouse and hamster immunoglobulin G (IgG) for an additional 30 min on ice. All the cells were washed, fixed, and analysed by FACScan (Becton Dickinson, Bedford, MA) with CellQuest analysis software (Becton Dickinson).

Vaccination

Groups of 4-week-old MT or MMT mice were vaccinated subcutaneously with 5×10^5 FC/MUC1 cells, FC/MC38 cells or MC38/MUC1 tumour cells that had been exposed to 60-Gy ionizing radiation (Gammacell 1000 Atomic Energy of Canada, Ottawa, Canada). In another experiment, MMT mice were immunized at varying ages. The immunization was repeated four additional times at monthly intervals. The mice were followed for up to 6 months. From 6 weeks of age, the mice were palpated every other day to assess the presence of mammary tumours. A progressively growing mass was regarded as tumour and was measured by calipers in two perpendicular diameters. Tumour incidence was determined and recorded. Mice with tumours ≥ 2 cm were killed. The mice were cared for according to the Institutional Animal Care and Use Committee Guidelines.

Humoral immune responses

Microtitre plates were precoated overnight at 4° with 100 μl/well of MUC1 antigen (5 units/ml in PBS, pH 7·4). MUC1 antigen was purified from supernatant of ZR-75 human breast cancer cells using the method previously described.[27–30] Briefly, the supernatant obtained by culturing ZR-75 cells for 3 or 4 days in the serum-free medium was concentrated in a stirred ultrafiltration cell (Millipore, Billerica, MA) on a YM30 filter. The concentrate was centrifuged and applied to an agarose-wheat germ lectin column (Pharmacia, Peapack, NJ). The DF3/MUC1 antigen containing fractions was eluted with 1 M N-acetylgulcosamine. The elute was dialysed, concentrated, and then applied to Sephacryl S-300 (Pharmacia). The DF3/MUC1 antigen-containing fractions were monitored by immunoassay, concentrated and then incubated with mAb DF3-Sepharose 4B. The MUC1 antigen was eluted with 3 M $MgCl_2$. The $MgCl_2$ fraction was dialysed against water and then concentrated. Anti-mouse IgG at 100 μl/well (1 μg/ml in PBS, pH 7·4) was used to precoat the well as a control. Each well was washed three times with PBS/Tween (0·05% v/v Tween 20) and blocked with 120 μl/well 5% horse serum in PBS for 1 hr at room temperature. After washing, 4-fold dilutions of mouse sera were added to each well for 2 hr. The plates were washed and incubated with sheep anti-mouse IgG conjugated to horseradish peroxidase (Amersham, Piscataway, NJ). Antibody complexes were detected by development with o-phenylenediamine (Sigma) and measured in an enzyme-linked immunosorbent assay (ELISA) microplate autoreader EL310 (Bio-Rad, Hercules, CA)at an OD of 490 nm.

^{51}Cr cytotoxicity assay

Splenocytes were isolated from MMT mice by Ficoll separation. The target cells include mammary carcinoma cells isolated from MMT or MT mice, MC38/MUC1, MC38 (the parent cells of MC38/MUC1), and YAC-1 cells. These target cells were prelabelled with ^{51}Cr for 1 hr at 37° and added to wells of 96-well v-bottom plates with T cells (effector cells) for 5 hr at 37°. The supernatants were assayed for ^{51}Cr release in a gamma counter and CTL activity was determined at the indicated effector:target (E:T) ratios. Percentage of specific ^{51}Cr release was determined by the following equation:

$$\text{Percentage specific release} = [(\text{experimental} - \text{spontaneous})/(\text{maximum} - \text{spontaneous})] \times 100.$$

Statistical analysis

Statistical significance was determined using Student's *t*-test.

RESULTS

Characterization of mammary carcinomas in MT and MMT mice

MMT mice have been generated by breeding MT mice with MUC1.Tg mice. Bitransgene-positive mice were selected using PCR. Mammary tumours first appeared in the female MMT mice at about 8 weeks of age. All mice developed mammary tumours by 15 weeks of age (range from 8 to 15 weeks) with a median of 12 weeks. The mammary tumours were multiple in nature with synchronous kinetics. The tumours progressed rapidly, and the mice became moribund at 16–18 weeks of age (Fig. 1a) when they were killed.

To establish the pattern of tumourigenesis, groups of MMT and MT mice were killed at varying time-points and their mammary tissue was subjected to histological examination. At least three stages of tumour development were observed. Mammary glands appeared normal until the 3rd week of age. Focal hyperplasia began to appear in the 4th week, which evolved into dysplasia and carcinoma *in situ*. Invasive tumours emerged at 8 to 9 weeks (Fig. 1b). A similar trend was observed in MT mice. These findings indicate that expression of PyMT resulted in transformation of the mammary epithelia and rapid production of mammary carcinomas in MT and MMT mice. Expression of MUC1 shortened the latency period to some extent, although no significant difference was found between the two groups. More importantly, multiple stages of tumour

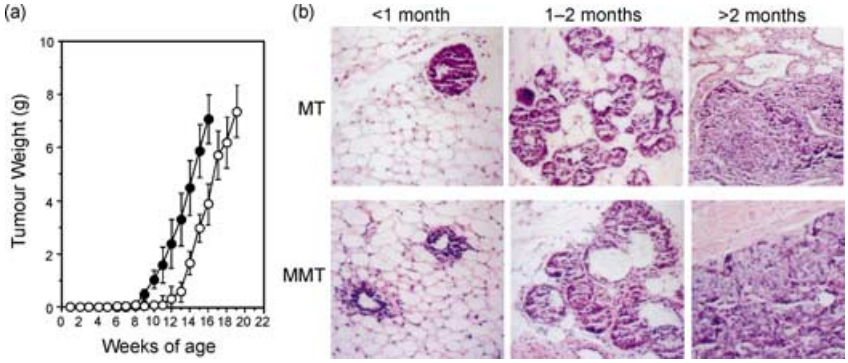

Figure 1. Mammary carcinoma development in MMT and MT mice. (a) Growth rate of spontaneous mammary carcinomas in MMT (●) and MT (○) mice. Three mice were used at each time-point. The error bars represent SE of the mean. (b) Histological examination with H&E staining of spontaneous mammary tumours in MT and MMT mice at different ages (×16).

development, similar to those found in human cancers, were observed.

Expression of MUC1 on mammary carcinoma cells in MMT mice

To assess expression of MUC1 in the mammary carcinomas of MMT mice, western blotting, PCR and immunohistochemical staining techniques were used. Western blot showed the expression of MUC1 in spontaneous mammary carcinoma cells from MMT, but not from MT, mice at a level comparable to that found in MCF-7 human breast cancer cells (Fig. 2a). At the DNA level, the presence of MUC1 and PyMT was detected in tumour cells from MMT mice by PCR analysis. In contrast, only PyMT was detected in tumour cells from MT mice (Fig. 2b). Furthermore, we detected MUC1 expression on mammary tumour cells from MMT, but not MT, mice with immunohistochemical staining (Figs 2c and d). Whereas MUC1 expression was confined to the apical or lumenal surface of normal mammary epithelia, MUC1 was detectable over the entire surface of spontaneous mammary tumour cells. Taken together, these results indicate that MUC1 is overexpressed on mammary carcinoma cells in MMT mice.

Induction of anti-MUC1 immunity in MMT mice by immunization with FC/MUC1

MC38/MUC1 carcinoma cells were successfully fused with syngeneic DCs. The fused cells (FC/MUC1) expressed tumour-derived MUC1 and DC-derived MHC class II molecules (Table 1a). In contrast, fusion of DC with MC38 tumour cells (FC/MC38) resulted in the expression of MHC class II molecules but not MUC1 (Table 1a). The fusion efficiency was 21·16%, as determined by dual expression of MUC1 and MHC class II. To assess induction of anti-MUC1 humoral immune response, MT and MMT mice were immunized subcutaneously with FC/MUC1. The immunization was repeated four additional times at 4-week intervals. Irradiated MC38/MUC1 tumour cells, fusions of DCs and MC38 tumour cells (FC/MC38) or PBS injection were used as controls. The sera from immunized and control mice were collected 7 days after each immunization and analysed for the presence of anti-MUC1 antibody by ELISA assay. An anti-MUC1 humoral response was induced in MMT mice immunized with FC/MUC1, but not with irradiated MC38/MUC1, FC/MC38 or PBS injection (Fig. 3a). The anti-MUC1 antibody titre increased after the second immunization, peaked after the third and fourth immunizations, then decreased and was maintained at lower levels at 6 months of age (Fig. 3b). In contrast, there was no anti-MUC1 antibody detected in MMT mice injected with PBS (Fig. 3b). These results indicate that immunization with FC/MUC1 is associated with production of anti-MUC1 antibodies in MMT mice.

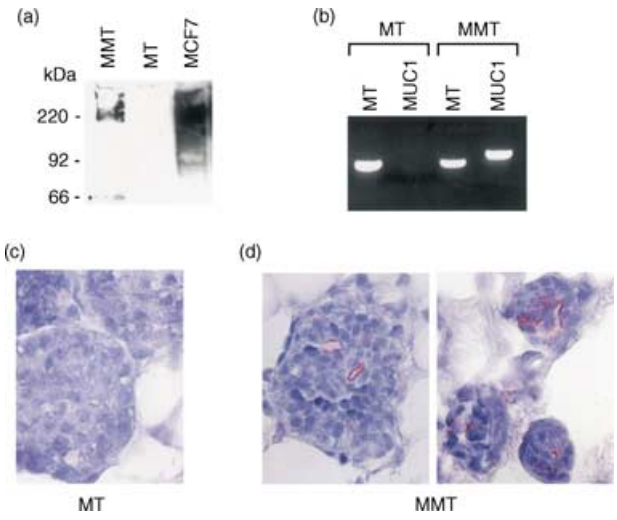

Figure 2. MUC1 expression on mammary carcinomas. (a) Lysates from MMT carcinoma (lane 1), MT carcinoma (lane 2) and human MCF-7 tumour cells (lane 3) were analysed by western immunoblotting with anti-MUC1 mAb DF3. (b) PCR was used to detect MT and MUC1 genes in mammary carcinoma from MMT and MT mice. (c, d) Immunohistochemical staining with mAb DF3 to detect the expression of MUC1 on mammary carcinomas from MT and MMT mice (×40).

Table 1. Phenotype of (a) DC/tumour fusions and (b) splenocytes

(a)

	% positive cells			
	DC	MC38/MUC1	FC/MUC1	FC/MC38
Anti-MUC1	0·10	98·01	68·14	0·24
Anti-MHC II	82·08	1·36	27·98	25·88
Anti-MUC1/MHC II*	0·22	0·13	21·16	4·02

(b)

	% positive splenocytes†		
Antibodies	PBS	MC38/MUC1	FC/MUC1
Anti-CD4	27·22	26·03	29·52
Anti-CD8	36·02	34·56	39·92
Anti-NK	8·92	7·98	8·04
Anti-αβ TCR	41·14	42·31	43·16
Anti-γδ TCR	2·22	2·08	1·96

*Percentage of double-positive cells.

†Splenocytes were collected from MMT mice immunized five times with FC/MUC1 or irradiated MC38/MUC1 tumour cells, or treated with PBS.

NK, natural killer; TCR, T-cell receptor.

To assess the induction of CTL against MUC1-positive tumour cells, splenocytes from MMT mice immunized with FC/MUC1 were collected at multiple time-points. Table 1b shows the phenotypes of the splenocytes. The standard ^{51}Cr release assay was used to determine the CTL activity against spontaneous mammary tumour cells from MMT mice (MMT tumour cells, MUC1-positive). CTL activity against MMT tumour cells (37%) was induced in splenocytes from MMT mice immunized with FC/MUC1 (Fig. 3c). In contrast, there was no apparent CTL activity induced in their littermates immunized with irradiated MC38/MUC1, FC/MC38 or PBS (Fig. 3c). The CTL activity against MUC1-positive targets was detectable at 20–38% lysis throughout the experiment (Fig. 3d). To assess the specificity of CTL activity, multiple targets were used. CTL activity against MC38/MUC1, MMT tumour and, to a lesser extent, MC38 cells was induced by FC/MUC1 immunization (Fig. 3e, right panel). This result is consistent with our previous findings that polyclonal CTLs are induced by the FC/MUC1 vaccination against MUC1 antigen as well as unknown tumour antigens expressed by MC38 and MC38/MUC1. In contrast, there was little, if any, CTL activity against MT and YAC-1 cells (Fig. 3e, right panel). As expected, no CTLs were induced in MMT mice immunized with irradiated MC38/MUC1 tumour cells (Fig. 3e, middle panel) or treated with PBS (Fig. 3e, left panel). Taken together, the results indicate that immunization with FC/MUC1 induces polyclonal and antigen-specific CTLs.

Inhibition of spontaneous mammary carcinomas in MMT mice by fusion cell immunization

To assess the efficacy of immunization with fusion cells *in vivo*, MMT mice were immunized with FC/MUC1 cells, FC/MC38

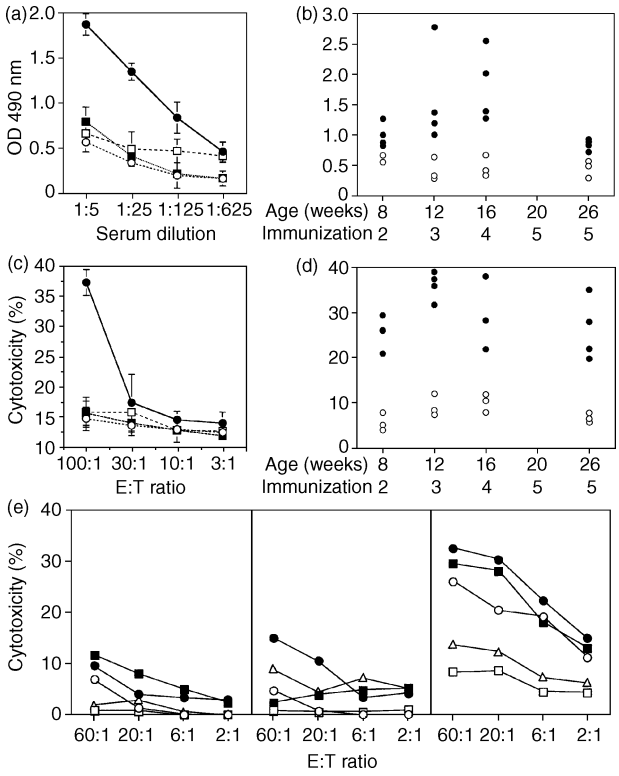

Figure 3. Anti-MUC1 humoral response induced in MMT mice by FC/MUC1 immunization. (a) The measurement of a single serum sample from one female MMT mouse or her littermates. The mice at 4 weeks of age were immunized with 5×10^5 FC/MUC1 cells (●), irradiated MC38/MUC1 cells (■) or FC/MC38 cells (□), or treated with PBS (○). The immunization was repeated at 8 and 12 weeks. Mice were killed 1 week after the last immunization. Serum from the mice was collected and anti-MUC1 antibodies were detected by ELISA. The results are expressed as the mean ± SD of three replicates. (b) Serum was collected from MMT mice of various ages (three or four mice per group) that had been immunized at different times with 5×10^5 FC/MUC1 cells (●) or treated with PBS (○) and assayed for the presence of anti-MUC1 antibody. Each dot represents the level of anti-MUC1 antibody (1 : 5 dilution) at the indicated age and number of immunizations. (c) MMT mice were immunized with 5×10^5 FC/MUC1 cells (●) at 4 weeks of age. The immunization was repeated at 8 and 12 weeks. Their littermates were immunized with FC/MC38 cells (□), irradiated MC38/MUC1 cells (■) or PBS (○). One week after the last immunization, the mice were killed and splenocytes were purified through nylon wool to remove antigen-presenting cells. T cells were incubated with mammary carcinoma cells from MMT mice at the indicated effector:-target ratios. CTL activity was determined by the ^{51}Cr release assay. The results are expressed as the mean ± SD of three replicates. (d) Splenocytes were isolated from MMT mice of various ages (three or four mice per group) that had been immunized at different times with 5×10^5 FC/MUC1 cells (●) or PBS (○). CTL activity against mammary carcinoma cells from MMT mice at an effector:target ratio of 100 : 1 was determined by ^{51}Cr release. Each dot represents the CTL activity at the indicated age and number of immunizations. (e) Splenocytes were isolated from MMT mice immunized five times with 5×10^5 FC/MUC1 (right panel) or irradiated MC38/MUC1 tumour cells (middle panel) or treated with PBS (left panel). CTL activity against MC38 (○) and MC38/MUC1 (●), MT (□) and MMT (■) mammary carcinoma cells, and YAC-1 (△) cells at the indicated effector:target ratio was determined by ^{51}Cr release.

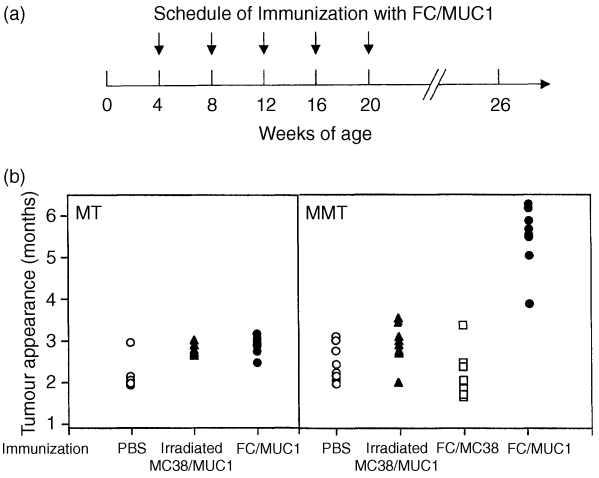

Figure 4. Inhibition of spontaneous mammary carcinoma *in vivo*. (a) Schedule of immunization with FC/MUC1. Female MMT and MT mice were vaccinated subcutaneously with 5×10^5 FC/MUC1 cells, FC/MC38 cells or irradiated MC38/MUC1 cells at the base of tail at <1 month of age. Immunization was repeated for four additional times at 4-week intervals. (b) Tumour incidence in MT (left panel) and MMT (right panel) mice immunized with FC/MUC1 cells (●), FC/MC38 cells (□), irradiated MC38/MUC1 cells (▲) or PBS (○). Each dot represents the appearance of tumour for individual mice at the indicated age.

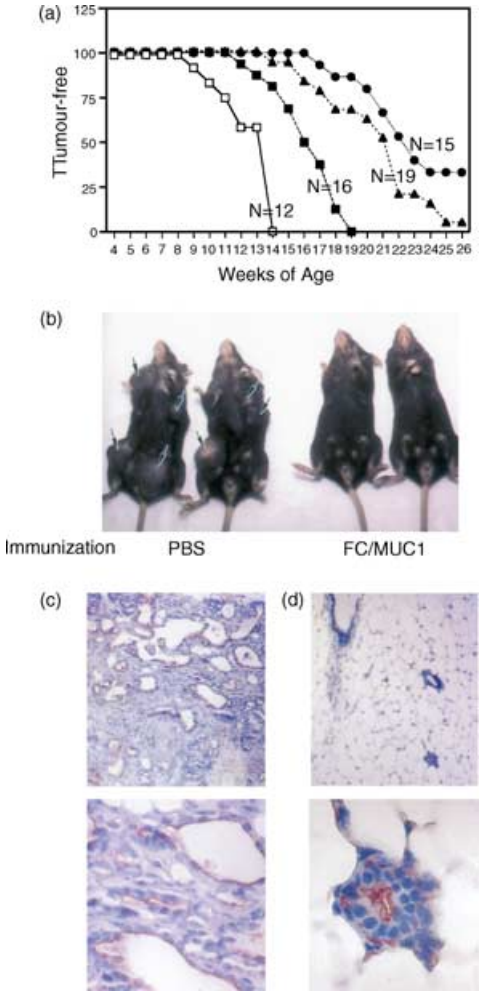

Figure 5. Immunoprevention and immunotherapy with FC/MUC1 immunization. (a) Tumour incidence in MMT mice in which immunization with FC/MUC1 cells was begun at <1 month (●), 1–2 months (▲), or over 2 months (■). Non-vaccinated age-matched MMT mice were used as the control (□). (b) Photograph of female littermates of MMT mice at age 14 weeks treated with PBS (left panel) or at age 26 weeks treated with FC/MUC1 fusion (right panel). The mice were <1 month old when treatment with PBS or FC/MUC1 immunization was commenced. (c, d) Photomicrograph of mammary carcinoma from a non-vaccinated MMT mouse at the age of 14 weeks (left panels) and of mammary tissue from a vaccinated MMT mouse at the age of 26 weeks (right panels). The mice were <1 month old when treatment with PBS or immunization was commenced. The upper panels have magnifications of $\times 10$ and the lower panels $\times 40$.

cells or irradiated MC38/MUC1 cells, or injected with PBS. Immunization was begun at 4 weeks of age. The mice received four additional immunizations at 4-week intervals (Fig. 4a). All MT mice treated with PBS, irradiated MC38/MUC1 cells or FC/MUC1 developed mammary tumours at 8–15 weeks and became moribund 4 weeks after tumour appearance (Fig. 4b, left panel). In contrast, immunization of MMT mice with FC/MUC1 significantly delayed the development of spontaneous mammary tumours (Fig. 4b, right panel). The specificity of these responses against MUC1 is supported by the finding that the immunization of MMT mice with FC/MC38 (MUC1-negative) or immunization of MT mice with FC/MUC1 gave no protection against the development of mammary carcinomas (Fig. 4b, left panel). These results indicate that the anti-MUC1 immune responses induced by the immunization with FC/MUC1 can block or delay the development of mammary tumours in a predisposed model.

Control of tumour progression with fusion cell immunization

One of the characteristics of MMT and MT mice is that they develop mammary tumours in multiple stages. We have shown that immunization of MMT mice in the early stage of tumourigenesis can block tumour development. Therefore, it would be of interest to determine whether immunization of MMT mice in the later stage of tumourigenesis can control the progression of spontaneous mammary tumour. To address this issue, MMT mice were divided into three groups according to age at initial immunization. The immunization was begun in the first group of mice at <1 month of age, in the second group of mice at 1–2 months and in the third group of mice at >2 months. The immunization was repeated four additional times at 4-week intervals. Immunization of MMT mice with FC/MUC1 at <1, 1–2 and >2 months of age rendered 33, 5 and 0% of mice free of tumours, respectively, up to 6 months (Fig. 5a). As expected, all the PBS-treated MMT mice developed mammary tumours and became moribund 4 weeks after tumour occurrence (Fig. 5b, left). However, immunization of MMT mice with FC/MUC1 in the early stages of tumour development rendered 33% mice free of the disease for at least 6 months (Fig. 5b, right), and delayed development of tumour in those in which

mammary tumour developed. The percentage of tumour-free mice was statistically significant compared with 1–2 month, >2 months, and non-vaccine groups respectively ($P < 0{\cdot}05$, $P < 0{\cdot}0001$ and $P < 0{\cdot}0001$). Invasive mammary carcinomas were found in samples from PBS-treated mice (Fig. 5c, upper and lower panels). In contrast, there was no tumour formation in MMT mice immunized with FC/MUC1 (Fig. 5d, upper and lower panels). These results indicate that the efficacy of immunization is dependent on the age at which the mice were immunized.

DISCUSSION

Cancers expressing MUC1 antigen occur in 72% of new cases.[31] MUC1 has been recognized as a multifunctional protein that is involved in protection and lubrication of mucous membrane, signal transduction and modulation of the immune system.[32] Although MUC1 is both tumour-associated and expressed in normal tissues, there is a striking difference in expression between normal tissues and cancer cells. MUC1 is normally expressed on the apical surface of secretory epithelia lining the lumen of ducts. Carcinoma cells, in contrast, exhibit loss of polarization and express MUC1 at high levels over the entire cell surface.[8] Moreover, sialyated O-linked glycans attached to the MUC1 tandem repeats differ structurally in normal and transformed epithelia.[33] Incomplete glycosylation of MUC1 in carcinoma cells could expose the tandem repeat epitopes that are normally cryptic.[9,34] Taken together, these features make MUC1 an attractive target for immunotherapy.

The aim of the present study was to determine whether immunization of MMT mice with FC/MUC1 can induce anti-MUC1 immunity that is sufficient to prevent or delay the development of spontaneous mammary tumour *in vivo*. The results demonstrate that immunization with FC/MUC1 induces anti-MUC1 immune responses. Such immune responses resulted in delay of mammary tumour development driven by a potent oncogene in a genetically modified mouse. Early immunization rendered 33% of mice free of disease for up to 6 months. These results are consistent with our previous findings that DC/tumour fusion cells induce potent antitumour immunity.[26,35]

Fusion cells express DC-derived costimulatory ligands, MHC class I and II molecules and tumour cell-derived antigens, including MUC1. The fusion cells process and present MUC1 in the context of MHC and costimulatory molecules and induce both arms of cellular-mediated immunity *in vivo* and *in vitro*.[35,36] In the present study, we showed that immunization with FC/MUC1 was associated with the induction of an anti-MUC1 immune response, a delay of mammary tumour development and control of tumour progression. These results further strengthen the notion that MUC1 is an immunogenic antigen capable of eliciting immune responses to reject MUC1-positive tumours.

The finding that the efficacy of the vaccine is correlated with the timing of initial vaccination is of interest but not unexpected. The MMT mice are born with a potent activated oncogene, PyMT. The PyMT antigen is associated with a number of signal transduction pathways[37–41] that promote cell growth and/or survival. This oncogene affects the entire mammary tree and results in widespread transformation of the mammary epithelia.[19,20] In this model, reversal of early tumour development or elimination of established tumour is needed to alter the progression of disease. In this context, immunization with FC/MUC1 significantly prolonged the latent period of tumour development, especially when the immunization was initiated in the early stage of tumour development. These results indicate that an effective immune response can be induced to counter the tumorigenesis driven by a potent oncogene. Furthermore, MUC1 was targeted in the present study. A possibility is that the efficacy of vaccine can be improved if multiple antigens are targeted. One of the advantages in using DC/tumour fusion cells is that the fusion cells are capable of processing and presenting multiple tumour antigens, including those unidentified, and inducing polyclonal CTLs. Collectively, the findings in the present study raise hope that a tumour vaccine can be developed for preventive and therapeutic use.

ACKNOWLEDGMENTS

This work was supported by National Cancer Institute Grant R01 CA87057; by the US Department of Defense Breast Cancer Research programs, Grant 990344; and by the Susan G. Komen Breast Cancer Foundation, Grant 9825.

REFERENCES

1 Hellstrom KE, Hellstrom I. Cellular immunity against tumor antigens. Adv Cancer Res 1969; **12:**167–223.
2 Rosato FE. Active specific immunotherapy of human solid tumors. Ann N Y Acad Sci 1976; **277:**332–8.
3 Boon T, van der Bruggen P. Human tumor antigens recognized by T lymphocytes. J Exp Med 1996; **183:**725–9.
4 Baum M. Immunotherapy in treatment of breast cancer. Proc R Soc Med 1974; **67:**294–6.
5 Jerome KR, Barnd DL, Bendt KM, Boyer CM, Taylor-Papadimitriou J, McKenzie IF, Bast RC Jr, Finn OJ. Cytotoxic T-lymphocytes derived from patients with breast adenocarcinoma recognize an epitope present on the protein core of a mucin molecule preferentially expressed by malignant cells. Cancer Res 1991; **51:**2908–16.
6 Taylor-Papadimitriou J, D'Souza B, Burchell J, Kyprianou N, Berdichevsky F. The role of tumor-associated antigens in the biology and immunotherapy of breast cancer. Ann N Y Acad Sci 1993; **698:**31–47.
7 Apostolopoulos V, Pietersz GA, McKenzie IF. MUC1 and breast cancer. Curr Opin Mol Ther 1999; **1:**98–103.
8 Kufe D, Inghirami G, Abe M, Hayes D, Justi-Wheeler H, Schlom J. Differential reactivity of a novel monoclonal antibody (DF3) with human malignant versus benign breast tumors. Hybridoma 1984; **3:**223–32.
9 Burchell J, Gendler S, Taylor-Papadimitriou J, Girling A, Lewis A, Millis R, Lamport D. Development and characterization of breast cancer reactive monoclonal antibodies directed to the core protein of the human milk mucin. Cancer Res 1987; **47:**5476–82.
10 Girling A, Bartkova J, Burchell J, Gendler S, Gillett C, Taylor-Papadimitriou J. A core protein epitope of the polymorphic epithelial mucin detected by the monoclonal antibody SM-3 is selectively exposed in a range of primary carcinomas. Int J Cancer 1989; **43:**1072–6.
11 Reddish M, MacLean GD, Koganty RR, Kan-Mitchell J, Jones V, Mitchell MS, Longenecker BM. Anti-MUC1 class I restricted CTLs in metastatic breast cancer patients immunized with a synthetic MUC1 peptide. Int J Cancer 1998; **76:**817–23.

12 Mukherjee P, Ginardi AR, Madsen CS, Sterner CJ, Adriance MC, Tevethia MJ, Gendler SJ. Mice with spontaneous pancreatic cancer naturally develop MUC-1-specific CTLs that eradicate tumors when adoptively transferred. J Immunol 2000; **165:**3451–60.
13 Morikane K, Tempero R, Sivinski CL, Kitajima S, Gendler SJ, Hollingsworth MA. Influence of organ site and tumor cell type on MUC1-specific tumor immunity. Int Immunol 2001; **13:**233–40.
14 Mukherjee P, Ginardi AR, Tinder TL, Sterner CJ, Gendler SJ. MUC1-specific cytotoxic T lymphocytes eradicate tumors when adoptively transferred in vivo. Clin Cancer Res 2001; **7:**848s–55s.
15 Mukherjee P, Madsen CS, Ginardi AR *et al.* Mucin 1-specific immunotherapy in a mouse model of spontaneous breast cancer. J Immunother 2003; **26:**47–62.
16 Steinman RM. The dendritic cell system and its role in immunogenicity. Annu Rev Immunol 1991; **9:**271–96.
17 Steinman RM. Dendritic cells and the control of immunity: enhancing the efficiency of antigen presentation. Mt Sinai J Med 2001; **68:**106–66.
18 Steinman RM, Dhodapkar M. Active immunization against cancer with dendritic cells: the near future. Int J Cancer 2001; **94:**459–73.
19 Guy CT, Cardiff RD, Muller WJ. Induction of mammary tumors by expression of polyomavirus middle T oncogene: a transgenic mouse model for metastatic disease. Mol Cell Biol 1992; **12:**954–61.
20 Cardiff RD, Muller WJ. Transgenic mouse models of mammary tumorigenesis. Cancer Surv 1993; **16:**97–113.
21 Maglione JE, Moghanaki D, Young LJ *et al.* Transgenic Polyoma middle-T mice model premalignant mammary disease. Cancer Res 2001; **61:**8298–305.
22 Rowse GJ, Tempero RM, VanLith ML, Hollingsworth MA, Gendler SJ. Tolerance and immunity to MUC1 in a human MUC1 transgenic murine model. Cancer Res 1998; **58:**315–21.
23 Ritland SR, Rowse GJ, Chang Y, Gendler SJ. Loss of heterozygosity analysis in primary mammary tumors and lung metastases of MMTV-MTAg and MMTV-neu transgenic mice. Cancer Res 1997; **57:**3520–5.
24 Siddiqui J, Abe M, Hayes D, Shani E, Yunis E, Kufe D. Isolation and sequencing of a cDNA coding for the human DF3 breast carcinoma-associated antigen. Proc Natl Acad Sci U S A 1988; **85:**2320–3.
25 Inaba K, Inaba M, Romani N, Aya H, Deguchi M, Ikehara S, Muramatsu S, Steinman RM. Generation of large numbers of dendritic cells from mouse bone marrow cultures supplemented with granulocyte/macrophage colony-stimulating factor. J Exp Med 1992; **176:**1693–702.
26 Gong J, Chen D, Kashiwaba M, Kufe D. Induction of antitumor activity by immunization with fusions of dendritic and carcinoma cells. Nat Med 1997; **3:**558–61.
27 Abe M, Kufe D. Structural analysis of the DF3 human breast carcinoma-associated protein. Cancer Res 1989; **49:**2834–9.
28 Sekine H, Ohno T, Kufe DW. Purification and characterization of a high molecular weight glycoprotein detectable in human milk and breast carcinomas. J Immunol 1985; **135:**3610–5.
29 Abe M, Kufe DW. Identification of a family of high molecular weight tumor-associated glycoproteins. J Immunol 1987; **139:** 257–61.
30 Abe M, Kufe D. Effects of maturational agents on expression and secretion of two partially characterized high molecular weight milk-related glycoproteins in MCF-7 breast carcinoma cells. J Cell Physiol 1986; **126:**126–32.
31 Greenlee RT, Murray T, Bolden S, Wingo PA. Cancer statistics 2000. CA Cancer J Clin 2000; **50:**7–33.
32 Gendler SJ. MUC1, the renaissance molecule. J Mammary Gland Biol Neoplasia 2001; **6:**339–53.
33 Hull SR, Bright A, Carraway KL, Abe M, Hayes DF, Kufe DW. Oligosaccharide differences in the DF3 sialomucin antigen from normal human milk and the BT-20 human breast carcinoma cell line. Cancer Commun 1989; **1:**261–7.
34 Perey L, Hayes DF, Kufe D. Effects of differentiating agents on cell surface expression of the breast carcinoma-associated DF3-P epitope. Cancer Res 1992; **52:**6365–70.
35 Gong J, Apostolopoulos V, Chen D, Chen H, Koido S, Gendler SJ, McKenzie IF, Kufe D. Selection and characterization of MUC1-specific CD8+ T cells from MUC1 transgenic mice immunized with dendritic-carcinoma fusion cells. Immunology 2000; **101:** 316–24.
36 Gong J, Chen D, Kashiwaba M *et al.* Reversal of tolerance to human MUC1 antigen in MUC1 transgenic mice immunized with fusions of dendritic and carcinoma cells. Proc Natl Acad Sci USA 1998; **95:**6279–83.
37 Courtneidge SA, Smith AE. Polyoma virus transforming protein associates with the product of the c- src cellular gene. Nature 1983; **303:**435–9.
38 Kornbluth S, Sudol M, Hanafusa H. Association of the polyomavirus middle-T antigen with c-yes protein. Nature 1987; **325:**171–3.
39 Guy CT, Muthuswamy SK, Cardiff RD, Soriano P, Muller WJ. Activation of the c-Src tyrosine kinase is required for the induction of mammary tumors in transgenic mice. Genes Dev 1994; **8:**23–32.
40 Webster MA, Hutchinson JN, Rauh MJ *et al.* Requirement for both Shc and phosphatidylinositol 3′ kinase signaling pathways in polyomavirus middle T-mediated mammary tumorigenesis. Mol Cell Biol 1998; **18:**2344–59.
41 Dankort DL, Muller WJ. Signal transduction in mammary tumorigenesis: a transgenic perspective. Oncogene 2000; **19:**1038–44.

Annals of Surgical Oncology, **11**(3):328–339
DOI: 10.1245/ASO.2004.05.027

Reduced T-Cell and Dendritic Cell Function Is Related to Cyclooxygenase-2 Overexpression and Prostaglandin E_2 Secretion in Patients With Breast Cancer

Barbara A. Pockaj, MD, Gargi D. Basu, PhD, Latha B. Pathangey, MS, Richard J. Gray, MD, Jose L. Hernandez, BA, Sandra J. Gendler, PhD, and Pinku Mukherjee, PhD

Background: In several neoplastic diseases, including breast cancer, immunosuppression correlates with disease stage, progression, and outcome. Thus, thorough analysis of immune parameters in breast cancer patients may be beneficial in designing effective anticancer immune-based therapies.

Methods: We investigated dendritic cell and T-cell function in breast cancer patients at various stages of the disease and in age-matched controls. We also evaluated cyclooxygenase-2 (COX-2) expression and prostaglandin E2 (PGE_2) levels within the tumor milieu and in the circulation.

Results: T cells from cancer patients showed decreased proliferation in response to CD3 antibody stimulation. Analysis of T-cell helper type 1 and 2 cytokines revealed reduced levels of interferon-γ, tumor necrosis factor-α, interleukin (IL)-12, and IL-2 and increased levels of IL-10 and IL-4. Dendritic cells from these patients showed significantly reduced expression of co-stimulatory molecules (B7 and CD40) and demonstrated reduced phagocytic ability, reduced antigen presentation to T cells, and reduced ability to mature in response to lipopolysaccharide. Data revealed increased synthesis of PGE_2, an immune suppressor, along with increased expression of COX-2, a key regulator of PGE_2 synthesis.

Conclusions: COX-2–induced PGE_2 may contribute to immunosuppression and may directly block antitumor immunity while promoting tumor growth, providing us with the rationale for using COX-2 inhibition combined with immunotherapy.

Key Words: Cyclooxygenase-2—Prostaglandin E_2—Dendritic cells—T cells—Breast cancer.

The defective function of the host's immune system is one of the major mechanisms by which tumors evade immune surveillance. T-cell anergy is thought to be an early event in tumor progression and may precede the generalized immunosuppression that is observed in cancer patients.[1] Multiple mechanisms of tumor-specific evasion have been demonstrated, including impaired HLA expression, modulation of surface antigens, lack of co-stimulatory molecules on dendritic cells (DCs) leading to impaired antigen presentation to T cells, impaired T-cell receptor (TCR) signal transduction through the TCR-ζ chain, and elaboration of immune-suppressive cytokines by tumor cells and T-regulatory cells such as interleukin-10 (IL-10) and transforming growth factor-β (TGF-β).[2]

Functional impairment of T cells has been well documented in patients with cancer.[3] This is true of both circulating and infiltrating lymphocytes in which there is reduced activation of the TCR and impaired production of interferon-γ (IFN-γ), IL-2, and tumor necrosis factor-α (TNF-α) in response to CD3 monoclonal antibodies.[4] Cytokine profiles of cancer patients demonstrate an abnormal balance between T-cell helper type 1 (Th1) and type 2 (Th2) cytokines, favoring a Th2 response.[5] Circulating and tumor-infiltrating DCs have also been

Received May 27, 2003; accepted November 4, 2003.

From the Departments of Surgery (BAP, RJG), Biochemistry and Molecular Biology (GDB, LBP, JLH, SJG, PM), and Biostatistics (JLH), Mayo Clinic College of Medicine, Scottsdale, Arizona.

Address correspondence and reprint requests to: Pinku Mukherjee, PhD, Department of Biochemistry and Molecular Biology, Mayo Clinic College of Medicine, 13400 E. Shea Blvd., Scottsdale, AZ 85259; Fax: 480-301-7017; E-mail: mukherjee.pinku@mayo.edu

shown to be functionally impaired. In metastatic melanoma patients, tumor-infiltrating DCs express low levels of co-stimulatory molecules (CD80 and CD86) and therefore are unable to activate T cells, whereas DCs isolated from breast cancer patients demonstrate a significantly reduced ability to stimulate allogeneic and antigen-specific T-cell responses.[6,7] In certain cancers, DCs derived from peripheral blood are lower in absolute number as compared with those in individuals without cancer and are predominantly immature in phenotype.[8]

Cyclooxygenase-2 (COX-2) is overexpressed in a variety of cancers, including breast cancer.[9–11] COX-2 is an enzyme that converts arachidonic acid to prostaglandin H_2, which is further metabolized to other prostaglandins, including prostaglandin E_2 (PGE_2).[12] COX-2 expression is rapidly induced secondary to a number of factors, including growth factors, tumor promoters, and hormones.[13] Transgenic mouse models demonstrated that overexpression of COX-2 leads to the development of mammary tumors.[14] Overexpression of COX-2 is also known to inhibit apoptosis[15] and promote angiogenesis.[16] This overexpression of COX-2 can lead to increased production of prostaglandins such as PGE_2, which has multiple downstream effects. PGE_2 is known to transactivate the epidermal growth factor receptor, which triggers mitogenic signaling in epithelial cells and induces cancer cell proliferation.[17] PGE_2 also causes immunosuppression in vitro[18] and can induce immunosuppression in vivo, enhancing tumor growth in animal models.[19,20] In this study, we tested the hypothesis that the COX-2–induced PGE_2 overexpression may correlate with the global immunosuppression observed in breast cancer patients.

Because T cells and DCs are pivotal in the development of antitumor immunity and are susceptible to tumor-mediated immune suppression, we investigated DC and T-cell function from 25 breast cancer patients at various stages of the disease and compared the data with those of 19 healthy age-matched controls. Although several studies have described the functional impairment of T cells and DCs in breast cancer patients, the studies have not evaluated both T-cell and DC function from the same breast cancer patients. Moreover, the mechanisms driving the functional impairment still remain elusive. The goal of our study was to evaluate the immune status of patients presenting with the diagnosis of breast cancer and to evaluate the immune-modulating factors within the tumor milieu that may account for the functional impairment of immune effector cells. This is the first study to describe a thorough analysis of both T-cell and DC function in patients with newly diagnosed breast cancer. Impaired functionality of T cells and DCs correlated with COX-2 and PGE_2 overexpression. These studies are of critical importance for designing novel immunotherapeutic strategies for breast cancer and for selecting the patients who may most benefit from such therapies.

METHODS

Study Characteristics

This research study was approved by the Mayo Clinic Institutional Review Board. Patients who presented to the Mayo Clinic Scottsdale Breast Clinic for initial treatment of disease were eligible for the protocol. The patients signed informed consent for peripheral blood and tumor samples. Informed consent for peripheral blood samples was also obtained from healthy, age-matched volunteers. Twenty-five patients with breast cancer and 19 healthy controls were studied. Patients and healthy donors who were chronic users of COX-2 inhibitors were excluded from the analysis. Staging of the patients was conducted by using the American Joint Committee on Cancer protocol. Breast cancer patient demographics and tumor characteristics are listed in Table 1. All patients were postmenopausal, with a mean age of 69 years. Controls were all postmenopausal, with a mean age of 60 years. Infiltrating ductal adenocarcinoma was the most common tumor subtype (64%). The mean size of the tumors was 2.3 cm, although 64% of lesions were ≤2 cm. Only 20% of patients had lymph node metastases,

TABLE 1. *Patient demographics and tumor characteristics*

Variable	Data
Age, y, median (range)	69 (36–80)
Presentation	
Mass	12 (48%)
Abnormal mammogram	13 (52%)
Tumor size, cm, median (range)	2.3 (0.3–13)
Tumors ≤2 cm	16 (64%)
Histology	
Infiltrating ductal	16 (64%)
Infiltrating lobular	3 (12%)
Mixed infiltrating ductal/lobular	3 (12%)
Infiltrating mucinous	3 (12%)
Grade	
1	9 (36%)
2	8 (32%)
3	8 (32%)
Angiolymphatic invasion	4 (16%)
Estrogen receptor positive	21 (84%)
Lymph node metastases	5 (20%)
Number of lymph nodes positive	1–8
Stage	
I	15 (60%)
II	7 (28%)
III	3 (12%)

and most patients presented with either stage I or stage II disease. In most cases, blood was drawn on the day of surgery, before resection of the tumor. In some cases, blood was drawn few days before surgery.

The overall scheme for the study design is shown in Fig. 1. Whole blood was obtained from the study subjects, and the peripheral blood mononuclear cells (PBMCs) were separated by using a Ficoll-Paque density gradient centrifugation. Sera from these patients were also collected and stored in a −80°C freezer. The PBMCs were used for isolation of T cells and DCs, and the serum was used for cytokine/chemokine and PGE_2 evaluation. Surgically resected tumor tissues and lymph node metastases were used to make tissue lysate for COX-2 and PGE_2 evaluation.

T-Cell Isolation

T cells were isolated from the PBMCs of patients as described in the scheme (Fig. 1). Briefly, mononuclear cells were obtained by centrifugation of peripheral blood over a Ficoll-Paque gradient (Amersham Biosciences, Uppsala, Sweden). Mononuclear cells were incubated for 2 hours at 37°C, and nonadherent lymphocytes were removed and used as T cells and adherent cells were used for generation of DCs. The processing of the blood was performed under the same conditions, and all assays were performed on freshly isolated buffy-coat cells.

T-Cell Proliferation Assay

The nonadherent lymphocyte population (1×10^6/mL) was subjected to in vitro stimulation with various concentrations of purified plate-bound CD3 antibody (BD Pharmingen, San Diego, CA). Cells were incubated for 4 days with CD3 antibody, and ^{3}H-thymidine was added 24 hours before collection. After excess thymidine was washed off, cells were lysed with 5% Triton X-100 (Fischer Scientific, Pittsburgh, PA), and incorporated thymidine was evaluated with the Topcount micro scintillation counter (Packard Biosciences, Shelton, CT). Evaluation of T-cell proliferation was also performed with varying concentrations of tumor lysates (12–200 μg/mL) and purified PGE_2 (Cayman Pharmaceuticals, Ann Arbor, MI). All assays were performed in triplicate. Control lymphocytes were included in every assay to control for interassay variation.

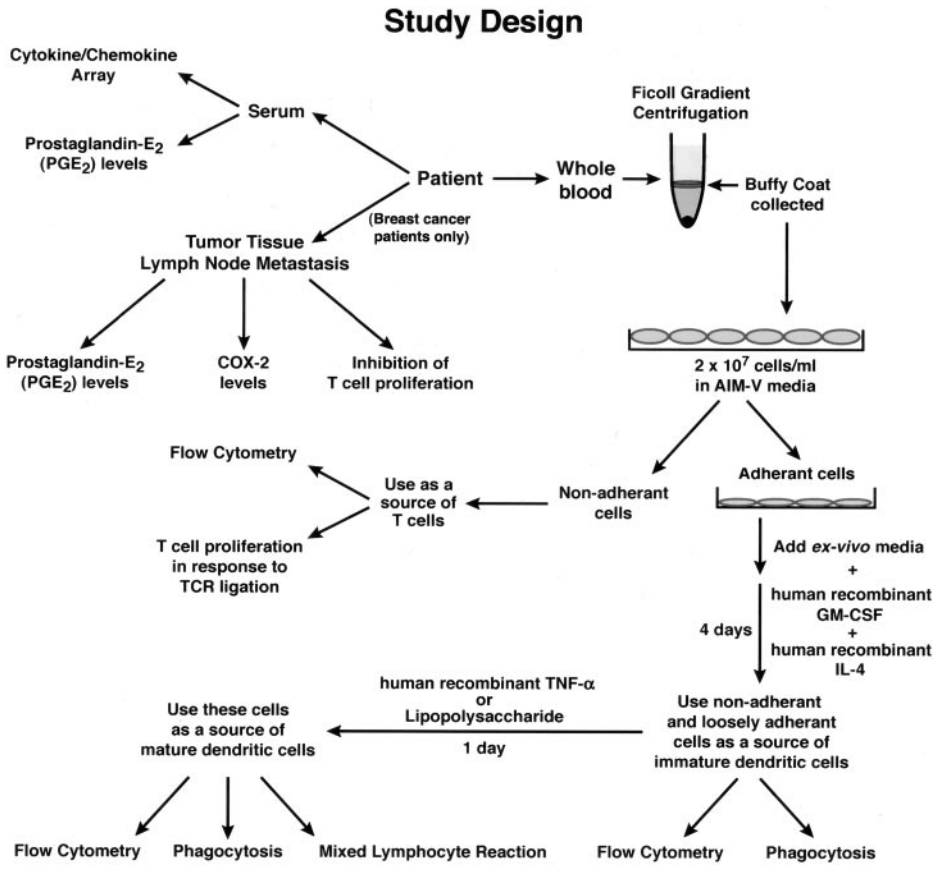

FIG. 1. Schematic representation of the study design. COX-2, cyclooxygenase-2; TCR, T-cell receptor; GM-CSF, granulocyte-macrophage colony-stimulating factor; IL, interleukin; TNF, tumor necrosis factor; AIM-V, serum free human lymphocyte culture media.

Analysis of Intracellular Cytokines

Intracellular cytokine levels were evaluated by two-color flow cytometric analysis after TCR ligation. Intracellular cytokines were determined post brefeldin A (BD Pharmingen) treatment of lymphocytes according to the manufacturer's recommendations (4 μL/1.2 $\times$ 10^7 cells per 6 mL for 3 hours at 37°C before staining). This treatment stops the release of cytokines in the culture media, and the cytokines accumulate within the cells. Cells were then stained for surface markers for T cells (CD3) or DCs (HLA-DR) at 4°C for 15 minutes, followed by washing excess stain and permeabilizing cells with Pharmingen permeabilization solution (containing saponin) for 30 minutes at 4°C. Cells were then stained for intracellular IL-2, IL-12, IFN-γ, IL-4, IL-10, and TNF-α for 30 minutes at 4°C. Cells were analyzed with the Becton Dickinson FACScan, and data were analyzed with the CellQuest program. All antibodies were purchased from BD Pharmingen.

Serum Analysis of Cytokines and Chemokines

A cytokine/chemokine array kit (Ray Biotech Inc., Norcross, GA) was used to detect a panel of 22 secreted cytokines and chemokines in the serum from healthy patients and those with breast cancer. The manufacturer's recommended protocol was used.

DC Isolation and Maturation

DCs were generated from a $CD14^+$ monocyte population isolated from PBMCs. Briefly, mononuclear cells were obtained by centrifugation of the peripheral blood over a Ficoll-Paque gradient. Mononuclear cells were incubated for 2 hours at 37°C, and nonadherent cells were removed. Adherent cells were incubated with granulocyte-macrophage colony-stimulating factor (5 ng/mL; PeproTech, Rocky Hill, NJ) and IL-4 (5 ng/mL; PeproTech) for 4 to 5 days. Cells were collected, counted, and phenotyped for immature DCs and were further cultured for one additional day with granulocyte-macrophage colony-stimulating factor (5 ng/mL), IL-4 (5 ng/mL), and lipopolysaccharide (LPS, 100 ng/mL; Sigma Pharmaceuticals, St. Louis, MO). Cells were collected on day 6 as mature DCs.

DC Phenotype

Control and breast cancer patient DCs were analyzed by two-color flow cytometric analysis. Cell-surface expression of several markers was evaluated: CD80 (B7.1), CD86 (B7.2), CD40, HLA-DR, HLA-ABC, CD1a, and CD14. All antibodies were purchased from BD Pharmingen. Stained cells were analyzed with the CellQuest program on a Becton Dickinson FACScan.

DC Function

Mixed Lymphocyte Reaction Assay

Control and patient-derived DCs were assayed for their ability to stimulate allogeneic T cells in a mixed lymphocyte reaction (MLR). T cells (1×10^5) from healthy donors were incubated with irradiated DCs (3000 rads; 1×10^4 cells) from allogeneic breast cancer patients for 5 days, and ^{3}H-thymidine was added 24 hours before the cells were collected. After the excess thymidine was washed off, cells were lysed with 5% Triton X-100, and incorporated thymidine was evaluated by using the Topcount micro scintillation counter.

Phagocytosis Ability

Immature and LPS-matured DCs from healthy donors and breast cancer patients were incubated with fluorescein isothiocyanate–conjugated dextran beads (molecular weight, 40,000; Molecular Probes Inc., Eugene, OR) at 1 mg/1×10^6 cells for 30 minutes at 37°C. Dextran beads were used as the exogenous antigen source. Because the beads were conjugated to fluorescein isothiocyanate, uptake of dextran beads by DCs was analyzed by flow cytometry, and mean fluorescence intensity was calculated.

Breast Tumor Cell Lysates

Tissue lysates were prepared within 1 hour after surgery by homogenizing the tumor tissue in lysate buffer containing 20 mM of 4-(2-hydroxyethyl)-1-piperazineethanesulfonic acid, .15 M of NaCl, and 1% Triton X-100 supplemented with phosphatase-inhibitor cocktail mix (1/100 dilution; Sigma Pharmaceuticals) and complete protease inhibitors (Roche Pharmaceuticals, Indianapolis, IN). Lysates were stored in a −80°C freezer for further use.

Expression of COX-2 Protein in Tumor Lysate

Protein concentrations of the lysates were determined with the Pierce BCA protein assay kit (Pierce, Rockford, IL). Sodium dodecyl sulfate-polyacrylamide gel electrophoresis was performed with 12% resolving gel; 100 μg of protein was loaded per lane. Gels were immunoblotted and probed for COX-2 with specific COX-2 monoclonal antibody (goat polyclonal antibody, clone C20; Santa Cruz Biotechnology Inc., Santa Cruz, CA) at a 1/200 dilution.

PGE_2 in Serum and Tumor Lysate

Levels in the lysates were determined with a specific enzyme-linked immunosorbent assay (ELISA) kit for PGE_2, and levels in serum were determined by using the

PGE_2 metabolite ELISA kit (Cayman Pharmaceuticals). The manufacturer's recommended protocols were followed.

Statistical Analysis

Statistical significance was assessed by using pairwise comparisons with the Tukey-Kramer adjustment for multiple comparisons. The margins of error for the comparisons were obtained by calculating the 95% confidence intervals for the differences between group proportions.

Immune function parameters were compared between a set of clinical indicators. The clinical parameters examined were stage, lymph node status, estrogen receptor status, tumor size (<2 vs. 2 cm), grade, presence of angiolymphatic invasion, multifocality, and previous breast cancer. Because of the nonnormality of the immune function data and the small sample size of the cohort, the exact Wilcoxon statistic was used for assessing significant differences between groups. All error bars in the figures represent the standard deviation of the mean.

RESULTS

The proliferative ability of T cells isolated from breast cancer patients just before surgical tumor resection was examined. T cells were stimulated by various concentrations of plate-bound CD3 antibody, and T-cell proliferation was measured by ^{3}H-thymidine uptake. T-cell proliferation was significantly reduced in cancer patients compared with controls ($P < .001$ at 1 μg and .5 μg/mL of CD3 antibody; Fig. 2A). The raw counts per minute for all patients (n = 25) and controls (n = 19) are presented in Fig. 2B for a 1 μg/mL CD3 antibody concentration. Figure 2B clarifies the number of patients who were immunosuppressed. Sixty percent (16 of 25) of the breast cancer patients had lower than 50,000 counts per minute, which is suggestive of impaired T-cell proliferation in response to TCR ligation. All controls had values greater than this value. Additional analysis of Th1/Th2 cytokines in activated cells revealed reduced intracellular levels of the immunostimulatory Th1 cytokines IFN-γ ($P < .001$), TNF-α ($P < .001$), IL-12 ($P < .001$), and IL-2 ($P < .001$) and increased levels of the Th2 cytokines IL-4 ($P = .1$) and IL-10 ($P = .01$; Fig. 3).

DCs from patients with breast cancer expressed reduced levels of co-stimulatory molecules such as CD80 (B7.1), CD86 (B7.2), and CD40 on maturation with LPS (Fig. 4). Similar results were obtained with TNF-α–induced maturation. Other markers used to determine DC phenotype included HLA-DR, HLA-ABC, CD1a, and CD14 (data not shown). No differences between cancer

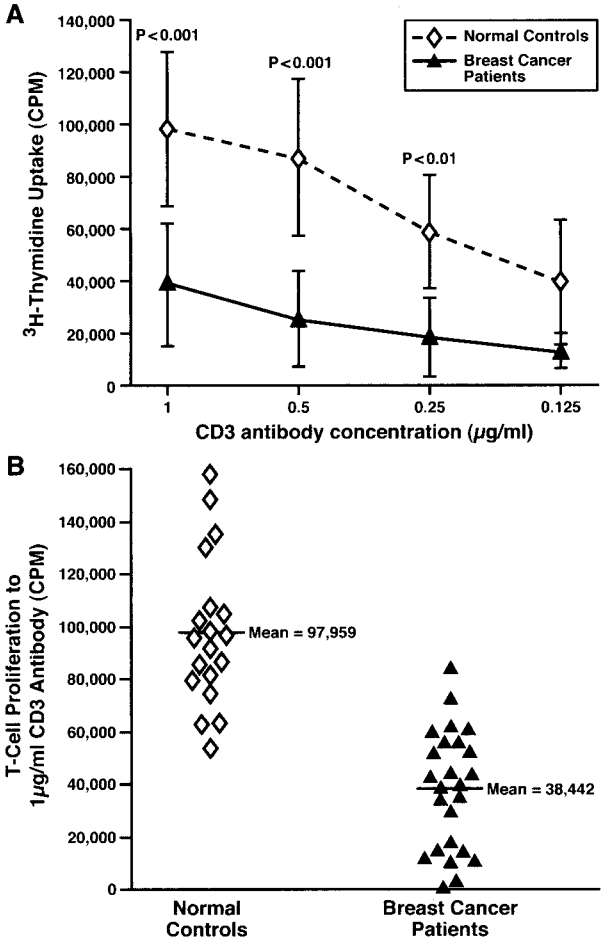

FIG. 2. T cells from breast cancer patients have markedly reduced proliferation in response to specific T-cell receptor ligation. (**A**) T-cell proliferation in response to plate-bound CD3 antibody comparing breast cancer patients (n = 25) and controls (n = 19). The amount of ^{3}H-thymidine uptake directly corresponds to the proliferative capacity of T cells. Error bars represent standard deviation of the mean. All assays were performed in triplicate with interassay controls. (**B**) Scatter plot of ^{3}H-thymidine uptake (in counts per minute; CPM) of T cells from individual patients (n = 25) and healthy donors (n = 19) in response to 1 μg/mL of plate-bound CD3 antibody.

patients and controls were observed in these markers. The reductions in expression of both CD80 and CD86 were statistically significant ($P < .001$). This low expression of co-stimulatory molecules is an indication that these DCs remain immature. It has been suggested (1) that immature DCs have a reduced ability for stimulating T cells and therefore may contribute to tumor-induced T-cell tolerance rather than immunity and (2) that mature DCs are essential for presenting tumor antigens and activating T cells to become cytolytic against tumor cells.

We therefore tested whether DCs from cancer patients had reduced antigen presentation. Data indicate that the

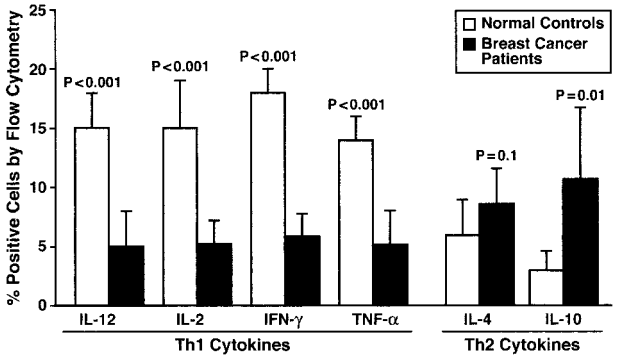

FIG. 3. Reduced T-helper type 1 (Th1) cytokines and increased T-helper type 2 (Th2) cytokines in the peripheral blood of patients with breast cancer. Intracellular cytokine levels were compared by flow cytometry. Interferon (IFN)-γ, tumor necrosis factor (TNF)-α, interleukin (IL)-12, IL-2, IL-10, and IL-4 levels were compared between breast cancer patients (solid bars; n = 9) and controls (open bars; n = 7). Error bars represent standard deviation of the mean.

function of DCs was significantly reduced. DCs from breast cancer patients demonstrated a significantly reduced ability to present antigens to allogeneic normal T cells in an MLR ($P < .001$; Fig. 5A). The MLR results support the previous findings shown in Fig. 4, in which the same DCs expressed low levels of co-stimulatory molecules and therefore failed to fully mature. Furthermore, the immature DCs from breast cancer patients demonstrated a significantly reduced ability to phagocytose exogenous antigens in vitro ($P < .001$; Fig. 5B and

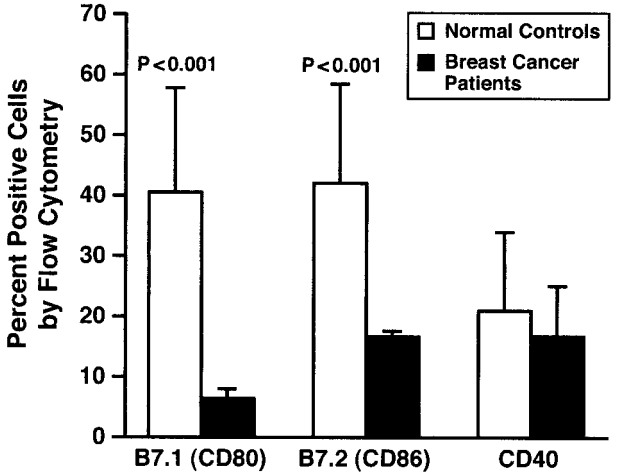

FIG. 4. Dendritic cells (DCs) from patients with breast cancer expressed reduced levels of co-stimulatory molecules. Flow cytometric analysis is shown of the surface expression of the co-stimulatory molecules CD80 (B7.1), CD86 (B7.2), and CD40 on lipopolysaccharide-matured DCs of breast cancer patients (solid bars; n = 25) versus controls (open bars; n = 19). Similar results were obtained with tumor necrosis factor-α–matured DCs (data not shown). Error bars represent standard deviation of the mean.

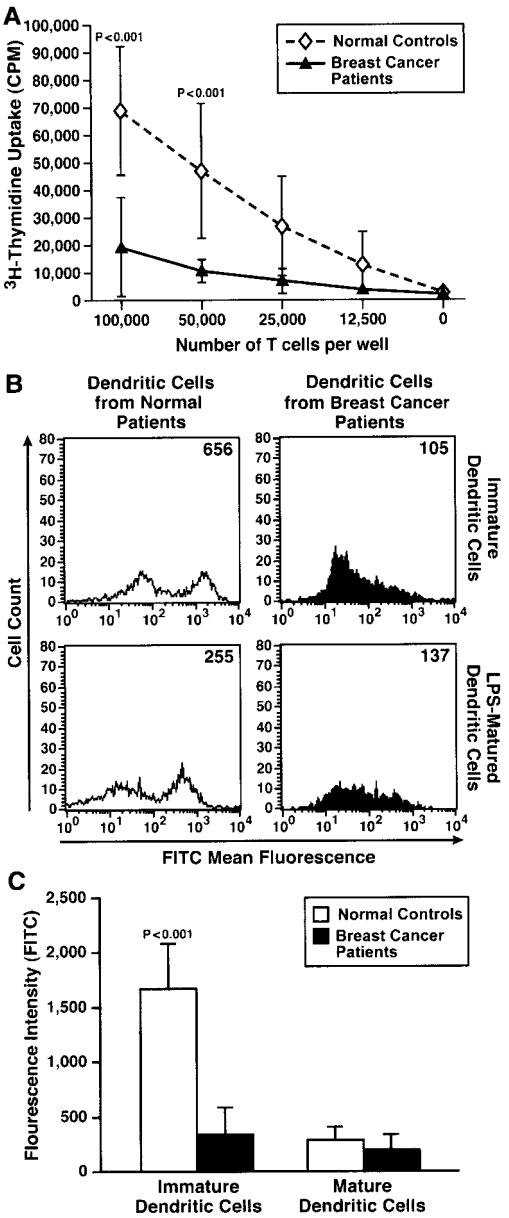

FIG. 5. Dendritic cells (DCs) from breast cancer patients demonstrate a significantly reduced ability to present antigens to allogeneic normal T cells and demonstrate reduced phagocytosis of exogenous antigen. (**A**) Allogeneic antigen presentation to normal T cells by DCs of breast cancer patients (n = 25) versus controls (n = 19) in a mixed lymphocyte reaction. The amount of ^{3}H-thymidine uptake directly corresponded to the proliferative capacity of T cells. (**B**) Representative histogram of immature and lipopolysaccharide-matured dendritic cell phagocytic ability of a cancer patient versus healthy donor (the numbers on the right corner are the mean fluorescence intensity). (**C**) Dendritic cell phagocytic ability (mean fluorescence intensity) in breast cancer patients (solid bars; n = 25) versus normal controls (open bars; n = 19) in the mature and immature state. In (**B**) and (**C**), the mean fluorescence intensity was used as a measure for the amount of fluorescein isothiocyanate–conjugated dextran beads engulfed by the DCs. Error bars represent standard deviation of the mean. CPM, counts per minute; FITC, fluorescein isothiocyanate.

C). They also demonstrated a maturation defect when stimulated with LPS treatment (Fig. 5C). Figure 5B shows a representative histogram from 1 patient, and Fig. 5C shows a bar graph of average values from the 24 patients and 19 controls. Immature DCs are known to be strong phagocytes but weak antigen presenters, whereas mature DCs are weak phagocytes and strong antigen presenters.[21] We found that immature DCs from healthy donors showed significantly higher ($P < .001$) fluorescence intensity (mean intensity of 1436), thus demonstrating good phagocytic ability, and on maturation with LPS, their phagocytic activity was reduced (mean intensity of 291; Fig. 5C). In comparison, the immature DCs from the breast cancer patients had significantly lower fluorescence intensity (mean intensity of 337), thus indicating poor phagocytosis; the florescence intensity of these DCs did not decrease with LPS treatment and remained at mean intensity of 207, once again indicating impaired maturation (Fig. 5C). Similar results were obtained when TNF-α instead of LPS was used to mature DCs (data not shown).

Tumor cells secrete factors that are known to induce immunosuppression and promote tumor cell proliferation. Prostaglandins, especially PGE_2, are such factors expressed within the tumor microenvironment and secreted in the serum. Because COX-2 is the key regulator of prostaglandin synthesis, we evaluated the COX-2 protein expression on Western blots of adjacent normal tissue lysates, tumor tissue lysates, and lysates from lymph nodes that contained metastases. The COX-2 protein was overexpressed in both the tumor and lymph node metastases compared with normal tissue. The highest expression was observed in lymph node metastases (Fig. 6A). Next, we evaluated the amount of PGE_2 in the serum of breast cancer patients and healthy donors by specific PGE_2 metabolite ELISA. Because PGE_2 is rapidly converted in the serum by 15-OH prostaglandin dehydrogenase to its 13,14-dihydro-15-keto metabolite, direct measurement of intact PGE_2 is not possible in sera or plasma. Thus, PGE_2 metabolite measurement is necessary to provide a reliable estimate of actual PGE_2 production.[22,23] However, in the tumor tissue lysates, PGE_2 levels can be evaluated directly by using a specific ELISA for PGE_2, because these cell types do not contain the enzymes required for metabolism of PGE_2, thus keeping the PGE_2 levels stable. Breast cancer patients had significantly increased levels of PGE_2 metabolite levels in their sera as compared with controls ($P < .001$; Fig. 6C). Similar to COX-2 expression, we observed high levels of PGE_2 in the tumor cell lysates ($P = .042$) and lymph node metastases ($P = .017$) as compared with normal adjacent breast tissue (Fig. 6B).

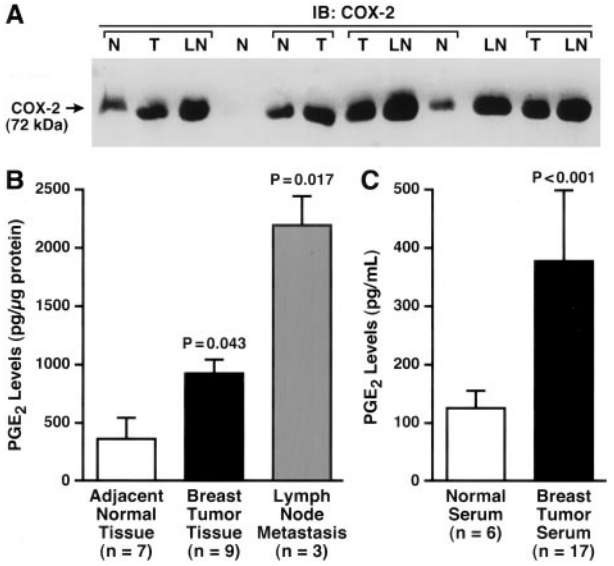

FIG. 6. Cyclooxygenase-2 (COX-2) and prostaglandin E_2 (PGE_2) are overexpressed in the tumor tissue and serum of patients with breast cancer. (**A**) COX-2 protein levels in tissue lysates (100 μg) from adjacent normal breast tissue, breast tumors, and lymph node metastases were analyzed by Western blot analysis. Brackets indicate tissues from a single patient. Six patient samples were analyzed. (**B**) PGE_2 levels in tissue lysates from adjacent normal breast tissue, breast tumors, and lymph node metastases were determined by specific enzyme-linked immunosorbent assay (ELISA). (**C**) Serum PGE_2 metabolite levels in breast cancer patients (solid bars) versus controls (open bars) were analyzed by specific PGE_2 metabolite ELISA. Error bars represent standard deviation of the mean. N, normal adjacent tissue; T, tumor; LN, lymph node metastasis; IB, immunonoblot.

Because tumor lysates contained COX-2, PGE_2, and, presumably, other immunosuppressive factors, we determined whether these lysates could directly block the T-cell signal transduction and activation that lead to T-cell proliferation. We evaluated the effect of the tumor lysates on the proliferation of T cells from the healthy donors. We used purified PGE_2 as a standard and compared it with the inhibition observed with the tumor lysate and lysate derived from adjacent normal tissue. There was direct inhibition of normal T-cell proliferation in response to CD3 antibody by the tumor lysates ($n = 3$) and lysates derived from lymph node metastasis ($n = 2$) at a 25 μg/mL concentration (Fig. 7). As expected, inhibition was also observed with purified PGE_2 at the same concentration (Fig. 7). Little inhibition of T-cell proliferation was observed with lysates derived from adjacent normal tissue, which did not express high levels of PGE_2 by ELISA (Fig. 6B). The inhibition observed with tumor and lymph node metastasis lysate was higher than with purified PGE_2, suggesting the presence of other T cell–inhibitory agents in the tumor lysate. Because normal lymph nodes express some PGE_2, normal

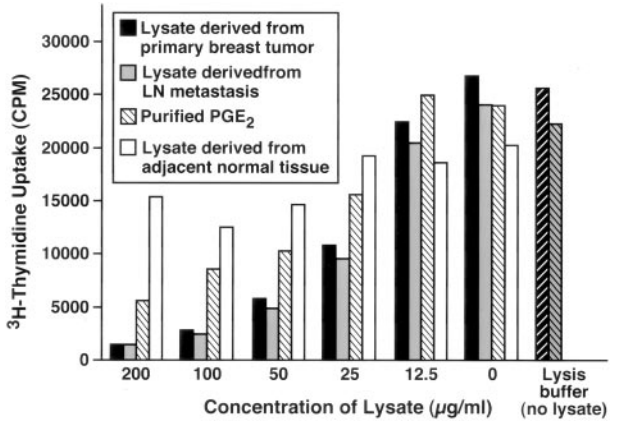

FIG. 7. Direct inhibition of normal T-cell proliferation by factors present in the tumor lysate. T-cell proliferation was determined in response to plate-bound CD3 antibody in the presence or absence of lysate derived from the primary tumor, lysate derived from lymph node (LN) metastasis, lysate derived from adjacent normal tissue, or purified prostaglandin E_2 (PGE_2) at varying concentrations (0 –200 μg/mL). T cells were generated from healthy donors (n = 4). The amount of ^{3}H-thymidine uptake directly corresponds to the proliferative capacity of T cells. Tissue lysis buffer and lysate from adjacent normal tissue were used as negative controls, and purified PGE_2 was used as the positive control. This assay was repeated three times, with similar results. CPM, counts per minute.

adjacent tissue may not be the ideal control for lymph node metastasis lysate. Thus, we evaluated normal lymph node lysates from mice (because normal human lymph nodes were not available) and determined that the PGE_2 levels in normal lymph nodes were minimal and were not sufficient to cause inhibition of mouse T-cell proliferation in response to TCR ligation (data not shown). Moreover, in humans, it has been well established that normal T cells that have not undergone any antigenic challenge or environmental insult generate very little PGE_2. In vitro studies have proven that normal T cells have to be stimulated with mitogen to express PGE_2.[24,25] Thus, we are confident that the inhibition of T-cell proliferation that we observed with lysates from lymph node metastasis was due to high levels of PGE_2 (Fig. 6B) and other unknown immunosuppressive factors.

We evaluated our data to see whether the patient's clinical variables correlated with immune function parameters. The clinical parameters examined were stage, lymph node status, estrogen receptor status, tumor size ($\leq$2 vs. 2 cm), grade, presence of angiolymphatic invasion, multifocality, and previous breast cancer. Immune function variables were compared between a set of clinical indicators. Because of the nonnormality of the immune function data and the small sample size of the cohort, the exact Wilcoxon statistic was used in assessing significant differences between groups. However, no significant correlation was reached except for impaired DC phagocytosis and antigen presentation in patients with lymph node–positive disease versus those who were lymph node negative ($P = .025$). The inability to elucidate any differences in any other parameters and clinical factors is due to small sample size.

DISCUSSION

There is evidence that tumor-specific antigens are present on cancer cells that could function as potential targets for the immune system. Unfortunately, cancer patients do not mount an effective immune response against them, indicating that the immune cells are tolerant to the tumor-specific antigens. Breaking this tolerance is one of the major goals of immunotherapy for cancer. Tumors also exhibit multiple immunosuppressive strategies, such as downregulation of major histocompatibility complex class I molecules, lack of co-stimulatory molecules on DCs, and secretion of immunosuppressive cytokines, as well as production of high levels of COX-2 and PGE_2. We first examined the immune status of patients recently diagnosed with breast cancer and then evaluated the effect of COX-2 overexpression by the tumor cells and subsequent synthesis of PGE_2 on the tumor's ability to evade immune surveillance.

Overall we found significant functional impairment in the T cells of patients who were diagnosed with breast cancer. T cells isolated from breast cancer patients before surgical removal of the tumor demonstrated a marked reduction in their proliferation response to CD3 antibodies (Fig. 2), suggesting a defect in activation of the TCR-mediated signal transduction pathways.[26] These described defects include reduced TCR-ζ chain expression, a defect in transcription factors such as nuclear factor-κB, upregulation of cyclin-dependent kinase inhibitor p27kip1, and hydrogen peroxide production by activated granulocytes.[26–30] A likely consequence of this ineffective T-cell signaling is impaired cytokine production by the T cells.[5,31] Nieland et al.[31] found that reduced cytokine expression was found in patients with early breast cancer with a normal TCR-ζ chain, suggesting involvement of other mechanisms in causing impaired cytokine production.

Th1 cytokines promote the development of cell-mediated antitumor responses.[32] However, Th2 cytokines are necessary for humoral immunity. Patients with carcinoma have a predominance of Th2 cytokines in the peripheral blood.[5] We found a similar increase in Th2 cytokines (IL-10 and IL-4) in our breast cancer cohort when compared with controls and found reduced Th1

cytokines (IFN-γ, IL-2, and IL-12; Fig. 3). A shift to a Th2 response has been correlated with increasing stage in patients with renal cell carcinoma.[33] Preliminary analysis of serum chemokine and cytokine levels by using a cytokine array system revealed a correlation between increasing levels of certain cytokines and chemokines with advanced-stage breast cancer (Fig. 8). RANTES (regulated on activation, normal T cells expressed and secreted), monokine induced by IFN-γ, monocyte chemoattractant protein-1, IL-8, and IL-10 levels (proteins that favor a Th2 response) were higher in the sera from patients with high-grade tumor and lymph node metastases as compared with patients with low-grade tumor and no lymph node metastases. Monocyte chemoattractant protein-1 is implicated in tumor cell migration and invasion and in multidrug resistance.[34] Similarly, monokine induced by IFN-γ and RANTES favor inflammation and tumor cell proliferation and invasion.[35,36] IL-8 is implicated in increased angiogenesis and multidrug resistance,[34] and IL-10 is known to cause T-cell anergy.[37] TGF-β1 is known to downregulate both cytotoxic T lymphocyte and T-helper signal transduction and function.[38]

These chemokines and cytokines are released by monocytes, macrophages, and lymphocytes that express the EP receptors for binding to PGE_2.[39] It is therefore plausible that the high levels of PGE_2 observed within the tumor microenvironment and in the circulation may

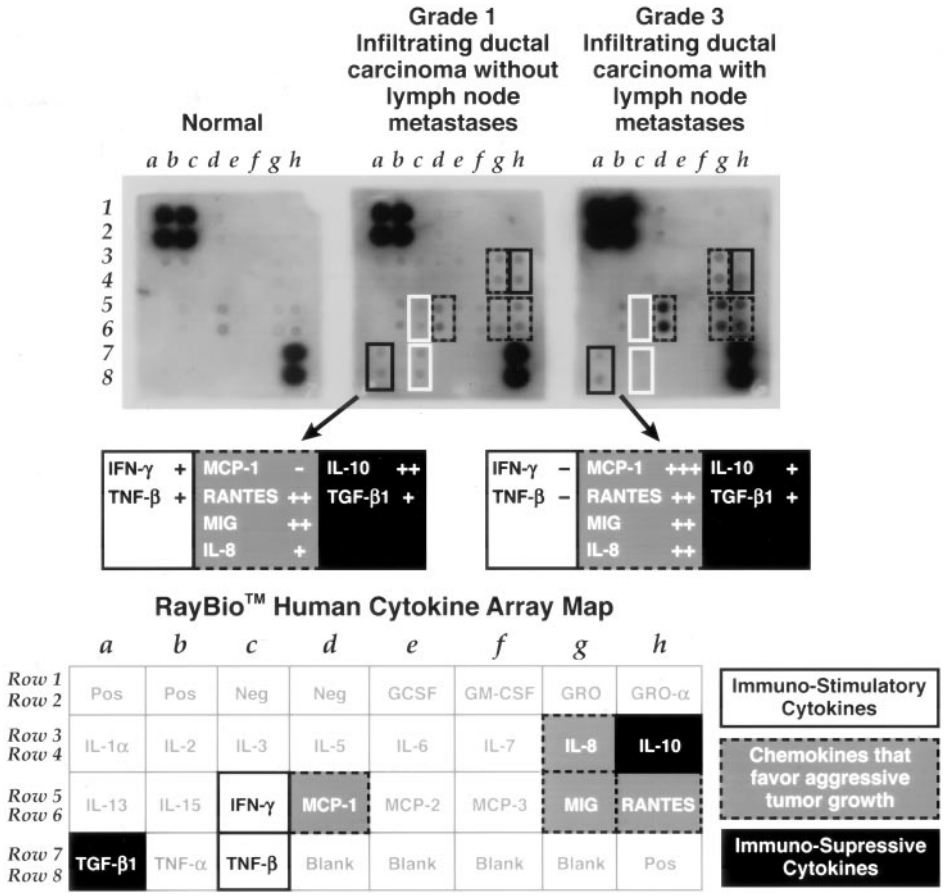

FIG. 8. Serum analysis of the chemokine/cytokine array revealed a correlation between increasing levels of certain cytokines and chemokines and advanced-stage breast cancer. Expression of a panel of 22 secreted cytokines and chemokines was detected in the serum of healthy and breast cancer patients by using the Ray Biotec cytokine array kit. Sera are shown from one control, one patient with a grade 1 invasive breast cancer without lymph node metastases, and one patient with a grade 3 invasive breast cancer with lymph node metastases. Similar results were observed with the other five breast cancer patients tested. The boxes on the blots and table demonstrate the cytokines and chemokines that are either upregulated (+) or downregulated (−) compared with the normal serum. The open box represents the immunostimulatory cytokines, the gray box represents chemokines that favor aggressive tumor growth, and the black box represents immunosuppressive cytokines. The actual cytokine array map from Ray Biotec is also provided. IFN, interferon; TNF, tumor necrosis factor; MCP, monocyte chemoattractant protein; RANTES, regulated on activation, normal T cells expressed and secreted; MIG, monokine induced by interferon-γ; IL, interleukin; TGF, transforming growth factor; GCSF, granulocyte colony-stimulating factor; GM-CSF, granulocyte-macrophage colony-stimulating factor; GRO, growth-related oncogene.

activate the tumor-infiltrating lymphocytes, monocytes, and macrophages via the EP receptors to release factors that favor tumor growth and invasion and suppress immune effector cells. These proteins were either absent or present in very low levels in the sera of controls. Conversely, serum levels of the immunostimulatory cytokines TNF-β1 and IFN-γ were higher in patients with low-grade/nonmetastatic tumors when compared with patients with high-grade/metastatic tumors, once again suggesting that advanced-stage patients are more likely to be immunosuppressed. The cytokine/chemokine array analysis was performed on six breast cancer patients and three healthy donors. Representative blots from two cancer patients and one healthy donor are shown in Fig. 8. The tumor milieu has been thought to play a significant role in the impairment of DCs. Release of such factors as IL-6, IL-10, macrophage colony-stimulating factor, vascular endothelial growth factor, and macrophage inflammatory protein-3α can prevent DC maturation and antigen-presenting functions. It is interesting to note that in our preliminary analysis of sera from four patients with breast cancer, we observed increased levels of vascular endothelial growth factor, macrophage colony-stimulating factor, IL-10, and macrophage inflammatory protein-3α (data not shown) as compared with controls. These results fit well with the concept that these increased chemokine levels favor a Th2 response that limits the DC allostimulatory capability.[7,40–42] In one study, it was shown that surgical removal of the primary tumor resulted in a dramatic reduction in the proportion of immature DCs, although the levels never reached those of controls.[8]

Mature DCs are the most powerful antigen-presenting cells and thus initiate the immune response.[21] The presence of immature DCs is thought to contribute to the induction of tolerance instead of immunity against the tumor antigens.[43] Low expression of co-stimulatory molecules on circulating DCs is an indication of immaturity. Low levels of co-stimulatory molecules in peripheral and draining lymph node DCs of breast cancer patients and impaired allostimulatory ability have been demonstrated in patients with breast cancer.[7,8] Our study confirms some of these findings as shown by the low expression of co-stimulatory molecules on circulating DCs from our breast cancer patients (Fig. 4). Our data further demonstrate the immaturity of DCs by the fact that DCs from cancer patients have a reduced ability to present antigens to allogeneic normal T cells in an MLR assay (Fig. 5A).

Heightened endocytic activity is characteristic of cytokine-derived DCs and their enhanced capacity to capture and process antigens.[21] Our study demonstrated impaired phagocytosis by the immature DCs from breast cancer patients (Fig. 5B and C). Attempts to mature the DCs with LPS did not change their phagocytic ability, once again suggesting a defect in DC maturation.

The mechanisms that underlie the T-cell and DC anergy in cancer patients are unknown but probably involve multiple events. We evaluated whether overexpression of COX-2 and downstream PGE_2 synthesis may be one of the mechanisms for immunosuppression. It is interesting to note that the COX-2 expression was high in primary tumors and was even more prominent in lymph node metastases (Fig. 6A). Because COX-2 was overexpressed, we evaluated the PGE_2 levels in the serum of the breast cancer patients and controls along with tumor lysates. Increased levels of PGE_2 were demonstrated in both the sera and tumor lysates of patients with cancer (Fig. 6B and C). PGE_2 is an immune suppressor that targets both cytotoxic and helper T-cell functions. PGE_2 is thought to suppress cell-mediated immune responses while enhancing humoral immune responses.[44,45] PGE_2 suppresses chemokine and cytokine production in humans, including IFN-γ–, TNF-α–, IL-12–, and IL-1β–mediated expression of chemokines. PGE_2 upregulates expression of immunosuppressive cytokines, such as IL-10 and TGF-β.[45,46] This immunosuppressive effect of PGE_2 was demonstrated by inhibition of normal T-cell proliferation to tumor lysates with high concentrations of PGE_2 (Fig. 7).

The ability of mature DCs to act as potent antigen-presenting cells is related to their production of IL-12.[47] DCs deficient of IL-12 generated in the presence of PGE_2 promote a Th2 response.[48] A recent study demonstrated that high concentrations of PGE_2 caused decreased IL-12 production via increases in IL-10 production and, therefore, decreased DC function.[18] This correlates well with our data, which clearly demonstrate increased PGE_2 levels in the serum and within the tumor milieu and also show increased levels of intracellular IL-10 and decreased levels of IL-12 in the T cells of the breast cancer patient population.

Thus, tumor overexpression of COX-2 via the elaboration of PGE_2 and other mechanisms could directly block the patient's defense mechanism against cancer and promote breast cancer growth.[49] We observed overexpression of COX-2 and PGE_2 and impaired T-cell and DC function in breast cancer patients. If the immune system of breast cancer patients were persistently compromised, the success of immunotherapies would be limited unless the immune system could be appropriately stimulated. Many immunotherapies for cancer treatment have been partially successful in eliciting a cellular immune response; however, this response has been downregulated by tumor-derived immunosuppressive factors.

If mediators of immune suppression, such as COX-2 and PGE_2, can be reduced; if co-stimulation for cytotoxic T-lymphocyte effector functions can be provided with appropriate immune-based therapy to overcome the tolerizing effects of the tumor; and, most importantly, if tumor cell proliferation can be restricted, then immunotherapy can be very effective. This study, along with other studies in the literature, provides us with an immunological rationale for using COX-2 inhibition that would reduce the PGE_2 levels and therefore reduce immunosuppression and tumor cell growth. COX-2 inhibition combined with immune-based therapy that would induce cytotoxic T-lymphocyte activity against tumor cells is a novel concept that needs further exploration in preclinical animal models and in clinical settings.

ACKNOWLEDGMENTS

The acknowledgments are available online in the full-text version at www.annalssurgicaloncology.org. They are not available in the PDF version.

REFERENCES

1. Staveley-O'Carroll K, Sotomayor E, Montgomery J, et al. Induction of antigen-specific T cell anergy: an early event in the course of tumor progression. *Proc Natl Acad Sci U S A* 1998;95:1178–83.
2. Pardoll D. Does the immune system see tumors as foreign or self? *Ann Rev Immunol* 2003;21:807–39.
3. Finke J, Ferrone S, Frey A, Mufson A, Ochoa A. Where have all the T cells gone? Mechanisms of immune evasion by tumors. *Immunol Today* 1999;20:158–60.
4. Keilholz U, Weber J, Finke JH, et al. Immunologic monitoring of cancer vaccine therapy: results of a workshop sponsored by the Society for Biological Therapy. *J Immunother* 2002;25:97–138.
5. Goto S, Sato M, Kaneko R, Itoh M, Sato S, Takeuchi S. Analysis of Th1 and Th2 cytokine production by peripheral blood mononuclear cells as a parameter of immunological dysfunction in advanced cancer patients. *Cancer Immunol Immunother* 1999;48: 435–42.
6. Enk AH, Jonuleit H, Saloga J, Knop J. Dendritic cells as mediators of tumor-induced tolerance in metastatic melanoma. *Int J Cancer* 1997;73:309–16.
7. Gabrilovich DI, Corak J, Ciernik IF, Kavanaugh D, Carbone DP. Decreased antigen presentation by dendritic cells in patients with breast cancer. *Clin Cancer Res* 1997;3:483–90.
8. Almand B, Resser JR, Lindman B, et al. Clinical significance of defective dendritic cell differentiation in cancer. *Clin Cancer Res* 2000;6:1755–66.
9. Singh B, Lucci A. Role of cyclooxygenase-2 in breast cancer. *J Surg Res* 2002;108:173–9.
10. Singh-Ranger G, Mokbel K. The role of cyclooxygenase-2 (COX-2) in breast cancer, and implications of COX-2 inhibition. *Eur J Surg Oncol* 2002;28:729–37.
11. Half E, Tang XM, Gwyn K, Sahin A, Wathen K, Sinicrope FA. Cyclooxygenase-2 expression in human breast cancers and adjacent ductal carcinoma in situ. *Cancer Res* 2002;62:1676–81.
12. Herschman HR. Regulation of prostaglandin synthase-1 and prostaglandin synthase-2. *Cancer Metastasis Rev* 1994;13:241–56.
13. Herschman HR. Prostaglandin synthase 2. *Biochim Biophys Acta* 1996;1299:125–40.
14. Liu CH, Chang SH, Narko K, et al. Overexpression of cyclooxygenase-2 is sufficient to induce tumorigenesis in transgenic mice. *J Biol Chem* 2001;276:18563–9.
15. Munkarah AR, Morris R, Baumann P, et al. Effects of prostaglandin E(2) on proliferation and apoptosis of epithelial ovarian cancer cells. *J Soc Gynecol Invest* 2002;9:168–73.
16. Amano H, Hayashi I, Endo H, et al. Host prostaglandin E(2)-EP3 signaling regulates tumor-associated angiogenesis and tumor growth. *J Exp Med* 2003;197:221–32.
17. Pai R, Soreghan B, Szabo IL, Pavelka M, Baatar D, Tarnawski AS. Prostaglandin E2 transactivates EGF receptor: a novel mechanism for promoting colon cancer growth and gastrointestinal hypertrophy. *Nat Med* 2002;8:289–93.
18. Harizi H, Juzan M, Pitard V, Moreau JF, Gualde N. Cyclooxygenase-2-issued prostaglandin e(2) enhances the production of endogenous IL-10, which down-regulates dendritic cell functions. *J Immunol* 2002;168:2255–63.
19. Sharma S, Stolina M, Lin Y, et al. T cell-derived IL-10 promotes lung cancer growth by suppressing both T cell and APC function. *J Immunol* 1999;163:5020–8.
20. Stolina M, Sharma S, Lin Y, et al. Specific inhibition of cyclooxygenase 2 restores antitumor reactivity by altering the balance of IL-10 and IL-12 synthesis. *J Immunol* 2000;164:361–70.
21. Lanzavecchia A, Sallusto F. Dynamics of T lymphocyte responses: intermediates, effectors, and memory cells. *Science* 2000;290:92–7.
22. Pradelles P, Grassi J, Maclouf J. Enzyme immunoassays of eicosanoids using acetylcholine esterase as label: an alternative to radioimmunoassay. *Anal Chem* 1985;57:1170–3.
23. Maxey KM, Maddipati KR, Birkmeier J. Interference in enzyme immunoassays. *J Clin Immunoassay* 1992;15:116–20.
24. Goodwin JS, Bankhurst AD, Messner RP. Suppression of human T-cell mitogenesis by prostaglandin. Existence of a prostaglandin-producing suppressor cell. *J Exp Med* 1977;146:1719–34.
25. Kabashima K, Sakata D, Nagamachi M, Miyachi Y, Inaba K, Narumiya S. Prostaglandin E2-EP4 signaling initiates skin immune responses by promoting migration and maturation of Langerhans cells. *Nat Med* 2003;9:744–9.
26. Finke JH, Zea AH, Stanley J, et al. Loss of T-cell receptor zeta chain and p56lck in T-cells infiltrating human renal cell carcinoma. *Cancer Res* 1993;53:5613–6.
27. Ghosh P, Sica A, Young HA, et al. Alterations in NF kappa B/Rel family proteins in splenic T-cells from tumor-bearing mice and reversal following therapy. *Cancer Res* 1994;54:2969–72.
28. Appleman LJ, Tzachanis D, Grader-Beck T, van Puijenbroek AA, Boussiotis VA. Helper T cell anergy: from biochemistry to cancer pathophysiology and therapeutics. *J Mol Med* 2001;78:673–83.
29. Schmielau J, Finn OJ. Activated granulocytes and granulocyte-derived hydrogen peroxide are the underlying mechanism of suppression of t-cell function in advanced cancer patients. *Cancer Res* 2001;61:4756–60.
30. Schmielau J, Nalesnik MA, Finn OJ. Suppressed T-cell receptor zeta chain expression and cytokine production in pancreatic cancer patients. *Clin Cancer Res* 2001;7(3 Suppl):933s–939s.
31. Nieland JD, Loviscek K, Kono K, et al. PBLs of early breast carcinoma patients with a high nuclear grade tumor unlike PBLs of cervical carcinoma patients do not show a decreased TCR zeta expression but are functionally impaired. *J Immunother* 1998;21: 317–22.
32. Lucey DR, Clerici M, Shearer GM. Type 1 and type 2 cytokine dysregulation in human infectious, neoplastic, and inflammatory diseases. *Clin Microbiol Rev* 1996;9:532–62.
33. Onishi T, Ohishi Y, Goto H, Tomita M, Abe K. An assessment of the immunological status of patients with renal cell carcinoma based on the relative abundance of T-helper 1- and -2 cytokine-producing CD4+ cells in peripheral blood. *BJU Int* 2001;87:755–9.
34. Duan Z, Feller AJ, Penson RT, Chabner BA, Seiden MV. Discovery of differentially expressed genes associated with paclitaxel resistance using cDNA array technology: analysis of interleukin

(IL) 6, IL-8, and monocyte chemotactic protein 1 in the paclitaxel-resistant phenotype. *Clin Cancer Res* 1999;5:3445–53.
35. Kunz M, Toksoy A, Goebeler M, Engelhardt E, Brocker E, Gillitzer R. Strong expression of the lymphoattractant C-X-C chemokine Mig is associated with heavy infiltration of T cells in human malignant melanoma. *J Pathol* 1999;189:552–8.
36. Baggiolini M, Dewald B, Moser B. Human chemokines: an update. *Annu Rev Immunol* 1997;15:675–705.
37. Groux H, Bigler M, de Vries JE, Roncarolo MG. Interleukin-10 induces a long-term antigen-specific anergic state in human CD4+ T cells. *J Exp Med* 1996;184:19–29.
38. Letterio JJ, Roberts AB. Regulation of immune responses by TGF-beta. *Annu Rev Immunol* 1998;16:137–61.
39. McCoy JM, Wicks JR, Audoly LP. The role of prostaglandin E2 receptors in the pathogenesis of rheumatoid arthritis. *J Clin Invest* 2002;110:651–8.
40. Menetrier-Caux C, Montmain G, Dieu MC, et al. Inhibition of the differentiation of dendritic cells from CD34(+) progenitors by tumor cells: role of interleukin-6 and macrophage colony-stimulating factor. *Blood* 1998;92:4778–91.
41. Jonuleit H, Schmitt E, Schuler G, Knop J, Enk AH. Induction of interleukin 10-producing, nonproliferating CD4(+) T cells with regulatory properties by repetitive stimulation with allogeneic immature human dendritic cells. *J Exp Med* 2000;192:1213–22.
42. Bell D, Chomarat P, Broyles D, et al. In breast carcinoma tissue, immature dendritic cells reside within the tumor, whereas mature dendritic cells are located in peritumoral areas. *J Exp Med* 1999; 190:1417–26.
43. Steinman RM, Hawiger D, Nussenzweig MC. Tolerogenic dendritic cells. *Ann Rev Immunol* 2003;21:685–711.
44. Roper RL, Phipps RP. Prostaglandin E2 regulation of the immune response. *Adv Prostaglandin Thromboxane Leukot Res* 1994;22: 101–11.
45. Snijdewint FG, Kalinski P, Wierenga EA, Bos JD, Kapsenberg ML. Prostaglandin E2 differentially modulates cytokine secretion profiles of human T helper lymphocytes. *J Immunol* 1993;150: 5321–9.
46. Misra N, Selvakumar M, Singh S, et al. Monocyte derived IL 10 and PGE2 are associated with the absence of Th 1 cells and in vitro T cell suppression in lepromatous leprosy. *Immunol Lett* 1995;48: 123–8.
47. Cella M, Scheidegger D, Palmer-Lehmann K, Lane P, Lanzavecchia A, Alber G. Ligation of CD40 on dendritic cells triggers production of high levels of interleukin-12 and enhances T cell stimulatory capacity: T-T help via APC activation. *J Exp Med* 1996;184:747–52.
48. Kalinski P, Vieira PL, Schuitemaker JH, de Jong EC, Kapsenberg ML. Prostaglandin E(2) is a selective inducer of interleukin-12 p40 (IL-12p40) production and an inhibitor of bioactive IL-12p70 heterodimer. *Blood* 2001;97:3466–9.
49. Morecki S, Yacovlev E, Gelfand Y, Trembovler V, Shohami E, Slavin S. Induction of antitumor immunity by indomethacin. *Cancer Immunol Immunother* 2000;48:613–20.

Cyclooxygenase-2 Inhibitor Induces Apoptosis in Breast Cancer Cells in an In vivo Model of Spontaneous Metastatic Breast Cancer11Susan G. Komen Breast Cancer Foundation.Note: G.D. Basu and L.B. Pathangey contributed equally to this work.

Gargi D. Basu, Latha B. Pathangey, Teresa L. Tinder, et al.

Mol Cancer Res 2004;2:632-642.

Cyclooxygenase-2 Inhibitor Induces Apoptosis in Breast Cancer Cells in an *In vivo* Model of Spontaneous Metastatic Breast Cancer

Gargi D. Basu,[1] Latha B. Pathangey,[1] Teresa L. Tinder,[1] Michelle LaGioia,[1] Sandra J. Gendler,[1,2] and Pinku Mukherjee[1]

[1]Mayo Clinic College of Medicine, Department of Biochemistry and Molecular Biology and [2]Tumor Biology Program, Scottsdale, Arizona

Abstract

Cyclooxygenase-2 (COX-2) inhibitors are rapidly emerging as a new generation of therapeutic drug in combination with chemotherapy or radiation therapy for the treatment of cancer. The mechanisms underlying its antitumor effects are not fully understood and more thorough preclinical trials are needed to determine if COX-2 inhibition represents a useful approach for prevention and/or treatment of breast cancer. The purpose of this study was to evaluate the growth inhibitory mechanism of a highly selective COX-2 inhibitor, celecoxib, in an *in vivo* oncogenic mouse model of spontaneous breast cancer that resembles human disease. The oncogenic mice carry the polyoma middle T antigen driven by the mouse mammary tumor virus promoter and develop primary adenocarcinomas of the breast. Results show that oral administration of celecoxib caused significant reduction in mammary tumor burden associated with increased tumor cell apoptosis and decreased proliferation *in vivo*. *In vivo* apoptosis correlated with significant decrease in activation of protein kinase B/Akt, a cell survival signaling kinase, with increased expression of the proapoptotic protein Bax and decreased expression of the antiapoptotic protein Bcl-2. In addition, celecoxib treatment reduced levels of proangiogenic factor (vascular endothelial growth factor), suggesting a role of celecoxib in suppression of angiogenesis in this model. Results from these preclinical studies will form the basis for assessing the feasibility of celecoxib therapy alone or in combination with conventional therapies for treatment and/or prevention of breast cancer.
(Mol Cancer Res 2004;2(11):632–42)

Introduction

In the United States, breast cancer is the second most common cancer and contributes to 40,000 deaths in a year. If confined within the breast, the tumor can be surgically removed with an increased survival rate. However, primary tumors that metastasize to distant sites such as lymph nodes, lungs, liver, and brain correlate with poor prognosis. Complications from metastatic disease are the leading cause of cancer-related deaths. Mean survival for patients with metastatic breast cancer is 18 to 24 months. Response to chemotherapy or endocrine therapy in metastatic breast cancer patients is ~50% (1). Clearly, a need for development of novel therapies to enhance the existing triad of surgery, radiation, and chemotherapy is evident. Cyclooxygenase-2 (COX-2), the inducible form of the COX enzymes, catalyzes conversion of arachidonic acid to prostaglandin H_2, which is further converted to several other prostaglandins with diversified functions. Deregulation of COX-2 activity and downstream prostaglandins plays a vital role in carcinogenesis, inflammation, and tissue damage (2-5). COX-2 is overexpressed in many cancers including breast cancer, and the major functional prostaglandin in breast cancer is prostaglandin E_2 (PGE_2). Overexpression of COX-2 protein and PGE_2 during carcinogenesis is implicated in proliferation, invasion, apoptosis, immune suppression, and angiogenesis. COX-2 is induced by a variety of factors including tumor promoters, cytokines, growth factors, and hypoxia. Importantly, selective inhibition of this enzyme reduces adenocarcinoma formation and cancer progression in preclinical animal models (6-8). The first direct evidence of COX-2 function in cancers came from the study by Eberhart et al. (9), documenting significant elevations in COX-2 expression in 85% of human colorectal carcinomas and 50% of colorectal adenomas. COX-2 overexpression has since been found in many other human cancers including breast (10, 11), esophageal (12, 13), lung (14, 15), prostate (16, 17), bladder (18, 19), skin (20, 21), and pancreas (22, 23).

Studies with specific inhibitors of COX-2 enzyme have shown significant effects in reducing the incidence and progression of tumors in both animal models and in treatment of cancer patients (6-8). Studies to evaluate effects of COX-2-specific inhibitors in the treatment of breast cancer have started recently; therefore, data are limited. In animal studies, COX-2 inhibitors have shown promising results. In rat models of chemical carcinogenesis, COX-2 inhibitors significantly reduced incidence and size of mammary tumors (31, 32). COX-2 inhibitors were also effective in retarding tumor progression and metastasis in mouse models of injected breast cancer cell lines and in xenograft models of human breast cancer cells in nude mice (24, 33, 34). Clinically, COX-2 inhibitors have been

Received 8/4/04; revised 10/5/04; accepted 10/18/04.
Grant support: Susan G. Komen Breast Cancer Foundation.
The costs of publication of this article were defrayed in part by the payment of page charges. This article must therefore be hereby marked advertisement in accordance with 18 U.S.C. Section 1734 solely to indicate this fact.
Note: G.D. Basu and L.B. Pathangey contributed equally to this work.
Requests for reprints: Pinku Mukherjee, Mayo Clinic College of Medicine, 13400 East Shea Boulevard, Scottsdale, AZ 85259. Phone: 480-301-6327; Fax: 480-301-7017. E-mail: mukherjee.pinku@mayo.edu

used in combination with other anticancer drugs or radiation therapy to treat solid tumors, mostly focusing on colon and colorectal cancers. Reports emerging from these studies strongly suggest that COX-2 inhibitors may emerge as a new generation of therapeutic drugs for cancer therapy. A recent report indicated that regular nonsteroidal anti-inflammatory drug use for 5 to 9 years was associated with a 21% reduction in the incidence of breast cancer and regular use for >10 years was associated with 28% reduction (35). This area of research is underexplored and more thorough preclinical trials are needed to further determine if COX-2 inhibition represents a useful approach to treatment of breast cancer.

Preclinical studies must precede clinical trials, and use of appropriate mouse models is key to the development of efficient therapeutic strategies. We have used in this study the oncogenic mice that carry the polyoma virus middle T antigen (MTag) driven by the mouse mammary tumor virus (MMTV) long terminal repeat promoter. These mice develop spontaneous tumors of the breast, which metastasize to the lungs and bone marrow. All mice are congenic on the C57BL/6 background to eliminate strain-specific modifier effects. In the MTag mice, mammary gland tumors are induced by the action of a potent tyrosine kinase activity associated with the polyoma virus MTag driven by the MMTV promoter (36). MTag specifically associates with and activates the tyrosine kinase activity of several c-*src* family members, eliciting tumors when a threshold level of gene product has been attained. In these mice, the MMTV promoter is transcriptionally active throughout all stages of mammary gland development, which results in widespread transformation of the mammary epithelium and the rapid production of multifocal mammary adenocarcinomas. Focal atypical lesions can be detected by whole mount as early as 21 days and palpable mammary gland tumors are detectable from ~60 days onward. Tumor progression is quite rapid, reaching 10% of body weight by ~20 to 24 weeks. All of the female mice get tumors. Tumors arise with synchronous kinetics and are highly fibrotic with dense connective tissue separating individual nests of tumor cells, a pathology that closely resembles scirrhous carcinomas of the human breast (37, 38). These mice exhibit metastasis in the lungs (60%) and micrometastasis in the bone marrow by 4 months of age (39). Therefore, the MTag mouse model is an appropriate model for human metastatic breast cancer in which to evaluate therapeutic strategies and to understand the mechanisms associated with therapy-induced growth inhibition. This is the first study to evaluate the efficacy and growth inhibitory mechanisms of celecoxib in an *in vivo* model of spontaneous metastatic breast cancer.

Results

Celecoxib Treatment Caused Significant Reduction in Primary Mammary Tumor Burden

Ten-week-old tumor-bearing female MTag mice were gavaged daily for 4 weeks with celecoxib at 5, 10, or 20 mg/kg body weight. In mice, at 10 and 20 mg/kg dose, the concentration of celecoxib in the plasma ranges from 6.5 to 13 μmol/L at 2 hours and from 4.2 to 8 μmol/L at 4 hours post-celecoxib treatment (40). This dose is attainable clinically and sufficient to inhibit PGE_2 (41). At 10 weeks, mice have small palpable tumors (1-2 tumors, ~0.1-0.5 mg tumor weight). One hundred percent of the MTag mice have hyperplastic mammary glands by 6 to 8 weeks (starting at time of puberty). Because the MTag is a strong oncogene, driven by the MMTV promoter, 100% of the MTag mice develop multifocal tumors with palpable tumors in at least 1 to 2 glands (of 10 mammary glands in mice) by 10 weeks. Every gland is hyperplastic by this time and every gland has palpable tumors by 14 weeks. Complete blood count analysis including hemoglobin levels was done to determine cytopenia and/or anemia post-celecoxib treatment. Regardless of the celecoxib dose, there was no detectable change in their complete blood count or hemoglobin levels (data not shown) as compared with untreated MTag mice. Flow cytometric analysis of T cells, B cells, and natural killer cells revealed no change in treated versus control MTag mice, nor were there any signs of weight loss in treated mice (data not shown). This suggested that celecoxib was well tolerated in these mice with no detectable signs of toxicity. Mice were sacrificed at 14 weeks of age, tumors were removed, and serum was collected. Tumor burden in MTag mice treated with 10 and 20 mg/kg dose was significantly reduced ($P < 0.003$ for 10 mg/kg and $P < 0.01$ for 20 mg/kg; Fig. 1). Note that in this study we started the treatment at 10 weeks when the mice had established tumors. The purpose of this study was to focus on the short-term effect of celecoxib on breast cancer cells *in vivo* at early times during tumor development and evaluate the mechanism of action of the drug on primary breast cancer cells. All mice were terminated at 14 weeks of age. The cumulative palpable tumors from 10 mammary glands at 14 weeks of age for individual mouse are presented in Fig. 1. Because metastasis in the MTag mice only develop between 19 and 24 weeks of age, we evaluated 6 MTag mice that received 20 mg/kg celecoxib and 10 vehicle-treated MTag mice between 20 and 24

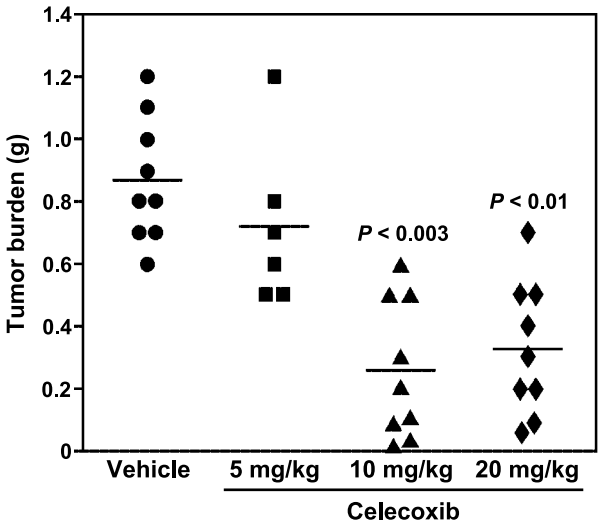

FIGURE 1. Reduced tumor burden in 14-week-old MTag mice post-celecoxib treatment. MTag mice were palpated weekly for presence of mammary tumors. Tumor weights plotted represent total tumor burden (including all mammary glands) per mice at 14 weeks of age ($n = 9$ mice for vehicle and 10 and 20 mg/kg celecoxib and $n = 6$ mice for 5 mg/kg celecoxib).

weeks of age. Gross microscopic examination of lungs revealed that the celecoxib-treated mice did not develop metastasis (0 of 6), whereas 6 of the 10 control mice developed lung metastasis (data not shown). These results are preliminary and we need to enroll more mice to the study to achieve statistical significance.

Celecoxib Induces Apoptosis in Breast Cancer Cells In vivo

We have reported recently that celecoxib induces growth inhibition of human and mouse breast cancer cells *in vitro* by simultaneously activating tumor cell apoptosis and inhibiting proliferation (42). Apoptosis of primary MTag tumor cells was determined by Annexin V/propidium iodide staining and flow cytometry. Data revealed significant increase in apoptotic cell population at 10 and 20 mg/kg celecoxib dose as compared with control MTag mice (39% in control mice versus 65% in 10 mg/kg dose, $P < 0.05$; 59% in 20 mg/kg dose, $P < 0.05$). The lowest dose (5 mg/kg) did not have a significant effect (Fig. 2A). Tumor cells from untreated MTag mice gave similar percentage of apoptotic cells (~35-40%) as vehicle-treated mice (data not shown). The high baseline apoptosis level in vehicle-treated and untreated mice is likely due to the method of isolating single cells. However, the 1.5- to 1.7-fold increase following celecoxib treatment was reproducibly observed.

We also evaluated celecoxib-induced apoptosis *in situ* by detection of DNA fragmentation using the terminal deoxynucleotidyl transferase–mediated dUTP nick end labeling (TUNEL) assay (43). We observed an increase in TUNEL-positive cells in celecoxib-treated tumor sections *in situ* as compared with control tumor sections, confirming the flow cytometry data (Fig. 2B). Representative immunohistochemical images of vehicle-treated and celecoxib-treated MTag tumor sections are shown at 100× magnification, demonstrating considerable TUNEL positivity in celecoxib-treated versus control MTag tumor sections.

Increased Bax and Decreased Bcl-2 in Tumor Lysate Derived from Celecoxib-Treated MTag Mice

The downstream signaling pathways involved in COX-2-induced apoptosis are not well understood, but at least three pathways have been suggested: Bcl-2-mediated pathway, nitric oxide pathway, and production of ceramide (44). Because it has been shown previously in cell lines that celecoxib-induced apoptosis is associated with decreased Bcl-2 (an antiapoptotic protein) and increased Bax (a proapoptotic protein), we evaluated the levels of Bcl-2 and Bax by Western blot analysis of whole MTag tumor lysate post-celecoxib treatment. Treatment with celecoxib at 10 and 20 mg/kg induced increased expression of Bax (inducer of apoptosis) in all five mice tested as compared with vehicle-treated tumors (Fig. 3A). The increase was most pronounced at the 10 mg/kg dose of celecoxib. Simultaneously, there was decrease in Bcl-2 (inhibitor of apoptosis) protein expression in the 10 and 20 mg/kg dose of celecoxib (Fig. 3B). Untreated MTag tumor lysate was used as positive control in the first lane. These tumor lysates were prepared from 21-week-old MTag tumors, whereas the treated mice were at 14 weeks of age. This could explain the difference in protein expression observed

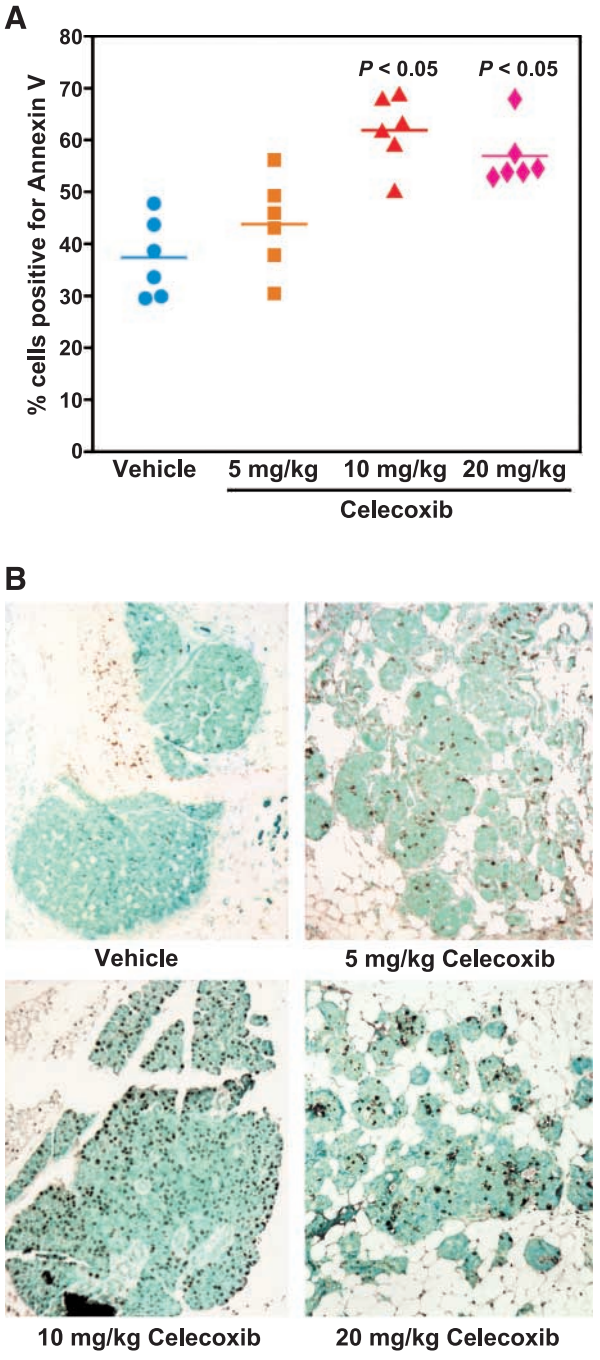

FIGURE 2. A. Increase in Annexin V–positive cells in celecoxib-treated MTag tumors *in vivo*. Tumor cells derived from vehicle-treated or celecoxib (5, 10, or 20 mg/kg body weight)–treated MTag mice were stained with Annexin V conjugated with FITC and propidium iodide, and percentage apoptotic cells (cells positive for Annexin V) were analyzed by flow cytometry. $n = 6$ mice per treatment group. *P,* significant difference between celecoxib-treated groups and vehicle control. **B.** Increase in TUNEL-positive cells in celecoxib-treated MTag tumors *in situ*. Light microscopic image of TUNEL-positive cells visualizing apoptosis *in situ* from mammary gland tumor sections isolated from vehicle and 5, 10, and 20 mg/kg celecoxib-treated MTag mice. *Brown,* apoptotic cells. All images are representative of five standardized fields from six separate mice. Magnification, ×100.

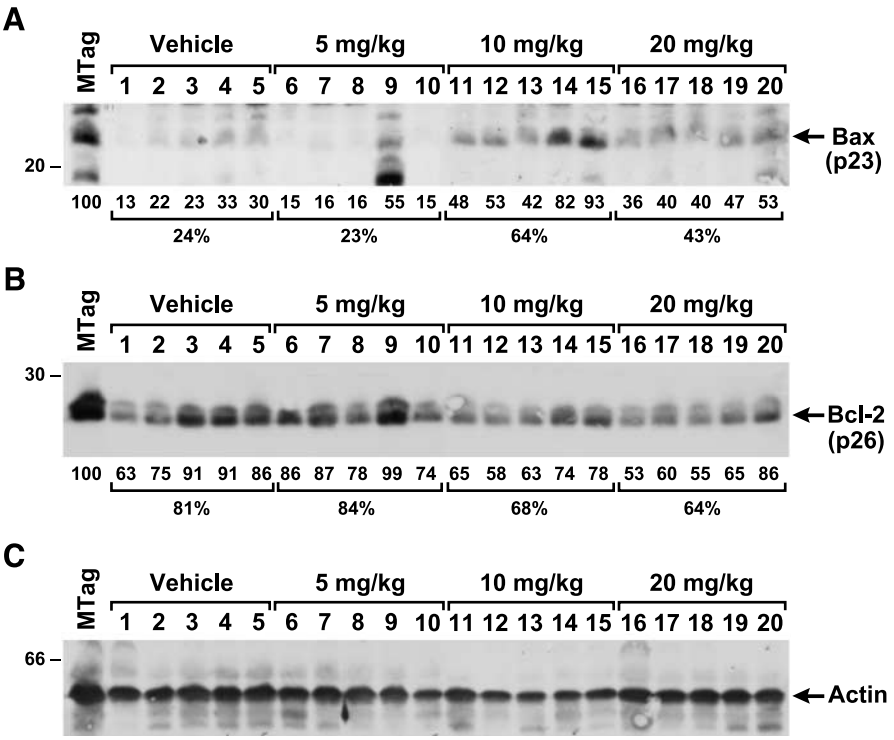

FIGURE 3. Increase in the proapoptotic protein Bax and decrease in the antiapoptotic protein Bcl-2 post-celecoxib treatment. Western blot analysis of Bax and Bcl-2 protein levels in mammary gland tumor lysates from vehicle and celecoxib (5, 10, and 20 mg/kg)–treated MTag mice; 100 μg of protein were loaded per lane. $n = 5$ individual mice. *Numbers below each lane,* percentage of protein expression compared with MTag lysate, which was set to equivalent of 100% as determined by densitometric analysis. Average percentage expression for each treatment group ($n = 5$ mice). *P,* significant difference between treatment groups and vehicle control. β-Actin is used as the protein loading control for all tumor lysates.

between vehicle-treated and untreated MTag tumors. Tumor lysate from 14-week-old MTag mice have similar Bcl-2 and Bax levels as vehicle-treated tumors (data not shown). Densitometric analysis of the Western blots indicates significant increase in Bax protein levels between vehicle-treated and 10 mg/kg ($P < 0.05$) and 20 mg/kg ($P < 0.06$) celecoxib-treated tumor lysates. Similarly, significant decrease in Bcl-2 was observed between vehicle-treated and 5 mg/kg celecoxib–treated mice versus 10 mg/kg ($P < 0.05$) and 20 mg/kg ($P < 0.05$) celecoxib-treated groups. All comparisons are between 14-week-old vehicle-treated tumors and age-matched celecoxib-treated tumors. Thus, data suggest that celecoxib-induced apoptosis in MTag tumor cells *in vivo* is associated with an elevated expression of Bax and reduced expression of Bcl-2 proteins. These results give further credence to the flow cytometry and TUNEL data, confirming that celecoxib induces apoptosis *in vivo* in a highly aggressive and metastatic breast cancer model.

Reduced Phosphorylation of Akt in Tumor Lysate Derived from Celecoxib-Treated MTag Mice

Protein kinase B/Akt is a serine/threonine protein kinase that is involved in promoting cell survival signals through the phosphatidylinositol 3-kinase (PI3K) pathway leading to inactivation of a series of proapoptotic proteins. These kinase activities are frequently deregulated in human disease including cancer (45). Akt represents a key signaling component in cell survival by activating downstream proapoptotic proteins and caspases (46-48). Celecoxib has been shown recently to induce apoptosis of cancer cells by blocking Akt activation in cultured prostate cancer cells (49, 50). To explore whether inhibition of Akt activation may be linked to the observed *in vivo* apoptosis in MTag tumors, we determined the effect of *in vivo* celecoxib administration on phosphorylation of Akt (at Ser^{473} in the carboxyl terminus) in MTag tumors. Data show that celecoxib substantially suppresses phosphorylation of Akt in MTag tumors. Two of five mice in the 5 mg/kg dose showed reduced phosphorylation, whereas four of five in 10 mg/kg and five of five mice in 20 mg/kg dose showed reduced Akt activation (Fig. 4). Densitometric analysis clearly indicates significant down-regulation of Akt phosphorylation in celecoxib-treated tumors as compared with vehicle-treated tumors ($P < 0.05$ for 10 and 20 mg/kg celecoxib). All tumors showed approximately equivalent levels of the Akt protein as shown in Fig. 4 (*bottom*). This result clearly suggested the involvement of the Akt pathway in induction of apoptosis *in vivo* in our mouse model of spontaneous breast cancer. Akt represents a key signaling component in cell survival by activating downstream proapoptotic proteins and caspases (46-48). Because we observed a decrease in Akt phosphorylation and increase in proapoptotic protein (Bax), we determined if caspases were activated post-celecoxib treatment. MTag tumor cells treated with celecoxib *in vitro* (20, 40, and 60 μmol/L) were analyzed for activation of effector caspase-3 and caspase-7. Most apoptotic signals induce intracellular cleavage of caspase-3 and caspase-7 and convert them into active forms. Caspase activity is presented as fluorescence emission, which is directly proportional to caspase-3/7 activities. Increase in fluorescence emission was observed with increasing dose of celecoxib, which correlates with increase in active forms of caspase-3 and caspase-7. Table 1 illustrates the fluorescence emission for untreated versus

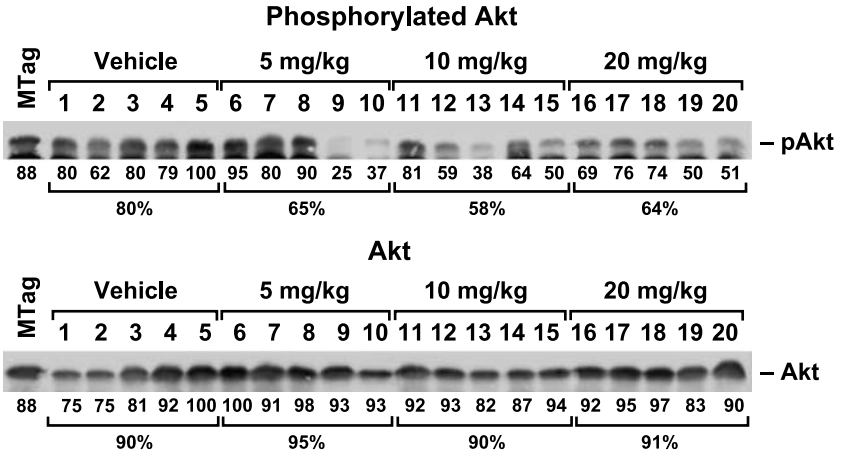

FIGURE 4. Decreased phosphorylation of protein kinase B/Akt post-celecoxib treatment. Western blot analysis of phospho-Akt (*pAkt*) and Akt protein levels in mammary gland tumor lysates from vehicle and celecoxib (5, 10, and 20 mg/kg)–treated MTag mice; 100 μg of protein were loaded per lane. $n = 5$ individual mice. *Numbers below each lane,* percentage of protein expression compared with mouse expressing the most protein, which was set equivalent to 100% as determined by densitometric analysis. Average percentage expression for each treatment group ($n = 5$ mice). *P,* significant difference between treatment groups and vehicle control.

celecoxib-treated MTag tumor cells. Significant increase in fluorescence emission was observed in 40 and 60 μmol/L celecoxib-treated cells compared with untreated or vehicle-treated cells ($P < 0.05$ and 0.01, respectively).

Celecoxib Inhibits Tumor Cell Proliferation

Antiproliferative effect of *in vivo* celecoxib treatment was determined by *in situ* immunohistochemical analysis of MTag tumor sections stained with proliferating cell nuclear antigen (PCNA). A representative light microscope image suggests inhibition of proliferation in MTag tumors *in vivo* with 10 and 20 mg/kg celecoxib treatment (Fig. 5). PCNA protein levels peak during the S phase of the cell cycle and is almost undetectable in other phases of the cycle. Vehicle and 5 mg/kg celecoxib treatments show almost every cell expressing PCNA, indicative of highly proliferative cells (Fig. 5A and B). With 10 and 20 mg/kg treatment, fewer cells expressed PCNA staining, suggestive of fewer cells undergoing proliferation (Fig. 5C and D). A lymph node within an untreated mammary tumor section shows only a few proliferating cells, confirming the specificity of the stain (Fig. 5E). Staining specificity is further confirmed with second antibody control (Fig. 5F).

Celecoxib Treatment Significantly Reduced Serum Levels of PGE_2 In vivo

Next, we analyzed sera and tumor lysate from celecoxib-treated and vehicle-treated MTag mice for PGE_2 levels to assess COX-2 activity *in vivo*. COX-2 converts arachidonic acid to bioactive prostaglandins. It has been shown that COX-2-derived PGE_2 is the major prostaglandin produced by breast cancer cells and may be required for the angiogenic switch leading to initiation and progression of mammary cancer in a MMTV-COX-2 transgenic mouse model (51). Production of secreted PGE_2 is an appropriate measure of COX-2 activity in the MTag mouse model. PGE_2 is unstable *in vivo* and

Table 1. Caspase-3 and Caspase-7 Activity of MTag Cells Treated with Celecoxib

Treatment	Caspase-3/7 Activity (Fluorescence Emission)
Vehicle	$1 \times 10^6 \pm 2.0 \times 10^5$
Celecoxib (20 μmol/L)	$2 \times 10^6 \pm 1.6 \times 10^5$
Celecoxib (40 μmol/L)	$4 \times 10^6 \pm 2.2 \times 10^5$*
Celecoxib (60 μmol/L)	$5 \times 10^6 \pm 2.0 \times 10^5$*

NOTE: Spectrofluorometric analysis of lysates prepared from 48-hour vehicle-treated and celecoxib (20, 40, and 60 μmol/L)–treated MTag cells. Activity of caspase-3 and caspase-7 was monitored by enzymatic cleavage using a fluorescence microplate reader with excitation at 485 ± 10 nm and emission detection at 530 ± 12.5 nm. Mean ± SD of three experiments.
*$P < 0.01$, significant difference between vehicle control and celecoxib treatment.

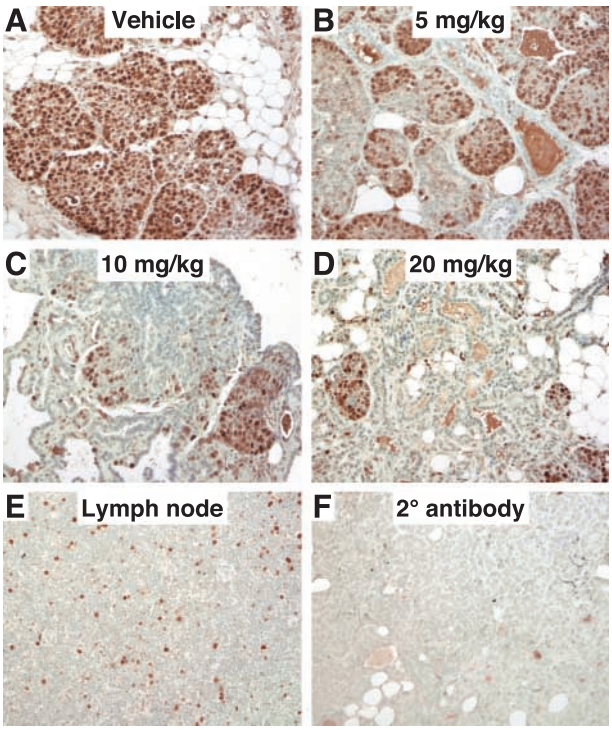

FIGURE 5. Celecoxib-induced inhibition of tumor cell proliferation *in vivo* in a dose-dependent manner. Light microscopy images of PCNA staining of mammary tumor sections from vehicle-treated (**A**) and celecoxib (5, 10, and 20 mg/kg)–treated (**B-D**) MTag mice. All images are representative of five standardized fields from six separate experiments. Inhibition of proliferation is most evident at 10 and 20 mg/kg dose of celecoxib. Lymph node section (**E**) and second antibody staining (**F**) are shown as controls. Magnification, ×200.

measurement of the metabolites is necessary to provide a reliable estimate of actual PGE_2 production. Thus, we measured PGE_2 metabolite (PGEM; i.e., 13,14-dihydro-15-keto prostaglandin A_2) using a commercially available ELISA. A significant reduction in serum PGEM is observed in 10 and 20 mg/kg celecoxib-treated MTag mice as compared with pretreatment and vehicle-treated mice (2,000 pg/mL in vehicle-treated mice versus <1,000 pg/mL in 10 mg/kg celecoxib-treated mice, $P < 0.01$; Fig. 6A). Similar reduction in PGEM was observed in tumor lysates (data not shown). Note that the serum PGEM levels never reached the values observed in nontumor C57BL/6 mice of 300 pg/mL (Fig. 6A). This suggests that, although celecoxib was partially effective in reducing PGEM levels, treatment was not sufficient to completely reverse the up-regulation of PGE_2 levels in MTag mice because these mice were not completely tumor free.

To test if celecoxib had a direct effect on COX-2 protein expression in the tumor, we evaluated COX-2 protein expression in tumor lysates from vehicle-treated and celecoxib-treated MTag tumors. MTag tumors from untreated and vehicle-treated mice expressed higher levels of COX-2 (Fig. 6B) as compared with celecoxib-treated (10 and 20 mg/kg) tumors, indicating that celecoxib has a direct effect on COX-2 protein expression *in vivo*. Densitometric analysis showed some difference between vehicle-treated and 10 or 20 mg/kg celecoxib-treated tumors ($P < 0.07$). However, the direct effect of celecoxib on COX-2 protein expression was less significant ($P < 0.07$) than its effect on COX-2 activity as measured by PGE_2 levels.

Celecoxib Treatment Reduced Vascular Endothelial Growth Factor Levels In vivo

It has been shown recently that COX-2-induced PGE_2 stimulated the expression of angiogenic regulatory genes including vascular endothelial growth factor (VEGF) in mammary tumor cells isolated from COX-2 transgenic mice and that treatment with indomethacin (nonspecific COX inhibitor) suppressed the expression of these genes *in vitro* (51). We therefore evaluated levels of *in vivo* VEGF protein levels in the tumor microenvironment of MTag tumors post-celecoxib treatment. Treatment with celecoxib (10 or 20 mg/kg) reduced VEGF levels in the tumor lysate in four of six treated mice as compared with vehicle-treated MTag tumors ($P < 0.05$; Fig. 7). No reduction was observed in mice treated with 5 mg/kg celecoxib. Untreated MTag tumor lysate had similar levels as vehicle-treated MTag mice (data not shown). Similar reduction in circulating VEGF levels was also

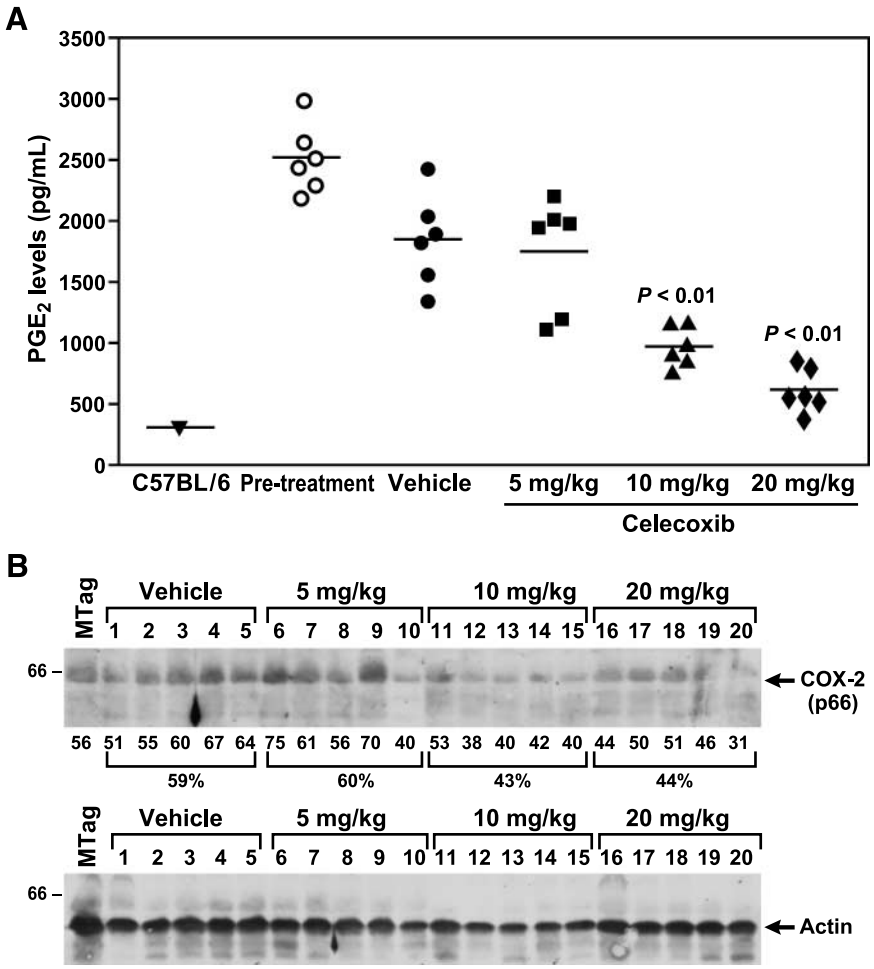

FIGURE 6. A. Dose-dependent inhibition of PGE_2 synthesis in serum of celecoxib-treated MTag mice. PGEM levels in serum were determined using specific ELISA (pg/mL serum). Serum from mice was collected either before treatment commenced or after 4 weeks of celecoxib treatment. *P,* significant difference between celecoxib-treated and untreated (pretreatment) or vehicle-treated mice. PGE_2 levels are also compared with serum from age-matched non-tumor-bearing wild-type C57BL/6 mice. Significant inhibition is evident at 10 and 20 mg/kg dose. **B.** Decrease in COX-2 protein expression is not significant in MTag tumors post-celecoxib treatment ($n = 5$ mice). Western blot analysis of tumor lysates from untreated, vehicle-treated, and celecoxib (5, 10, and 20 mg/kg)–treated MTag mice; 100 μg of protein were loaded per lane. All tumor lysates expressed COX-2. Untreated and vehicle-treated tumors expressed higher levels of COX-2 than tumor lysates from celecoxib (10 and 20 mg/kg)–treated mice. *Numbers below each lane,* percentage of protein expression compared with mouse expressing the most protein, which was set equivalent to 100% as determined by densitometric analysis. Average percentage expression for each treatment group ($n = 5$ mice). β-Actin is used as the protein loading control for all tumor lysates.

observed. Serum levels of VEGF in untreated or vehicle-treated 14-week-old MTag mice were found to be between 150 and 400 pg/mL, whereas in the mice treated with celecoxib (10 or 20 mg/kg) the levels ranged from 20 to 90 pg/mL. In some of the treated mice, the VEGF levels were too low to be detected by ELISA. Preliminary histologic evaluation also suggests the presence of fewer blood vessels in the celecoxib-treated tumor sections versus control tumor using the Masson's trichrome staining. A representative picture of vehicle, 5, 10, and 20 mg/kg celecoxib-treated MTag tumor is shown in Fig. 7B.

Discussion

We show for the first time that *in vivo* treatment with celecoxib causes significant reduction in mammary gland tumor burden in a mouse model of spontaneous breast cancer. Recently, we have evaluated 6 MTag mice that received 20 mg/kg celecoxib and 10 control MTag mice between 20 and 24 weeks of age. None of the celecoxib-treated mice developed lung metastasis, whereas 5 of the 10 control mice developed lung metastasis (data not shown).

Tumor reduction was associated with induction of tumor cell apoptosis *in vivo*. Investigation into the potential molecular pathway revealed that treatment with celecoxib caused reduction in activation of antiapoptotic/prosurvival kinase (Akt). Increased apoptosis was associated with increased expression of the proapoptotic protein Bax and decreased expression of the antiapoptotic protein Bcl-2. Concurrently, we observed decreased tumor cell proliferation and decreased synthesis of VEGF in mammary gland tumors treated with celecoxib *in vivo*, most probably associated with decreased PGE_2 synthesis.

The importance of this study lies in the use of a mouse model system that resembles human disease in many aspects of tumor progression. The MTag tumors start as hyperplasia, like early proliferative lesions seen in the human breast; show indication of histologic progression to malignant mammary adenocarcinomas and metastasis; are heterogenous with respect their malignant potential; and trigger signaling pathways inactive in normal breast epithelium (38). One of the pathways that is activated in these mice is the arachidonic acid/COX-2 pathway (52), similar to that described in many human breast cancers. Furthermore, we have shown recently that COX-2 protein and its downstream product PGE_2 were highly elevated in human breast tumors and lymph node metastasis compared with normal tissue, with the highest expression being observed in lymph node metastasis (53). There was a direct correlation between increased COX-2 and PGE_2 expression with impaired immune cell function in newly diagnosed stage I and II breast cancer patients (53). Our observations are similar to the reports that have shown significant elevation of COX-2 protein levels in 43% of human invasive breast cancers and 63% of ductal carcinomas *in situ* (11, 54). Thus, the MTag model offers the potential to evaluate chemoprevention with a highly specific COX-2 inhibitor, celecoxib.

Celecoxib has been shown to target multiple pathways of tumorigenesis including proliferation, apoptosis, angiogenesis, invasion, and tumor-induced immune suppression in various

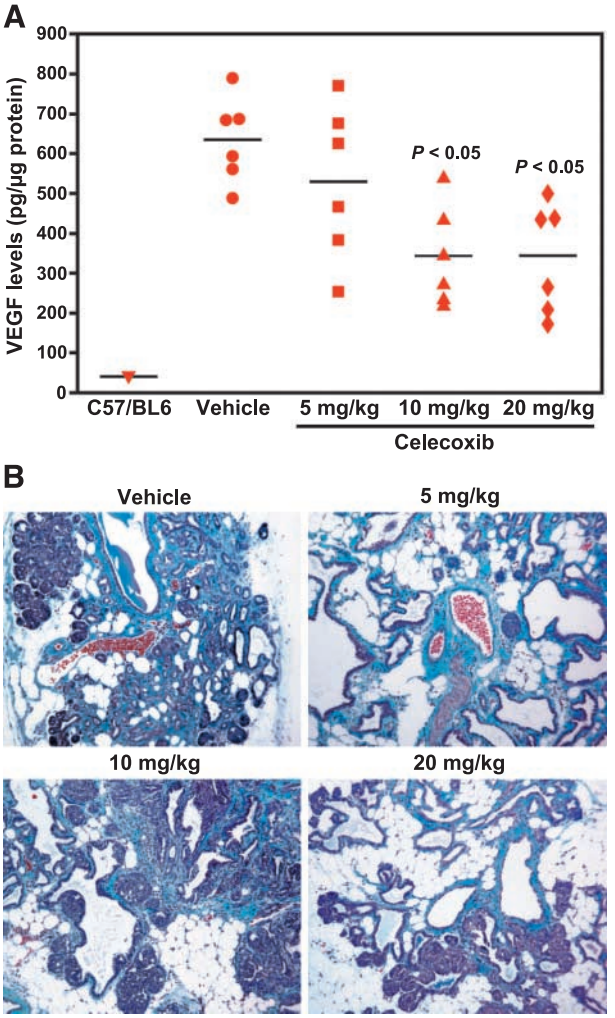

FIGURE 7. A. Decreased VEGF levels in MTag tumors from celecoxib-treated mice. VEGF levels were determined in the tumor lysates using specific ELISA (pg/μg protein lysate). Tumor lysate was prepared from untreated, vehicle-treated, and celecoxib (5, 10, and 20 mg/kg)–treated MTag mice. *P,* significant difference between celecoxib-treated and vehicle-treated mice. Values are also compared with mammary gland lysate from age-matched non-tumor-bearing wild-type C57BL/6 mice. Significant inhibition is evident at 10 and 20 mg/kg dose. **B.** Fewer blood vessels in 10 and 20 mg/kg celecoxib-treated tumor sections compared with vehicle-treated tumor. Blood vessels in MTag tumor sections were histologically evaluated by Masson's trichrome. This method stains fibrous tissue and stroma green. Blood vessels containing RBC stain bright red. Fewer blood vessels in the tumor section of the celecoxib-treated tumors (10 and 20 mg/kg) relative to those obtained from vehicle-treated animals. Magnification, ×100.

breast tumor cell lines. The current report by Chang et al. (51) supports the concept that COX-2 may provide an early target for breast cancer prevention. We show that early intervention with celecoxib causes reduced primary tumor burden in the MTag model (Fig. 1). We further show that reduced PGE_2 synthesis (Fig. 6A) and reduced PI3K/Akt kinase activation (Fig. 4) post-celecoxib treatment may be the mechanism(s) underlying enhanced tumor cell apoptosis (Fig. 2) and reduced tumor cell proliferation (Fig. 5) *in vivo*. Our data are in line with the recent *in vitro* study in prostate cancer cell lines, where

it was shown that celecoxib induces apoptosis by blocking or suppressing Akt activation (50). The PI3K/Akt pathway is typically activated in response to oncogenes that bind to receptor kinases at the plasma membrane and lead to the activation of PI3K (55, 56). Activated Akt targets multiple factors involved in cell proliferation, migration, and survival/apoptosis. Mechanistically, activated Akt is known to trigger several cyclins including cyclin D1 that affects all stages of the cell cycle and induces downstream proliferation (56). Preliminary data suggest decreased levels of cyclin D1 in tumor lysates of mice treated with celecoxib, with significant arrest of the mammary tumor cells at the G_2-M checkpoint phase of cell cycle (data not shown). Thus far, our results implicate the PI3K/Akt pathway to be critical in the celecoxib-induced apoptosis and inhibition of tumor cell proliferation. However, other pathways such as the Raf/mitogen-activated protein kinase-extracellular signal-regulated kinase/mitogen-activated protein kinase pathway may also be affected by celecoxib, and future studies will be designed to evaluate these pathways *in vivo* in the MTag mouse model. One potential mechanism that has been associated with PGE_2-related inhibition of apoptosis is that PGE_2 reduces the basal apoptotic rate by increasing the level of antiapoptotic proteins such as Bcl-2 (54, 57). Our *in vivo* data support this concept, because inhibiting PGE_2 production by targeting COX-2 activity in the MTag tumors led to decrease in Bcl-2 protein levels and concurrent increase in the proapoptotic protein Bax (Fig. 3A and B) as well as activate effector caspase-3 and caspase-7 (Table 1).

Finally, angiogenesis plays a crucial role in tumor development and progression. COX-2-dependent PGE_2 is a potent inducer of angiogenesis *in vivo* and induces expression of angiogenic regulatory proteins such as VEGF (51, 58, 59). It has been shown recently that overexpression of COX-2 in the mammary gland by MMTV promoter induces mammary carcinogenesis and that the major prostaglandin that is produced in these tumors is PGE_2 (51, 54). These authors further defined the role of COX-2-dependent PGE_2 production in transforming local tumors to invasive cancer by triggering a so-called angiogenic switch by increasing expression of proangiogenic mediators such as VEGF and its receptors. Thus, we examined whether celecoxib treatment *in vivo* was effective in reducing the exaggerated VEGF levels observed in MTag tumors and in the serum. Significant decrease in levels of VEGF in the mammary gland tumors accompanied by fewer blood vessels in the celecoxib-treated tumor sections versus control was observed (Fig. 7), once again suggesting a role of COX-2 and PGE_2 in mediating angiogenesis in the polyoma virus MTag-induced breast tumors. Although additional mechanisms are involved in mediating the angiogenic effects of COX-2, our data suggest that COX-2 influences angiogenesis at least in part by enhancing VEGF secretion by tumor endothelial cells. Additional studies are needed to fully elucidate the complex events involved in COX-2-mediated angiogenesis in our model. Our data clearly show extensive down-regulation of PGE_2 in serum (Fig. 6A) post-celecoxib treatment *in vivo*. PGE_2 binds to cell surface receptors that belong to the family of seven-transmembrane domain G protein-coupled receptors, designated EP1, EP2, EP3, and EP4 (54, 60). Future studies will determine the pattern of prostanoid receptor distribution in the MMTV-MTag mice and whether COX-2 inhibitors can modulate prostanoid receptor expression and its activation state. Although we suggest that PGE_2 down-regulation may be in part responsible for the reduced VEGF levels, we fully recognize that much work is required to define a direct relationship between PGE_2 and VEGF and that other pathways and angiogenic markers may be involved. We also acknowledge that the effect of celecoxib in the MTag mice may be COX independent; indeed, we do not see a dramatic down-regulation of COX-2 expression in celecoxib-treated compared with vehicle-treated mice (Fig. 6B). However, we must point out that we have published that the MTag tumors overexpress COX-2 and the expression increases as tumors progress and that the PGE_2 levels are significantly decreased with celecoxib treatment.

In summary, celecoxib treatment may exert its antiproliferative, antiangiogenic, and proapoptotic effects by regulating the PGE_2-prostanoid receptor–associated pathways and by decreasing PI3K/Akt phosphorylation. This leads to significant reduction in primary breast tumor burden. Furthermore, this effect may or may not be dependent on down-regulation of COX-2 protein expression in the tumor. Thus, we believe that COX-2 inhibitors not only represents a future therapeutic option for the treatment of human breast cancer in combination with standard therapies but also may be considered as a potent chemopreventive agent for individuals with high risk of developing breast cancer and for individuals with high risk of disease relapse.

Materials and Methods

Generation of MTag Mouse Model

MTag oncogenic mice was originally a kind gift from Dr. W.J. Muller (McGill University, Toronto, Ontario, Canada; ref. 36). MTag male mice were mated to C57BL/6 mice to maintain the MTag mice as heterozygous. Approximately 50% of the pups carry the oncogene, and in these pups, ~50% are females that develop mammary gland adenocarcinomas and are used for the experiments. PCR was used to routinely identify the MTag oncogene. PCR was carried out as described previously (39). Primer pairs for MTag transgene are 5′-AGTCACTGCT-ACTGCACCCAG-3′ (282-302 bp) and 5′-CTCTCCTCAGT-TCCTCGCTCC-3′ (817-837 bp). The amplification program for MTag consisted of 1 cycle of 5 minutes at 95°C and 40 cycles of 30 seconds at 95°C, 1 minute at 61°C, and 30 seconds at 72°C followed by 1 cycle of 10 minutes at 72°C. The PCR product was analyzed by size fractionation through a 1% agarose gel. Amplification of MTag gene results in a 480-bp fragment. All mice are congenic on the C57/BL6 background at $n \geq 10$. All mice were bred and maintained in specific pathogen-free conditions in the Mayo Clinic Scottsdale Natalie Schafer Transgenic Animal Facility. All experimental procedures were conducted according to Institutional Animal Care and Use Committee guidelines.

Celecoxib Treatment

Celecoxib was purchased from Pharmacia Pharmaceuticals (Skokie, IL) as 100-mg capsules. Drug was prepared for p.o. administration according to the manufacturer's recommendation.

Briefly, the drug was dissolved in DMSO, rotated at low speed in a 37°C hot room for 12 hours, and centrifuged at 1,800 rpm for 10 minutes, and the supernatant was collected and stored at 4°C as stock solution of 20 mg/mL. Ten-week-old female MTag mice were gavaged p.o. with 20-gauge barrel tip feeding needles (Fine Science Tools, Foster City, CA) at 5, 10, or 20 mg/kg body weight daily (5 days on with 2 days off) for 4 weeks. Control mice were gavaged with DMSO. Six mice per treatment group were used. Following 4 weeks of treatment, mice were sacrificed and mammary tumors dissected and divided into three parts: (*a*) to generate single cell suspension for flow cytometry, (*b*) to prepare tumor lysate for Western blot analysis and ELISA, and (*c*) to fix in formalin and embedded in paraffin blocks for immunohistochemical analysis. Serum was collected for ELISA. A dose range of 5 to 20 mg/kg body weight was used in our spontaneous mouse model based on previous reports in the literature (24, 34). These doses correspond to physiologic dose of celecoxib and are clinically relevant because the doses of COX-2 inhibitors recommended to patients are in the range of 5 to 20 mg/kg body weight (29).

Tumor Burden

From 10 weeks of age until sacrifice, control and celecoxib-treated mice were palpated weekly for presence of mammary tumors. Palpable tumors were measured by calipers and tumor weight was calculated according to the following formula: $g = L$ (cm) $\times$ W (cm^2) / 2 (39).

Analysis of Apoptosis by Flow Cytometry

Part of the tumor tissue was dissociated to generate single cell suspension by incubating in 5 mmol/L EDTA solution for 1 hour at 37°C. Apoptosis was determined by staining single cells (1×10^6) with Annexin V and propidium iodide using the BD PharMingen (San Diego, CA) apoptosis kit following the manufacturer's protocol. Cell staining was determined by flow cytometry using the CellQuest program. Percentage apoptotic cells were determined by CellQuest statistical analysis program as the cumulative percentage cells that were stained positive for both propidium iodide and Annexin V (upper right quadrant) and cells that were stained for Annexin V only (lower right quadrant).

Analysis of Apoptosis, Proliferation, and Blood Vessels by Immunohistochemistry

Part of the tumor was formalin fixed [10% neutral-buffered formalin (pH 6.8-7.2), Fisher Scientific, Pittsburgh, PA] and paraffin embedded and 5-μm sections were prepared by the Mayo Clinic Scottsdale Histology Core Facility. Immunohistochemistry was done using the ApopTag Peroxidase *In situ* Apoptosis Detection kit (Serologicals Corp., Norcross, GA). 3,3′-Diaminobenzidine was used as the chromogen and hematoxylin was used as counterstain. TUNEL-positive cells were examined under light microscopy and representative images taken at 200×. For PCNA staining, paraffin-embedded and 5-μm sections were subjected to antigen retrieval using the DAKO Target Retrieval (Carpinteria, CA) at 95°C for 40 minutes. Primary antibody (PCNA antibody, BD Biosciences, San Jose, CA) was used at 5 μg/mL at 4°C overnight and DAKO anti-mouse secondary conjugated to horseradish peroxidase was used at 1:200 for 2 hours at room temperature. 3,3′-Diaminobenzidine was used as the chromogen and hematoxylin was used as counterstain. Histologic evaluation of vascularity was determined by Masson's trichrome staining (61). This method stains fibrous tissue and stroma green. Blood vessels containing RBC stain bright red.

Assay for Caspase-3 and Caspase-7

Primary MTag tumor cells derived from 17-week-old MTag mice were treated with increasing concentrations (20-60 μmol/L) of celecoxib or DMSO (vehicle) in medium supplemented with 5% FCS for 48 hours. To evaluate if celecoxib treatment can induce activation of caspase-3 and caspase-7, we detected levels of active forms of caspase-3 and caspase-7 in freshly prepared cell lysates from treated and untreated MTag tumor cells using the EnzChek Caspase-3/7 Assay Kit (Molecular Probes, Eugene, OR) following the manufacturer's protocol. In principle, active caspase-3 or caspase-7 will cleave a fluorogenic substrate releasing the fluorochrome, and the fluorescence was detected and quantified by spectrofluorometry using UV excitation of 380 nm and detected at an emission wavelength range of 430 to 460 nm. Fluorescence emission is an indication of caspase-3 and caspase-7 activity. Thus, apoptotic cell lysates containing active caspase-3 and caspase-7 yield considerable emission as compared with nonapoptotic lysates that do not contain the active forms of the enzymes.

ELISA for PGE_2 and VEGF

PGE_2 and VEGF enzyme immunoassay kits (Cayman Chemical Co., Ann Arbor, MI for PGE_2 and Oncogene Research Products, La Jolla, CA for VEGF) were used to assay the levels of PGE_2 and VEGF in tumor lysates and serum derived from treated and control mice. All tumor lysates were made in tissue lysis buffer containing 20 mmol/L HEPES, 0.15 mol/L NaCl, and 1% Triton X-100 supplemented with 80 μL/mL phosphatase inhibitor cocktail II (Sigma P-5726, St. Louis, MO) and 10 μL/mL complete protease inhibitor cocktail (Boehringer Mannheim GmbH, Indianapolis, IN). The PGE_2 and VEGF assays were done according to the manufacturer's recommendation. Lysates were diluted appropriately to ensure that readings were within the limits of accurate detection. Results are expressed as picogram of PGE_2 or VEGF per milliliter of serum or per microgram protein of tumor lysate for individual mice.

Western Blot Analysis for COX-2, Phospho-Akt, Bax, and Bcl-2

Tumor lysates from treated and untreated mice prepared as stated previously were resolved by SDS-PAGE on 10% to 15% resolving gels. Tumor lysate (100 μg) was loaded per lane. Gels were blotted and probed for COX-2 (p70, 1:200, Santa Cruz Biotechnology, Santa Cruz, CA), phospho-Akt and Akt protein (p60, 1:1,000, Cell Signaling, Beverly, MA), Bax-horseradish peroxidase conjugated (p23, 1:200, Santa Cruz Biotechnology), and Bcl-2 (p26, 1:1,000, Trevigen, Gaithersburg, MD). Mammary gland tumor lysates from 20- to 22-week-old MTag

mouse are used as positive control for COX-2. Jurkat T lymphoma cell lysate was used as positive control for the other proteins. Individual animal protein expression data are shown.

Statistical Analysis

All data are expressed as means ± SD. Statistically significant difference between experimental groups was assessed by one-way ANOVA with Dunnett adjustment.

Acknowledgments

We thank Dr. Eric Thompson for critical review of the article, Jim Tarara (Mayo Clinic Flow Cytometry Core) for helping with the cell cycle analysis, Marvin Ruona (Mayo Clinic Visual Communications Core) for the graphics and densitometry, Carol Williams for help with preparation of the article, and all personnel in the Mayo Clinic Natalie Schafer Transgenic Facility and the Histology Core.

References

1. Ellis MJ, Hayes DF, Lippman ME. Treatment of metastatic breast cancer. Diseases of the breast. In: Harris JR, Lippman ME, Morrow M, Osborne CK, editors. Philadelphia (PA): Lippincott Williams & Wilkins; 2000. p. 749–99.

2. Kujubu DA, Fletcher BS, Varnum BC, Lim RW, Herschman HR. TIS10, a phorbol ester tumor promoter-inducible mRNA from Swiss 3T3 cells, encodes a novel prostaglandin synthase/cyclooxygenase homologue. J Biol Chem 1991; 266:12866–72.

3. Kutchera W, Jones DA, Matsunami N, et al. Prostaglandin H synthase 2 is expressed abnormally in human colon cancer: evidence for a transcriptional effect. Proc Natl Acad Sci U S A 1996;93:4816–20.

4. Smith WL, Garavito RM, DeWitt DL. Prostaglandin endoperoxide H synthases (cyclooxygenases)-1 and -2. J Biol Chem 1996;271:33157–60.

5. Smith WL, DeWitt DL, Garavito RM. Cyclooxygenases: structural, cellular, and molecular biology. Annu Rev Biochem 2000;69:145–82.

6. Oshima M, Dinchuk JE, Kargman SL, et al. Suppression of intestinal polyposis in ApcΔ716 knockout mice by inhibition of cyclooxygenase 2 (COX-2). Cell 1996;87:803–9.

7. Subbaramaiah K, Zakim D, Weksler BB, Dannenberg AJ. Inhibition of cyclooxygenase: a novel approach to cancer prevention. Proc Soc Exp Biol Med 1997;216:201–10.

8. Taketo MM. Cyclooxygenase-2 inhibitors in tumorigenesis (Part II). J Natl Cancer Inst 1998;90:1609–20.

9. Eberhart CE, Coffey RJ, Radhika A, Giardiello FM, Ferrenbach S, DuBois RN. Up-regulation of cyclooxygenase 2 gene expression in human colorectal adenomas and adenocarcinomas. Gastroenterology 1994;107:1183–8.

10. Soslow RA, Dannenberg AJ, Rush D, et al. COX-2 is expressed in human pulmonary, colonic, and mammary tumors. Cancer 2000;89:2637–45.

11. Half E, Tang XM, Gwyn K, Sahin A, Wathen K, Sinicrope FA. Cyclooxygenase-2 expression in human breast cancers and adjacent ductal carcinoma *in situ*. Cancer Res 2002;62:1676–81.

12. Li M, Lotan R, Levin B, Tahara E, Lippman SM, Xu XC. Aspirin induction of apoptosis in esophageal cancer: a potential for chemoprevention. Cancer Epidemiol Biomarkers Prev 2000;9:545–9.

13. Zimmermann KC, Sarbia M, Weber AA, Borchard F, Gabbert HE, Schror K. Cyclooxygenase-2 expression in human esophageal carcinoma. Cancer Res 1999; 59:198–204.

14. Hosomi Y, Yokose T, Hirose Y, et al. Increased cyclooxygenase 2 (COX-2) expression occurs frequently in precursor lesions of human adenocarcinoma of the lung. Lung Cancer 2000;30:73–81.

15. Hida T, Yatabe Y, Achiwa H, et al. Increased expression of cyclooxygenase 2 occurs frequently in human lung cancers, specifically in adenocarcinomas. Cancer Res 1998;58:3761–4.

16. Uotila P, Valve E, Martikainen P, Nevalainen M, Nurmi M, Harkonen P. Increased expression of cyclooxygenase-2 and nitric oxide synthase-2 in human prostate cancer. Urol Res 2001;29:23–8.

17. Yoshimura R, Sano H, Masuda C, et al. Expression of cyclooxygenase-2 in prostate carcinoma. Cancer 2000;89:589–96.

18. Mohammed SI, Knapp DW, Bostwick DG, et al. Expression of cyclooxygenase-2 (COX-2) in human invasive transitional cell carcinoma (TCC) of the urinary bladder. Cancer Res 1999;59:5647–50.

19. Ristimaki A, Nieminen O, Saukkonen K, Hotakainen K, Nordling S, Haglund C. Expression of cyclooxygenase-2 in human transitional cell carcinoma of the urinary bladder. Am J Pathol 2001;158:849–53.

20. Tang Q, Gonzales M, Inoue H, Bowden GT. Roles of Akt and glycogen synthase kinase 3β in the ultraviolet B induction of cyclooxygenase-2 transcription in human keratinocytes. Cancer Res 2001;61:4329–32.

21. Neufang G, Furstenberger G, Heidt M, Marks F, Muller-Decker K. Abnormal differentiation of epidermis in transgenic mice constitutively expressing cyclooxygenase-2 in skin. Proc Natl Acad Sci U S A 2001;98:7629–34.

22. Tucker ON, Dannenberg AJ, Yang EK, et al. Cyclooxygenase-2 expression is up-regulated in human pancreatic cancer. Cancer Res 1999;59:987–90.

23. Molina MA, Sitja-Arnau M, Lemoine MG, Frazier ML, Sinicrope FA. Increased cyclooxygenase-2 expression in human pancreatic carcinomas and cell lines: growth inhibition by nonsteroidal anti-inflammatory drugs. Cancer Res 1999;59:4356–62.

24. Kundu N, Fulton AM. Selective cyclooxygenase (COX)-1 or COX-2 inhibitors control metastatic disease in a murine model of breast cancer. Cancer Res 2002;62:2343–6.

25. Gupta RA, Dubois RN. Colorectal cancer prevention and treatment by inhibition of cyclooxygenase-2. Nat Rev Cancer 2001;1:11–21.

26. Jacoby RF, Seibert K, Cole CE, Kelloff G, Lubet RA. The cyclooxygenase-2 inhibitor celecoxib is a potent preventive and therapeutic agent in the min mouse model of adenomatous polyposis. Cancer Res 2000;60:5040–4.

27. Reddy BS, Hirose Y, Lubet R, et al. Chemoprevention of colon cancer by specific cyclooxygenase-2 inhibitor, celecoxib, administered during different stages of carcinogenesis. Cancer Res 2000;60:293–7.

28. Schreinemachers DM, Everson RB. Aspirin use and lung, colon, and breast cancer incidence in a prospective study. Epidemiology 1994;5:138–46.

29. Steinbach G, Lynch PM, Phillips RK, et al. The effect of celecoxib, a cyclooxygenase-2 inhibitor, in familial adenomatous polyposis. N Engl J Med 2000;342:1946–52.

30. Williams CS, Watson AJ, Sheng H, Helou R, Shao J, DuBois RN. Celecoxib prevents tumor growth *in vivo* without toxicity to normal gut: lack of correlation between *in vitro* and *in vivo* models. Cancer Res 2000;60:6045–51.

31. Nakatsugi S, Ohta T, Kawamori T, et al. Chemoprevention by nimesulide, a selective cyclooxygenase-2 inhibitor, of 2-amino-1-methyl-6-phenylimidazo[4, 5-b]pyridine (PhIP)-induced mammary gland carcinogenesis in rats. Jpn J Cancer Res 2000;91:886–92.

32. Alshafie GA, Abou-Issa HM, Seibert K, Harris RE. Chemotherapeutic evaluation of celecoxib, a cyclooxygenase-2 inhibitor, in a rat mammary tumor model. Oncol Rep 2000;7:1377–81.

33. Rozic JG, Chakraborty C, Lala PK. Cyclooxygenase inhibitors retard murine mammary tumor progression by reducing tumor cell migration, invasiveness and angiogenesis. Int J Cancer 2001;93:497–506.

34. Blumenthal RD, Waskewich C, Goldenberg DM, Lew W, Flefleh C, Burton J. Chronotherapy and chronotoxicity of the cyclooxygenase-2 inhibitor, celecoxib, in athymic mice bearing human breast cancer xenografts. Clin Cancer Res 2001;7:3178–85.

35. Harris RE, Chlebowski RT, Jackson RD, et al. Breast cancer and nonsteroidal anti-inflammatory drugs: prospective results from the Women's Health Initiative. Cancer Res 2003;63:6096–101.

36. Guy CT, Cardiff RD, Muller WJ. Induction of mammary tumors by expression of polyomavirus middle T oncogene: a transgenic mouse model for metastatic disease. Mol Cell Biol 1992;12:954–61.

37. Cardiff RD, Muller WJ. Transgenic mouse models of mammary tumorigenesis. Cancer Surv 1993;16:97–113.

38. Maglione JE, Moghanaki D, Young LJ, et al. Transgenic polyoma middle-T mice model premalignant mammary disease. Cancer Res 2001;61:8298–305.

39. Mukherjee P, Madsen CS, Ginardi AR, et al. Mucin 1-specific immunotherapy in a mouse model of spontaneous breast cancer. J Immunother 2003;26: 47–62.

40. Paulson SK, Kaprak TA, Gresk CJ, et al. Plasma protein binding of celecoxib in mice, rat, rabbit, dog and human. Biopharm Drug Dispos 1999;20: 293–9.

41. Niederberger E, Tegeder I, Vetter G, et al. Celecoxib loses its anti-inflammatory efficacy at high doses through activation of NF-κB. FASEB J 2001;15:1622–4.

42. Basu GD, LaGioia M, Tinder TL, et al. The COX-2 selective inhibitor, celecoxib mediates growth inhibition in breast cancer cell lines via diverse pathways. Cancer Epidemiol Biomarkers Prev 2003;12:1298S.

43. Gavrieli Y, Sherman Y, Ben-Sasson SA. Identification of programmed cell death *in situ* via specific labeling of nuclear DNA fragmentation. J Cell Biol 1992;119:493–501.

44. Cao Y, Prescott SM. Many actions of cyclooxygenase-2 in cellular dynamics and in cancer. J Cell Physiol 2002;190:279–86.

45. Scheid MP, Woodgett JR. Unravelling the activation mechanisms of protein kinase B/Akt. FEBS Lett 2003;546:108–12.

46. Datta SR, Dudek H, Tao X, et al. Akt phosphorylation of BAD couples survival signals to the cell-intrinsic death machinery. Cell 1997;91:231–41.

47. del Peso L, Gonzalez-Garcia M, Page C, Herrera R, Nunez G. Interleukin-3-induced phosphorylation of BAD through the protein kinase Akt. Science 1997; 278:687–9.

48. Cardone MH, Roy N, Stennicke HR, et al. Regulation of cell death protease caspase-9 by phosphorylation. Science 1998;282:1318–21.

49. Lai GH, Zhang Z, Sirica AE. Celecoxib acts in a cyclooxygenase-2-independent manner and in synergy with emodin to suppress rat cholangiocarcinoma growth *in vitro* through a mechanism involving enhanced Akt inactivation and increased activation of caspases-9 and -3. Mol Cancer Ther 2003;2:265–71.

50. Hsu AL, Ching TT, Wang DS, Song X, Rangnekar VM, Chen CS. The cyclooxygenase-2 inhibitor celecoxib induces apoptosis by blocking Akt activation in human prostate cancer cells independently of Bcl-2. J Biol Chem 2000; 275:11397–403.

51. Chang SH, Liu CH, Conway R, et al. Role of prostaglandin E_2-dependent angiogenic switch in cyclooxygenase 2-induced breast cancer progression. Proc Natl Acad Sci U S A 2004;101:591–6.

52. Mukherjee P, Tinder TL, Basu GD, Pathangey LB, Chen L, Gendler SJ. Therapeutic efficacy of MUC1-specific cytotoxic T lymphocytes and CD137 co-stimulation in a spontaneous breast cancer model. Breast Dis. In press 2004.

53. Pockaj B, Basu GD, Pathangey LB, et al. Reduced T cell and dendritic cell function is related to COX-2 over-expression and PGE_2 secretion in patients with breast cancer. Ann Surg Oncol 2003;11:328–39.

54. Wang D, DuBois RN. Cyclooxygenase 2-derived prostaglandin E_2 regulates the angiogenic switch. Proc Natl Acad Sci U S A 2004;101:415–6.

55. Cantley LC. The phosphoinositide 3-kinase pathway. Science 2002;296: 1655–7.

56. Soengas MS, Lowe SW. Apoptosis and melanoma chemoresistance. Oncogene 2003;22:3138–51.

57. Sheng H, Shao J, Morrow JD, Beauchamp RD, DuBois RN. Modulation of apoptosis and Bcl-2 expression by prostaglandin E_2 in human colon cancer cells. Cancer Res 1998;58:362–6.

58. Ben-Av P, Crofford LJ, Wilder RL, Hla T. Induction of vascular endothelial growth factor expression in synovial fibroblasts by prostaglandin E and interleukin-1: a potential mechanism for inflammatory angiogenesis. FEBS Lett 1995;372:83–7.

59. Seno H, Oshima M, Ishikawa TO, et al. Cyclooxygenase 2- and prostaglandin E(2) receptor EP(2)-dependent angiogenesis in Apc(Δ716) mouse intestinal polyps. Cancer Res 2002;62:506–11.

60. Breyer RM, Bagdassarian CK, Myers SA, Breyer MD. Prostanoid receptors: subtypes and signaling. Annu Rev Pharmacol Toxicol 2001;41:661–90.

61. Jadeski LC, Lala PK. Nitric oxide synthase inhibition by *N*(G)-nitro-L-arginine methyl ester inhibits tumor-induced angiogenesis in mammary tumors. Am J Pathol 1999;155:1381–90.

Breast Disease 20 (2004) 53–63
IOS Press

Therapeutic Efficacy of MUC1-Specific Cytotoxic T Lymphocytes and CD137 Co-Stimulation in a Spontaneous Breast Cancer Model

Pinku Mukherjee[a], Teresa L. Tinder[a], Gargi D. Basu[a], Latha B. Pathangey[a], Lieping Chen[b] and Sandra J. Gendler[a,*]
[a]*Mayo Clinic College of Medicine, Department of Biochemistry and Molecular Biology, Mayo Clinic, Scottsdale, AZ, USA*
[b]*Mayo Clinic College of Medicine, Department of Immunology, Mayo Clinic, Rochester, MN, USA*

Abstract. To study immunology in breast tumors, we have utilized a mammary gland adenocarcinoma model in which mice develop spontaneous tumors of the mammary gland which are initiated at puberty and express a human tumor antigen, MUC1. MUC1 (CD227) is over-expressed in 90% of human breast cancers and its glycosylation status and pattern of expression in cancer cells is altered. Humoral and cellular responses to MUC1 have been reported in breast cancer patients and therefore, MUC1 is being evaluated as a target for immune intervention. This mouse model of spontaneous breast cancer allows the evaluation of anti-MUC1 immune responses at all stages of the disease. In this report, we review the model as it pertains to a) the development of the tumor, b) MUC1 expression, and the native immune responses against MUC1 as tumors progress, and c) the immune suppressive microenvironment within the developing tumor. Finally, we report our latest findings describing the therapeutic efficacy of adoptively transferred MUC1-specific cytotoxic T lymphocytes (MUC1-CTL) in these mice and discuss ways to increase their effectiveness by agonistic monoclonal antibody against CD137 T cell costimulatory molecule.

INTRODUCTION

Breast cancer remains a major health problem, accounting for approximately 40,000 deaths each year in the United States. Interest is high in developing non-toxic therapeutic approaches to complement toxic surgical and chemotherapeutic strategies. The recent molecular identification of tumor antigens recognized by cytotoxic T cells (CTLs) derived from cancer patients has initiated a new era in tumor immunology. MUC1 (CD227) is a cell-associated mucin that is developmentally regulated and aberrantly expressed by more than ninety percent of breast carcinomas [1–3]. The recent description of MUC1 as a target for CTLs has raised interest in using this protein as a target for immunotherapy.

MUC1 is a transmembrane protein that exists as a large extended rod protruding from the cell membrane into the lumen of ducts and glands. The core protein consists mainly of a twenty amino acid sequence repeated from 30–90 times. These tandem repeats (TR) serve as the scaffold for O-linked oligosaccharides that cover the polypeptide core. In cancer, MUC1 expression is greatly increased on cells and in circulation, its expression is no longer restricted to the apical cell surface, and its glycosylation is altered. Both cellular and humoral immune responses to MUC1 have been reported (reviewed in [4]). However, these responses

*Corresponding author: Sandra J. Gendler, Mayo Clinic College of Medicine, Dept. of Biochemistry and Molecular Biology and Tumor Biology Program, Mayo Clinic, Scottsdale, 13400 E. Shea Blvd., Scottsdale, AZ 85259, USA. Tel.: +1 480 301 7062; Fax: +1 480 301 7017; E-mail: gendler.sandra@mayo.edu.

are not sufficiently strong to stimulate CTL killing, as most breast adenocarcinomas express MUC1 and these tumors still progress. Thus, there is a need for studies to devise effective presentation of MUC1 immunogens to stimulate immune cells to kill tumor cells. The mouse has not been a suitable preclinical model for testing vaccines, as human MUC1 differs in sequence from mouse Muc1 and is a foreign antigen in the mouse. (Human MUC1 is designated MUC1, mouse as Muc1.) We have developed MUC1-expressing mice that spontaneously develop mammary gland tumors for use in pre-clinical studies. This model effectively mimics the human situation and provides a powerful system in which to study tolerance and inactivation of CTLs in the tumor microenvironment.

Bitransgenic Mice Develop Spontaneous Mammary Gland Cancer Accompanied by Lung and Bone Marrow Metastases

Human MUC1 transgenic mice (MUC1.Tg) were bred with mice carrying the MMTV-driven polyoma middle T antigen (MT) to create MMT mice [5–7]. MUC1.Tg mice carry the full-length human MUC1 gene driven by its own promoter; they express normal levels of MUC1 in a tissue specific manner and are therefore not a model of MUC1 over expression [8]. These mice exhibit T and B cell tolerance to the MUC1 antigen, thus providing an excellent model system where MUC1-specific therapy can be studied in the context of immune tolerance [5,9]. In the MMT mice, mammary gland tumors are induced by the action of a potent tyrosine kinase activity associated with the polyoma virus middle T antigen driven by the mouse mammary tumor virus long terminal repeat (MMTV) [10]. Middle T specifically associates with and activates the tyrosine kinase activity of a number of c-src family members, eliciting tumors when a threshold level of gene product has been attained. This promoter is transcriptionally active throughout all stages of mammary gland development and results in widespread transformation of the mammary epithelium and the rapid production of multifocal mammary adenocarcinomas. Hyperplastic alveolar nodules (HANs) can be detected by whole mount as early as 21 days and palpable mammary gland tumors are detectable from approximately 49 days onwards (a schematic representing the model and the tumor progression is shown in Fig. 1). Tumor progression is quite rapid, reaching 10% of body weight by about 24 weeks [6]. 100% of the female MMT mice get tumors. Tumors arise with synchronous kinetics

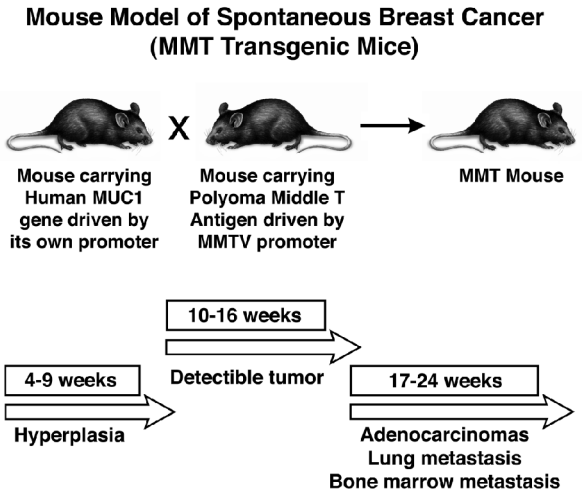

Fig. 1. Schematic representation of a mouse model of spontaneous metastatic breast cancer and approximate time-line of tumor progression from hyperplasia to adenocarcinomas and metastasis.

and are highly fibrotic with dense connective tissue separating individual nests of tumor cells, a pathology that closely resembles scirrhous carcinomas of the human breast [11]. Lung and bone marrow metastases were detected in MMT mice by 4 months of age [6]. Bone marrow metastasis was determined by staining bone marrow cells from MMT mice with pan-cytokeratin and MUC1, markers commonly used to detect epithelial tumor cells. About four percent of bone marrow cells were positive for both pan-cytokeratin and MUC1 by flow cytometry [6]. It is important to note that mortality in human breast cancer patients is directly associated with lung and bone metastasis. The MMT mouse is, therefore, an appropriate model for human cancer and allows us to study the effects of self-tolerance, immunity and auto-immunity to MUC1 as mammary tumors develop spontaneously.

MUC1 Expression Increases as MMT Tumors Progress

Tumor sections from 6, 12 and 20 week old non-immunized MMT mice show strong heterogeneous expression of MUC1 as tumors progress (Fig. 2). As compared to normal mammary gland, tumors express higher levels of MUC1 with increase in expression as tumors progressed from 6 weeks to 18 weeks (Fig. 2). MUC1 staining was determined using two antibodies, one recognizing the cytoplasmic tail of MUC1 (CT2) and the other recognizing the tandem repeat (TR) epitope of MUC1 (B27.29). CT2 antibody recognizes both mouse and human cytoplasmic tail (CT) of MUC1. It

is a monoclonal antibody raised in Armenian hamster. B27.29 is a mouse monoclonal reactive only against human MUC1 [12,13]. The staining pattern for B27.29 and CT2 was similar, hence, only B27.29 is shown in Fig. 2. MUC1 was expressed throughout the cytoplasm and around the cells in a pattern similar to that observed in human breast carcinomas. Thus, mammary gland tumors that occurred spontaneously in the MMT mice over-expressed the transgene protein, MUC1, in a manner similar to humans.

Cellular and humoral responses are not evidenced in MMT mice as tumors progress

In some breast cancer patients, humoral and cellular immune responses against MUC1 have been demonstrated. Thus, we determined native cellular and humoral immune responses in the non-immunized MMT mice as tumors progressed. At different stages of the tumor (6, 14, and 21 weeks), T cells were examined for expression of early and late activation markers (CD69 and CD25), as well as for expression of intracellular cytokines including IFN-γ, IL-2, IL-4, IL-5, and IL-10 in response to MUC1. No significant anti-MUC1 immune responses were evident in MMT mice as tumors progressed. Furthermore, we were unable to detect presence of T cells recognizing H-2D^b/MUC1 tetramer nor did we detect precursor cytotoxic T lymphocytes (CTLs) against MUC1 at any stage during tumor progression. Dendritic cell (DC) maturation status as determined by B7 co-stimulatory receptor expression and IL-12 production also remained unchanged as the tumor progressed. With regards to humoral immune response, circulating antibody to MUC1 was undetectable by specific ELISA at any time during tumor progression. These data taken together clearly indicate that naturally occurring cellular or humoral immune responses in non-immunized MMT mice were non-detectable [6]. This lack of detectable anti-MUC1 immune response in the MMT mice implies that the immune tolerance to MUC1 is not broken by aberrantly expressed tumor-specific MUC1. In general, immune tolerance to a particular self-antigen can be broken if the immune cells encounter large amounts of the antigen systemically. In some human breast cancers, a low level anti-MUC1 immune response is generally associated with high levels of shed MUC1 in the serum which is not the case in MMT mice.

Increased Levels of MUC1 in the Serum Determine if MUC1-Specific Immune Responses will be Elicited

As tumors progressed in the MMT mice, MUC1 serum levels increased only slightly as compared to age matched MUC1.Tg mice with maximum reaching to 1500–2500 Units/ml of serum at 24 weeks of age. In age matched female MUC1.Tg mice, serum MUC1 levels ranged from 500 to 1200 Units/ml, which is likely to depend upon their estrous cycle status. The low levels of circulating MUC1 may explain the lack of an immune response to MUC1 in non-immunized MMT mice. When MMT mice were immunized with liposomal MUC1-TR and human recombinant interleukin-2, we observed significant increase in the levels of serum MUC1 as compared to untreated MMT mice. This increase in serum MUC1 directly corresponded to the increased CTL activity in these mice [6]. These results suggested that high levels of circulating tumor antigen, MUC1, may activate MUC1-specific CTL that are capable of specifically lysing MUC1-expressing tumor cells *in vitro*. We also detected low levels of circulating antibodies to MUC1 in the immunized mice suggesting that the high level of circulating tumor-associated MUC1 has changed the antigenic profile and elicited a moderate level of humoral response to MUC1. Antibodies reactive with MUC1 have been reported in a small percent of breast cancer patients [14,15]. Although the effectiveness of a humoral immune response against solid tumors is not established, it once again parallels that observed in humans. Taken together, these data demonstrate that as observed in humans, immunization strategies elicited MUC1-specific CTLs which were unable to kill the spontaneously arising breast tumors. These CTLs were found to kill MUC1$^+$ tumor cells *in vitro*, secrete IFN-γ, and express perforin and granzyme B. Despite the presence of mature functional CTLs, these mice grew tumors [6,16]. We therefore postulated that the growing MMT tumor cells evaded immune recognition and killing, a phenomenon that is becoming increasingly critical to consider in designing future immune-based therapies.

Characteristics of the MUC1-Specific CTLs

To test whether MUC1-specific CTLs enter the mammary tumor bed and are active within the tumor microenvironment, we adoptively transferred the cytolytically active MUC1-specific CTL clone into MMT mice [17,18]. These MUC1-specific CTL clone were generated from a CTL line that was originally derived

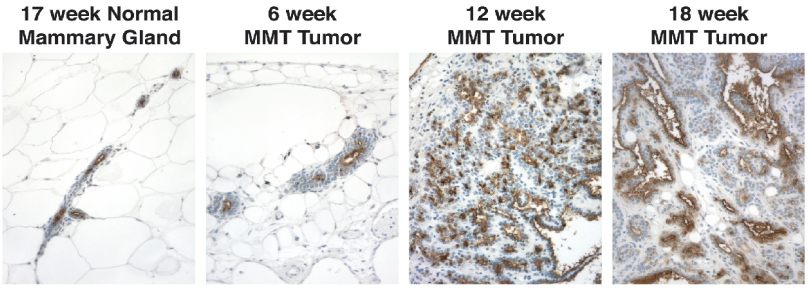

Fig. 2. MUC1 expression increases as tumors develop in MMT mice. Methacarn fixed and paraffin-embedded sections of mammary gland tumors from 6, 12 and 18 week old MMT mice were stained with B27.29, a monoclonal antibody reactive with MUC1 TR. B27.29 antibody is directly conjugated to horse radish peroxidase (HRP). specific staining was observed on lumenal surface of mammary epithelial cells and staining pattern is similar to that seen in humans. Increase in MUC1 expression is observed as tumors developed from 6 weeks to 18 weeks. As control, normal mammary gland from 17-week old MUC1.Tg mice was used. MUC1 expression is restricted to the apical surface in normal glands as compared to tumors and the staining is less intense than in MMT tumors. Images were captured at 200X magnification.

from a MUC1-expressing pancreatic cancer mouse model that develops spontaneous tumors of the pancreas [17]. Unlike the MMT model, these mice naturally developed MUC1-specific CTLs as the pancreatic tumor progressed. The MUC1-specific CTL lines are CD8+ T cells that recognize several of the MUC1-derived peptides (Fig. 3(A)). Fourteen different MUC1 TR 9 mer peptide sequences and one MUC1 cytoplasmic tail (CT) 17 mer peptide were used to determine epitope recognition. Dendritic cells were pulsed with these peptides prior to use as targets for the CTL line and CTL clone. The line recognizes several of the MHC class I-restricted MUC1 TR peptides and the CT peptide as illustrated in Fig. 3(A). Thus, the CTL line is comprised of a heterogeneous population of T cells, expressing predominantly T cell receptor (TCR) Vβ5, 11, 13 and 2 and V*a*8, 3, 11, and 2. The CTL clone, on the other hand, recognizes only a H-2D^b MHC class I-restricted immunodominant epitope of MUC1 (APGSTAPPA) and expresses Vβ5 and Vα2 [18]. When CTL line was adoptively transferred (intravenously) into MUC1.Tg mice prior to challenge with either the B16 melanoma cells expressing MUC1 transgene (B16.MUC1), or the C57 mammary tumor cells expressing MUC1 (C57mg.MUC1), the mice were protected against both types of tumor cell challenge and furthermore, developed memory T cells that could be transferred to protect naive MUC1.Tg mice from further tumor challenge [17,18]. These MUC1-specifc CTL clones expressed high levels of perforin and granzyme B as determined by confocal microscopy and flow cytometry. Perforin and granzyme B are cellular components of cytolytic granule of CTLs and NK cells that mediate lymphocyte-dependent killing and low expression of these proteins on CTLs suggest weak cytotoxicity [19,20]. Figure 3(B) shows a representative flow cytometric dot plot of CTLs stained with anti-granzyme B antibody that was directly conjugated to phycoerythrin (PE). Almost 100% of the cells express high levels of intracellular granzyme B (Fig. 3(B)). Similarly, CTLs stained with a specific perforin antibody showed high intensity of intracellular staining by confocal microscopy (Fig. 3(B)), thus, confirming the high cytolytic activity of the MUC1-specifc CTLs.

MUC1-Specific CTLs Delay Tumor Growth in MMT Mice

To test the efficacy of the MUC1-specific CTL in MMT mice, we determined if the CTLs could enter the mammary tumor bed and whether they remained active within the tumor micro-environment. We adoptively transferred cytolytically active MUC1-specific CTL clones into 14-week-old MMT mice, which had palpable tumors. To determine if the infused CTLs could home to the tumor site, we labeled the CTL clone with carboxy-fluoresceinsuccinimidyl ester (CFSE, an *in vivo* tracking dye) prior to adoptive transfer of 1 x 10^7 CTLs intravenously. We observed that CFSE-labeled CTL home to the tumor site and lymph node by 2 days post infusion and undergo proliferation as evidenced by the discrete population of cells with distinct CFSE staining intensities. CTLs were detected up to 20 days post infusion (Fig. 4). Few to no CTLs were detected within the thymus or the spleen. To determine if the infused CTLs remained active within the tumor environment, we infused 3 week-old MMT mice with unlabeled 1 x 10^7 CTLs intravenously and boosted every 3 weeks with the same. Final infusion was given at 15 weeks and at 17 weeks of age, the mammary tumors were removed, tumor-infiltrated lymphocytes (TILs) were isolated and sorted for the infused CD8+ CTL

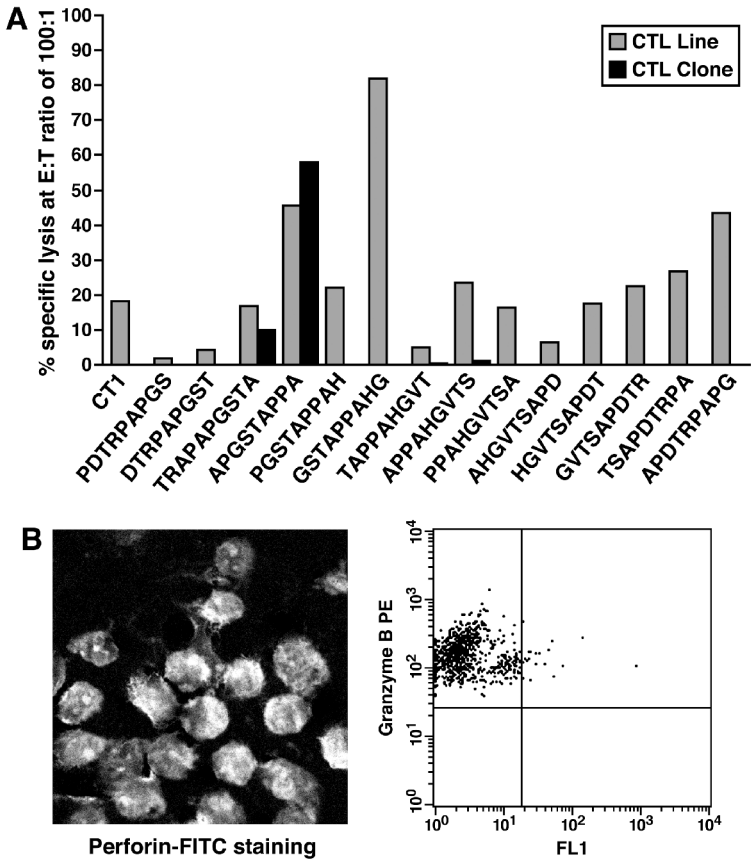

Fig. 3. A. Epitopes recognized by MUC1-specific CTL line and clone. Fourteen different MUC1 TR 9 mer peptide sequences and a MUC1 cytoplasmic tail 17 mer peptide were used to determine epitope recognition. Dendritic cells were pulsed with the peptides at 10(-6)M concentration prior to use as targets for the CTL line and CTL clone. A standard 8hr ^{51}Cr-release assay was performed. Specific lysis was performed with several effector to target (E : T) ratios. Figure shows data from 100:1 effector to target ratio. Recognition of the peptides by CTLs is gauged by the percent of specific lysis. Lysis at and above 18-20% is thought to be significant. Thus, MUC1 line consists of several CTL populations that recognize eight different TR peptides and the CT peptide. MUC1 clone recognizes only APGSTAPPA peptide. Degree of lysis directly correlates to the affinity by which the peptide is recognized by the CTL. CTLs seem to recognize APGSTAPP Aand GSTAPPAHG with the highest affinity. B. MUC1-specific CTLs express high levels of perforin and granzyme B. CTLs were permeabilized using the Pharmingen Permeabilization kit and stained with either perforin-FITC antibody (Alexis Biochemicals, San Diego, CA) and examined by confocal microscopy (left panel); or with granzyme B antibody directly conjugated to PE (Caltag Laboratories, Burlington, CA) and analyzed by flow cytometry (right panel).

clone based on their CD8 expression and TCR Vβ5 expression (Fig. 5(A), 2nd panel). TILs isolated from age matched MMT mice that were not infused with CTLs were used as controls (Fig. 5(A), 4th panel). The CTL clone maintained *in vitro* with the same profile as the sorted TILs were used as positive control (Fig. 5(A), 1st panel). The sorted cells were used in three assays to determine: 1) if these cells were hypo-responsive to MUC1 and therefore were tolerant to MUC1 antigen, 2) if these cells maintained their cytotoxicity after encounter with the tumor cells *in vivo*, and 3) if the sorted CTLs expressed granzyme B, a protein needed for the CTLs to be functionally lytic. In Fig. 5(B), we clearly show that in contrast to the CTL clone, the sorted Vβ5$^+$ /CD8$^+$ TILs had significantly reduced proliferation in response to MUC1 presented on irradiated DCs, suggesting that the infused CTLs become tolerized to tumor antigen MUC1 after encounter with the growing mammary tumor cells. Similarly, the sorted Vβ5$^+$ /CD8$^+$ TILs were unable to kill tumor cells expressing MUC1 *in vitro*, while the same cells that had not encountered tumor cells and were maintained in tissue culture remained highly cytolytic (Fig. 5(C)), suggesting that the infused CTL became cytolytically nonfunctional in the tumor environment. This cytolytic capability of the sorted TILs was further confirmed by the observation that the sorted Vβ5$^+$/CD8$^+$ TILs from the tumors showed significantly lower levels of granzyme

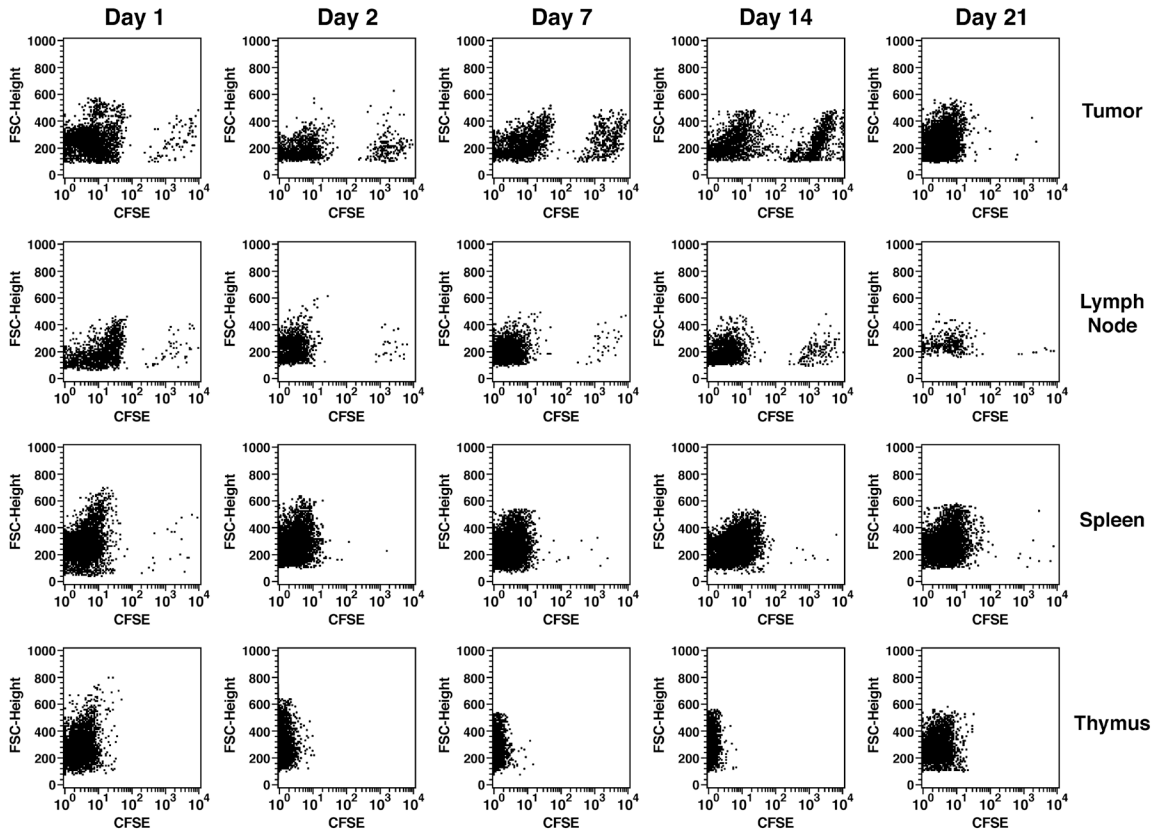

Fig. 4. CFSE labeled MUC1-specific CTL home to the lymph node and mammary gland tumor. CTL clone were stained with carboxyfluorescein diacetate succinimidyl ester (CFSE). Cells were incubated with 2 µl of 5 mM CFSE per 1×10^7 cells/ml in PBS-0.1% FBS for 10 minutes at 37°C and quenched by adding 5 times the volume of ice-cold media. 2×10^7 CFSE-stained CTLs were injected intravenously into 14-week old tumor bearing MMT mice. At various times post CTL infusion, TILs, lymph node cells, spleen cells and thymic cells were isolated and monitored for CFSE staining by flow cytometry. $n = 5$ mice and a representative dot plot is shown. By 21 days post infusion, CFSE labeled cells were undetectable.

B staining as compared to the CTLs that were maintained in culture (Fig. 5(D)). These findings are extremely significant, as immunotherapy can now be designed to reverse this established tolerance or prevent the induction of tolerance. The treatment group that includes CTL + CD137 monoclonal antibody (mAb) is represented in this Figure, but the experiment is described in a later section.

Nevertheless, when CTLs were continuously infused in MMT mice starting at 3 weeks of age, we observed a significant reduction in tumor growth and progression (Fig. 6). Clearly, adoptive transfer of MUC1-specific CTL early during tumorigenesis can reduce tumor burden and enhance survival in these mice. However, once CTL infusions were stopped, the tumors grew back. These results suggest strongly that immunotherapy can work if the tumor microenvironment is somehow altered. For example, if mediators of tumor-induced immune-suppression can be reduced, co-stimulation for CTL function can be provided to overcome the tolerizing effects of the tumor microenvironment, and most importantly, if tumor-cell proliferation can be restricted.

Immunosuppressive Tumor Microenvironment in the Mammary Gland Tumor

Since infused CTLs became tolerant and cytolytically non-functional within the tumor microenvironment, we evaluated the presence of immunosuppressive mediators in mammary tumors. Data revealed that the tumor cells secrete IL-10 and TGF-β that are partly responsible for the down-regulation of CTL activity [6]. IL-12 production and expression of co-stimulatory receptors by DCs was also found to be reduced, suggesting sub-optimal antigen presentation within the tumor micro-environment. In addition, tumor cells down-regulated surface major histocompati-

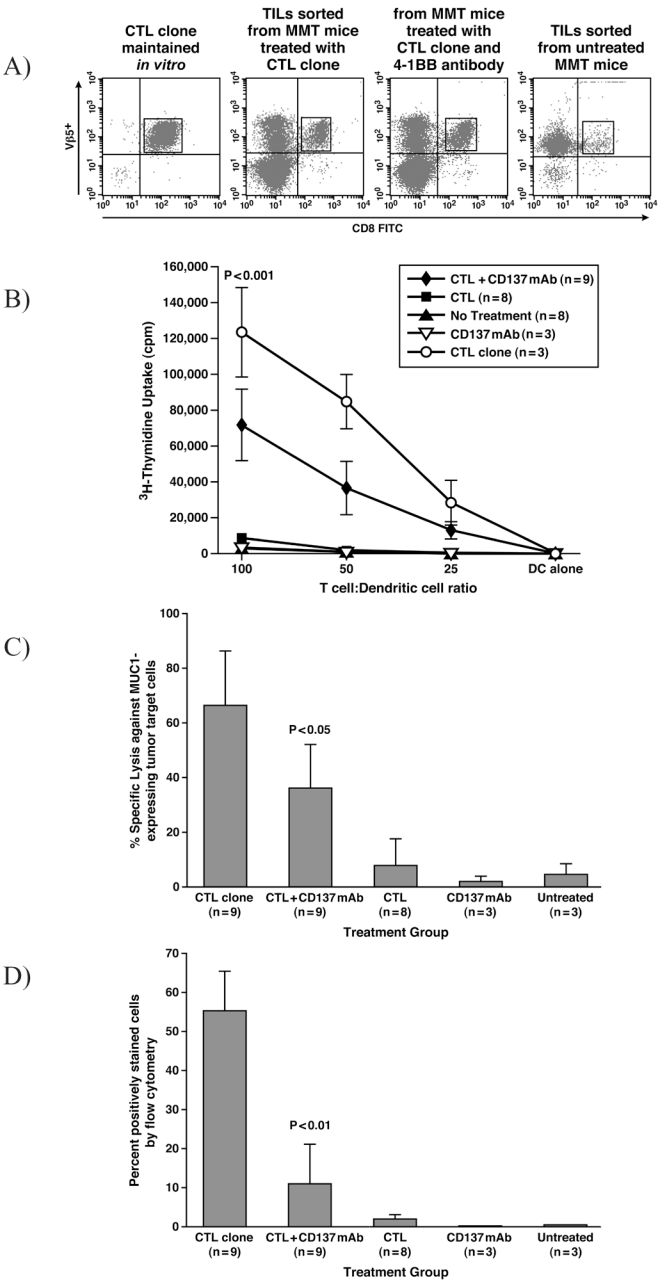

Fig. 5. Adoptively transferred CTL become tolerant to MUC1 antigen and are cytolytically inactive within the tumor microenvironment. TILs were isolated from tumors of MMT mice that received adoptively transferred MUC1-specific CTL clone ($V\beta5^+/CD8^+$ T cells). CD137 mAb was injected every week at 100 ng/mouse/100 µl intraperitoneally. A) Flow cytometric profile of TCR $V\beta5^+/CD8^+$ T cells sorted from TILs by flow cytometry (box represents the population that was sorted). Profile of untreated MMT and MMT treated with CD137 mAb alone looked identical and therefore we chose to show only one group. B) Proliferation by 3H-thymidine uptake of the sorted T cells. Proliferation was determined in response to 25 mer MUC1 peptide (STAPPAHGVTSAPDTRPAPGSTAPP) presented on dendritic cells. C) Cytotoxic activity by 51Cr-release assay of sorted T cells against MUC1-expressing B16.MUC1 melanoma tumor cells. As positive controls, CTL clone maintained *in vitro* was used and as negative controls TCR $V\beta5^+/CD8^+$T cells from mammary tumor of age matched untreated MMT mice was used. D) Granzyme B staining of sorted T cells by flow cytometry. Cells were permeabilized and antibody to Granzyme B directly conjugated to PE from B.D. Pharmingen was used at 1 ug/10^6 cells to determine intracellular staining using flow cytometry. Treatment groups include: MMT treated with CTL; MMT treated with CTL + CD137 mAb; MMT treated with CD137 mAb; and untreated MMT. p-values are shown in the figure and represent significant differences between CTL + CD137 group as compared to untreated or α–CD137 alone or CTL alone groups. 6 mice were enrolled in the α–CD137, however, 3 mice were found morbid prior to end of experiment and were removed from the study.

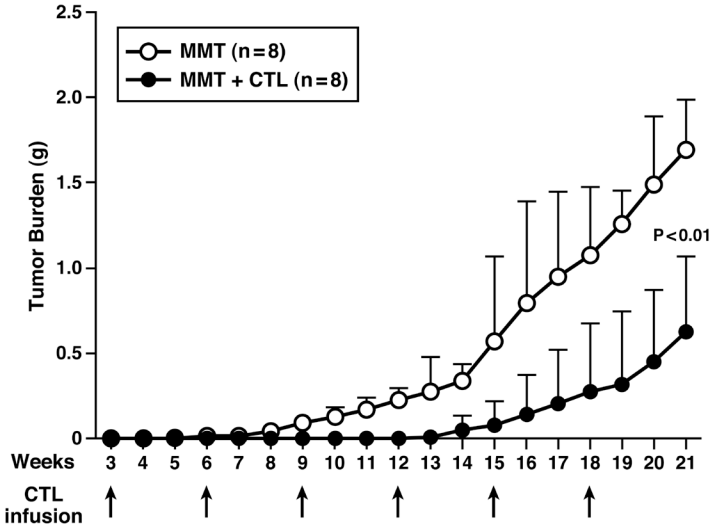

Fig. 6. Adoptively transferred MUC1-specific CTL clone inhibits tumor progression in MMT mice. MUC1-specific CTLs (2×10^7 cells i.v.) were infused into MMT mice starting at three weeks of age. Infusions were given every three weeks from week 3 onward. Six infusions were performed. Tumor growth was inhibited until the cessation of CTL injections, at which time tumors began to progress. CTL infused MMT mice showed significantly lower tumor burden as compared to untreated MMT mice ($p < 0.01$).

bility complex (MHC) class I molecules to avoid immune recognition as well as expressed higher levels of $CD4^+CD25^+$ T regulatory cells [6,16]. Recently, we have found over expression of COX-2 in the MMT tumors by western blot analysis (Fig. 7) as well as by immunohistochemistry (data not shown). COX-2 is an inducible enzyme that is over expressed in many tumors and is involved in many aspects of tumorigenesis. COX-2 converts arachidonic acid to prostaglandins, especially prostaglandin E2 (PGE2), a well-characterized immune cell suppressor [21–24]. In MMT mice, we found significantly higher levels of serum PGE2 as compared to normal mouse sera, suggesting that the COX-2/PGE2 pathway may be partly responsible for the immune suppressive tumor micro-environment in MMT mice. We have recently shown that T cell and DC functions in newly diagnosed breast cancer patients are impaired and that over expression of COX-2 and PGE2 may play a significant role in inducing such suppression [25]. Together, these data indicate that mammary gland tumor cells utilize a variety of immune evasion mechanisms to avoid CTL killing. Managing all of these immune evasion pathways seems formidable. On one hand, we have immune responses against the tumor and, on the other hand, there is tumor-induced immune suppression. Tilting the balance towards more sustained and increased CTL activity may be easier to accomplish than addressing every one of the tumor evasion mechanisms. One way to accomplish this is by providing the activated CTLs with appropriate co-stimulation to increase their efficiency in killing tumor cells.

CD137 mAb can Reverse Tolerance in vivo in MMT Mice and has a Synergistic Anti-Tumor Effect when Combined with MUC1-Specific CTL Therapy

The CD137 glycoprotein is a member of the tumor necrosis factor receptor superfamily expressed on primed but not on naïve $CD4^+$ and $CD8^+$ T cells. CD137 binds to a specific ligand (CD137L) expressed on several antigen presenting cells (APCs) and signals either through ligand binding or by specific agonistic antibody to deliver a dual mitogenic signal for further T cell activation and proliferation. It has been shown that administration of CD137 mAb can amplify T cell-mediated immune responses and can eradicate established tumors [26,27]. Recent experiments suggest that anti-tumor effect of CD137 antibody is to reverse T cell tolerance/anergy [28] that is so often induced by tumor cells. Thus, we evaluated the efficacy of CD137 antibody therapy in reversing tolerance in our *in vivo* breast cancer model, since we have already established that adoptively transferred CTLs become tolerized to MUC1 and are cytolytically non-functional within the tumor microenvironment. We were therefore able to specifically answer whether treatment with CD137 antibody could reverse this tolerizing effect within the mammary gland tumor. MMT mice were infused with 1×10^7 CTLs starting at 3 weeks of age and boosted

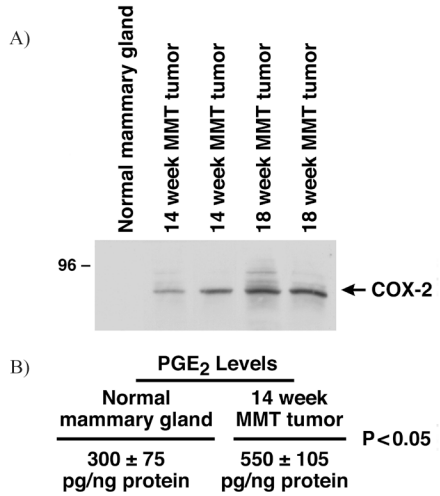

Fig. 7. MMT tumors express COX-2 and the downstream product PGE2. A) Western blot analysis of mammary tumor lysate derived from 14 and 18-week old MMT mice compared to normal mammary gland lysate. SDS-PAGE electrophoresis was performed using 12% resolving gel. 50 μgs of protein was loaded per lane. Gels were immunoblotted and probed for COX-2 with specific COX-2 monoclonal antibody (goat polyclonal, clone C20, Santa Cruz Biotechnology Inc., Santa Cruz, CA) at 1:200 dilution. MMT tumors over express COX-2 as tumors progress. B) PGE2 levels determined by specific ELISA in 14-week old MMT tumor lysate as compared to normal mammary gland lysate (n = average of 6 mice). Levels in the lysates were determined using a specific ELISA kit for PGE2 (Cayman Pharmaceuticals, Ann Arbor, MI). Manufacturer's recommended protocols were followed. Compared to normal mammary gland, PGE2 in tumor is significantly higher ($p < 0.05$).

every 3 weeks with the same. Final infusion was given at 15 weeks and TILs were sorted for $CD8^+V\beta5^+$ T cells at 17 weeks (Fig. 5(A), 3rd panel). Along with the CTL infusions, these mice received CD137 mAb at 100 ug/mouse intraperitoneally every week until mice were sacrificed at 17 weeks of age. Data clearly indicate that CD137 mAb treatment was extremely effective in reversing tolerance such that the CTL clone regains responsiveness to MUC1 antigen post CD137 treatment (Fig. 5(B)). Treatment with this antibody was also effective in restoring the cytolytic activity of the CTL clone as measured by the ^{51}Cr-release assay and granzyme B staining (Figs 5(C) and (D)). Most importantly, this reversal of CTL tolerance *in vivo* translated well to anti-tumor response. When mice were sacrificed at 17 weeks, tumor burden was evaluated. MMT mice treated with CTL alone had a tumor burden of 0.5 g that was significantly lower than untreated control mice with 0.9 g tumor ($p < 0.05$) or mice treated with CD137 mAb alone with 1 g tumor. Treatment with CD137 increased the effectiveness of CTLs since MMT mice treated with CTL and CD137 mAb had a tumor burden of 0.2 g ($p < 0.01$) (Fig. 8). The unresponsiveness of MMT tumors to CD137 mAb alone can be explained by the fact that CD137 is only expressed on activated T cells and does not work on naïve, non-primed T cells [29] and untreated MMT mice have no detectable primed T cells. Although 6 mice were enrolled in the anti-CD137 treatment arm, 3 mice were found morbid prior to end of experiment and were removed from the study. These results demonstrate that MUC1-specific CTLs are very effective against spontaneously arising MUC1 expressing breast tumors and that their efficacy can be increased and maintained for longer time with appropriate co-stimulation such as with anti-CD137 antibody. Lung metastasis was not evaluated in these mice, since tumor burden at 17 weeks even in the untreated mice is not large enough for lung metastasis to develop. The next set of experiments will determine the effect such a treatment on lung and bone marrow metastasis.

CONCLUSIONS

We have shown that the spontaneous mammary gland tumors that arise in the transgenic MMT mice appropriately models the human metastatic breast cancer. Several features of the tumor resemble the human disease, for example, the tumors arise in an immune competent host within the context of MUC1-tolerence; the tumors aberrantly over express MUC1, the tumors metastasize to the lungs and the bone marrow, and very little to no immune response against the tumor antigen, MUC1, is evident in the model. As observed in humans, treatment with anti-MUC1 immunotherapy leads to a robust cellular immune response accompanied with a moderate humoral immune response against the immunizing antigen, MUC1, which does not translate efficiently to a clinical response. We further show that the inefficiency of MUC1-specific CTLs to affect tumor burden and survival is partly due to the immunosuppressive tumor microenvironment that renders the infiltrating CTLs inactive with regards to antigen recognition and killing. Similar to observations in human breast cancer, several immunosuppressive factors were identified in the MMT tumor microenvironment. In fact, in human disease, immunosuppression has not only been described within the tumor microenvironment but also systemically. Finally, we show in our model, that the most effective anti-tumor response was generated when mice were treated with continuous intravenous infusions of MUC1-specific CTLs and that the CTL

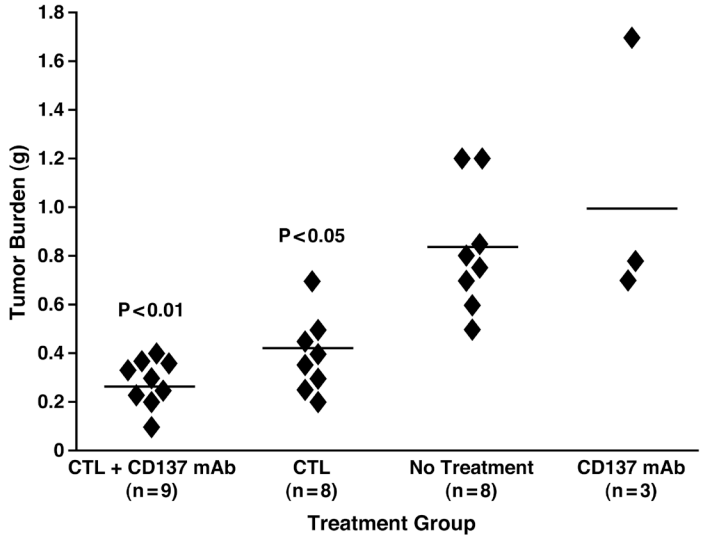

Fig. 8. CD137 mAb in combination with MUC1-specific CTL therapy is more efficient in reducing tumor burden than CTL therapy alone. MMT mice were injected with MUC1-specific CTLs (2×10^7 cells i.v.) every three weeks starting at 3 weeks; and CD137 mAb was injected at 100 ug/mice (i.p.) every week starting at 6 weeks. Individual animal data are shown as scatter plot. P values indicate significant differences between treatment groups and untreated control mice. Tumor burden was significantly lower in CTL + CD137 mAb treated mice ($p < 0.01$) and in CTL treated mice ($p < 0.05$) as compared to untreated and CD137 mAb treated mice. 6 mice were enrolled in the CD137 mAb group; however, 3 mice were found morbid prior to end of experiment and were removed from the study. CD137 mAb, clone 2A, was raised in rats against a fusion protein consisting of the extracellular domain of murine CD137 and the human immunoglobulin C region [26].

efficiency was significantly enhanced when treatment was combined with CD137 co-stimulation. From our data, we suggest that one of the mechanisms by which CD137 co-stimulation increases CTL activity is by reversing tumor-induced CTL tolerance and hence inactivity *in vivo*. These results allow us to propose that such a therapy may be beneficial for the treatment of metastatic breast cancer in humans.

ACKNOWLEDGEMENTS

We acknowledge the funding provided by Susan G. Komen Breast Cancer Foundation, the DOD Breast Cancer Research Program DAMD17-01-1-0318 and National Institutes of Health grant CA79915. We thank Biomira Inc. for providing conjugated B27.29 monoclonal antibody and Dr. Olivera Finn for MUC1 tandem repeat peptides. We also acknowledge Jim Tarara in the FACs Core for providing expertise in flow cytometry and CTL sorting; all animal technicians in the Natalie Schaffer Transgenic Core; Cathy Madsen and Kari Kotlarczyk for maintaining the MTag and MUC1.Tg mouse colonies; Marvin Ruona in our Visual Communications Core for his expertise in preparation of the figures; and Carol Williams for help in preparing and submitting the manuscript.

REFERENCES

[1] S. Zotter, P.C. Hageman, A. Lossnitzer, W.J. Mooi and J. Hilgers, Tissue and tumor distribution of human polymorphic epithelial mucin, *Cancer Reviews* (11–12) (1988), 55–101.

[2] J.J. Rahn, L. Dabbagh, M. Pasdar and J.C. Hugh, The importance of MUC1 cellular localization in patients with breast carcinoma, *Cancer* **91** (2001), 1973–1982.

[3] M.V. Croce, M.T. Isla-Larrain, C.E. Rua, M.E. Rabassa, S.J. Gendler and A. Segal-Eiras, Patterns of MUC1 tissue expression defined by an anti-MUC1 cytoplasmic tail monoclonal antibody in breast cancer, *J Histochem Cytochem* **51** (2003), 781–788.

[4] S.J. Gendler, MUC1, the renaissance molecule, *J Mammary Gland Biol Neoplasia* **6** (2001), 339–353.

[5] G.J. Rowse, R.M. Tempero, M.L. VanLith, M.A. Hollingsworth and S.J. Gendler, Tolerance and immunity to MUC1 in a human MUC1 transgenic murine model, *Cancer Res* **58** (1998), 315–321.

[6] P. Mukherjee, C.S. Madsen, A.R. Ginardi, T.L. Tinder, F. Jacobs, J. Parker, B. Agrawal, B.M. Longenecker and S.J. Gendler, Mucin 1-specific immunotherapy in a mouse model of spontaneous breast cancer, *J Immunother* **26** (2003), 47–62.

[7] J. Xia, Y. Tanaka, S. Koido, C. Liu, P. Mukherjee, S.J. Gendler and J. Gong, Prevention of spontaneous breast carcinoma by prophylactic vaccination with dendritic/tumor fusion cells, *J Immunol* **170** (2003), 1980–1986.

[8] L.M. Silver, *In Mouse Genetics Concepts and Applications*, Oxford University Press, 1995, 32–61.

[9] R.M. Tempero, M.L. Vanlith, K. Morikane, G.J. Rowse, S.J. Gendler and M.A. Hollingsworth, CD4(+) lymphocytes provide MUC1-specific tumor immunity *in vivo* that is undetectable *in vitro* and is absent in MUC1 transgenic mice, *J Immunol* **161** (1998), 5500–5506.

[10] C.T. Guy, R.D. Cardiff and W.J. Muller, Induction of mammary tumors by expression of polyomavirus middle T oncogene: a transgenic mouse model for metastatic disease, *Mol. Cell. Biol.* **12** (1992), 954–961.
[11] R.D. Cardiff and W.J. Muller, Transgenic mouse models of mammary tumorigenesis, *Cancer Surveys* **16** (1993), 97–113.
[12] M.A. Reddish, N. Helbrecht, A.F. Almeida, R. Madiyalakan, M.R. Suresh and B.M. Longenecker, Epitope mapping of mab B27.29 within the peptide core of the malignant breast carcinoma-associated mucin antigen coded for by the human MUC1 gene, *J Tumor Marker Oncol* **7** (1992), 19–27.
[13] R. Sikut, A. Sikut, K. Zhang, D. Baeckstrom, G.C. Hansson, in: *Tumor Biology*, P.D. Rye and M.R. Price, eds, S. Karger Medical and Scientific Publishers, 1998, p. 122–126.
[14] A. Rughetti, V. Turchi, C.A. Ghetti, G. Scambia, P.B. Panici, G. Roncucci, S. Mancuso, L. Frati and M. Nuti, Human B-cell immune response to the polymorphic epithelial mucin, *Cancer Res* **53** (1993), 2457–2459.
[15] Y. Kotera, J.D. Fontenot, G. Pecher, R.S. Metzgar and O.J. Finn, Humoral immunity against a tandem repeat epitope of human mucin MUC-1 in sera from breast, pancreatic, and colon cancer patients, *Cancer Res* **54** (1994), 2856–2860.
[16] P. Mukherjee, A.R. Ginardi, C.S. Madsen, T.L. Tinder, F. Jacobs, J. Parker, B. Agrawal, B.M. Longenecker and S.J. Gendler, MUC1-specific CTLs are non-functional within a pancreatic tumor microenvironment, *Glycoconj J* **18** (2001), 931–942.
[17] P. Mukherjee, A.R. Ginardi, C.S. Madsen, C.J. Sterner, M.C. Adriance, M.J. Tevethia and S.J. Gendler, Mice with spontaneous pancreatic cancer naturally develop MUC1-specific CTLs that eradicate tumors when adoptively transferred, *J Immunol* **165** (2000), 3451–3460.
[18] P. Mukherjee, A.R. Ginardi, T.L. Tinder, C.J. Sterner and S.J. Gendler, MUC1-specific CTLs eradicate tumors when adoptively transferred *in vivo*, *Clin Can Res* **7** (2001), 848s–855s.
[19] E.J. Wherry, V. Teichgraber, T.C. Becker, D Masopust, S.M. Kaech, R. Antia, U.H. von Andrian and R. Ahmed, Lineage relationship and protective immunity of memory CD8 T cell subsets, *Nat Immunol* **4** (2003), 225–234.
[20] V. Appay et al., HIV-specific CD8(+) T cells produce antiviral cytokines but are impaired in cytolytic function, *J Exp Med* **192** (2000), 63–75.
[21] K. Okuno, H. Jinnai, Y.S. Lee, K. Nakamura, T. Hirohata, H. Shigeoka and M. Yasutomi, A high level of prostaglandin E2 (PGE2) in the portal vein suppresses liver-associated immunity and promotes liver metastases, *Surg Today* **25** (1995), 954–958.
[22] K. Takayama, G. Garcia-Cardena, G.K. Sukhova, J. Comander, M.A. Gimbrone, Jr. and P. Libby, Prostaglandin E2 suppresses chemokine production in human macrophages through the EP4 receptor, *J Biol Chem* **277** (2002), 44147–44154.
[23] M. Stolina et al., Specific inhibition of cyclooxygenase 2 restores antitumor reactivity by altering the balance of IL-10 and IL-12 synthesis, *J Immunol* **164** (2000), 361–370.
[24] M. Huang, M. Stolina, S. Sharma, J.T. Mao, L. Zhu, P.W. Miller, J. Wollman, H. Herschman and S.M. Dubinett, Non-small cell lung cancer cyclooxygenase-2-dependent regulation of cytokine balance in lymphocytes and macrophages: up-regulation of interleukin 10 and down-regulation of interleukin 12 production, *Cancer Res* **58** (1998), 1208–1216.
[25] B. Pockaj, G.D. Basu, L.B. Pathangey, R.J. Gray, J.L. Hernandez, S.J. Gendler, P. Mukherjee and T. Reduced, cell and dendritic cell function is related to COX-2 over-expression and PGE2 secretion in patients with breast cancer, *Ann Surg Onc* **11** (2004), 328–339.
[26] I. Melero, W.W. Shuford, S.A. Newby, A. Aruffo, J.A. Ledbetter, K.E. Hellstrom, R.S. Mittler and L. Chen, Monoclonal antibodies against the 4-1BB T-cell activation molecule eradicate established tumors, *Nat Med* **3** (1997), 682–685.
[27] R.A. Wilcox, D.B. Flies, G. Zhu, A.J. Johnson, K. Tamada, A.I. Chapoval, S.E. Strome, L.R. Pease and L. Chen, Provision of antigen and CD137 signaling breaks immunological ignorance, promoting regression of poorly immunogenic tumors, *J Clin Invest* **109** (2002), 651–659.
[28] R.A. Wilcox, K. Tamada, D.B. Flies, G. Zhu, A.I. Chapoval, B.R. Blazar, W.M. Kast and L. Chen, Ligation of CD137 receptor prevents and reverses established anergy of CD8+ cytolytic T lymphocytes *in vivo*, *Blood* **103** (2004), 177–184.
[29] K.E. Pollok, Y.J. Kim, Z. Zhou, J. Hurtado, K.K. Kim, R.T. Pickard, B.S. Kwon and T. Inducible, cell antigen 4-1BB. Analysis of expression and function, *J Immunol* **150** (1993), 771–781.

Research article

Open Access

Mechanisms underlying the growth inhibitory effects of the cyclo-oxygenase-2 inhibitor celecoxib in human breast cancer cells

Gargi D Basu, Latha B Pathangey, Teresa L Tinder, Sandra J Gendler and Pinku Mukherjee

Department of Biochemistry and Molecular Biology, Mayo Clinic College of Medicine, Scottsdale, Arizona, USA

Corresponding author: Pinku Mukherjee, mukherjee.pinku@mayo.edu

Received: 1 Oct 2004 Revisions requested: 14 Dec 2004 Revisions received: 1 Mar 2005 Accepted: 4 Mar 2005 Published: 4 Apr 2005

Breast Cancer Research 2005, **7**:R422-R435 (DOI 10.1186/bcr1019)
This article is online at: http://breast-cancer-research.com/content/7/4/R422

Abstract

Introduction Inhibitors of cyclo-oxygenase (COX)-2 are being extensively studied as anticancer agents. In the present study we evaluated the mechanisms by which a highly selective COX-2 inhibitor, celecoxib, affects tumor growth of two differentially invasive human breast cancer cell lines.

Methods MDA-MB-231 (highly invasive) and MDA-MB-468 (moderately invasive) cell lines were treated with varying concentrations of celecoxib *in vitro*, and the effects of this agent on cell growth and angiogenesis were monitored by evaluating cell proliferation, apoptosis, cell cycle arrest, and vasculogenic mimicry. The *in vitro* results of MDA-MB-231 cell line were further confirmed *in vivo* in a mouse xenograft model.

Results The highly invasive MDA-MB-231 cells express higher levels of COX-2 than do the less invasive MDA-MB-468 cells. Celecoxib treatment inhibited COX-2 activity, indicated by prostaglandin E_2 secretion, and caused significant growth arrest in both breast cancer cell lines. In the highly invasive MDA-MB-231 cells, the mechanism of celecoxib-induced growth arrest was by induction of apoptosis, associated with reduced activation of protein kinase B/Akt, and subsequent activation of caspases 3 and 7. In the less invasive MDA-MB-468 cells, growth arrest was a consequence of cell cycle arrest at the G_0/G_1 checkpoint. Celecoxib-induced growth inhibition was reversed by addition of exogenous prostaglandin E_2 in MDA-MB-468 cells but not in MDA-MB-231 cells. Furthermore, MDA-MB-468 cells formed significantly fewer extracellular matrix associated microvascular channels *in vitro* than did the high COX-2 expressing MDA-MB-231 cells. Celecoxib treatment not only inhibited cell growth and vascular channel formation but also reduced vascular endothelial growth factor levels. The *in vitro* findings corroborated *in vivo* data from a mouse xenograft model in which daily administration of celecoxib significantly reduced tumor growth of MDA-MB-231 cells, which was associated with reduced vascularization and increased necrosis in the tumor mass.

Conclusion The disparate molecular mechanisms of celecoxib-induced growth inhibition in human breast cancer cells depends upon the level of COX-2 expression and the invasive potential of the cell lines examined. Data suggest a role for COX-2 not only in the growth of cancer cells but also in activating the angiogenic pathway through regulating levels of vascular endothelial growth factor.

Introduction

The incidence of breast cancer – the second leading cause of cancer death in women in the USA – is increasing, and current therapy is unable to achieve clinical responses in patients with highly invasive metastatic disease. There is a consequent need for more effective approaches to prevention and treatment of breast cancer. Nonsteroidal anti-inflammatory drugs (NSAIDs) show great promise in this respect. Recent data on regular NSAID use for 5–9 years indicated a 21% reduction in the incidence of breast cancer, and regular NSAID use for 10 or more years produced a 28% reduction in the incidence of breast cancer [1]. Preclinical studies [2-4] have consistently shown that NSAIDs inhibit mammary carcinogenesis.

CDK = cyclin-dependent kinase; COX = cyclo-oxygenase; DMEM = Dulbecco's modified eagle medium; DMSO = dimethyl sulfoxide; FCS = fetal calf serum; NSAID = nonsteroidal anti-inflammatory drug; pAkt = phosphorylated Akt; PBS = phosphate-buffered saline; PG = prostaglandin; PI = propidium iodide; VEGF = vascular endothelial growth factor.

Various mechanisms may be responsible for the observed effects of NSAIDs against breast cancer. Inhibition of cyclooxygenase (COX), particularly the COX-2 isozyme, and blockade of the prostaglandin (PG) cascade may have impacts on neoplastic growth and development by inhibiting several key features of mammary carcinogenesis – namely proliferation, angiogenesis and metastasis. Inhibition of COX also causes induction of apoptosis in malignant cells and enhances antineoplastic activity of cytotoxic T lymphocytes [5-8]. Our study conducted in newly diagnosed stage I and stage II breast cancer patients [9] showed impaired functionality of T cells and dendritic cells, which correlated with COX-2 overexpression in the tumors and increased levels of PGE_2 in the serum and tumor milieu. Therefore, a convincing case has been made for COX-2 being an important target for the antineoplastic action of NSAIDs. Unlike NSAIDs, COX-2 selective inhibitors such as celecoxib and rofecoxib do not inhibit COX-1 and thus show promise as drugs that spare the gastrointestinal system.

COX-2 is overexpressed in breast cancer tissues, and greater extent of its expression is associated with poorer prognosis [10]. Various environmental and nutritional risk factors induce COX-2 expression in animal models of breast cancer [11,12]. Moreover, COX-2 selective inhibitors significantly delayed the incidence of mammary tumors in transgenic mice expressing the Her2/Neu, and polyoma-middle T oncogenes [13,14]. Recently, a transgenic mouse model was developed in which the human COX-2 gene was expressed in the mammary gland under the control of the murine mammary tumor virus promoter [15]. That study demonstrated that enhanced COX-2 expression strongly predisposes to transformation of the mammary gland in multiparous animals. These data strongly suggest that local expression of COX-2 is sufficient for *in situ* tumor initiation and/or progression. Another transgenic overexpression study with COX-2 targeted to the epidermis also supports the concept that COX-2 is a critical regulator of tumor progression [16]. Transfections of the breast cancer cell line Hs578T with cDNA for COX-2 led to an increase in expression and activity of matrix metalloproteinase-2, resulting in increasingly invasive behavior of the cells [17]. COX-2 specific inhibitors have the ability to block cell growth, and induce apoptosis and cell cycle arrest in murine mammary tumor cell lines [18]. However, the molecular mechanisms involved are not well understood. If COX-2 inhibitors act only by modulating COX-2 expression, then that would imply that this therapy would be limited to COX-2 overexpressing tumors; hence, this question is of considerable clinical importance.

In the present study we established that the level of COX-2 expression and the invasive property of breast cancer cells determines the mechanism of celecoxib-induced growth inhibition; that COX-2 is involved in extracellular matrix associated microvascular channel formation by breast cancer cells; and that COX-2 inhibits angiogenesis *in vivo*. The study should further our understanding of the cellular and molecular mechanisms underlying the chemopreventive effect of a COX-2 selective inhibitor in breast cancer. To the best of our knowledge, this is the first study demonstrating the diverse mode of action of celecoxib on human breast cancer cells, which may be dependent upon the cells' invasive properties and levels of COX-2 expression. This is also the first report suggesting a direct role for COX-2 in matrix associated microvascular channel formation by breast cancer cells.

Methods

Cell culture

The human breast cancer cell lines MDA-MB-231 and MDA-MB-468 were obtained from the American Type Culture Collection (ATCC; Rockville, MD, USA) and cultured following instructions from the ATCC. Briefly, cells were grown in Dulbecco's modified eagle medium (DMEM; GIBCO-BRL, Rockville, MD, USA) supplemented with 5% fetal calf serum (FCS), 100 U penicillin, 0.1 μg streptomycin and 2 mmol/l L-glutamax. Cells were maintained in log phase in 37°C incubator with 10% carbon dioxide. For each experiment cells were plated in FCS-containing media in 58 cm^2 culture dishes at a cell density of approximately 1×10^6 cells/dish and incubated for another 48 hours. Cell cultures were treated with increasing concentrations of celecoxib (20–60 μmol/l; Pfizer, New York, NY, USA) and with dimethyl sulfoxide (DMSO; the vehicle in which celecoxib was dissolved). The concentration of celecoxib used in our experiments is clinically relevant because the serum concentrations of COX-2 inhibitors in patients range from 20 to 100 μmol/l [19]. The concentrations used in the study are based on our titrations with celecoxib for the two cell lines and from several published references on other cell lines [20-22]. In both the cell lines tested there was no evidence of apoptosis or cell cycle arrest at concentrations below 20 μmol/l.

SDS-PAGE immunoblotting

Following harvesting of adherent cells by scraping, cell lysates were prepared and quantified by BCA assay. Lysates (100 μg) were resolved on a 10–15% acrylamide gel and electroblotted onto immobilon-P polyvinylidene diflouride membranes (Sigma, St. Louis, MO, USA). These were probed with primary antibodies for COX-2 (p66), BAX (p23), Bcl-2 (p26), and vascular endothelial growth factor (VEGF; p20), all from Santa Cruz Biotechnology Inc. (Santa Cruz, CA, USA), and phosphorylated Akt (pAkt; p60; Cell Signaling, Beverly MA, USA), and then probed with the appropriate secondary antibodies. Bound antibodies were detected using an enhanced chemiluminescence detection kit (SuperSignal West Dura, Pierce, Rockford, IL, USA), and developed on high performance chemiluminescence films (Amersham Pharmacia Biotech, Piscataway, NJ, USA).

Proliferation assay

Cell proliferation was determined by using [^{3}H]thymidine incorporation, in which 1 μCi of [^{3}H]thymidine was added to

the drug or vehicle treated cultures 16 hours before harvesting using a Packard Cell Harvester (Packard Biosciences, Shelton, CT, USA). Incorporated thymidine was evaluated using the Topcount micro-scintillation counter (Packard Biosciences). Results were expressed as [^{3}H]thymidine uptake. All determinations were performed in triplicate. Proliferation is directly correlated to radioactive counts/min. In order to determine whether added PGE_2 could counteract the growth inhibitory effect of celecoxib, we treated cells with celecoxib (40 μmol/l) and 12.5–200 pg/ml PGE_2 and incubated them for 96 hours before determining [^{3}H]thymidine incorporation, as mentioned above.

Assay for apoptosis

Following treatment of cells with celecoxib for 48 hours, apoptosis was determined by staining the cells with annexin V and propidium iodide (PI), in accordance with the manufacturer's instructions for use of the BD Pharmingen (San Diego, CA, USA) apoptosis kit. Briefly, an aliquot of 10^5 cells was incubated with annexin V–fluorescein isothiocyanate and PI for 15 min at room temperature in the dark. Cells were immediately analyzed by flow cytometry. Viable cells exclude PI and are negative for annexin V staining, whereas early apoptotic cells are annexin V positive and PI negative. Cells that are not viable due to apoptotic cell death stain positive for annexin V and PI. The percentage of stained cells in each quadrant was quantified using CellQuest software (BD Biosciences, San Jose, CA, USA) and the total number of apoptotic cells (both early and late apoptosis) was quantified.

Confocal microscopy for detection of apoptotic bodies

Cells were grown with celecoxib (60 μmol/l) for 48 hours and then trypsinized. Cells were resuspended in phosphate-buffered saline (PBS) with 0.1% bovine serumn albumin at a final concentration of 5×10^7 cells/ml and 2 μl of 5 mmol/l carboxyfluoroscein succinimidyl ester (CFSE)/ml (Molecular Probes, Eugene, OR, USA) was added. After 10 min of incubation at 37°C the staining was quenched by adding five times the volume of ice-cold PBS and excess stain was washed off by repeated washes in PBS. Cells were fixed in 95% ethanol for 1 hour on ice and resuspended in PBS containing 20 μg/ml PI (Sigma) and 15 μg/ml RNase A (Sigma). Images were captured on the LSM510 confocal microscope (Carl Zeiss Inc., Gottingen, Germany) using excitation wavelengths of 488 nm (for CFSE) and 543 nm (for PI).

Assay for caspases 3 and 7

To evaluate whether celecoxib treatment can induce activation of caspases 3 and 7, we detected levels of active forms of caspases 3 and 7 in cell lysates from treated and untreated cells using the EnzChek Caspase-3/7 Assay Kit (Molecular Probes), in accordance with the manufacturer's protocol. In principle, active caspase 3 or 7 cleaves a fluorogenic substrate; this releases the fluorochrome, which is detected using a spectrofluorometer.

Cell cycle analysis

Cells were treated with increasing concentrations (20–60 μmol/l) of celecoxib or DMSO (vehicle) in medium supplemented with 5% FCS for 48 hours. The adherent and the non-adherent cell fractions were harvested and cell pellets were fixed and permeabilized in 95% cold ethanol, and resuspended in PBS containing 20 μg/ml PI (Sigma) and 15 μg/ml RNase A (Sigma). Samples were incubated in the dark at 37°C for 30 min and analyzed by flow cytometry (Becton Dickinson, San Diego, CA, USA). For each sample, 50,000 fluorescent cells were counted. Data were analyzed using the ModFit software (Verity Software House Inc., Topsham, ME, USA) to determine DNA content and cell cycle phase (G_0/G_1–S–G_2/M phase). Cell doublets and clumps were eliminated from the analyses by gating.

Prostaglandin E_2 production

Cells were treated with increasing concentrations (20–60 μmol/l) celecoxib or DMSO (vehicle) in medium supplemented with 5% FCS for 48 hours. Levels of PGE_2 released in media were measured using a PGE_2 enzyme immunoassay kit from Cayman Chemical Co. (Ann Arbor, MI, USA). Medium was sampled, centrifuged to remove floating cells and frozen immediately at -70°C until assay. The PGE_2 assay was performed in accordance with the manufacturer's instructions, following dilution to ensure that readings were within the limits of accurate detection by the assay. The results are expressed as pg PGE_2/ml ± standard deviation.

Assay for vasculogenic mimicry

This assay was performed as described [23]. Cells were grown until they were about 80% confluent. The growth medium was replaced with serum-free DMEM supplemented with 100 μg/ml heparin (Elkins-Sinn, Inc. Cherry Hill, NJ, USA) and antibiotics, and cells were incubated for 24 additional hours. The cells were trypsinized, counted, and resuspended in media (at a concentration of 4×10^4 cells/ml) containing 40 and 60 μmol/l concentrations of celecoxib or vehicle. The wells of a 24-well tissue culture plate were evenly coated with 0.1 ml/well growth factor reduced Matrigel (BD Biosciences), which was allowed to solidify at 37°C for 30 min, in accordance with the manufacturer's instructions, before the cells were plated. The cell suspension was plated (1 ml/well) onto the surface of Matrigel and incubated at 37°C for 48 hours and photographed using a Nikon inverted phase contrast photomicroscope (Nikon USA, Garden City, NY, USA). Channel formation was quantified as percentage of channels formed by counting the number of connected cells in five randomly selected fields, using 200× magnification, and dividing the number by the total number of cells in the same field.

Xenografts

Male athymic nude mice (age 6–8 weeks) were obtained from NxGen Biosciences Inc. (San Diego, CA, USA) and animals were housed under specific pathogen-free conditions. Five

mice/group were prophylactically treated with either celecoxib (25 mg/kg body weight) or vehicle DMSO for 7 days before the tumor cells were inoculated. MDA-MB-231 cells were harvested by centrifugation and 5×10^6 cells were suspended in 150 μl of serum free DMEM with an equal volume of cold liquid Matrigel (10 mg/ml). The suspension was injected subcutaneously in the mice. In order to determine the optimal cell number to be injected, titration with varying cell numbers was done on nude mice and the tumorigenicity of the cell line determined. The growth of these tumors was monitored by weekly examination, and growth rates were determined using caliper measurements. Tumor weight was calculated according to the following equation [24]: tumor weight (g) = (length (cm) × width $(cm)^2$) × 0.5. Experiments were terminated 45 days after tumor cell injection. It was necessary to kill some of the mice earlier because of the aggressive nature of the tumor.

Histologic studies

All solid tumors resulting were excised and fixed in formaldehyde, and paraffin-embedded blocks was sectioned at a thickness of 7 μm. Histologic evaluation of vascularity was determined by Masson's trichrome staining [25]. This method stains fibrous tissue and stroma green. Blood vessels containing red blood cells stain bright red. Immunohistochemical localization of factor VIII related antigen on endothelial cells was determined using the polyclonal rabbit antihuman von Willebrand factor purchased from Dako Cytomation (Glostrup, Denmark), using the manufacturer's recommended staining protocol.

Statistical analysis

The celecoxib experiments were run in triplicate; the mean as well as standard deviations were computed. The means were then compared using one-way analysis of variance with Dunnett adjustment.

Results

Cyclo-oxygenase-2 protein is differentially expressed in breast cancer cell lines

We studied two human breast cancer cell lines, MDA-MB-231 and MDA-MB-468, for COX-2 expression by western blotting. Both cell lines expressed COX-2, although MDA-MB-468 cells exhibited lower protein expression than did MDA-MB-231 cells. Western blot analysis for COX-2 protein in the MDA-MB-231 cell line showed little change in protein expression after treatment with 20–40 μmol/l celecoxib. At the level of 60 μmol/l there was a slight increase in COX-2 expression. However, in the MDA-MB-468 cell line there was significant downregulation of COX-2 expression upon drug treatment (Fig. 1a).

Celecoxib inhibits growth and proliferation of breast cancer cell lines

Celecoxib at concentrations of 20, 40, and 60 μmol/l was used to treat the two cell lines for 48 hours. Under the phase contrast microscope, both cell lines exhibited a dramatic morphologic change as well as growth arrest after 48 hours of drug treatment (data not shown). The rate of proliferation in response to celecoxib treatment was assayed by measuring incorporation of $[^3H]$thymidine uptake. Significant inhibition of proliferation was observed in both cell lines in a dose-dependent manner, in response to varying concentrations of celecoxib at 96 hours after treatment ($P < 0.001$; Fig. 1b). Similar growth inhibition was observed at earlier time points (48 and 72 hours after treatment (data not shown).

Celecoxib induces apoptosis in MDA-MB-231 but not in MDA-MB-468 cells

Because COX inhibitors have been reported to mediate apoptosis in many cells [26,27], we investigated whether the observed growth inhibition mediated by celecoxib was associated with induction of programmed cell death. Flow cytometric analysis of annexin V/PI staining in celecoxib-treated and vehicle-treated cells was used to analyze apoptosis. Following 48 hours of drug treatment, induction of apoptosis was observed in the MDA-MB-231 cells in a dose-dependent manner (Fig. 2a). Celecoxib at concentrations of 40 and 60 μmol/l caused significant increases in the percentage apoptotic cells ($P = 0.01$ and $P < 0.001$, respectively). In the MDA-MB-468 cell line apoptosis was not induced with celecoxib treatment (Fig. 2a). In spite of the lack of evidence of increased apoptosis, MDA-MB-468 cells had significantly lower proliferation after drug treatment (Fig. 1b). Treated cells appeared rounded up and exhibited atypical morphology (data not shown), which suggested that alterations in the adhesive properties of these cells might have occurred and other pathways may be involved in the growth inhibition observed in MDA-MB-468 cells.

Celecoxib induces formation of apoptotic bodies and loss of nuclear envelope integrity in MDA-MB-231 cells

To follow up on the celecoxib-induced apoptosis of the MDA-MB-231 cells, we analyzed morphological changes in MDA-MB-231 cells after celecoxib treatment using confocal microscopy. Celecoxib at concentrations of 40 and 60 μmol/l caused loss of integrity of nuclear envelope and induced formation of peripheral, sharply delineated masses of condensed chromatin or apoptotic bodies, which are characteristic structural features of apoptosis (Fig. 2b–e). Membrane blebbing was also observed, along with loss of plasma membrane integrity in some cells (data not shown). These results indicate that celecoxib treatment caused architectural changes in membrane and cell nucleus within 48 hours of treatment. No such changes were observed in MDA-MB-468 cells (data not shown), which correlated with our observation that there was no significant induction of apoptosis in these cells after celecoxib treatment (Fig. 2a).

Figure 1

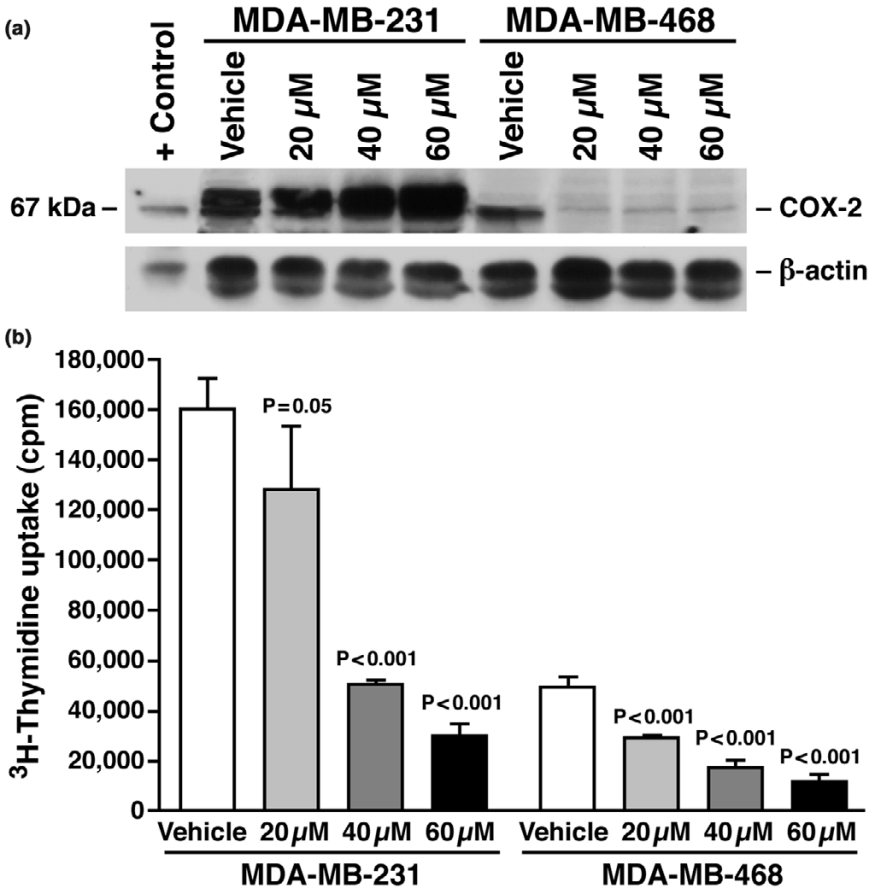

Celecoxib regulates COX-2 levels and causes growth arrest in human breast cancer cells. **(a)** Cyclo-oxygenase (COX)-2 is expressed in both MDA-MB-231 and MDA-MB-468 cell lines. Western blot analysis of vehicle and celecoxib (20–60 μmol/l) treated cells. SDS-PAGE electrophoresis was performed using a 10% resolving gel. Protein was loaded at 100 μg per lane. Lipopolysaccharide/phorbol 12-myristate 13-acetate treated whole cell lysate from RAW264.7 cell line was used as positive control. Gels were blotted and probed with COX-2 monoclonal antibody. Both cell lines expressed COX-2. MDA-MB-231 cells expressed higher levels of COX-2 than did MDA-MB-468 cells. With drug treatment, COX-2 protein level did not change in the MDA-MB-231 cells, but there was reduction in the level of COX-2 protein in the MDA-MB-468 cells after treatment. β-Actin blot is included to confirm equal loading. These experiments were repeated three times with similar results. **(b)** Celecoxib induced dose-dependent inhibition of proliferation of breast cancer cell lines. Cells were incubated for 4 days with vehicle or celecoxib, and [^{3}H]thymidine was added 24 hours before harvest. After washing off excess thymidine, cells were lysed with 5% Triton X-100, and incorporated thymidine was evaluated. Celecoxib treatment caused significant dose-dependent growth inhibition in both human breast cancer cell lines. Mean values of three experiments ± standard deviation is shown. *P* values represent significant differences between vehicle control and celecoxib treatment.

Celecoxib inhibits activation of protein kinase B/Akt kinase in MDA-MB-231 cells

Protein kinase B, Akt, is a serine/threonine protein kinase that is involved in promoting cell survival signals through the phosphoinositide 3-kinase pathway, leading to inactivation of a series of proapoptotic proteins. Akt also represents a key signaling component in cell survival by mediating the activation of downstream effectors such as BAD [28,29] and procaspase-9 [30]. Celecoxib was recently shown to induce apoptosis of cancer cells by blocking Akt activation in rat cholangiocarcinoma and human prostate cancer cells *in vitro* [21,22]. To explore whether inhibition of Akt activation may be the mechanism responsible for induction of apoptosis in MDA-MB-231 cells, we determined the effect of celecoxib on phosphorylation of Akt on breast cancer cell lines. Breast cancer cells were exposed to varying doses of celecoxib for 48 hours, and Akt and pAkt in cell lysates were determined by western blot analysis. At a concentration of 20 μmol/l, celecoxib caused slight increase in pAkt in MDA-MB-231 cells. At a concentration of 60 μmol/l, celecoxib treatment significantly ($P = 0.002$) downregulated the level of phosphorylation of Akt in MDA-MB-231 cells but not in MDA-MB-468 cells (Fig. 3a,b), suggesting that the mechanism of apoptosis induction in MDA-MB-231 cells was, in part, dependent upon decreased phosphorylation of Akt protein. Because Akt represents a key signaling component in cell survival by activating downstream apoptotic proteins [28-31], we evaluated the levels of Bax and Bcl-2 by western blot analysis of lysates derived from both cell lines

Figure 2

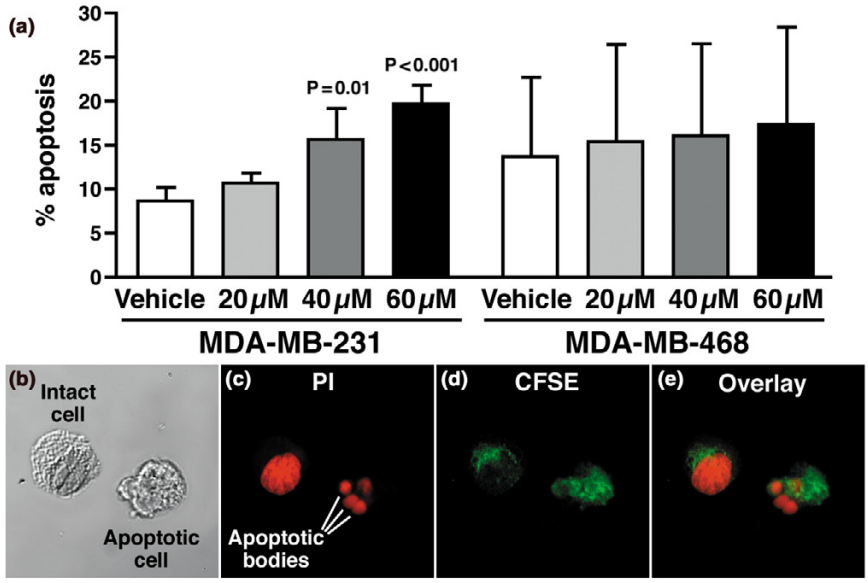

Celecoxib induces apoptosis in MDA-MB-231 cells. **(a)** Flow cytometric analysis of vehicle-treated and celecoxib-treated cells stained with annexin V and propidium iodide (PI) was done 48 hours after treatment. The population shown in the figure is total apoptotic cells, which includes early and late apoptosis. Significant induction of apoptosis was observed in the MDA-MB-231 cells at 40 and 60 μmol/l concentrations of celecoxib. Apoptosis was not induced in MDA-MB-468 cells. Mean values of three experiments ± standard deviation is shown. *P* values represent significant differences between vehicle control and celecoxib treatment. **(b–e)** Celecoxib induces formation of apoptotic bodies in MDA-MB-231 cells. Shown are confocal images of MDA-MB-231 cells subjected to 48 hours of celecoxib (60 μmol/l) treatment. Cells were stained with CFSE (panel d) and then fixed in 95% ethanol and stained with PI (panel c). Cells were visualized in a confocal microscope (Carl Zeiss Inc.) using excitation wavelengths of 488 nm (for CFSE) and 543 nm (for PI). Loss of integrity of nuclear envelope and formation of peripheral, sharply delineated masses of condensed chromatin or apoptotic bodies are visualized. Panel b represents phase contrast images of the cells and panel e represents colocalization of CFSE and PI. Images were taken 200×.

after celecoxib treatment. Treatment with celecoxib at concentrations of 40 and 60 μmol/l induced increased expression of Bax in the MDA-MB-231 cells (Fig. 3c), but no significant decrease in Bcl-2 was observed (data not shown). In MDA-MB-468 cells, in which apoptosis was not evident, levels of pAkt and Bax remained unchanged with treatment (Fig. 3a,b).

Celecoxib induces caspase-3/7 activation in MDA-MB-231 cells

Caspases are responsible for many of the biochemical and morphological changes that occur during apoptosis. Most apoptotic signals induce intracellular cleavage of caspases 3 and 7 from an inactive precursor (p32–p35) to the active forms (p17 and p12); hence, these proteins are the most extensively studied apoptotic proteins. The effector caspases 3 and 7 proteolytically cleave and activate several other caspases as well as several other apoptotic proteins, including the DNA fragmentation protein poly-ADP-ribose polymerase (PARP), which is one of the primary activators of DNA fragmentation and cell death [32-34].

We investigated whether celecoxib induced the activation of caspase 3 and caspase 7 in MDA-MB-231 cells in which apoptosis was induced. Caspase activity is presented as fluorescence emission, which is directly proportional to activities of caspases 3 and 7. Treatment with celecoxib (40 and 60 μmol/l) for 48 hours caused significant increases in activation of caspases 3 and 7 (fivefold increase at the 40 μmol/l concentration [$P = 0.008$] and sixfold increase at the 60 μmol/l concentration [$P = 0.002$]; Fig. 3d). Caspase activation was completely blocked by incubation with the caspase inhibitor Ac-DEVD-CHO (data not shown). These results suggest that celecoxib-induced apoptosis in MDA-MB-231 cells is due to activation of caspases 3 and 7, which is corroborated by studies indicating that the blockade or absence of caspase activation is sufficient to inhibit effective apoptosis [35]. In contrast, caspase activation was not observed in celecoxib-treated MDA-MB-468 cells, which correlated with no significant increase in apoptosis with celecoxib treatment (Fig. 2).

Celecoxib induces cell cycle arrest at the G_0/G_1 checkpoint in MDA-MB-468 but not in MDA-MB-231 cells

To determine whether celecoxib-induced growth inhibition was due to changes in cell cycle progression, flow cytometric analysis was performed on cells treated with increasing concentrations of celecoxib (20–60 μmol/l) for 48 hours. In MDA-MB-468 cells, in which celecoxib did not induce apoptosis, there was induction of cell cycle arrest. At 40 and 60 μmol/l concentrations of celecoxib, significant increases ($P = 0.02$ and $P < 0.001$, respectively) in the proportion of cells that

Figure 3

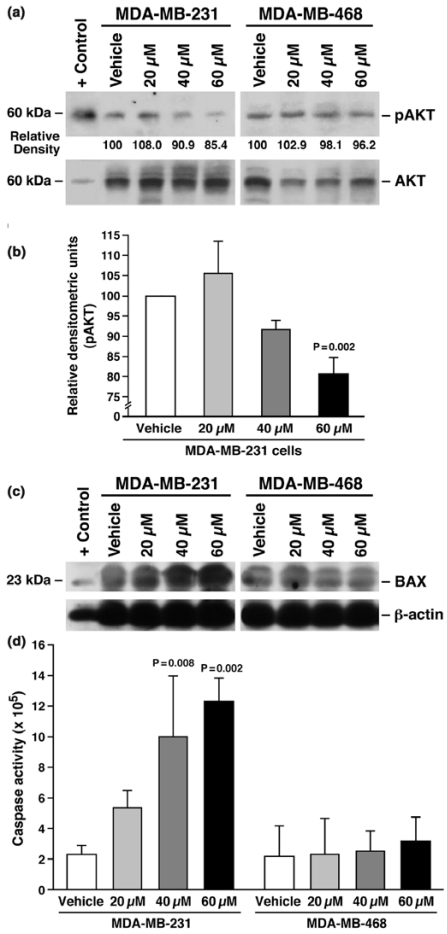

Celecoxib induced down-regulation of pAkt, increase in Bax, and caspase 3/7 in MDA-MB-231 cells. (a) Total Akt and phosphorylated Akt (pAkt). Western blot analysis of cell lysates prepared from vehicle and celecoxib (20–60 μmol/l) treated cells. SDS-PAGE electrophoresis was performed using 10% resolving gel. Protein was loaded at 100 μg per lane and the protein of interest was detected using specific antibodies. Celecoxib treatment at 40 and 60 μmol/l caused decreases in the levels of pAkt in MDA-MB-231 cells, with no change in MDA-MB-468 cells. Numbers below each lane represents percentage of protein expression compared with vehicle-treated cell lysate, which was set to equivalent to 100%, as determined by densitometric analysis. Control cell extracts from Jurkats were used as positive control for Akt and pAkt. **(b)** Average densitometric values of three separate experiments showing reduction in pAkt with celecoxib treatment. There was a significant decrease ($P = 0.002$) in the levels of pAkt with 60 μmol/l celecoxib treatment. **(c)** Western blot analysis of BAX. Increased expression of BAX protein was observed with increasing concentrations of celecoxib in MDA-MB-231 cells but not in MDA-MB-468 cells. The experiment was repeated three times with similar results. A β-actin blot is included to show equal loading. **(d)** Spectrofluorometric analysis of lysates prepared from vehicle and celecoxib (20–60 μmol/l) treated cells at 48 hours. Activity of caspases 3 and 7 was monitored by enzymatic cleavage using a fluorescence microplate reader with excitation at 485 ± 10 nm and emission detection at 530 ± 12.5 nm. In MDA-MB-231 cells, activities of caspases 3 and 7 were increased significantly at 40 μmol/l and 60 μmol/l drug concentrations. No increase in caspase activity was evident in the MDA-MB-468 cells. Mean values from three experiments ± standard deviation is shown. *P* values represent significant differences between vehicle control and celecoxib treatment.

Figure 4

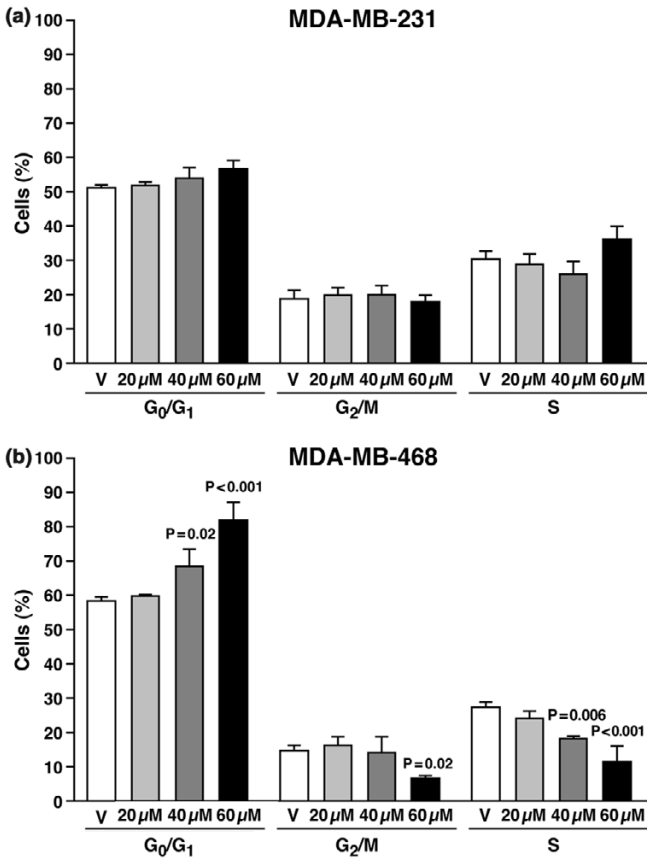

Celecoxib causes cell cycle arrest in MDA-MB-468 cells. **(a,b)** Flow cytometric analysis of cells subjected to treatment with vehicle or celecoxib (20–60 μmol/l) for 48 hours. Cells were fixed and permeabilized with 95% ethanol, stained with propidium iodide, and analyzed by flow cytometry. Celecoxib induced growth arrest at the G_0/G_1 cell cycle checkpoint in MDA-MB-468 cells (panel b) with no cell cycle arrest in the MDA-MB-231 cells (panel a). Mean values for three experiments ± standard deviation of the mean is shown. *P* values represent significant difference between vehicle control and celecoxib treatment. Experiments were repeated three times, with similar results.

were arrested at the G_0/G_1 checkpoint of the cell cycle were observed. Subsequently, significant inhibition of transition to the G_2/M phase ($P = 0.02$ at 60 μmol/l) and S phase ($P = 0.006$ and $P < 0.001$ at 40 and 60 μmol/l) was observed (Fig. 4b). Thus, growth inhibitory activity of celecoxib on these MDA-MB-468 cells was due to cell cycle arrest at G_0/G_1 phase and not due to induction of apoptosis. The cell cycle arrest persisted at 72 hours after drug treatment (data not shown). In MDA-MB-231 cells there was no significant difference in cell cycle progression with celecoxib treatment for 48 hours (Fig. 4a).

Celecoxib inhibits cyclo-oxygenase-2 induced prostaglandin E_2 production in both cell lines

COX-2 converts arachidonic acid to bioactive prostanoids. It has been demonstrated that COX-2 derived PGE_2 is the major

Table 1

Celecoxib inhibited prostaglandin E_2 secretion by breast cancer cells

Treatment	MDA-MB-231	*P* value	MDA-MB-468	*P* value
Vehicle	430.0 ± 178.2		76.6 ± 15.2	
Celecoxib 20 μmol/l	30.1 ± 2.9	<0.01	39.0 ± 16.5	0.03
Celecoxib 40 μmol/l	30.7 ± 4.7	<0.01	37.3 ± 11.0	0.02
Celecoxib 60 μmol/l	37.7 ± 13.6	<0.01	30.3 ± 13.6	0.01

Forty-eight hours post treatment, conditioned medium from vehicle and celecoxib (20–60 μmol/l) treated cells were harvested and prostaglandin (PG)E_2 levels (pg/ml) determined by enzyme-linked immunosorbent assay. In all cell lines, PGE_2 levels were significantly reduced at all doses of celecoxib. The experiment was repeated three times and in triplicate. *P values* represent significant differences between vehicle control and celecoxib treatment.

prostaglandin produced by breast cancer cells [36]. To determine whether COX-2 activity was affected by celecoxib treatment, PGE_2 production using a PGE_2-specific enzyme-linked immunosorbent assay was measured in conditioned medium collected from the breast cancer cell lines after celecoxib-treatment (20–60 μmol/l) for 48 hours. All doses of celecoxib significantly reduced PGE_2 secretion by both cell lines ($P < 0.01$ for MDA-MB-231 and $P = 0.03$, 0.02 and 0.01 for MDA-MB-468 cells; Table 1), indicating that celecoxib is a potent inhibitor of COX-2 induced PGE_2 production.

Celecoxib-induced growth inhibition is reversed by exogenous prostaglandin E_2 only in MDA-MB-468 cells

Because celecoxib caused growth inhibition in the two breast cancer cell lines and inhibited PGE_2 secretion, we hypothesized that this growth inhibition was PGE_2 dependent. To determine whether celecoxib-induced growth inhibition could be reversed by exogenous PGE_2, PGE_2 was added to cultures of MDA-MB-231 and MDA-MB-468 cells treated with constant dose (40 μmol/l) of celecoxib. Varying amounts of PGE_2 (12.5–200 pg/ml) were added to the medium in order to take into account the fact that some of the PGE_2 may degrade or be internalized into cells. In MDA-MB-231 cells, growth inhibition induced by 40 μmol/l celecoxib could not be restored by addition of exogenous PGE_2 (Fig. 5a), thereby suggesting that celecoxib-induced growth inhibition in MDA-MB-231 cells may be independent of PGE_2 levels. However, addition of 200 pg/ml PGE_2 completely reversed the growth inhibition induced by 40 μmol/l celecoxib in the less invasive MDA-MB-468 cells (Fig. 5b), suggesting that celecoxib-induced growth regulation of these cell lines may be dependent on the levels of PGE_2.

Celecoxib inhibits *in vitro* matrix-associated vascular channel formation

Recent findings demonstrate the unusual ability of aggressive human breast cancer cells to form tubular structures in three-dimensional Matrigel cultures. The generation of these channels by epithelial tumor cells is called vascular mimicry [37-39]. One study [40] suggested a connection between angiogenesis and formation of these channels. Because celecoxib is known to act as an inhibitor of angiogenesis, we investigated the ability of MDA-MB-231 and MDA-MB-468 cells to form the microvascular channels with and without celecoxib treatment. MDA-MB-231 cells, which express elevated levels of COX-2 and are highly invasive, begin to form tubular structures in under 16 hours when plated on Matrigel (data not shown) and form very characterized microvascular channels by 48 hours. In contrast, MDA-MB-468 cells, which have lower COX-2 and are less invasive, start tubule formation much later, at approximately 30 hours, and exhibit significantly fewer microvascular channels at 48 hours than do MDA-MB-231 cells. These observations were specific for the high or moderately invasive cells, because the noninvasive breast cancer cells (ZR-75-1) did not form channels *in vitro* under identical culture conditions (data not shown).

We found that celecoxib treatment at concentrations of 40 and 60 μmol/l was able to reduce significantly the formation of channels in both breast cancer cell lines in a dose-dependent manner, as compared with vehicle treated cells ($P < 0.001$ for MDA-MB-231 cells and $P < 0.001$ for MDA-MB-468 cells; Fig. 6a), suggesting a role for COX-2 in channel formation. The effect of celecoxib on channel formation was only quantified on live adherent cells in Matrigel as the apoptosed and dead cells float into the media. Thus, we believe that the negative effect of celecoxib on channel formation was not due to cell death, which was also measured by trypan blue exclusion (data not shown).

Celecoxib inhibits expression of vascular endothelial growth factor protein in MDA-MB-231 cells

Recent reports have shown that a nonspecific COX inhibitor (indomethacin) suppresses the expression of VEGF gene expression *in vitro* in mammary tumor cells [41]. We evaluated the levels of VEGF protein from tumor lysate of cells treated with vehicle or increasing doses of celecoxib. Compared with control, celecoxib (20–60 μmol/l) treatment reduced expression of VEGF in the MDA-MB-231 cells in a dose-dependent manner (Fig. 6b). No such reduction was observed in the MDA-MB-468 cells treated with celecoxib (Fig. 6b), suggesting that in the highly aggressive MDA-MB-231 cells the COX-2/PGE_2 pathway may play a critical role in channel formation

Figure 5

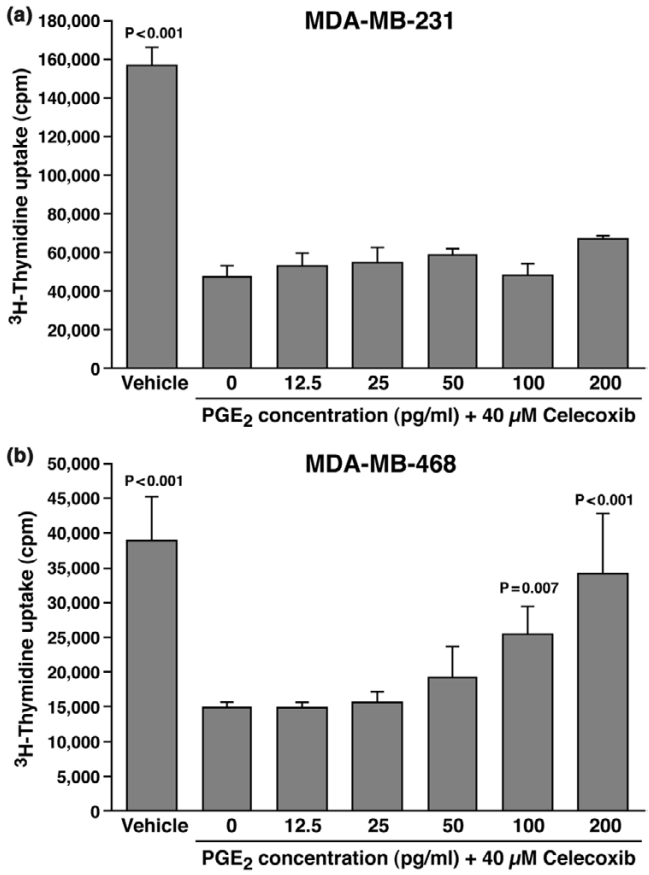

Growth inhibition of MDA-MB-468 cells was abrogated by exogenous prostaglandin (PG)E_2 addition. [^{3}H]thymidine uptake assay was done to determine proliferation of **(a)** MDA-MB-231 and **(b)** MDA-MB-468 cells treated with 40 μmol/l celecoxib with or without varying amounts of exogenous PGE_2 (12.5–200 pg/ml). Cells were harvested after 96 hours in culture. In MDA-MB-231 cells, growth inhibition induced by 40 μmol/l celecoxib could not be restored by addition of exogenous PGE_2; however, addition of 200 pg/ml PGE_2 completely reversed the growth inhibition induced by 40 μmol/l celecoxib in the less invasive MDA-MB-468 cells. Average values of three experiments ± standard deviation is shown. *P* values represent significant differences between vehicle control and celecoxib treatment.

and angiogenesis, in part by activating proangiogenic proteins such as VEGF. Future studies will evaluate other proteins associated with the angiogenic pathway.

In vivo tumor growth was reduced with celecoxib treatment

Nude mice were prophylactically treated with celecoxib or vehicle for 1 week before tumor challenge with MDA-MB-231 cells in Matrigel. Celecoxib treatment was continued for 45 days after tumor challenge. Mice treated with celecoxib (25 mg/kg body weight) exhibited significant ($P = 0.01$) reduction in tumor growth as compared with vehicle-treated mice without evidence of systemic toxicity (Fig. 7a). A representative mouse from each treatment group is shown in Fig. 7b; the treated mouse has reduced tumor mass compared with the control mouse.

In vivo inhibition of angiogenesis and increase in necrosis with celecoxib treatment

Vascularity of tumor implants was histologically evaluated using Masson's trichrome and factor VIII-related antigen staining. Tumors from celecoxib-treated mice showed reduced blood vessels as compared with tumors excised from vehicle-treated mice (Fig. 8). Furthermore, there was evidence of necrosis in the celecoxib-treated tumors relative to those obtained from vehicle-treated animals (Fig. 8a,b).

Discussion

The results presented here clearly show that celecoxib strongly suppresses cell growth and proliferation in both human breast cancer cell lines (Fig. 1b). However, the mechanism of antitumor effect is dependent upon COX-2 expression and the invasive properties of the cancer cell. The highly invasive MDA-MB-231 cells undergo induction of apoptosis (Fig. 2) and the less invasive MDA-MB-468 cells undergo cell cycle arrest (Fig. 4) after treatment with celecoxib. The two cell lines exhibit different levels of COX-2 protein expression, with MDA-MB-231 cells expressing much higher levels than MDA-MB-468 cells (Fig. 1a), which directly correlated with the amount of PGE_2 production by the cells (Table 1) and their invasive properties. Our data are in good agreement with the postulate that elevated production of COX-2-induced prostanoids is a hallmark of highly metastasizing breast cancer cells [41,42]. The two cell lines regulate COX-2 protein differently after celecoxib treatment, with downregulation of the protein observed in MDA-MB-468 cells but not in MDA-MB-231 cells (Fig. 1a). In fact there was an increase in COX-2 expression in MDA-MB-231 cells at the 60 μmol/l level of celecoxib, the mechanism for which is not known. However, one or more COX-produced products may repress COX expression in a negative feedback loop. Removal of negative feedback by celecoxib treatment would result in COX-2 induction. There are similar reports on celecoxib treatment leading to strong upregulation of COX-2 protein expression in 184htert breast cancer cells [43].

Regardless of COX-2 expression and regulation patterns, celecoxib treatment reduced PGE_2 secretion by both cell lines (Table 1), but provision of exogenous PGE_2 reversed celecoxib-induced growth inhibition in the MDA-MB-468 cells only, and not in the MDA-MB-231 cells (Fig. 5). This suggests that celecoxib-induced growth inhibition of the highly aggressive MDA-MB-231 cells is independent of PGE_2. Corroborating our findings are previous reports that growth inhibition induced by COX-2 inhibitors in some carcinoma cell lines can be completely abrogated by exogenous addition of PGE_2 [44], whereas in other studies addition of PGE_2 had no effect [45,46]. One possible PGE_2-independent mechanism by which celecoxib may have caused apoptosis in MDA-MB-231

Figure 6

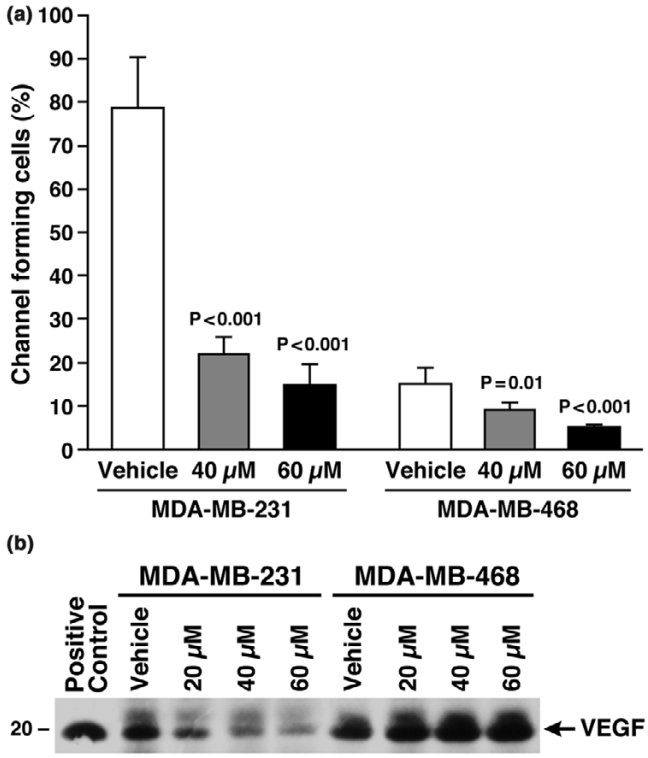

Celecoxib treatment causes reduction in microvascular channel formation by regulating VEGF levels. **(a)** The percentage of cells forming channels was much greater in MDA-MB-231 cells than in MDA-MB-468 cells. In both cells, treatment with 40 and 60 μmol/l celecoxib caused significant reduction in the number of channels. *P* values represent significant differences between vehicle control and celecoxib treatment. **(b)** Western blot analysis of cell lysates prepared from vehicle and celecoxib (20–60 μmol/l) treated cells. SDS-PAGE electrophoresis was performed using 15% resolving gel. Protein was loaded at 100 μg per lane and the protein was detected using vascular endothelial growth factor (VEGF) antibody. Celecoxib treatment decreased VEGF levels in MDA-MB-231 cells in a dose-dependent manner.

cell lines could be through the accumulation of the prostaglandin precursor arachidonic acid. Arachidonic acid is known to be converted to an intermediate, apoptosis-signaling compound, namely ceramide, which causes NSAID-induced apoptosis in cancer cells [47]. This phenomenon of ceramide-induced apoptosis has been proven in a murine mammary tumor cell line treated with celecoxib [18]. Because PGE_2 is the major prostanoid released from breast cancer cells [41], we focused our studies on PGE_2 levels. However, a possible role of other prostanoids such as PGD_2, PGI, $PGF_{2\alpha}$ and $thromboxane_2$ cannot be ruled out, and future studies will include analyses of other prostanoids.

Thus, we observed that the mechanisms driving celecoxib-induced growth inhibition are very diverse in the two cells lines, depending upon COX-2 expression levels, invasive properties, and dependence on PGE_2. At the cellular level, celecoxib induced the characteristic features of apoptosis in the MDA-MB-231 cells (Fig. 2). At the molecular level, activation of protein kinase B/Akt was significantly reduced at 60 μmol/l concentration of celecoxib, with increased activation of proapoptotic protein Bax and caspases 3 and 7 (Fig. 3). These results are in agreement with those of other studies in which it was suggested that activation of effector caspases 3 and 7 and Bax proteins, downstream of phosphoinositide 3-kinase/Akt inactivation, was the mechanism of celecoxib-induced tumor cell apoptosis [22,48]. Mechanisms leading to the downregulation of Akt activation are not clear. It has been suggested that inhibition of the tumor suppressor PTEN, a phosphatase that targets phosphoinositol triphosphate, or inhibition of 3-phosphoinositide-dependent kinase 1 activity may be involved [48-50].

In contrast to MDA-MB-231 cells, growth of MDA-MB-468 cells was inhibited by induction of cell cycle arrest at the G_0/G_1 phase of the cell cycle (Fig. 4). Similar cell cycle arrest has been reported using a murine mammary tumor cell line derived from a spontaneously occurring tumor [18], human pancreatic cancer cell lines [51], and human ovarian cancer cell lines [52]. It is not clear from our studies that celecoxib directly affects cell cycle distribution by regulating cyclin D_1 levels, which is one of the major cyclins known to be upregulated during cancer. Preliminary data evaluating cyclin D_1 levels in MDA-MB-468 cells after celecoxib treatment were inconclusive (data not shown) and more thorough analysis is needed. The question remains whether COX-2 induced PGE_2 can directly regulate cyclin D_1 or other network of cyclins, cyclin-dependent kinases (CDKs) or CDK inhibitors. For other cell types, including colon, lung and squamous cell carcinomas, it has been reported that treatment with NSAIDs results in upregulation of CDK inhibitors that regulate accumulation of cells in G_0/G_1 [53-55]. In breast cancer cells, this remains to be examined.

Angiogenesis plays a crucial role in tumor development and progression. COX-2 dependent PGE_2 production represents a likely candidate for the angiogenic response observed in several tumors, including mammary tumors [36,56-58]. To explore the role played by COX-2 inhibitors in angiogenesis, we used both *in vitro* and *in vivo* model systems. Aggressive breast epithelial cells are known to differentiate into tubules when cultured on growth factor reduced Matrigel. This phenomenon is known as vasculogenic mimicry. Its presence has been reported in inflammatory breast cancer patients and is associated with reduced 5-year survival and higher percentage of recurrence [59]. Shirakawa and coworkers [40] suggested a connection between vascular mimicry and angiogenesis, based on the existence of blood flow in the vascular channels. When plated on growth factor reduced Matrigel, human breast cancer cell lines have the unique ability to form tubular channels. We showed that the more aggressive MDA-MB-231 cells generate channels more efficiently and in higher numbers than do the less aggressive MDA-MB-

Figure 7

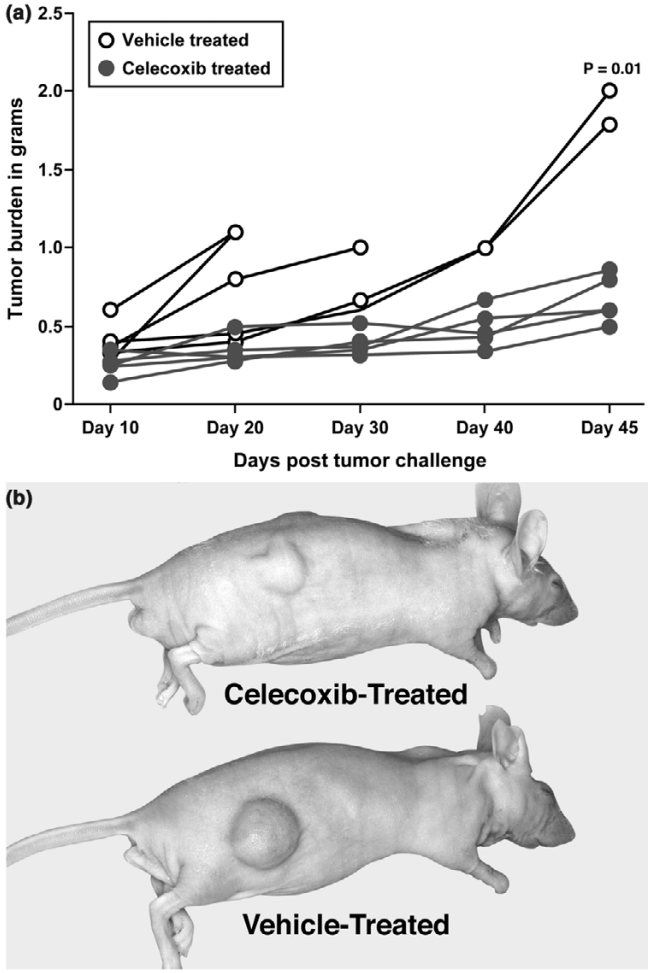

Celecoxib treatment reduced MDA-MB-231 tumor growth in nude mice. **(a)** Five mice per group were treated with either celecoxib (25 mg/kg body weight) or vehicle (dimethyl sulfoxide) and the mice were killed 45 days after the tumor cells were inoculated. Tumor growth was monitored by weekly examination using digital calipers, and tumor weight was calculated using to the following equation [23]: tumor weight (g) = (length (cm) × width (cm)^2) × 0.5. Three mice from the vehicle-treated group had to be killed early because of the aggressive nature of the tumor. The other two mice in the vehicle-treated group had significantly greater tumor burden ($P = 0.01$) than did the five mice in celecoxib-treated group. **(b)** A representative mouse from each treatment group is illustrated; lower tumor mass Is evident in the treated animal as compared with the vehicle control.

Figure 8

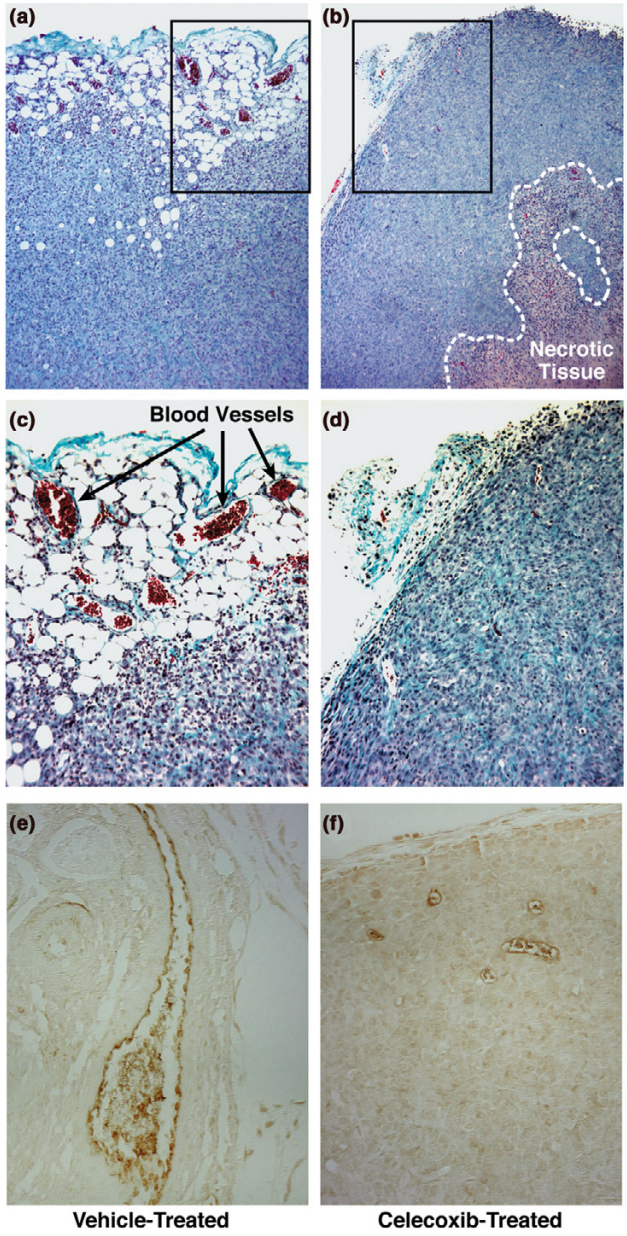

In vivo inhibition of angiogenesis and increase in necrosis with celecoxib treatment. Vascularity of tumor implants was histologically evaluated by Masson's trichrome and factor VIII related antigen staining. Shown is evidence of central necrosis and decreased number of blood vessels in **(b)** a section of celecoxib-treated tumors relative to **(a)** a section obtained from a vehicle-treated animal (magnification 50×). Greater magnification (100×) of **(c)** panel a and **(d)** panel b are shown in the next two panels. Arrows in panel c point to blood vessels. Endothelial cells lining the blood vessels stained positively for factor VIII related antigen and showed larger blood vessels in the **(e)** vehicle-treated than in the **(f)** celecoxib-treated samples (magnification 100×).

468 cell line (Fig. 6a). Similarly, it was shown that highly aggressive melanoma cells, when seeded on three-dimensional matrices of collagen I, form extracellular matrix-rich patterned networks that surround clusters of tumor cells; however, under the same culture conditions, poorly aggressive melanoma cells did not form the patterned networks [38]. When treated with increasing concentrations of celecoxib (40–60 μmol/l) we observed a dose-dependent decrease in the ability of both cell lines to differentiate into channels (Fig. 6a). Our findings are in accordance with those of other reports, in which capillary-like tube formation by human umbilical vein endothelial cells cocultured with COX-2 overexpress-

ing Caco-2 cells was inhibited by a COX-2 selective inhibitor, NS-398, in a dose-dependent manner [60].

COX-2 inhibitors have already been reported to inhibit angiogenesis, and our study shows for the first time that COX-2 regulates vascular channel formation in human breast cancer cells. The mechanism of action of celecoxib in inhibiting channel formation is not known. Our data suggest that treatment with celecoxib caused a dose-dependent downregulation of VEGF in the MDA-MB-231 cells but not in the MDA-MB-468 cells (Fig. 6b). Although additional mechanisms are involved in mediating the angiogenic effects of COX-2, our data imply that COX-2 inhibitors influence angiogenesis at least in part by decreasing the release of VEGF. It was recently reported that COX-2 induced PGE_2 stimulated the expression of angiogenic regulatory genes, including VEGF, in mammary tumor cells isolated from COX-2 transgenic mice, and that treatment with indomethacin (a nonspecific COX inhibitor) suppressed the expression of these genes *in vitro* [36]. To confirm the *in vitro* data, the antiangiogenic effects of celecoxib were evaluated in an *in vivo* xenograft model using MDA-MB-231 cell containing Matrigel implants. Results showed that celecoxib dramatically reduced the vascularity within the tumor tissue (Fig. 8). In addition, the treatment caused increased necrosis and reduced viable tissue mass within the tumor (Figs 7 and 8). Therefore, the reduced tumor burden in the treated mice can be explained in part by the inhibition of angiogenesis and confirms our *in vitro* data. Previous studies have reported similar effects of COX-2 inhibitors in an *in vivo* angiogenesis assay using the highly metastatic murine mammary tumor cell line C3L5 [45]. Additional studies are needed to fully elucidate the complex events involved in COX-2 mediated angiogenesis in human mammary tumors.

To our knowledge, this is the first study to identify some key mechanisms of action of celecoxib *in vitro* and *in vivo* in human breast cancer cells. More cell lines must be evaluated to characterize fully the antitumor actions of celecoxib, including identification of its primary targets, the precise molecular mechanism of cell damage, and the basis for its preferential effect on tumor cells. Although COX-2 inhibitor treatment alone is unlikely to eliminate an existing tumor, it is likely that it can confer significant benefit as part of a carefully chosen regimen involving other drugs. The strategy to target multiple pathways simultaneously may be critical to improving the efficacy of therapy in the treatment of breast cancer, especially for metastatic breast cancer. Moore and coworkers [61] reported that celecoxib, in combination with 5-fluorouracil or cyclophosphamide, greatly enhanced the antitumor effects of chemotherapy in a colon cancer model. In another tumor model, COX-2 selective inhibitors showed promise in combination with radiation therapy, enhancing tumor radiation responses [62]. Celecoxib was recently shown to have chemopreventive effects against the development of chemically induced mammary tumors in the rat [12]. Finally, recent evidence that combined treatment with a nonselective NSAID and EGFR tyrosine kinase inhibitor significantly decreased polyp formation in Min $APC^{+/-}$ mice supports the notion that combination therapy may be more effective [63]. These studies, combined with the present study and the reports of aberrant COX-2 expression in human breast cancer [9,64], suggest that selective COX-2 inhibitors have an important role to play in chemoprevention, chemo-intervention, and therapy of human breast cancer.

Conclusion

We showed that the mechanisms driving celecoxib-induced growth inhibition of human breast cancer cells are dependent upon COX-2 expression levels, invasive properties, and dependence on PGE_2. At the cellular level, celecoxib induced apoptosis in highly invasive cells, but it caused cell cycle arrest at the G_0/G_1 phase of the cell cycle without causing apoptosis in the less invasive cells. At the molecular level, pAkt was inactivated with increased activation of proapoptotic protein Bax and caspases 3 and 7. Furthermore, we showed for the first time that celecoxib inhibited microvascular channel formation in a dose-dependent manner, associated with downregulation of VEGF in the highly invasive cells. An *in vivo* xenograft model confirmed the *in vitro* data and showed dramatic reduction in tumor mass accompanied by reduced vascularity and increased necrosis within the tumor, suggesting that the reduced tumor burden in the treated mice may in part be due to reduced angiogenesis.

Competing interests

The author(s) declare that they have no competing interests.

Authors' contributions

GDB conducted the mouse studies including daily gavaging, palpating tumors and monitoring tumor growth, as well as endpoint assays such as apoptosis, and caspase assays. LBP and TLT performed the western blotting and PGE_2 assays. SJG provided expert scientific advice with regard to the MTag transgenic mice and mammary carcinogenesis. PM is the PI of the laboratory in which all experiments were conducted and is the recipient of the grant that funded the project. She was instrumental in writing the manuscript.

Acknowledgements

This study was supported by a grant from the Susan G Komen Breast Cancer Foundation (BCTR0202089) to PM. We thank Dr Ronald J Marler for his help in evaluating the histologic specimens, Leslie Dixon for helping with histology, Jim Tarara for helping with the confocal studies and flow cytometry, Marvin H Ruona for help with the graphic production, Scott Dulla for helping with photography, and Carol Williams for preparation of the manuscript.

References

1. Harris RE, Chlebowski RT, Jackson RD, Frid DJ, Ascenseo JL, Anderson G, Loar A, Rodabough RJ, White E, McTiernan A: **Breast cancer and nonsteroidal anti-inflammatory drugs: pro-**

spective results from the Women's Health Initiative. *Cancer Res* 2003, **63:**6096-6101.
2. Lee PP, Ip MM: **Regulation of proliferation of rat mammary tumor cells by inhibitors of cyclooxygenase and lipoxygenase.** *Prostaglandins Leukot Essent Fatty Acids* 1992, **45:**21-31.
3. Robertson FM, Parrett ML, Joarder FS, Ross M, Abou-Issa HM, Alshafie G, Harris RE: **Ibuprofen-induced inhibition of cyclooxygenase isoform gene expression and regression of rat mammary carcinomas.** *Cancer Lett* 1998, **122:**165-175.
4. Alshafie GA, Harris RE, Robertson FM, Parrett ML, Ross M, Abou-Issa H: **Comparative chemopreventive activity of ibuprofen and N-(4-hydroxyphenyl) retinamide against the development and growth of rat mammary adenocarcinomas.** *Anticancer Res* 1999, **19:**3031-3036.
5. Zhao Y, Agarwal VR, Mendelson CR, Simpson ER: **Estrogen biosynthesis proximal to a breast tumor is stimulated by PGE2 via cyclic AMP, leading to activation of promoter II of the CYP19 (aromatase) gene.** *Endocrinology* 1996, **137:**5739-5742.
6. Brueggemeier RW, Quinn AL, Parrett ML, Joarder FS, Harris RE, Robertson FM: **Correlation of aromatase and cyclooxygenase gene expression in human breast cancer specimens.** *Cancer Lett* 1999, **140:**27-35.
7. Richards JA, Brueggemeier RW: **Prostaglandin E2 regulates aromatase activity and expression in human adipose stromal cells via two distinct receptor subtypes.** *J Clin Endocrinol Metab* 2003, **88:**2810-2816.
8. Bandyopadhyay GK, Imagawa W, Wallace D, Nandi S: **Linoleate metabolites enhance the in vitro proliferative response of mouse mammary epithelial cells to epidermal growth factor.** *J Biol Chem* 1987, **262:**2750-2756.
9. Pockaj B, Basu GD, Pathangey LB, Gray RJ, Hernandez JL, Gendler SJ, Mukherjee P: **Reduced T cell and dendritic cell function is related to COX-2 over-expression and prostaglandin E2 secretion in patients with breast cancer.** *Ann Surg Oncol* 2004, **11:**328-339.
10. Ristimaki A, Sivula A, Lundin J, Lundin M, Salminen T, Haglund C, Joensuu H, Isola J: **Prognostic significance of elevated cyclooxygenase-2 expression in breast cancer.** *Cancer Res* 2002, **62:**632-635.
11. Harris RE, Namboodiri KK, Farrar WB: **Nonsteroidal antiinflammatory drugs and breast cancer.** *Epidemiology* 1996, **7:**203-205.
12. Harris RE, Alshafie GA, Abou-Issa H, Seibert K: **Chemoprevention of breast cancer in rats by celecoxib, a cyclooxygenase 2 inhibitor.** *Cancer Res* 2000, **60:**2101-2103.
13. Howe LR, Subbaramaiah K, Patel J, Masferrer JL, Deora A, Hudis C, Thaler HT, Muller WJ, Du B, Brown AM, *et al.*: **Celecoxib, a selective cyclooxygenase 2 inhibitor, protects against human epidermal growth factor receptor 2 (HER-2)/neu-induced breast cancer.** *Cancer Res* 2002, **62:**5405-5407.
14. Basu GD, Pathangey LB, Tinder TL, LaGioia M, Gendler SJ, Mukherjee P: **Cyclooxygenase-2 inhibitor induces apoptosis in breast cancer cells in an *in vivo* model of spontaneous metastatic breast cancer.** *Proc Natl Acad Sci USA* 2002, **2:**632-642.
15. Liu CH, Chang SH, Narko K, Trifan OC, Wu MT, Smith E, Haudenschild C, Lane TF, Hla T: **Overexpression of cyclooxygenase-2 is sufficient to induce tumorigenesis in transgenic mice.** *J Biol Chem* 2001, **276:**18563-18569.
16. Muller-Decker K, Neufang G, Berger I, Neumann M, Marks F, Furstenberger G: **Transgenic cyclooxygenase-2 overexpression sensitizes mouse skin for carcinogenesis.** *Proc Natl Acad Sci USA* 2002, **99:**12483-12488.
17. Takahashi Y, Kawahara F, Noguchi M, Miwa K, Sato H, Seiki M, Inoue H, Tanabe T, Yoshimoto T: **Activation of matrix metalloproteinase-2 in human breast cancer cells overexpressing cyclooxygenase-1 or -2.** *FEBS Lett* 1999, **460:**145-148.
18. Kundu N, Smyth MJ, Samsel L, Fulton AM: **Cyclooxygenase inhibitors block cell growth, increase ceramide and inhibit cell cycle.** *Breast Cancer Res Treat* 2002, **76:**57-64.
19. Munkarah AR, Genhai Z, Morris R, Baker VV, Deppe G, Diamond MP, Saed GM: **Inhibition of paclitaxel-induced apoptosis by the specific COX-2 inhibitor, NS398, in epithelial ovarian cancer cells.** *Gynecol Oncol* 2003, **88:**429-433.
20. Williams CS, Watson AJ, Sheng H, Helou R, Shao J, DuBois RN: **Celecoxib prevents tumor growth in vivo without toxicity to normal gut: lack of correlation between in vitro and in vivo models.** *Cancer Res* 2000, **60:**6045-6051.
21. Hsu AL, Ching TT, Wang DS, Song X, Rangnekar VM, Chen CS: **The cyclooxygenase-2 inhibitor celecoxib induces apoptosis by blocking Akt activation in human prostate cancer cells independently of Bcl-2.** *J Biol Chem* 2000, **275:**11397-11403.
22. Lai GH, Zhang Z, Sirica AE: **Celecoxib acts in a cyclooxygenase-2-independent manner and in synergy with emodin to suppress rat cholangiocarcinoma growth in vitro through a mechanism involving enhanced Akt inactivation and increased activation of caspases-9 and -3.** *Mol Cancer Ther* 2003, **2:**265-271.
23. Jones MK, Wang H, Peskar BM, Levin E, Itani RM, Sarfeh IJ, Tarnawski AS: **Inhibition of angiogenesis by nonsteroidal anti-inflammatory drugs: insight into mechanisms and implications for cancer growth and ulcer healing.** *Nat Med* 1999, **5:**1418-1423.
24. Simpson-Herrerns L, Lloyd HH: **Kinetic parameters and growth curves for experimental tumor systems.** *Cancer Chemother Rep* 1970, **54:**143-174.
25. Jadeski LC, Lala PK: **Nitric oxide synthase inhibition by N(G)-nitro-L-arginine methyl ester inhibits tumor-induced angiogenesis in mammary tumors.** *Am J Pathol* 1999, **155:**1381-1390.
26. Tsujii M, DuBois RN: **Alterations in cellular adhesion and apoptosis in epithelial cells overexpressing prostaglandin endoperoxide synthase 2.** *Cell* 1995, **83:**493-501.
27. Liu XH, Yao S, Kirschenbaum A, Levine AC: **NS398, a selective cyclooxygenase-2 inhibitor, induces apoptosis and down-regulates bcl-2 expression in LNCaP cells.** *Cancer Res* 1998, **58:**4245-4249.
28. Datta SR, Dudek H, Tao X, Masters S, Fu H, Gotoh Y, Greenberg ME: **Akt phosphorylation of BAD couples survival signals to the cell-intrinsic death machinery.** *Cell* 1997, **91:**231-241.
29. del Peso L, Gonzalez-Garcia M, Page C, Herrera R, Nunez G: **Interleukin-3-induced phosphorylation of BAD through the protein kinase Akt.** *Science* 1997, **278:**687-689.
30. Cardone MH, Roy N, Stennicke HR, Salvesen GS, Franke TF, Stanbridge E, Frisch S, Reed JC: **Regulation of cell death protease caspase-9 by phosphorylation.** *Science* 1998, **282:**1318-1321.
31. Scheid MP, Woodgett JR: **Unravelling the activation mechanisms of protein kinase B/Akt.** *FEBS Lett* 2003, **546:**108-112.
32. Susin SA, Zamzami N, Castedo M, Daugas E, Wang HG, Geley S, Fassy F, Reed JC, Kroemer G: **The central executioner of apoptosis: multiple connections between protease activation and mitochondria in Fas/APO-1/CD95- and ceramide-induced apoptosis.** *J Exp Med* 1997, **186:**25-37.
33. Keane RW, Srinivasan A, Foster LM, Testa MP, Ord T, Nonner D, Wang HG, Reed JC, Bredesen DE, Kayalar C: **Activation of CPP32 during apoptosis of neurons and astrocytes.** *J Neurosci Res* 1997, **48:**168-180.
34. Krajewski S, Gascoyne RD, Zapata JM, Krajewska M, Kitada S, Chhanabhai M, Horsman D, Berean K, Piro LD, Fugier-Vivier I, *et al.*: **Immunolocalization of the ICE/Ced-3-family protease, CPP32 (Caspase-3), in non-Hodgkin's lymphomas, chronic lymphocytic leukemias, and reactive lymph nodes.** *Blood* 1997, **89:**3817-3825.
35. Hirpara JL, Seyed MA, Loh KW, Dong H, Kini RM, Pervaiz S: **Induction of mitochondrial permeability transition and cytochrome C release in the absence of caspase activation is insufficient for effective apoptosis in human leukemia cells.** *Blood* 2000, **95:**1773-1780.
36. Chang SH, Liu CH, Conway R, Han DK, Nithipatikom K, Trifan OC, Lane TF, Hla T: **Role of prostaglandin E2-dependent angiogenic switch in cyclooxygenase 2-induced breast cancer progression.** *Proc Natl Acad Sci USA* 2004, **101:**591-596.
37. Shirakawa K, Tsuda H, Heike Y, Kato K, Asada R, Inomata M, Sasaki H, Kasumi F, Yoshimoto M, Iwanaga T, *et al.*: **Absence of endothelial cells, central necrosis, and fibrosis are associated with aggressive inflammatory breast cancer.** *Cancer Res* 2001, **61:**445-451.
38. Maniotis AJ, Folberg R, Hess A, Seftor EA, Gardner LM, Pe'er J, Trent JM, Meltzer PS, Hendrix MJ: **Vascular channel formation by human melanoma cells in vivo and in vitro: vasculogenic mimicry.** *Am J Pathol* 1999, **155:**739-752.
39. Folberg R, Hendrix MJ, Maniotis AJ: **Vasculogenic mimicry and tumor angiogenesis.** *Am J Pathol* 2000, **156:**361-381.

40. Shirakawa K, Kobayashi H, Heike Y, Kawamoto S, Brechbiel MW, Kasumi F, Iwanaga T, Konishi F, Terada M, Wakasugi H: **Hemodynamics in vasculogenic mimicry and angiogenesis of inflammatory breast cancer xenograft.** *Cancer Res* 2002, **62:**560-566.
41. Timoshenko AV, Xu G, Chakrabarti S, Lala PK, Chakraborty C: **Role of prostaglandin E2 receptors in migration of murine and human breast cancer cells.** *Exp Cell Res* 2003, **289:**265-274.
42. Liu XH, Rose DP: **Differential expression and regulation of cyclooxygenase-1 and -2 in two human breast cancer cell lines.** *Cancer Res* 1996, **56:**5125-5127.
43. Levitt RJ, Buckley J, Blouin MJ, Schaub B, Triche TJ, Pollak M: **Growth inhibition of breast epithelial cells by celecoxib is associated with upregulation of insulin-like growth factor binding protein-3 expression.** *Biochem Biophys Res Commun* 2004, **316:**421-428.
44. Minter HA, Eveson JW, Huntley S, Elder DJ, Hague A: **The cyclooxygenase 2-selective inhibitor NS398 inhibits proliferation of oral carcinoma cell lines by mechanisms dependent and independent of reduced prostaglandin E2 synthesis.** *Clin Cancer Res* 2003, **9:**1885-1897.
45. Rozic JG, Chakraborty C, Lala PK: **Cyclooxygenase inhibitors retard murine mammary tumor progression by reducing tumor cell migration, invasiveness and angiogenesis.** *Int J Cancer* 2001, **93:**497-506.
46. Elder DJ, Halton DE, Crew TE, Paraskeva C: **Apoptosis induction and cyclooxygenase-2 regulation in human colorectal adenoma and carcinoma cell lines by the cyclooxygenase-2-selective non-steroidal anti-inflammatory drug NS-398.** *Int J Cancer* 2000, **86:**553-560.
47. Chan TA, Morin PJ, Vogelstein B, Kinzler KW: **Mechanisms underlying nonsteroidal antiinflammatory drug-mediated apoptosis.** *Proc Natl Acad Sci USA* 1998, **95:**681-686.
48. Soengas MS, Lowe SW: **Apoptosis and melanoma chemoresistance.** *Oncogene* 2003, **22:**3138-3151.
49. Maehama T, Taylor GS, Dixon JE: **PTEN and myotubularin: novel phosphoinositide phosphatases.** *Annu Rev Biochem* 2001, **70:**247-279.
50. Arico S, Pattingre S, Bauvy C, Gane P, Barbat A, Codogno P, Ogier-Denis E: **Celecoxib induces apoptosis by inhibiting 3-phosphoinositide-dependent protein kinase-1 activity in the human colon cancer HT-29 cell line.** *J Biol Chem* 2002, **277:**27613-27621.
51. Yip-Schneider MT, Sweeney CJ, Jung SH, Crowell PL, Marshall MS: **Cell cycle effects of nonsteroidal anti-inflammatory drugs and enhanced growth inhibition in combination with gemcitabine in pancreatic carcinoma cells.** *J Pharmacol Exp Ther* 2001, **298:**976-985.
52. Denkert C, Furstenberg A, Daniel PT, Koch I, Kobel M, Weichert W, Siegert A, Hauptmann S: **Induction of G0/G1 cell cycle arrest in ovarian carcinoma cells by the anti-inflammatory drug NS-398, but not by COX-2-specific RNA interference.** *Oncogene* 2003, **22:**8653-8661.
53. Goldberg Y, Nassif II, Pittas A, Tsai LL, Dynlacht BD, Rigas B, Shiff SJ: **The anti-proliferative effect of sulindac and sulindac sulfide on HT-29 colon cancer cells: alterations in tumor suppressor and cell cycle-regulatory proteins.** *Oncogene* 1996, **12:**893-901.
54. Toyoshima T, Kamijo R, Takizawa K, Sumitani K, Ito D, Nagumo M: **Inhibitor of cyclooxygenase-2 induces cell-cycle arrest in the epithelial cancer cell line via up-regulation of cyclin dependent kinase inhibitor p21.** *Br J Cancer* 2002, **86:**1150-1156.
55. Hung WC, Chang HC, Pan MR, Lee TH, Chuang LY: **Induction of p27(KIP1) as a mechanism underlying NS398-induced growth inhibition in human lung cancer cells.** *Mol Pharmacol* 2000, **58:**1398-1403.
56. Ben-Av P, Crofford LJ, Wilder RL, Hla T: **Induction of vascular endothelial growth factor expression in synovial fibroblasts by prostaglandin E and interleukin-1: a potential mechanism for inflammatory angiogenesis.** *FEBS Lett* 1995, **372:**83-87.
57. Seno H, Oshima M, Ishikawa TO, Oshima H, Takaku K, Chiba T, Narumiya S, Taketo MM: **Cyclooxygenase 2- and prostaglandin E(2) receptor EP(2)-dependent angiogenesis in Apc(Delta716) mouse intestinal polyps.** *Cancer Res* 2002, **62:**506-511.
58. Chu J, Lloyd FL, Trifan OC, Knapp B, Rizzo MT: **Potential involvement of the cyclooxygenase-2 pathway in the regulation of tumor-associated angiogenesis and growth in pancreatic cancer.** *Mol Cancer Ther* 2003, **2:**1-7.
59. Shirakawa K, Wakasugi H, Heike Y, Watanabe I, Yamada S, Saito K, Konishi F: **Vasculogenic mimicry and pseudo-comedo formation in breast cancer.** *Int J Cancer* 2002, **99:**821-828.
60. Tsujii M, Kawano S, Tsuji S, Sawaoka H, Hori M, DuBois RN: **Cyclooxygenase regulates angiogenesis induced by colon cancer cells.** *Cell* 1998, **93:**705-716.
61. Moore RJ, Zweifel BS, Heuvelman DM, Leahy KM, Edwards DA, Woerner BM, Ornberg RL, Seibert K, Koki AT, Masferrer JL: **Enhanced antitumor activity co-administration of celecoxib and the chemotherapeutic agents cyclophosphamide and 5-fu.** *Proceedings of the American Association for Cancer Research: 1–5 April 2000. Cadmus Journal Services, Linthicum, MD. USA. Abstract 2600* :409.
62. Kishi K, Petersen S, Petersen C, Hunter N, Mason K, Masferrer JL, Tofilon PJ, Milas L: **Preferential enhancement of tumor radioresponse by a cyclooxygenase-2 inhibitor.** *Cancer Res* 2000, **60:**1326-1331.
63. Torrance CJ, Jackson PE, Montgomery E, Kinzler KW, Vogelstein B, Wissner A, Nunes M, Frost P, Discafani CM: **Combinatorial chemoprevention of intestinal neoplasia.** *Nat Med* 2000, **6:**1024-1028.
64. Soslow RA, Dannenberg AJ, Rush D, Woerner BM, Khan KN, Masferrer J, Koki AT: **COX-2 is expressed in human pulmonary, colonic, and mammary tumors.** *Cancer* 2000, **89:**2637-2645.

Available online at www.sciencedirect.com
ScienceDirect
Vaccine 25 (2007) 1607–1618
Vaccine
www.elsevier.com/locate/vaccine

MUC1-specific immune therapy generates a strong anti-tumor response in a MUC1-tolerant colon cancer model

P. Mukherjee [a,*], L.B. Pathangey [a], J.B. Bradley [a], T.L. Tinder [a], G.D. Basu [a], E.T. Akporiaye [b], S.J. Gendler [a]

[a] *Mayo Clinic College of Medicine, Mayo Clinic Arizona, 13400 E. Shea Boulevard, Scottsdale, AZ 85259, United States*
[b] *Department of Immunobiology and Arizona Cancer Center, University of Arizona, Tucson, AZ 85724, United States*

Received 20 September 2006; received in revised form 27 October 2006; accepted 2 November 2006
Available online 16 November 2006

Abstract

A MUC1-based vaccine was used in a preclinical model of colon cancer. The trial was conducted in a MUC1-tolerant immune competent host injected with MC38 colon cancer cells expressing MUC1. The vaccine included: MHC class I-restricted MUC1 peptides, MHC class II-restricted pan-helper-peptide, unmethylated CpG oligodeoxynucleotide, and granulocyte macrophage-colony stimulating factor. Immunization was successful in breaking MUC1 self-tolerance, and in eliciting a robust anti-tumor response. The vaccine stimulated IFN-γ-producing $CD4^+$ helper and $CD8^+$ cytotoxic T cells against MUC1 and other undefined MC38 tumor antigens. In the prophylactic setting, immunization caused complete rejection of tumor cells, while in the therapeutic regimen, tumor burden was significantly reduced.

Keywords: MUC1; CpG ODN; GM-CSF; Colon cancer

1. Introduction

Colorectal cancer is the third most common malignancy in the US with 75% of cases diagnosed early and treated effectively with surgery, chemotherapy, radiation therapy, or a combination of these modalities. However, 25% of patients that present with metastatic disease have a 5-year survival of only 10%. Complications from metastatic disease are the leading causes of cancer-related deaths. In recent years there has been great interest in cancer vaccines, which have the potential of controlling metastatic disease, prolonging time to recurrence, and ultimately serving as a preventive measure. MUC1 (CD227) is a membrane-tethered mucin glycoprotein expressed on the apical surfaces of normal glandular epithelia and it is over expressed and aberrantly glycosylated in >70% of human colon cancer [1–3]. Recent description of MUC1 as a target for cytotoxic T lymphocytes (CTLs) has raised interest in using this protein as a target for immunotherapy [4–14]. Several preclinical and clinical trials targeting the tumor associated MUC1 antigen have elicited strong anti-tumor CTLs [1,2,12,14–24]. Importantly, there have been several reports of two HLA-A2 binding peptides derived from the MUC1 protein [25–27]. MUC1-specific CTLs have also been induced in vivo after vaccination of breast, ovarian, and metastatic renal cancer patients with peptide-pulsed dendritic cells (DCs) [16,28,29]. However, these approaches have generated only modest and infrequent clinical responses. One reason may be that traditionally, cancer-specific vaccines have focused on the activation of the $CD8^+$ CTLs, often involving direct stimulation of immunity using HLA-class I binding peptide epitopes. Recently it has become clear that activation of the CTL immune effector arm alone is insufficient to mediate an effective anticancer response. A major problem is that $CD8^+$ T cells alone cannot be sustained without the concomitant activation of $CD4^+$ T helper (Th) cells. In fact, it is now widely

* Corresponding author at: Biochemistry and Molecular Biology, Cellular Immunology, Mayo Clinic College of Medicine, 13400 E. Shea Blvd., Scottsdale, AZ 85259, United States. Tel.: +1 480 301 6327; fax: +1 480 301 7017.
E-mail address: mukherjee.pinku@mayo.edu (P. Mukherjee).

0264-410X/$ – see front matter © 2006 Elsevier Ltd. All rights reserved.
doi:10.1016/j.vaccine.2006.11.007

recognized that the Th cell regulates nearly all aspects of the adaptive immune response [30]. In addition, Th cells can recruit the innate immune system during immune augmentation. Therefore, the focus of the immune response in cancer has shifted away from activating CTL immunity alone to activating Th cell immunity concurrently with CTLs. In this study, in addition to the MHC class I MUC1 epitopes, we have utilized a MHC class II pan T helper peptide, TPPAYRPPNAPIL, derived from the hepatitis B virus core antigen sequence that is capable of activation of Th cells [30]. This vaccine formulation achieves an effective anti-tumor immunity.

In addition to the peptide vaccine, we have used adjuvants that include synthetic oligonucleotides containing CpG motifs and GM-CSF. CpG ODN are recognized by cells of the innate immune system through the Toll-like receptor 9 (TLR9), leading to potent stimulation of both the innate and the adaptive immune responses [31–33]. The net effect of TLR9 activation is to induce Th1 biased cellular and humoral effector functions with strong CTL generation [33]. In murine models of cancer and in phase I/II clinical trials in patients with metastatic melanoma and non-small cell lung cancer, CpG ODN has improved tumor responses to conventional therapies such as chemotherapy, radiotherapy, and immunotherapy [34–41]. GM-CSF is a commercially available cytokine currently used in patients undergoing chemotherapy to shorten the duration of post-chemotherapy neutropenia. Recently published evidence also suggests that GM-CSF plays an important role as an immune adjuvant [42,43]. The following observations illustrate the mechanisms by which GM-CSF can potentiate the immunogenicity of an antigen: (1) GM-CSF is a key mediator of DC maturation and function [44]; (2) GM-CSF increases surface expression of class I and II MHC molecules as well as co-stimulatory molecules of DCs in vitro [44]; (3) GM-CSF enhances antibody responses to known immunogens in vivo [45]; (4) tumor cells transfected with genes encoding/expressing GM-CSF are able to induce long lasting, specific anti-tumor immune responses in vivo [46]; (5) GM-CSF encapsulated in biodegradable microspheres mixed with whole tumor cells resulted in systemic anti-tumor immune responses comparable to those of GM-CSF transfected tumor cells [47]. Addition of GM-CSF to a peptide vaccine has been successfully utilized in patients with metastatic melanoma [48]. Thus, GM-CSF was included in our MUC1-peptide vaccine formulation with the expectation that it would enhance immunogenicity of the peptides. Based on existing data suggesting the potent immune adjuvant properties of CpG ODN and GM-CSF, we elected to test the efficacy of both these agents in the setting of a MUC1/pan T helper peptide vaccine immunization in a MUC1-tolerant colon cancer mouse model. To optimally enhance the antigenicity, the peptides and immune adjuvants were delivered emulsified in incomplete Freund's adjuvant (IFA). In addition, the local inflammatory properties of IFA may play an important role in attracting antigen presenting cells to the site of injection [49,50].

Herein we present results of the vaccination strategy containing MHC class I-binding MUC1 peptides along with a MHC class II-binding pan-helper-peptide and adjuvants in a colon cancer mouse model. Subcutaneous tumors were elicited by injecting the syngeneic MC38 colon cancer cell line expressing full-length human MUC1 into human MUC1.Tg mice. These mice exhibit T and B cell tolerance and are immune competent [51]. Both clinical and immunological responses were achieved in the preclinical study with induction of Th cells and CTLs against MUC1 and other undefined tumor antigens presented by the MC38 colon cancer cells.

2. Materials and methods

2.1. Tumor generation

MC38 colon cancer cells transfected with full-length human MUC1 (MC38.MUC1) or empty vector containing the neomycin resistance gene (MC38.neo) were maintained in DMEM medium supplemented with 10% fetal calf serum (FCS), 100 U of penicillin, 0.1 μg of streptomycin, 2 mM L-glutamine, 1% Na-pyruvate, 1% non-essential amino acids and 150 ug/ml G418. Cells were maintained in log phase at 37 °C with 5% CO_2. Eight to 10-week-old MUC1.Tg mice were injected subcutaneously in the left flank with 1×10^6 MC38 colon cancer cells in 100 μl of PBS. For prophylactic experiments, MC38 cells were injected 7 days after the first immunization (Fig. 1A). For therapeutic experiments, tumors were allowed to grow for 7 days prior to the first immunization (Fig. 1B).

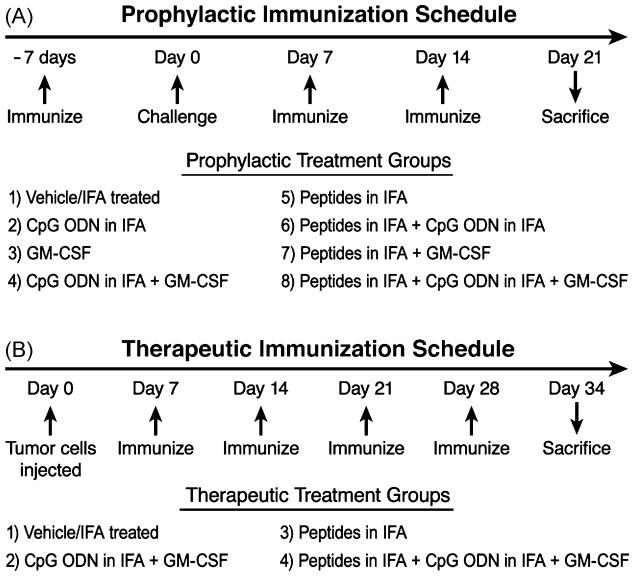

Fig. 1. Schematic representation of the experimental design: (A) prophylactic study and (B) therapeutic study.

2.2. Vaccination strategy

The vaccine included: (a) two MHC class I-restricted MUC1 peptides, APGSTAPPA (100 μg) and SAPDTRPAP (100 μg); (b) one MHC class II helper peptide TPPAYRPPNAPIL (140 μg) (hepatitis B virus core antigen sequence 128–140 [52]); (c) mouse unmethylated CpG oligodeoxynucleotide constructs (CpG ODN, (100 μg) Coley Pharmaceuticals, Canada); (d) granulocyte macrophage-colony stimulating factor (GM-CSF, 10,000 units or 2 μg, Cell Sciences, Canton, MA). All peptides and adjuvants were emulsified in IFA and administered subcutaneously at a site away from the tumor injection. Schematic representation of the treatment schedules for the prophylactic and therapeutic studies are shown in Fig. 1.

2.3. Tumor palpation

Mice were palpated every day starting at day 7 post-tumor cell injection until sacrifice. At time of sacrifice, tumors in the vehicle-treated mice were approximately 1 g in weight and were well-vascularized. MC38.MUC1 tumors stained positive for human MUC1 and MC38.neo tumors were negative by immunohistochemistry (data not shown). Palpable tumors were measured by calipers and tumor weight was calculated according to the formula: grams = (length in cm) × (width)^2/2 [53]. In accordance with IACUC regulations, all surviving mice were sacrificed when tumors reached 10% of body weight. Mice were carefully observed for signs of ill health, including lethargy, abdominal distention, failure to eat or drink, marked weight loss and hunched posture.

2.4. IFN-γ ELISPOT assay

From the tumor draining lymph nodes (TDLNs), CD4$^+$ and CD8$^+$ T cells were isolated using the magnetic activated cell sorter (MACS, Miltenyi Biotech, Auburn, CA). IFN-γ ELISPOT assay was performed using capture IFN-γ antibody as recommended by the manufacturer (Mabtech, Stockholm, Sweden). Autologous irradiated DCs pulsed with the immunizing peptides (class I-restricted H2-D^b binding APGSTAPPA + H2-K^b binding SAPDTRPAP + class II-restricted pan-helper-peptide TPPAYRPPNAPIL) were used as stimulator cells at a responder to stimulator ratio of 10:1. DCs were prepared according to the protocol published previously [10,54]. In some experiments, DCs were pulsed with either the MUC1 peptides or the helper peptide separately. Control wells contained T cells stimulated with DCs pulsed with irrelevant peptide (vesicular stomatitis virus peptide, RGYKYQGL). Spot numbers were determined using computer assisted video image analysis by Zellnet Consulting Inc. (FortLee, NJ). DCs pulsed with irrelevant peptides were used as control. Splenocytes from a C57BL/6 mice stimulated with concavalin A (Con A) was used as positive control (data not shown).

2.5. ^{51}Chromium (Cr)-release assay

Determination of CTL activity was performed using a standard ^{51}Cr-release method. Splenocytes, CD4$^+$ and CD8$^+$ T cells from TDLN served as effector cells. Autologous irradiated DCs pulsed with immunizing peptide were used as stimulator cells and co-incubated with the effector cells at an effector: stimulator ratio of 10:1 for 48 h. Effector cells were then recovered and incubated with ^{51}Cr-labeled tumor target cells at effector: target ratios of 100:1, 50:1, and 25:1. Target cells included MC38.MUC1, MC38.neo, B16.MUC1, and B16.neo cell lines. Epithelial tumor targets express low levels of MHC class I on the cell surface. Thus, target cells were treated with 5 ng/ml IFN-γ (Amersham, Piscataway, NJ) 1 day prior to the assay to up-regulate MHC class I surface expression and loaded with radioactivity (100 μCi ^{51}Cr (Amersham) per 10^6 target cells) for 3 h. Effectors and targets were co-incubated for 6 h. Radioactive ^{51}Cr released at the end of 6 h was determined using the Topcount Micro-scintillation Counter (Packard Biosciences, Shelton, CT). Specific lysis was calculated according to the following formula: (experimental cpms − spontaneous cpms/complete cpms − spontaneous cpms) × 100. Spontaneous ^{51}Cr release in all experiments was 10–15% of complete ^{51}Cr release.

3. Statistical analysis

Biostatisticians at the Mayo Clinic Biostatistics Core Facility conducted statistical analysis for all data. A two-factor ANOVA was used to generate significant differences between experimental groups. For the ELISPOT analysis, data were adjusted for operator (different days at which assays were conducted).

4. Results

4.1. Complete prevention of MC38.MUC1 tumor growth in MUC1.Tg mice immunized with the vaccine formulation

In a prophylactic setting, MC38.MUC1 or MC38.neo tumor cells (1 × 10^6 cells per mouse) were injected 7 days post-first immunization. Two more immunizations were administered at days 7 and 14 post-tumor challenge and mice were sacrificed on day 21 (Fig. 1A). We observed complete rejection of MC38.MUC1 tumors in MUC1.Tg mice receiving MUC1-specific immunization in combination with CpG ODN and GM-CSF ($p < 0.001$ compared to all other groups) (Fig. 2A). Tumor burden for all experimental groups is represented as percent of tumor burden in vehicle-treated mice. All eight mice in the peptide + adjuvant group remained tumor free. Mice in all other treatment groups developed tumor but with lower incidence and lower tumor weight compared to mice treated with vehicle (Fig. 2A, $p < 0.001$ for peptides,

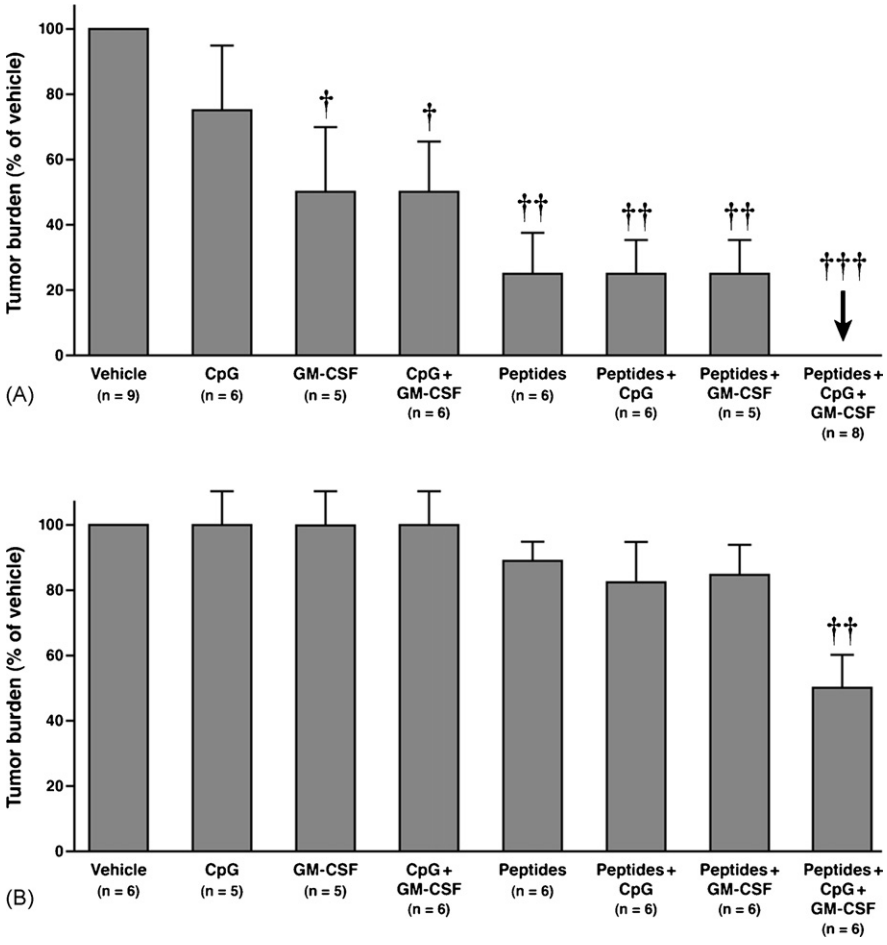

Fig. 2. (A) Complete inhibition of MC38.MUC1 colon cancer tumor cells in a MUC1.Tg mice post-peptide immunization. MUC1.Tg mice immunized with MUC1-based peptide vaccine in combination with pan-helper-peptide, GM-CSF and CpG ODN. Immunizations were given 1 week prior to tumor challenge with MC38.MUC1 cells followed by two boosts 1 week apart. Tumors were measured using digital calipers and final weight calculated as $(L \times W^2)/2$. Each point represents data from one mouse. The vehicle group was significantly different from the other groups ($p < 0.001$ compared to all other groups). Other significant differences were also determined ($p < 0.001$ for peptides, peptides + CpG ODN and peptides + GM-CSF groups compared to vehicle; $p < 0.04$ for GM-CSF and CpG + GM-CSF groups compared to vehicle). (B) Reduced tumor burden of MC38.neo colon cancer tumor cells in a MUC1.Tg model post-peptide immunization. MUC1.Tg mice immunized with MUC1-based peptide vaccine in combination with pan-helper-peptide, GM-CSF and CpG ODN. Immunizations were given 1 week prior to tumor challenge with MC38.MUC1 cells followed by two boosts 1 week apart. Tumors were measured using digital calipers and final weight calculated as $(L \times W^2)/2$. Each point represents data from one mouse. Immunization with peptides + CpG ODN + GM-CSF was successful in significantly but partially reducing MC38.neo tumor growth in MUC1.Tg mice ($p < 0.01$ compared to all other groups). $^{\dagger}p < 0.04$, $^{\dagger\dagger}p < 0.01$, $^{\dagger\dagger\dagger}p < 0.001$.

peptides + CpG ODN and peptides + GM-CSF groups compared to vehicle; $p < 0.04$ for GM-CSF and CpG + GM-CSF groups compared to vehicle). Mice treated with CpG ODN alone was the only group that did not show lower tumor burden compared to vehicle-treated mice. Four of the eight mice in the full treatment group (peptide + GM-CSF + CpG ODN) were re-challenged with MC38.MUC1 tumor cells 2 months post-primary vaccination. All four mice rejected the tumor cells, suggesting a strong memory response against MC38.MUC1 cells (data not shown).

4.2. Partial effect of the vaccine on MC38.neo tumor growth in MUC1.Tg mice

Interestingly, the immunization strategy with peptides + CpG ODN + GM-CSF was also successful in partially reducing MC38.neo tumor growth in MUC1.Tg mice (Fig. 2B, $p < 0.01$ compared to all other groups), presumably due to an immune response elicited by the pan-helper-peptide immunization, CpG ODN and GM-CSF. Mice in all other treatment groups had slightly lower tumor weights but were not significantly different from mice treated with vehicle (Fig. 2B). Thus, the vaccine formulation not only elicited a MUC1-specific immune response but also an MC38 tumor-specific immune response.

4.3. In vivo stimulation of IFN-γ-producing $CD4^+$ helper T cells and $CD8^+$ cytotoxic T cells in MUC1.Tg mice immunized with the vaccine formulation

To elucidate the mechanism of anti-tumor response, $CD4^+$ and $CD8^+$ T cells were isolated from lymph nodes

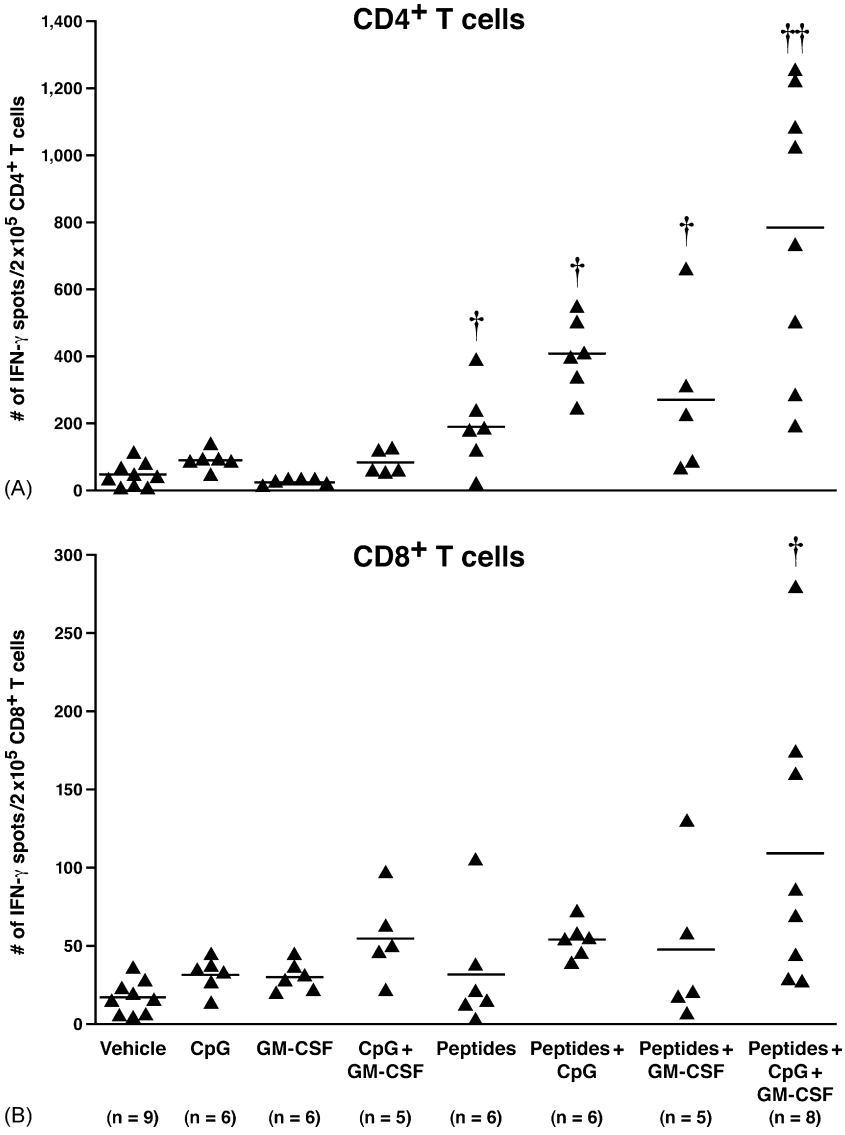

Fig. 3. Induction of IFN-γ production by $CD4^+$ and $CD8^+$ T cells in response to MUC1 and pan-helper-peptides, which was enhanced by GM-CSF and CpG ODN in MC38.MUC1 challenged mice. At sacrifice, $CD4^+$ and $CD8^+$ T cells were sorted from lymph nodes. Cells were stimulated for 24 h with irradiated DCs pulsed with the immunizing peptides on an ELISPOT plate. Each point represents data from one mouse. (A) Number of IFN-γ spots in $CD4^+$ T cells: a significant increase was noted in peptides + CpG ODN and peptides + CpG ODN + GM-CSF groups compared to the vehicle group ($p < 0.05$ for peptides + CpG ODN, and $p < 0.001$ for peptides + CpG ODN + GM-CSF). (B) Number of IFN-γ spots in $CD8^+$ T cells: the only group that showed significant increase in IFN-γ producing $CD8^+$ T cells were mice treated with peptides + adjuvants compared to mice treated with vehicle ($p < 0.05$). $^{\dagger\dagger}p < 0.001$, $^{\dagger}p < 0.05$ compared to vehicle treatment. Note that the *y*-axes differ in (A) and (B).

of immunized and non-immunized mice and analyzed for MUC1-specific IFN-γ spot formation (ELISPOT). $CD4^+$ and $CD8^+$ T cells were stimulated overnight with syngeneic DCs pulsed with the three immunizing peptides. In the MC38.MUC1 challenged mice, both IFN-γ-producing $CD4^+$ and $CD8^+$ T cells were observed (Fig. 3A and B). An irrelevant peptide, vesicular stomatitis virus peptide (RGYKYQGL, VSV $NP_{52–59}$) showed numbers of spots similar to vehicle (data not shown). Compared to $CD4^+$ T cells, we observed lower numbers of IFN-γ spot-forming $CD8^+$ T cells (Fig. 3A and B, note the difference in scale for the *y*-axis). A strong $CD4^+$ helper T cell response was elicited, possibly due to the presence of the pan-helper-peptide and CpG ODN, both known to target the $CD4^+$ helper T cell population [33,55–57]. A significant increase in IFN-γ-producing $CD4^+$ T cells was noted in peptide + CpG ODN and peptide + CpG ODN + GM-CSF groups compared to the vehicle group ($p < 0.05$ for peptides + CpG ODN, and $p < 0.001$ for peptides + CpG ODN + GM-CSF). The only group that showed significant increase in IFN-γ-producing $CD8^+$ T cells were mice treated with peptides + both adjuvants compared to mice treated with vehicle and all other groups including the adjuvants alone group ($p < 0.05$). We therefore selected to confirm the ELISPOT data with an in vitro CTL assay only from the two groups (vehicle versus peptides + adjuvants). Tumor targets were MC38.MUC1 and

MC38.neo tumor cells and effectors were either splenic T cells, or sorted $CD4^+$ or $CD8^+$ T cells from TDLNs. Compared to vehicle-treated mice, splenic T cells from mice immunized with peptides + adjuvants showed the highest CTL activity against MC38.MUC1 targets (data not shown). Moderate levels of CTL activity were also observed with MC38.neo target cells, suggesting that the immunization elicited CTLs not only against MUC1 tumor antigen but also against other unknown MC38 tumor antigens (data not shown). This result substantiates the moderate decrease in tumor burden observed with the immunization in the MC38.neo challenged mice (Fig. 2B).

In the MC38.neo challenged mice, immunization stimulated the $CD4^+$ T cells to produce IFN-γ in all groups compared to vehicle. However, significantly higher spot formation was detected in the groups treated with peptides + CpG ODN and peptides + CpG ODN + GM-CSF ($p < 0.05$ and $p < 0.01$, respectively). These groups were also significantly different from adjuvants alone or peptide alone groups suggesting the important role of pan-helper-peptide and CpG ODN. GM-CSF by itself did not have much effect. The $CD8^+$ T cells showed only modest increase in spot formation with no statistical significance between groups (Fig. 4A and B). The modest increase is once again due to the adjuvants (particularly CpG ODN), since groups that received CpG ODN in the vaccine formulation showed increased spot formation. The data suggest that the pan-helper-peptide + CpG ODN can elicit a reasonable immune response against MC38 tumor cells and mount a partial anti-tumor response regardless of the presence of MUC1 antigen. Furthermore, the data imply that both adjuvants administered with the peptide vaccination may be better than one adjuvant alone in eliciting a robust anti-tumor response (Fig. 2). It should be noted that in Fig. 4, the mice were challenged with MC38.neo cells and not MC38.MUC1 cells; therefore, there is no MUC1-specific response but the response is due to the adjuvants and helper peptide. If you compare Fig. 4 with Fig. 3 (in which the mice were challenged with MC38.MUC1 cells), there is a significant increase in the $CD8^+$ T cell response with peptides + adjuvants versus all

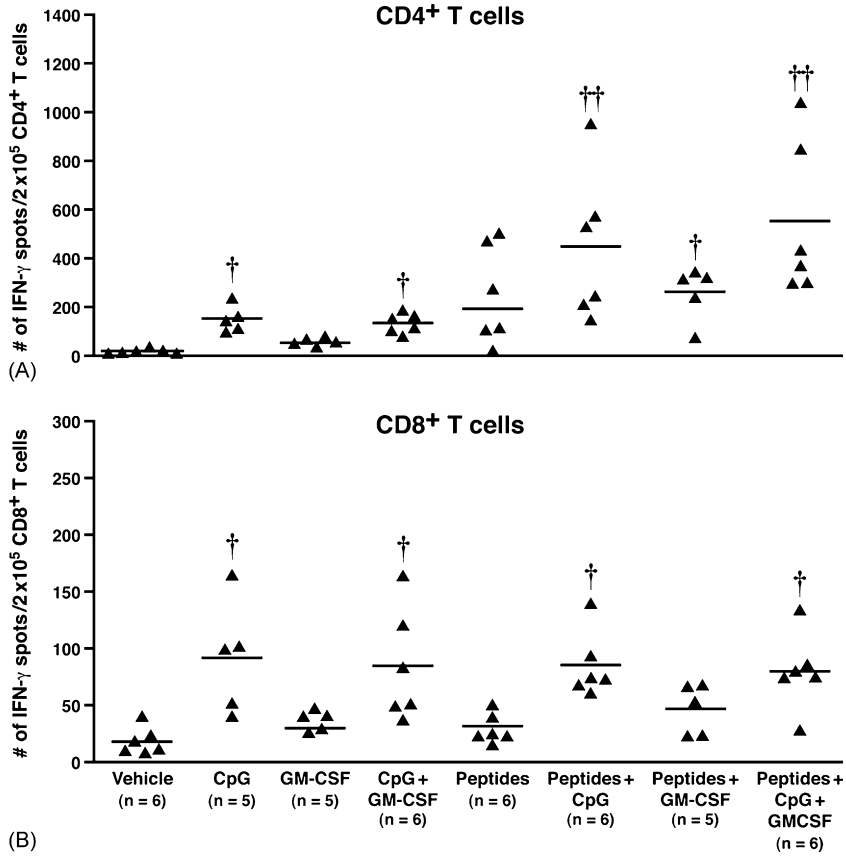

Fig. 4. Induction of IFN-γ production by $CD4^+$ but not $CD8^+$ T cells in response to MUC1 and pan-helper-peptides, was enhanced by GM-CSF and CpG ODN in MC38.neo challenged mice. At sacrifice, $CD4^+$ and $CD8^+$ T cells were sorted from lymph nodes. Cells were stimulated for 24 h with irradiated DCs pulsed with the immunizing peptides on an ELISPOT plate. Each point represents data from one mouse. (A) Number of IFN-γ spots in $CD4^+$ T cells: significantly higher spot formation was detected in the groups treated with peptides + CpG ODN and peptides + CpG ODN + GM-CSF ($p < 0.05$ and $p < 0.01$, respectively). These groups were also significantly different from adjuvants alone or peptide alone groups ($p < 0.05$). (B) Number of IFN-γ spots in $CD8^+$ T cells: a modest increase in spot formation was noted with no statistical significance between groups. $^{\dagger\dagger}p < 0.01$, $^{\dagger}p < 0.05$ compared to vehicle treatment. Note that the *y*-axis differs in (A) and (B).

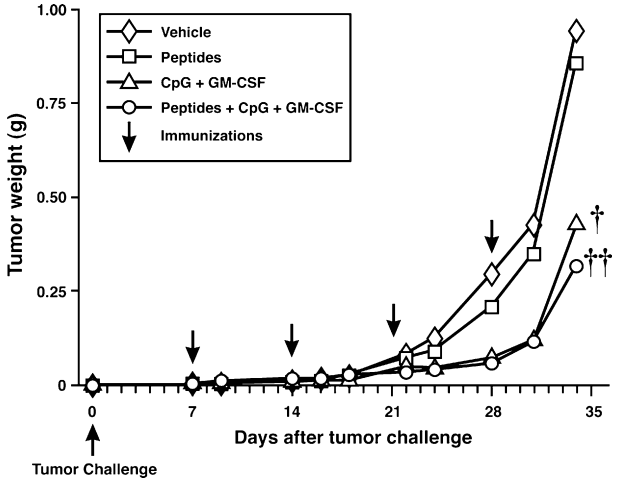

Fig. 5. MUC1 peptide vaccine significantly reduced burden of established MC38.MUC1 tumors in MUC1.Tg mice. Tumors were established for 7 days by subcutaneous injection of MC38.MUC1 cells (1×10^6) into the flanks of MUC1.Tg mice. Tumor-bearing mice were immunized weekly with MUC1-based peptide vaccine in combination with pan-helper-peptide, CpG ODN and GM-CSF. Tumors were measured (cm) and final weight (gm) calculated as $(L \times W^2)/2$. A significant reduction in tumor growth was observed in the vaccine treatment compared to vehicle control or peptide alone ($^{\dagger\dagger}p = 0.003$). The adjuvants alone (CpG ODN + GM-CSF) also showed a significant reduction in tumor burden compared to vehicle or peptides only ($^{\dagger}p = 0.01$).

other groups, suggesting that the response is clearly MUC1 peptide-specific.

4.4. Significant reduction in established MC38.MUC1 tumors in MUC1.Tg mice immunized with the vaccine formulation

To test the efficacy of the vaccine formulation in a therapeutic setting, MC38.MUC1 tumor cells (1×10^6 cells/mouse) were established in MUC1.Tg mice for 7 days. Tumors were well-vascularized and palpable by this time. Immunization was administered on days 7, 14, 21, and 28 post-tumor injection and mice were sacrificed on day 34 (Fig. 1B). We opted to conduct the therapeutic part of the study using MC38.MUC1 tumor cells with four groups of mice. The experimental groups included: (a) peptides + CpG ODN + GM-CSF, (b) peptides, (c) CpG ODN + GM-CSF, and (d) vehicle. A significant reduction in tumor growth was observed in the group treated with peptides + adjuvants compared to mice treated with vehicle (Fig. 5, $p = 0.003$). Although tumor burden in the peptide alone group was not significantly different from the control ($p = 0.12$), the adjuvants alone group (GM-CSF + CpG ODN) showed a significant reduction in tumor burden as compared to vehicle ($p = 0.011$), suggesting that the adjuvants were strong enough to cause a reduction in tumor burden even without the tumor associated antigen (TAA)-specific peptides. The MUC1 peptide vaccine did not significantly affect the growth of the established MC38.neo tumors compared to peptides alone or adjuvants (data not shown).

4.5. Immunization elicited a strong IFN-γ response in CD4$^+$ T cells isolated from mice bearing established MC38.MUC1 tumors

At sacrifice, CD4$^+$ and CD8$^+$ T cells were sorted from TDLNs. Cells were stimulated for 24 h with irradiated DCs pulsed with the immunizing peptides on an ELISPOT plate. To delineate the effect of the MUC1 peptide from the pan-helper-peptide, the DCs were pulsed with either the MUC1 peptides, or the pan-helper-peptide or both. Compared to the vehicle-treated group, CD4$^+$ T cells from mice treated with adjuvants, peptides, or peptides + adjuvants showed significantly increased IFN-γ spot formation (Fig. 6A, $p < 0.02$ for adjuvants, $p < 0.001$ for peptides and $p < 0.001$ for peptides + adjuvants). Significant differences were also achieved between adjuvants and peptides groups ($p < 0.001$ except for the DCs pulsed with MUC1 peptide arm) and between adjuvants and peptides + adjuvant group ($p < 0.001$). Similarly a significant difference was noted between peptides and peptides + adjuvants groups in all three DC arms ($p < 0.001$). Thus, an additive effect of adjuvants + peptides is detected in the IFN-γ-producing CD4$^+$ T cell parameter with our immunization strategy in a therapeutic setting. As can be appreciated from Fig. 6A, IFN-γ production in the CD4$^+$ T cells was stimulated primarily by the pan-helper-peptide since there was no difference in spot formation between DCs stimulated with pan-helper-peptide alone or pan-helper-peptide + MUC1 peptide in any of the experimental groups. DCs pulsed with MUC1 peptide alone showed significantly lower spot formation than DCs pulsed with pan-helper-peptide in mice treated with peptides or peptides + adjuvants ($p < 0.001$), once again confirming that the pan-helper-peptide is the main stimulator of IFN-γ production by CD4$^+$ T cells. CD8$^+$ T cells showed modest albeit significant increase in IFN-γ production in the adjuvants group as well as in the peptides + adjuvants group compared to the vehicle regardless of the peptides used to pulse the DCs (Fig. 6B, $p = 0.02$). The peptides group did not show significant difference in IFN-γ-spot formation compared to vehicle and like the vehicle group, showed significantly lower spot formation than the other two groups (adjuvants alone or peptides + adjuvants, $p = 0.02$) except for the DCs pulsed with pan-helper-peptide alone arm ($p = 0.6$, Fig. 6B), suggesting that the CD8$^+$ T cells were less influenced by the pan-helper-peptides compared to the CD4$^+$ T cells. Thus, the immunization strategy stimulated a strong CD4$^+$ IFN-γ-producing T cell response primarily to the pan-helper-peptide.

4.6. Immunization elicited CTLs against MC38 and MUC1 tumor antigens in mice bearing established MC38.MUC1 tumors

Although the CD8$^+$ T cells did not produce much IFN-γ in the ELISPOT assay, we determined if splenic T cells from immunized mice showed lytic activity against the tumor, since we did observe a significant decrease in the tumor bur-

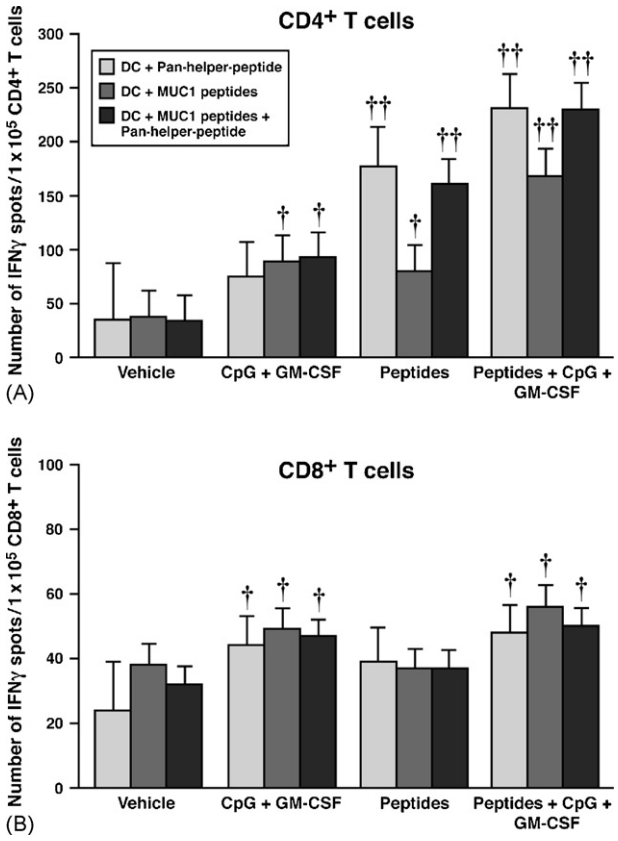

Fig. 6. IFN-γ production by $CD4^+$ T cells was induced in response to pan-helper-peptides, which was enhanced by CpG ODN and GM-CSF. At sacrifice, $CD4^+$ and $CD8^+$ T cells were sorted from TDLN. Cells were stimulated for 24 h with irradiated DCs pulsed with the immunizing peptides on an ELISPOT plate. (A) Number of IFN-γ spots from $CD4^+$ T cells: compared to vehicle-treated, mice treated with adjuvants, peptides, or peptides + adjuvants showed significantly increased IFN-γ spot formation ($p < 0.02$ for adjuvants, $p < 0.001$ for peptides and $p < 0.001$ for peptides + adjuvants). Significant differences were also achieved between adjuvants and peptides group ($p < 0.001$ except for the DCs pulsed with the MUC1 peptide arms) and between adjuvants and peptides + adjuvant groups ($p < 0.001$). Significant differences were noted between peptides and peptides + adjuvants group in all three DC arm ($p < 0.001$). (B) Number of IFN-γ spots from $CD8^+$ T cells: there was a significant increase in IFN-γ production in the adjuvants group as well as in the peptides + adjuvants group compared to the vehicle regardless of the peptides used to pulse the DCs ($p = 0.02$). The peptides group did not show significant difference in IFN-γ-spot formation compared to vehicle but showed significantly lower spot formation than the other two groups (adjuvants alone or peptides + adjuvants, $p = 0.02$) except for the DCs pulsed with pan-helper-peptide alone ($p = 0.6$). $^{\dagger}p \leq 0.02$, $^{\dagger\dagger}p < 0.001$ compared to vehicle. Note that *y*-axis differs in (A) and (B).

den with immunization (Fig. 5). To further establish if the CTLs were specific against MUC1 and/or the tumor cell itself, we utilized two different tumor cell targets, one specific for the immunized mice, MC38 colon cancer cells, and the other, an irrelevant melanoma cell line, namely, B16. Both cell lines expressed either full-length MUC1 or empty vector (neo). The results are summarized in Fig. 7. When B16 cells were utilized as the target, the CTLs were lytic only against the cells that expressed MUC1 but not against B16.neo ($p < 0.001$). Note that there is no cytolysis from mice immunized with vehicle or adjuvants alone when B16 was used as the target. Lytic activity was only observed when mice were immunized with peptides alone ($p < 0.001$ compared to vehicle) or peptides + adjuvants ($p < 0.001$ compared to vehicle) confirming that the immunization elicited CTLs specifically against the MUC1 antigen and not against a non-specific tumor cell. In contrast, when MC38 cells were used as targets, the lytic activity was not only against the MC38.MUC1 but also against MC38.neo cells ($p < 0.001$ for all experimental groups compared to the vehicle group). Another important data that emerged from this experiment was that mice treated with adjuvants alone elicited a cytolytic response against the MC38 tumors regardless of whether MUC1 was expressed or not. These results explain clearly the lower tumor burden in the adjuvants group as well as begin to explain the anti-tumor effect on MC38.neo tumors (Fig. 2). The peptides alone group generated CTLs only against the MC38.MUC1 but not against MC38.neo ($p < 0.001$ between MC38.MUC1 and MC38.neo targets). Mice treated with vehicle showed no lytic activity against any tumor target.

5. Discussion

Although MUC1-based immunotherapy has been able to induce MUC1-specific CTL responses in a substantial number of cancer patients, the response has not been long lasting, and has mostly remained without a significant clinical response. We hypothesize that this may be because less focus has been given to the generation of Th cells that are required to sustain a long-lasting anti-tumor response. We have developed a MUC1-based vaccine strategy that generates a robust $CD4^+$ Th cell response with sustained antigen-specific $CD8^+$ CTL response that clearly translated to a successful anti-tumor response. The vaccine consisted of peptides derived from MHC class I-restricted MUC1 epitopes and MHC class II-restricted pan-helper T cell epitope. CpG ODN and GM-CSF were used as adjuvants. The vaccine was tested both in a prophylactic and a therapeutic setting in an appropriate mouse model of MUC1 tolerance. The MUC1.Tg mice were challenged with MC38 colon cancer cell lines transfected with full-length human MUC1 (MC38.MUC1) or empty vector containing the neomycin resistance gene (MC38.neo). In the prophylactic setting, the vaccine specifically caused rejection of the MC38.MUC1 tumors but not the MC38.neo tumors, although a 50% reduction in tumor burden was observed in these tumors (Fig. 2). This apparently was due to the robust $CD4^+$ Th cell response elicited by the pan-helper-peptide and the adjuvants, CpG ODN and GM-CSF, present in the vaccine formulation (Fig. 4). This Th response facilitated the generation of a moderate $CD8^+$ CTL response accompanied by a modest anti-tumor response. In contrast, both the $CD4^+$ Th and $CD8^+$ CTL responses were highly significant in the immunized mice challenged with the MC38.MUC1 tumor cells compared to mice treated with vehicle (Fig. 3). This immune response translated to a significant anti-tumor

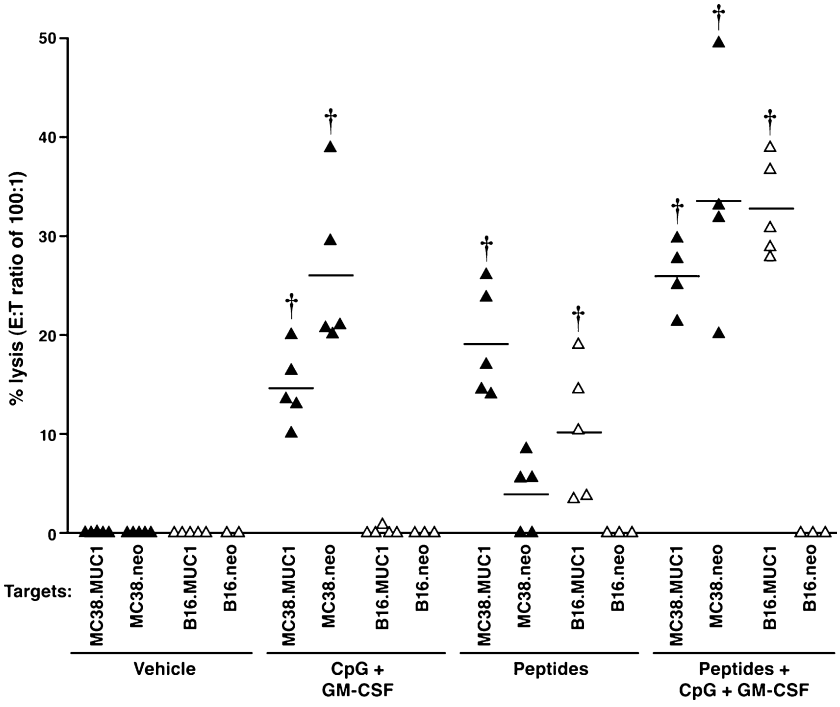

Fig. 7. Immunization with MUC1-peptide vaccine increased MUC1-specific CTL activity in mice with established MC38.MUC1 tumors. Effector cells (splenocytes) from immunized mice were subjected to a standard ^{51}Cr-release assay. Targets were MC38.MUC1, MC38.neo, B16.MUC1, and B16.neo cells. $N = 4$ to 6 mice per group. MC38 targets are designated with (▲) and B16 targets with (△). CTLs were lytic against the B16.MUC1 cells but not against B16.neo ($p < 0.001$). Note that there is no cytolysis from mice immunized with vehicle or adjuvants alone when B16 was used as the target. Lytic activity was only observed when mice were immunized with peptide alone ($p < 0.001$) or peptides + adjuvants ($p < 0.001$). With MC38 tumor targets, lytic activity was against MC38.MUC1 and MC38.neo cells ($p < 0.001$ for all experimental groups compared to the vehicle group). The peptides alone group generated CTLs only against the MC38.MUC1 but not against MC38.neo cells ($p < 0.001$). Mice treated with vehicle showed no lytic activity against any tumor target. $^{\dagger}p < 0.001$ compared to vehicle. E:T ratios of 100:1, 50:1 and 25:1 were conducted and titrations were observed. Due to multiple targets and multiple animals per experimental group, we selected to show E:T ratio of 100:1.

response (Fig. 2). Even more important is that the vaccination strategy generated a strong memory response against the MC38.MUC1 tumor cells, such that mice that were tumor free after primary immunization remained tumor free for months after re-challenge with the same MC38.MUC1 tumor cells (data not shown). Since the peptide vaccine was utilized in the study, we monitored the humoral response by testing for MUC1 antibody levels in the serum of immunized mice using a specific ELISA. The levels of MUC1 antibody were found to be below the detectable levels (data not shown). Similarly, we tested for Th1 versus Th2 cytokines in the T cell supernatant collected from the ELISPOT plates at 24 h post-stimulation with DCs pulsed with the immunizing peptide. Cytokine bead array (CBA) analysis revealed an increase in IFN-γ and TNF-α levels, although IL-4, IL-5 and IL-10 were undetectable (data not shown). Together, these data suggest a predominantly Th1-type cellular immune response with minimal Th2 response. This is not surprising since both CpG ODN and GM-CSF are known to promote a Th1-type response [48,49,55].

In the therapeutic setting, the vaccination was effective in significantly reducing the tumor burden compared to the vehicle or peptides alone treated groups (Fig. 5). To our surprise there was no significant difference between the adjuvant and the adjuvant + peptides group (Fig. 5), suggesting that the adjuvants alone were potent enough to cause a clinically significant anti-tumor response. This was most prominent in the therapeutic setting and was much less obvious in the prophylactic setting (compare Fig. 2A with Fig. 5). In fact, in the prophylactic setting the peptides alone group had a much more significant anti-tumor response than the adjuvants alone group. These data raise several questions regarding the differences in immune status of tumor-bearing mice versus non-tumor-bearing mice and how the two respond to the same vaccination. Tumor-bearing mice (in this case the mice in the therapeutic arm with 7-day established tumor) may have existing low-level anti-MUC1 or anti-MC38 responses, which were accentuated with the addition of the adjuvants. In the prophylactic setting the immunization was given prior to tumor challenge and therefore the response to the peptides was stronger than to the adjuvants alone. Thus, the global immune status of the host receiving the vaccination impacts greatly on the host's ability to generate CTL immune responses to the peptide vaccines. It is clear from the therapeutic study that CTLs were generated not only against MUC1 but also against other tumor antigens presented by the MC38 colon cancer cells (Fig. 7). This represents an important mechanism by which the immune system can effi-

ciently eliminate malignant cells and suggests the induction of epitope spreading.

Although patients with advanced colorectal cancer have thus far derived no substantial clinical benefit from peptide vaccination, we do not know enough regarding the global immune status of the patients to abandon our efforts in this direction. We agree with those who find it premature to give up on active cancer vaccines because much work remains [58–61]. For example, we must gain a better understanding of T cell functions, such as T cell avidity for tumor cells, T cell homing to the tumor site, durability of the T cell response, and activation of more than one effector mechanism.

To address the limitation of previous peptide-based therapeutic anti-tumor vaccine strategies and low clinical efficacy in the clinic, scientists have used several approaches to improve vaccine potency. These include selection of more immunogenic peptides, modifying naturally occurring peptides by increasing affinity to MHC class I molecules, combining peptides derived from multiple tumor associated antigens, combining MHC class I and class II binding peptides from the same antigen, and by using novel immune adjuvants. We have successfully combined the last two strategies and as a result increased the Th cell response and therefore the CTL response in our model system.

MUC1 occurs naturally as a heavily glycosylated protein which contains two well-known tumor associated carbohydrate antigens (TACA): the disaccharide Thomsen–Friedenreich (TF) antigen (β-Gal-(1 → 3)-α-GalNAc-*O*-serine/threonine and its precursor, the monosaccharide Tn (GalNAc-*O*-serine/threonine) [62,63]. TACA-containing glycopeptides are appealing CTL-based vaccines as they are widely expressed in a variety of tumors including colon cancer, their expression is largely tumor specific, they are induced early in neoplastic transformation, and they elicit a high affinity, degenerate carbohydrate-specific response [64]. Future studies will focus on generating glycosylated and/or anchor-improved MUC1 peptides that will have higher MHC binding and thus greater ability to activate T cells [65]. The idea that the glycopeptides from highly glycosylated proteins can serve as CTL-based vaccines has been pioneered by Olivera Finn (Vlad et al. [66]), Apostolopoulos et al. [67] and Franco and colleagues [52,64]. Eliciting immunity to the novel anchor-modified glycosylated MUC1 peptides may result in robust anti-tumor immunity and long-term immune memory.

Acknowledgements

This work was supported by the SPORE in Gastrointestinal Cancers NIH P50 CA95060 and by the Mayo Foundation. We would like to thank Drs. D. Kufe and J. Schlom for providing the MC38.MUC1 and MC38.neo cell lines. We also thank Marvin Ruona in the Visual Communications core for preparing the figures in the correct format, Irene Beauvais for her assistance in submitting the manuscript, Dr. Joe Hentz and Noble Brie in the Biostatistics core for performing the statistical analysis and all technicians in the animal core facility for help in maintaining our mice.

References

[1] Zotter S, Hageman PC, Lossnitzer A, Mooi WJ, Hilgers J. Tissue and tumor distribution of human polymorphic epithelial mucin. Cancer Rev 1988;11–12:55–101.
[2] Croce MV, Isla-Larrain MT, Rua CE, Rabassa ME, Gendler SJ, Segal-Eiras A. Patterns of MUC1 tissue expression defined by an anti-MUC1 cytoplasmic tail monoclonal antibody in breast cancer. J Histochem Cytochem 2003;51(6):781–8.
[3] Girling A, Bartkova J, Burchell J, Gendler S, Gillet C, Taylor-Papadimitriou J. A core protein epitope of the polymorphic epithelial mucin detected by the monoclonal antibody SM-3 is selectively exposed in a range of primary carcinomas. Int J Cancer 1989;43:1072–6.
[4] Domenech N, Henderson RA, Finn OJ. Identification of an HLA-A11-restricted epitope from the tandem repeat domain of the epithelial tumor antigen mucin. J Immunol 1995;155(10):4766–74.
[5] Agrawal B, Reddish MA, Longenecker BM. In vitro induction of MUC-1 peptide-specific type 1 T lymphocyte and cytotoxic T lymphocyte responses from healthy multiparous donors. J Immunol 1996;157(5):2089–95.
[6] Apostolopoulos V, Haurum JS, McKenzie IFC. Muc1 peptide epitopes associated with five different H-2 class I molecules. Eur J Immunol 1997;27(10):2579–87.
[7] Apostolopoulos V, Karanikas V, Haurum JS, McKenzie IF. Induction of HLA-A2-restricted CTLs to the mucin 1 human breast cancer antigen. J Immunol 1997;159(11):5211–8.
[8] Reddish M, MacLean GD, Koganty RR, Kan-Mitchell J, Jones V, Mitchell MS, et al. Anti-MUC1 class I restricted CTLs in metastatic breast cancer patients immunized with a synthetic MUC1 peptide. Int J Cancer 1998;76(6):817–23.
[9] Mukherjee P, Ginardi AR, Madsen CS, Sterner CJ, Adriance MC, Tevethia MJ, et al. Mice with spontaneous pancreatic cancer naturally develop MUC1-specific CTLs that eradicate tumors when adoptively transferred. J Immunol 2000;165(6):3451–60.
[10] Mukherjee P, Madsen CS, Ginardi AR, Tinder TL, Jacobs F, Parker J, et al. Mucin 1-specific immunotherapy in a mouse model of spontaneous breast cancer. J Immunother 2003;26(1):47–62.
[11] Mukherjee P, Ginardi AR, Tinder TL, Sterner CJ, Gendler SJ. MUC1-specific CTLs eradicate tumors when adoptively transferred in vivo. Clin Cancer Res 2003;7:848s–55s.
[12] North SA, Graham K, Bodnar D, Venner P. A pilot study of the liposomal MUC1 vaccine BLP25 in prostate specific antigen failures after radical prostatectomy. J Urol 2006;176(1):91–5.
[13] Kohlgraf KG, Gawron AJ, Higashi M, Meza JL, Burdick MD, Kitajima S, et al. Contribution of the MUC1 tandem repeat and cytoplasmic tail to invasive and metastatic properties of a pancreatic cancer cell line. Cancer Res 2003;63(16):5011–20.
[14] Ramanathan RK, Lee KM, McKolanis J, Hitbold E, Schraut W, Moser AJ, et al. Phase I study of a MUC1 vaccine composed of different doses of MUC1 peptide with SB-AS2 adjuvant in resected and locally advanced pancreatic cancer. Cancer Immunol Immunother 2005;54(3):254–64.
[15] Treon SP, Mollick JA, Urashima M, Teoh G, Chauhan D, Ogata A, et al. MUC1 core protein is expressed on multiple myeloma cells and is induced by dexamethasone. Blood 1999;93(4):1287–98.
[16] Brossart P, Schneider A, Dill P, Schammann T, Grunebach F, Wirths S, et al. The epithelial tumor antigen MUC1 is expressed in hematological malignancies and is recognized by MUC1-specific cytotoxic T-lymphocytes. Cancer Res 2001;61(18):6846–50.
[17] Loveland BE, Zhao A, White S, Gan H, Hamilton K, Xing PX, et al. Mannan-MUC1-pulsed dendritic cell immunotherapy: a phase I

trial in patients with adenocarcinoma. Clin Cancer Res 2006;12(3 Pt 1):869–77.
[18] Apostolopoulos V, Pietersz GA, Tsibanis A, Tsikkinis A, Drakaki H, Loveland BE, et al. Pilot phase III immunotherapy study in early-stage breast cancer patients using oxidized mannan-MUC1 [ISRCTN71711835]. Breast Cancer Res 2006;8(3):R27.
[19] Pantuck AJ, van Ophoven A, Gitlitz BJ, Tso CL, Acres B, Squiban P, et al. Phase I trial of antigen-specific gene therapy using a recombinant vaccinia virus encoding MUC-1 and IL-2 in MUC-1-positive patients with advanced prostate cancer. J Immunother 2004;27(3):240–53.
[20] North S, Butts C. Vaccination with BLP25 liposome vaccine to treat non-small cell lung and prostate cancers. Expert Rev Vaccines 2005;4(3):249–57.
[21] Pecher G, Haring A, Kaiser L, Thiel E. Mucin gene (MUC1) transfected dendritic cells as vaccine: results of a phase I/II clinical trial. Cancer Immunol Immunother 2002;51(11–12):669–73.
[22] Kontani K, Taguchi O, Ozaki Y, Hanaoka J, Sawai S, Inoue S, et al. Dendritic cell vaccine immunotherapy of cancer targeting MUC1 mucin. Int J Mol Med 2003;12(4):493–502.
[23] Scholl S, Squiban P, Bizouarne N, Baudin M, Acres B, Von Mensdorff-Pouilly S, et al. Metastatic breast tumour regression following treatment by a gene-modified vaccinia virus expressing MUC1 and IL-2. J Biomed Biotechnol 2003;2003(3):194–201.
[24] Snyder LA, Goletz TJ, Gunn GR, Shi FF, Harris MC, Cochlin K, et al. A MUC1/IL-18 DNA vaccine induces anti-tumor immunity and increased survival in MUC1 transgenic mice. Vaccine 2006;24(16):3340–52.
[25] Brossart P, Heinrich KS, Stuhler G, Behnke L, Reichardt VL, Stevanovic S, et al. Identification of HLA-A2-restricted T-cell epitopes derived from the MUC1 tumor antigen for broadly applicable vaccine therapies. Blood 1999;93(12):4309–17.
[26] Heukamp LC, van der Burg SH, Drijfhout JW, Melief CJ, Taylor-Papadimitriou J, Offringa R. Identification of three non-VNTR MUC1-derived HLA-A*0201-restricted T-cell epitopes that induce protective anti-tumor immunity in HLA-A2/K(b)-transgenic mice. Int J Cancer 2001;91(3):385–92.
[27] Tsang KY, Palena C, Gulley J, Arlen P, Schlom J. A human cytotoxic T-lymphocyte epitope and its agonist epitope from the nonvariable number of tandem repeat sequence of MUC-1. Clin Cancer Res 2004;10(6):2139–49.
[28] Wierecky J, Mueller M, Brossart P. Dendritic cell-based cancer immunotherapy targeting MUC-1. Cancer Immunol Immunother 2006;55(1):63–7.
[29] Wierecky J, Muller MR, Wirths S, Halder-Oehler E, Dorfel D, Schmidt SM, et al. Immunologic and clinical responses after vaccinations with peptide-pulsed dendritic cells in metastatic renal cancer patients. Cancer Res 2006;66(11):5910–8.
[30] Knutson KL, Disis ML. Tumor antigen-specific T helper cells in cancer immunity and immunotherapy. Cancer Immunol Immunother 2005;54(8):721–8.
[31] Krieg AM, Yi AK, Matson S, Waldschmidt TJ, Bishop GA, Teasdale R, et al. CpG motifs in bacterial DNA trigger direct B-cell activation. Nature 1995;374(6522):546–9.
[32] Krieg AM. CpG motifs in bacterial DNA and their immune effects. Annu Rev Immunol 2002;20:709–60.
[33] Krieg AM. Therapeutic potential of Toll-like receptor 9 activation. Nat Rev Drug Discov 2006;5(6):471–84.
[34] Ballas ZK, Krieg AM, Warren T, Rasmussen W, Davis HL, Waldschmidt M, et al. Divergent therapeutic and immunologic effects of oligodeoxynucleotides with distinct CpG motifs. J Immunol 2001;167(9):4878–86.
[35] Heckelsmiller K, Rall K, Beck S, Schlamp A, Seiderer J, Jahrsdorfer B, et al. Peritumoral CpG DNA elicits a coordinated response of CD8 T cells and innate effectors to cure established tumors in a murine colon carcinoma model. J Immunol 2002;169(7):3892–9.
[36] Milas L, Mason KA, Ariga H, Hunter N, Neal R, Valdecanas D, et al. CpG oligodeoxynucleotide enhances tumor response to radiation. Cancer Res 2004;64(15):5074–7.
[37] Brunner C, Seiderer J, Schlamp A, Bidlingmaier M, Eigler A, Haimerl W, et al. Enhanced dendritic cell maturation by TNF-alpha or cytidine-phosphate-guanosine DNA drives T cell activation in vitro and therapeutic anti-tumor immune responses in vivo. J Immunol 2000;165(11):6278–86.
[38] Schneeberger A, Wagner C, Zemann A, Luhrs P, Kutil R, Goos M, et al. CpG motifs are efficient adjuvants for DNA cancer vaccines. J Invest Dermatol 2004;123(2):371–9.
[39] Bourquin C, Schreiber S, Beck S, Hartmann G, Endres S. Immunotherapy with dendritic cells and CpG oligonucleotides can be combined with chemotherapy without loss of efficacy in a mouse model of colon cancer. Int J Cancer 2006;118(11):2790–5.
[40] Krieg AM. Antitumor applications of stimulating toll-like receptor 9 with CpG oligodeoxynucleotides. Curr Oncol Rep 2004;6(2):88–95.
[41] Speiser DE, Lienard D, Rufer N, Rubio-Godoy V, Rimoldi D, Lejeune F, et al. Rapid and strong human CD8+ T cell responses to vaccination with peptide, IFA, and CpG oligodeoxynucleotide 7909. J Clin Invest 2005;115(3):739–46.
[42] Jones T, Stern A, Lin R. Potential role of granulocyte-macrophage colony-stimulating factor as vaccine adjuvant. Eur J Clin Microbiol Infect Dis 1994;13(Suppl. 2):S47–53.
[43] Jager E, Ringhoffer M, Dienes HP, Arand M, Karbach J, Jager D, et al. Granulocyte-macrophage-colony-stimulating factor enhances immune responses to melanoma-associated peptides in vivo. Int J Cancer 1996;67(1):54–62.
[44] Fagerberg J. Granulocyte-macrophage colony-stimulating factor as an adjuvant in tumor immunotherapy. Med Oncol 1996;13(3):155–60.
[45] Carlsson T, Struve J. Granulocyte-macrophage colony-stimulating factor given as an adjuvant to persons not responding to hepatitis B vaccine [letter]. Infection 1997;25(2):129.
[46] Pardoll DM. Paracrine cytokine adjuvants in cancer immunotherapy. Annu Rev Immunol 1995;13:399–415.
[47] Golumbek PT, Azhari R, Jaffee EM, Levitsky HI, Lazenby A, Leong K, et al. Controlled release, biodegradable cytokine depots: a new approach in cancer vaccine design. Cancer Res 1993;53(24):5841–4.
[48] Markovic SN, Suman VJ, Ingle JN, Kaur JS, Pitot HC, Loprinzi CL, et al. Peptide vaccination of patients with metastatic melanoma: improved clinical outcome in patients demonstrating effective immunization. Am J Clin Oncol 2006;29(4):352–60.
[49] Disis ML, Bernhard H, Shiota FM, Hand SL, Gralow JR, Huseby ES, et al. Granulocyte-macrophage colony-stimulating factor: an effective adjuvant for protein and peptide-based vaccines. Blood 1996;88(1):202–10.
[50] Kaplan C, Morel-Kopp MC, Verdy E, Pron B, Tchernia G. Fetal and neonatal immune thrombocytopenias. Study group "mother–child immune thrombopenias". Presse Med 1992;21(36):1717–24.
[51] Rowse GJ, Tempero RM, VanLith ML, Hollingsworth MA, Gendler SJ. Tolerance and immunity to MUC1 in a human MUC1 transgenic murine model. Cancer Res 1998;58:315–21.
[52] Franco A, Yokoyama T, Huynh D, Thomson C, Nathenson SG, Grey HM. Fine specificity and MHC restriction of trinitrophenyl-specific CTL. J Immunol 1999;162(6):3388–94.
[53] Simpson-Herrerns L, Lloyd HH. Kinetic parameters and growth curves for experimental tumor systems. Cancer Chemother Rep 1970;54:143–74.
[54] Inaba K, Inaba M, Romani N, Aya H, Deguchi M, Ikehara S, et al. Generation of large numbers of dendritic cells from mouse bone marrow cultures supplemented with granulocyte/macrophage colony-stimulating factor. J Exp Med 1992;176(6):1693–702.
[55] Miconnet I, Koenig S, Speiser D, Krieg A, Guillaume P, Cerottini JC, et al. CpG are efficient adjuvants for specific CTL induction against tumor antigen-derived peptide. J Immunol 2002;168(3):1212–8.
[56] Davila E, Celis E. Repeated administration of cytosine-phosphorothiolated guanine-containing oligonucleotides together with peptide/protein immunization results in enhanced CTL responses with anti-tumor activity. J Immunol 2000;165(1):539–47.

[57] Davila E, Velez MG, Heppelmann CJ, Celis E. Creating space: an antigen-independent, CpG-induced peripheral expansion of naive and memory T lymphocytes in a full T-cell compartment. Blood 2002;100(7):2537–45.
[58] Finn O. History of tumour vaccines and novel approaches for preventive cancer vaccines. Dev Biol (Basel) 2004;116:3–12.
[59] Finn OJ. Tumor immunology at the service of cancer immunotherapy. Curr Opin Immunol 2004;16(2):127–9.
[60] Finn OJ. Cancer vaccines: between the idea and the reality. Nat Rev Immunol 2003;3(8):630–41.
[61] Pure E, Allison JP, Schreiber RD. Breaking down the barriers to cancer immunotherapy. Nat Immunol 2005;6(12):1207–10.
[62] Springer GF. T and Tn, general carcinoma autoantigens. Science 1984;224(4654):1198–206.
[63] Muller S, Hanisch FG. Recombinant MUC1 probe authentically reflects cell-specific *O*-glycosylation profiles of endogenous breast cancer mucin. High density and prevalent core 2-based glycosylation. J Biol Chem 2002;277(29):26103–12.
[64] Xu Y, Gendler SJ, Franco A. Designer glycopeptides for cytotoxic T cell-based elimination of carcinomas. J Exp Med 2004;199(5):707–16.
[65] Sidney J, Grey HM, Kubo RT, Sette A. Practical, biochemical and evolutionary implications of the discovery of HLA class I supermotifs. Immunol Today 1996;17(6):261–6.
[66] Vlad AM, Muller S, Cudic M, Paulsen H, Otvos Jr L, Hanisch FG, et al. Complex carbohydrates are not removed during processing of glycoproteins by dendritic cells: processing of tumor antigen MUC1 glycopeptides for presentation to major histocompatibility complex class II-restricted T cells. J Exp Med 2002;196(11):1435–46.
[67] Apostolopoulos V, Yuriev E, Ramsland PA, Halton J, Osinski C, Li W, et al. A glycopeptide in complex with MHC class I uses the GalNAc residue as an anchor. Proc Natl Acad Sci USA 2003;100(25):15029–34.

Mayo Clinic Cancer Center

MUC1/HER-2/neu Peptide Based Immunotherapeutic Vaccines for Breast Adenocarcinomas

Principal Investigators/Study Chairs: Svetomir Markovic, M.D., Ph.D. *+
Mayo Clinic Cancer Center
200 First Street, SW
Rochester, MN 55905
507/284–2511
507/284-5280 (FAX)

Sandra J. Gendler, Ph.D. √
Mayo Clinic Scottsdale
13400 E. Shea Boulevard
Scottsdale, AZ 85255
480/301-7062
480/301-7017 (FAX)

Study Co-chairs: James N. Ingle, M.D (Mayo Clinic, Rochester)

Tom Fitch, M.D (Mayo Clinic, Scottsdale)
Barbara Pockaj, M.D (Mayo Clinic, Scottsdale)
Edith A. Perez, M.D. (Mayo Clinic, Jacksonville)

Statistician: Vera J. Suman, Ph.D. √

* Investigator having primary responsibility for this protocol
+ IND sponsor (IND# 12155)
√ Study contributor(s) not responsible for patient care.

Document History	**(effective date)**
Activation	August 28, 2008
MCCC Addendum 1	May 19, 2009
MCCC Addendum 2	December 23, 2009
MCCC Addendum 3	May 12, 2010

Protocol Resources

Questions:	Contact Name:
Review all unanticipated problems involving risk to volunteers or others, serious adverse events and all volunteer deaths associated with the protocol and provide an unbiased written report of the event	Robert R. McWilliams, M.D. Medical Monitor Phone: 507-284-8432 E-mail: mcwilliams.robert@mayo.edu
Patient eligibility*****, test schedule, treatment delays/interruptions/adjustments, dose modifications, adverse events, forms completion	Carol Leonard Quality Control Specialist Phone: 507-284-3121 Fax: 507-284-1902 E-mail: leonard@mayo.edu
Drug administration, infusion pumps, nursing guidelines	Lisa Kottschade, NP Mayo Clinic Cancer Center Nurse Phone: 507-538-2958 E-mail: kottschade.lisa@mayo.edu
Clinical data submission and record maintenance	Renee Bradshaw Clinic Research Associate Phone: 507-284-2041 E-mail: Bradshaw.renee@mayo.edu
Protocol document, consent form, Regulatory issues	Jane M. Milburn, MBA Protocol Development Coordinator Phone: 507-266-0743 Fax: 507-284-5280 E-mail: milburn@mayo.edu
Technical problems with electronic form entry	Vicki Bryhn Data Management Specialist Phone: 507-266-5350 Fax:: 507-538-0906 E-mail: bryhn@mayo.edu

Index

Schema

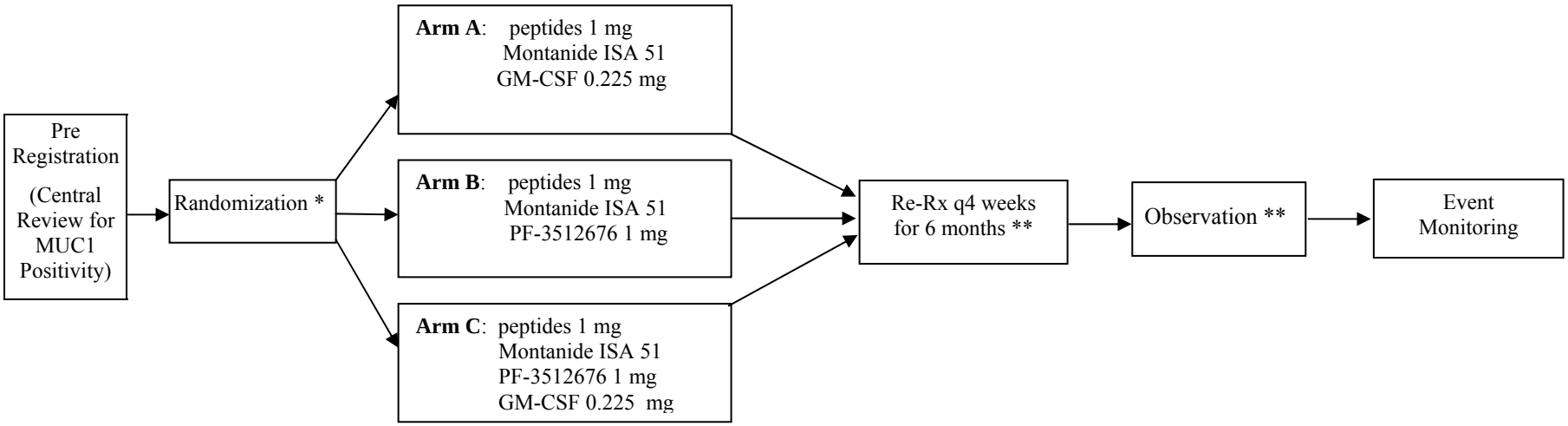

* Patient must have MUC1 positive breast cancer confirmed by central review prior to randomization.
** At relapse, patients enter event monitoring phase (see Section 13)

Generic Name	Brand Name	Mayo Abbreviation	Availability
MUC1 (STAPPVHNV)		MUC1	Clinalfa
HER2 Peptide-1 (ILHNGAYSL)		HER2-1	Clinalfa
HER2 Peptide 2 (KVPIKWMALESILRRRF)		HER2-2	Clinalfa
Montanide ISA-51 or Montanide ISA-51 VG		MONTAN	Purchased, study funded
Sargramostim (GM-CSF)	Leukine	GM-CSF	Purchased, study funded
PF-3512676 (CPG7909)		CP7909	Pfizer Pharm, Inc.

1.0 Background

1.1 Breast cancer is diagnosed in 200,000 individuals in the United States annually and contributes to approximately 40,000 deaths each year. For tumors confined to the breast, surgical removal provides a good prognosis. However, primary tumor that metastasizes to distant sites, such as lymph nodes, lungs, liver and brain, correlates with a poor prognosis. Patients with advanced stage breast cancer are at high risk of relapse. Complications from metastatic disease are the leading causes of cancer-related deaths. Novel adjuvant strategies, such as breast cancer specific vaccines, are being considered as a clinical intervention that may reduce the chance of recurrence.

In recent years there has been great interest in the development of these cancer vaccines, which are designed to immunize individuals to antigens present on tumors. Cancer vaccines are a non-toxic therapy, which have been shown in several melanoma trials to have the potential of controlling disease and prolonging survival because tumors can be surgically removed and there is often a long period of time before the tumor recurs at metastatic sites, cancer vaccines have been proposed as an optimal therapy that could prolong the time to recurrence. This optimal opportunity of immunization in the situation of minimal residual disease has rarely been tested, however, as most vaccines have been given to patients with large tumor burden after the failure of standard therapies in Phase I and Phase II trials. Recently, several groups have addressed the use of adjuvant immunotherapy following complete surgical resection [1]. Data from these studies are not yet complete.

1.2 The past two decades in tumor immunology have led to the discovery of specific tumor antigens that have been shown in preclinical studies to elicit tumor-specific immunity and establish long term memory without autoimmunity. For breast cancer, vaccines composed of epitopes derived of MUC1, HER-2/neu, MAGE3, CEA have been studied and shown to be immunogenic without causing autoimmunity [2-5].

1.3 It is now clear that tumor antigens are presented in the context of specific class I and Class II HLA molecules. Class I presentation, in the presence of appropriate co-stimulation, is thought to stimulate a cytolytic $CD8^+$ T cell response, while antigen presentation in the context of Class II molecules stimulates a $CD4^+$ helper T cell response [6].

1.4 One approach for the development of a cancer vaccine is the use of tumor associated synthetic antigens for immunologic priming. Because specific peptides are ubiquitous in tumors of the same histologic type, identical peptide vaccines may be employed in allogeneic hosts bearing the same tumor histology. Additionally, the use of single peptides for immunization limits the potential induction of undesired autoimmunity [7-9]. Recent developments in the use of soluble MHC Class I/peptide tetramers and elispot technology have enabled rapid characterization of epitope-specific CTL responses [10, 11]. In addition to being well-explored and understood, many of these antigens are shared tumor antigens. Vaccines that are composed of these antigens can be developed for use in a large number of patients. The primary limitations to peptide based vaccine strategies are haplotype restriction, potential for degradation, and uncertainty regarding which peptides, used alone or in combination, are the most immunogenic [12, 13]. This study is designed to test these uncertainties.

1.5 One attractive and broadly applicable target for immunotherapeutic strategies is the MUC1 tumor antigen. MUC1, a cell-associated mucin, is expressed on the cell surface of many epithelial malignancies as well as by hematological malignancies [14-17]. These include multiple myeloma (92%) and acute myelogenous leukemia (67%) [18]. Greater than 90% of breast carcinomas express MUC1; high levels are also found in adenocarcinomas originating from most tissues [14, 16]. MUC1 expression is greatly up-regulated on tumors (reviewed in

Gendler [19]). Expression on tumors is no longer apical, but it is found all around the cell surface and in the cytoplasm. In addition, glycosylation on tumor-synthesized MUC1 is aberrant, with greater exposure of the peptide core than is found in normal tissues. MUC1 has long been an interesting target molecule for immunotherapeutic strategies, given its high level and ubiquitous expression. Patients with tumors, especially with breast, pancreas and ovarian tumors, have exhibited immune responses to MUC1 with the presence of antibodies and T cells specific for MUC1 detected in about 10% of individuals. An HLA unrestricted T cell response among cancer patients has also been described [20-23]. There is increasing evidence from murine and human studies that MHC-restricted T cells can be induced in mice and humans after immunization with the MUC1 peptide or MUC1 antigenic epitopes [24-32]. Importantly, there have been reports of two HLA-A2 binding peptides derived from the MUC1 protein [33]. One of the peptides is from the tandem repeat sequence of MUC1 and the second peptide is from the signal sequence. MUC1-specific cytotoxic T cells (CTLs) have been induced in T cells from healthy donors following *in vitro* immunization using peptide-pulsed dendritic cells. MUC1-specific CTLs have also been induced *in vivo* after vaccination of breast and ovarian cancer patients with peptide-pulsed DCs [18].

1.6 A second candidate for peptide-based immunotherapy is HER-2/neu, the gene product of the erbB2/neu protooncogene. HER-2/neu is overexpressed in approximately 30% of breast cancer patients. HER-2/neu is also expressed by multiple types of tumors, including ovarian, lung, colon, pancreas and gastric tumors [34-36]. HER-2/neu has particular relevance, as it is expressed at high levels in early *in situ* lesions in breast carcinoma [37]. Thus, it is a target for early disease. Immunologic responses to HER-2/neu have been detected in a minority of patients with advanced stage breast and ovarian cancer, including antibodies, T helper and CD8 responses [38, 39]. Several HLA-class I binding peptides have been previously identified. A novel HLA-A2.1 binding peptide from the HER-2/neu extracellular domain [HER-2(9_{435})] was recently identified [40]. This peptide (ILHNGAYSL) bound to HLA-A2.1 with intermediate affinity (IC50 74.6 nM). The HER-2(9_{435}) epitope was tested using an *in vitro* immunization protocol and found to elicit CTLs that killed peptide-sensitized target cells. The CTLs elicited also recognized the HER-2/neu antigens, as it specifically killed tumor cells expressing the HLA-A2.1 and HER-2/neu antigens (see below in preliminary data). Furthermore, recognition of the tumor cell targets was significantly inhibited by unlabeled (cold) targets pulsed with HER-2(9_{435}), but not by unlabeled targets either unpulsed or pulsed with a control HLA-A2.1 binding peptide (see below). Thus, the CTLs induced by HER-2(9_{435}) are antigen specific.

A potential limiting factor for peptide based immunotherapy is related to a defined antigenic repertoire which is HLA restricted. This factor, inherent to all peptide-based approaches, restricts patient access. Additionally, because individual peptides only have the potential to induce epitope-specific CTL, the vast majority of potential tumor antigens are not targeted. In this setting, tumor down regulation of individual antigens or HLA epitopes promotes immune evasion. Recent evidence, however, suggests that this problem of epitope restriction may not be as physiologically important as was previously postulated. Specifically, it has now been clearly demonstrated that a T cell response induced against one epitope can stimulate CTL response to other target epitopes through a mechanism termed epitope spreading [3, 41, 42]. Using an experimental autoimmune encephalitis model, Vanderlugt et al. have demonstrated that disease progression is associated with the development of epitope-specific helper T cells, which are distinct from those initiating the disease. Transfer of secondary $CD4^+$ cells to naïve mice induces the disease phenotype and the disease is abrogated by blocking the secondary T cell response even though the primary T cell response remains intact [43, 44]. Disis demonstrated epitope spreading in 84% of patients vaccinated with HER-2/neu peptides, reflecting the initiation of an endogenous immune response. The immunity persisted after active immunizations ended [3]. These data suggest that peptide based approaches to cancer immunotherapy may indirectly stimulate multiple tumor reactive CTL against minor antigens in

the presence of residual tumor. Based on this concept, the current study is designed as a therapeutic approach, with peptide epitope selection designed to enhance the number of potential candidates.

In addition to class I epitopes, immunogenic HLA-DR restricted class II epitopes have been defined for HER-2/neu. $CD4^+$ helper T lymphocytes (T_H) responses play an essential role in immunologically mediated anti-tumor immunity [45]. T_H lymphocytes provide CTLs with growth-stimulating cytokines, prime/activate DCs to effectively present antigen to naive CTL precursors [46-48] and they are important in the development of immune memory [49-51]. The development of IgG antibodies to HER-2/neu and the identification of $CD4^+$ T cells that secrete cytokines in response to HER-2/neu peptides or recombinant HER-2/neu protein suggest responses to helper T cells [52-57]. A promiscuous MHC class II T_H epitope has been identified for the HER-2/neu antigen ($HER\text{-}2_{883}$). T cell responses are restricted by HLA-DR1, HLA-DR4, HLA-DR52, and HLA-DR53 [58]. Peptide-induced T cells were effective in recognizing naturally processed HER-2/neu protein. The peptide $HER\text{-}2_{883}$, (KVPIKWMALESILRRRF), which was selected by computer algorithm, was tested for its capacity to stimulate $CD4^+$ T cells isolated from four healthy, MHC-typed individuals (DR1/11, DR1/13, DR4/15, DR7/17) in primary *in vitro* culture using peptide pulsed autologous DCs. T cells that proliferated were found to react with peptide and recombinant HER-2/neu intracellular domain protein presented by autologous DCs (see below). These results, showing reactivity with recombinant protein, suggest that $HER\text{-}2_{883}$ is naturally processed, as the peptide stimulated T cells react with DCs primed with recombinant protein. Clearly, $HER\text{-}2_{883}$ is a naturally processed peptide epitope and is promiscuous for multiple HLA-DR epitopes, making it an ideal candidate for therapeutic applications.

1.7 Because of the expression of MUC1 and HER-2/neu in multiple cancers, the development of this peptide-based immunotherapy can potentially impact the treatment of multiple disease entities, not only adenocarcinomas but hematopoietic malignancies as well. There is considerable interest in the use of the MUC1 peptide vaccination for treatment of multiple myeloma following transplant when there is minimal residual disease prior to remission.

1.8 GM-CSF

Granulocyte-macrophage colony stimulating factor (sargramostim, GM-CSF) is a commercially available cytokine currently used in patients undergoing chemotherapy to shorten the duration of post-chemotherapy neutropenia. Recently published evidence also suggests that GM-CSF may play a role as an immune adjuvant [59, 60]. The following observations illustrate the mechanisms by which GM-CSF can potentiate the immunogenicity of an antigen: 1) GM-CSF is a key mediator of dendritic cell (DC) maturation and function [61]; 2) GM-CSF increases surface expression of class I and II MHC molecules as well as co-stimulatory molecules of dendritic cells *in vitro* [61]; 3) GM-CSF enhances antibody responses to known immunogens *in vivo* [62]; 4) tumor cells transfected with genes encoding/expressing GM-CSF are able to induce long lasting, specific anti-tumor immune responses *in vivo* [63]; 5) GM-CSF encapsulated in biodegradable microspheres mixed with whole tumor cells resulted in systemic anti-tumor immune responses comparable to those of GM-CSF transfected tumor cells [64]. Therefore, addition of GM-CSF to an oligopeptide antigen may substantially enhance its immunogenicity.

In an attempt to optimally enhance the immunogenicity of the peptides we will deliver the antigens and GM-CSF emulsified in incomplete Freund's adjuvant (IFA, Montanide ISA-51). This delivery mechanism should be comparable to a previously demonstrated delivery mechanism utilizing GM-CSF suspended in microspheres and mixed with tumor cells (antigens). We hypothesize that the emulsified GM-CSF in close proximity to tumor antigen peptides will substantially enhance their immunogenicity. This proximity of antigen and GM-

CSF seems to be necessary for the adjuvant effect of GM-CSF, as systemic administration of equivalent doses in animal models has not demonstrated adjuvant activity. Also, the adjuvant/local inflammatory properties of IFA may play a role in attracting antigen presenting cells to the site of injection [53]. We have preliminary data demonstrating the plausibility of such a mechanism.

1.9a Preliminary data demonstrating the feasibility of this approach already exists. Rosenberg and investigators published effective generation of peptide-specific T cells in melanoma patients immunized with peptides derived from gp100 [65]. Despite the demonstration of a specific immune response, no clinical responses were detected. Addition of systemic GM-CSF resulted in more pronounced CTL and delayed type hypersensitivity reactions and in a few cases objective tumor regressions. Salgaller et al. utilized a peptide derived from the gp100 epitope suspended in IFA and demonstrated generation of specific T cell responses to the peptide in melanoma patients [66]. Both studies suggest that increased immunogenicity of the peptide antigens leads to a more pronounced T cell response, which in some cases results in a clinically relevant anti-tumor effect. In the proposed study, we will combine the immunoadjuvant effects of both IFA and GM-CSF with the goal of increasing the immunogenicity of the MUC1 and HER-2/neu immunodominant peptides.

Preliminary observations in an ongoing clinical study (MC9973) utilizing HLA-A2 specific melanoma differentiation antigen peptide vaccines in which the peptide is emulsified in a suspension of IFA and GM-CSF is demonstrating enhanced skin reactions if peptide emulsified in IFA is administered in the presence of GM-CSF. A dose of 50 mcg of GM-CSF in the presence of IFA and peptide results in extensive local skin reactions as well as evidence of a clinical response in one of seven patients thus far. No changes in the numbers of peptide specific CTLs were observed. However, a recent publication demonstrated superior numbers of vaccine specific CTLs generated in a peptide vaccine utilizing 225 mcg of GM-CSF in IFA) [67]. This would suggest a dose/response relationship of GM-CSF and anti-peptide vaccine CTL frequencies as determined by ELISPOT and tetramer assays. Therefore, in the current trial we propose to use 225 mcg of GM-CSF suspended in IFA (montanide ISA-51).

1.9b CpG (PF-3512676)

Therapeutic properties of bacteria in the treatment of malignant diseases (i.e. Coley's toxin) is an observation that has permeated the oncology literature for almost a century. More recently, it has been demonstrated that bacterial DNA possesses unique immunomodulatory features of potential utility in cancer therapy. Specifically, unmethylated CpG are able to stimulate NK cells and B cells. Furthermore, synthetic oligodeoxynucleotide (ODN) constructs containing unmethylated CpG motifs (CpG-ODN) were able to activate dendritic cells (DC) enhancing their antigen processing/presentation properties and stimulating production of Th1 cytokines necessary for CTL immune responses. Thus, CpG ODN appeared to function as an immune adjuvant. Several preclinical and clinical works illustrate the ability of CpG-ODN to function as a potent immune adjuvant for various forms of vaccines. One of the more interesting works, pertinent to this study, demonstrates the ability of CpG ODN to induce CTLs against a peptide vaccine when administered in conjunction with incomplete Freund's adjuvant (IFA) [68]. These authors used a MART-1/Melan-A_{26-35} peptide emulsified in IFA with or without the addition of 50ug of CpG ODN to immunize human D^b (HHD) A2 transgenic mice. Their data suggest superior anti-peptide immunization in the CpG-ODN immunized group as determined by the frequency of tetramer positive CTLs. Our own data support these findings demonstrating superior immunization efficacy of IFA+CpG-ODN with ova peptide of C57BL/6 mice when compared to either IFA+peptide or complete Freund's adjuvant (CFA) + peptide (data not shown). An additional benefit to the CpG-ODN adjuvant is that it has been shown to be especially good at enhancing cellular and humoral immunity and promoting a Th1-type of response in older mice [69]. The population that develops cancer is mainly older individuals,

thus the CpG-ODN adjuvant may be particularly relevant for this trial. Based on preclinical data suggesting the potent immune adjuvant properties of CpG co-emulsified with peptides in IFA, we elected to test the efficacy of CpG-ODN in the setting of a peptide vaccine immunization in this clinical trial. The dose of CpG-ODN that we decided to use in this study is 2mg/vaccine. The dose is based on published data demonstrating a direct dose-dependent relationship of CpG-ODN (0.125 –1 mg) and magnitude of measured immune responses (HepB vaccine adjuvant [70]). This is well below the highest tested doses of 20mg/week. Based on these observations we feel that the 2 mg dose is a reasonable starting point for a CpG-ODN adjuvant suspended in Montanide ISA 51 alone or in combination with GM-CSF.

1.9c Preliminary Data

Preliminary data will be presented in multiple sections. First, we will provide data to support the choice of MUC1 and HER-2/erbB2 antigenic epitopes for this trial. Next, we will define our experience using peptides to stimulate tumor reactive T cells for cancer immunotherapy. Finally, we will discuss our experience with the immune adjuvants GM-CS and CpG-ODN. These preliminary data provide a strong foundation for the current proposal.

1.9c1 Identification of CTL Epitopes from MUC1

Using a computer analysis of the MUC1 amino acid sequence, two novel peptides were identified with a high binding probability to the HLA-A2 molecule [33]. Two peptides from MUC1 were identified; one from the tandem repeat M1.1 ($STAPPVHNV_{950-958}$) and one from the leader sequence M1.2 ($LLLLTVLTV_{12-20}$). The presence of the V in position 6 increases the binding of the M1.1 peptide to the HLA-A2 molecule. There is some variability in the tandem repeats in MUC1 and this sequence is found in the last tandem repeat. Cytotoxic T cells were induced from healthy donors by primary *in vitro* immunization using peptide-pulsed dendritic cells. The peptide-induced CTL lysed tumors endogenously expressing MUC1 in an antigen-specific and HLA-A2-restricted fashion..

CTL.M1.1

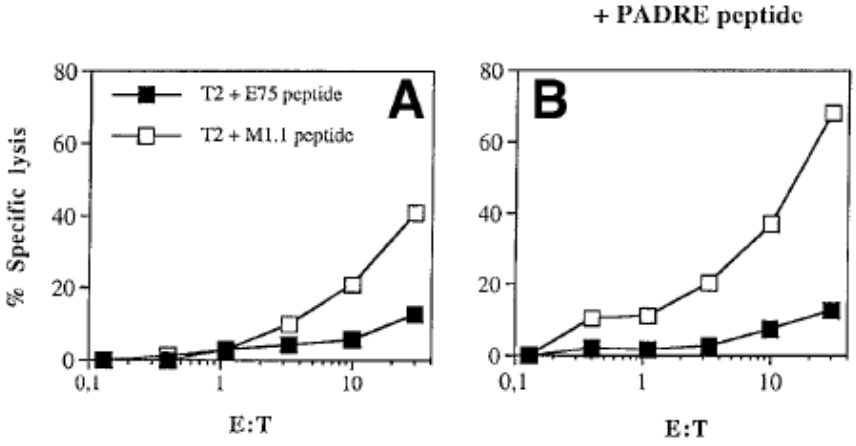

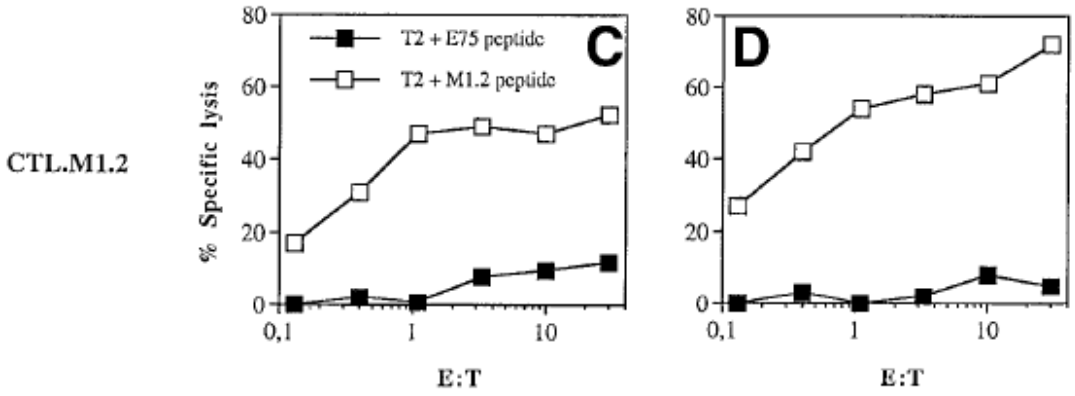

Figure 1. *Induction of CTL responses by peptide-pulsed dendritic cells. Adherent peripheral blood mononuclear cells were grown for 7 days with GM-CSF, IL-4, and TNF alpha. DCs pulsed with the synthetic peptides derived from the MUC1 protein (M1.1 and M 1.2) were used to induce a CTL response in vitro. In addition to the MUC1 peptide DCs were incubated with the PAN-DR binding peptide PADRE as a T-helper epitope. Cytotoxic activity of induced CTL was determined in a standard ^{51}Cr-release assay using T2 cells as targets pulsed for 2 hours with 50 μg of the cognate (open symbols) or irrelevant HER-2/neu protein-derived protein derived E75 peptide (solid symbols). (data reproduced from Brossart 1999 [33])*

Next, the ability of the induced MUC1-specific CTL lines to lyse tumors expressing MUC1 was tested. MCF-7 cells that express MUC1 endogenously and are HLA-A2 positive were used as targets in a standard ^{51}Cr-release assay. The controls were SK-OV-3 cells, which express MUC1, but are HLA-A2 negative and the immortalized B cell line, Croft, which is A2 positive and was pulsed with MUC1 M1.1 or M1.2 peptides or the irrelevant HER-2/neu E75 peptide.

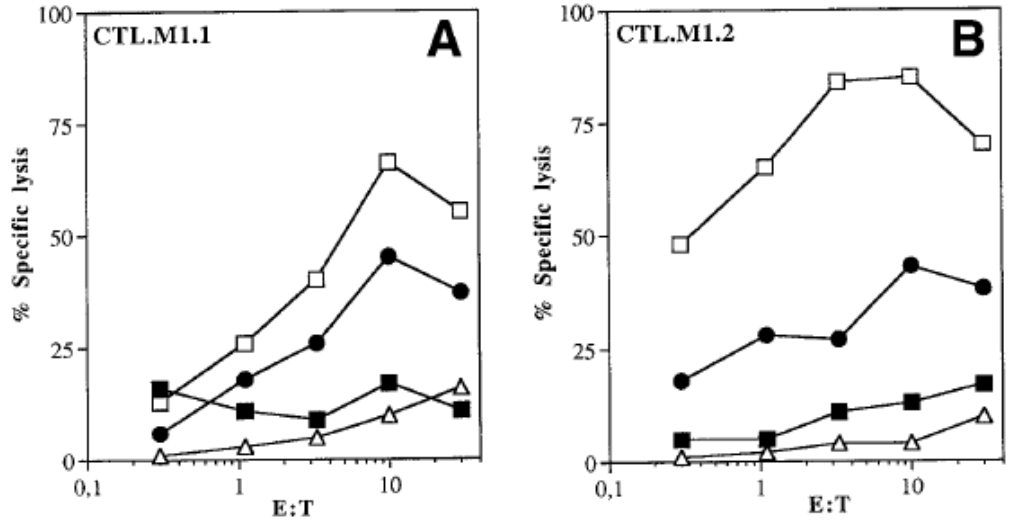

Figure 2. *Lysis of cancer cells endogenously expressing MUC1 by CTL.M1.1 (A) and CTL.M1.2 (B). Human breast cancer cell line MCF-7 (HLA-A2$^+$/MUC1$^+$), ovarian cancer cell line SK-OV-3 (HLA-A2$^-$/MUC1$^+$), and the immortalized B-cell line Croft (HLA-A2$^+$/MUC1$^-$) were used as targets in a standard ^{51}Cr-release assay. Croft cells were pulsed with the MUC1 peptides or an irrelevant HER-2/neu-derived peptide E75. (■) Croft + E75 peptide; (□) Croft + M1.1 (A) or M1.2 (B); (●)MCF-7; (Δ) SK-OV-3.*

We have chosen to use the M1.1 peptide based on the large amount of data on the response to the MUC1 tandem repeat peptide, both in the human situation as well as in the mouse. Obviously only the human data are relevant for the clinical trials. We will use a HER-2/neu helper epitope (see below, not the PADRE helper epitope)

In the case of HER-2/neu, we have identified a novel CTL epitope HER-2 (9_{435}), which bound HLA-A2.1 with intermediate affinity (IC_{50} 74.6 nM). The peptide identified is: ILHNGAYSL. The .221(A2.1) cell line, produced by transferring the HLA-A2.1 gene into the HLA-A, -B, -C null mutant human lymphoblastoid cell line .221, was used as target (peptide loaded) to measure activity of HLA-A2.1 restricted CTL [71]. The CTLs elicited following in vitro stimulation effectively killed HLA-A2.1$^+$ tumor cells, showing that the antigen is appropriately processed by tumors (Fig. 3A). In addition, recognition of the tumor cell target was significantly inhibited by unlabeled (cold) target pulsed with HER-2 (9_{435}) peptide, but not by unlabeled targets either unpulsed or pulsed with a control HLA-A2.1 binding peptide (Fig. 3B).

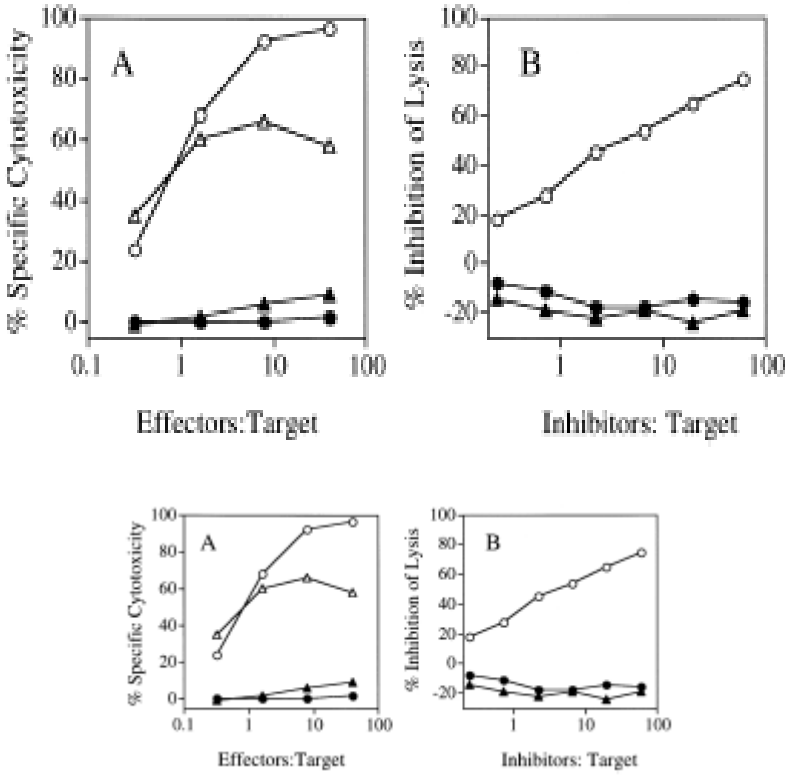

Figure 3. *HER-2(9_{435}) specific CTL can kill tumor cells. (A) HER-2(9_{435}) specific CTL were used as effector cells to test for the lysis of the following target cell lines: o, .221A2.1 pulsed with HER-2(9_{435}); ●, .221A2.1 without peptide; Δ, SW403 (colon CA, A2$^+$, HER-2/neu$^+$); ▲, HT-29 (colon ca, A2$^-$, HER-2/neu$^+$). (B): Antigen specificity demonstrated by cold target inhibition assay. Lysis of ^{51}Cr labeled SW403 cells at an effectors/target ratio of 10:1 by the HER-2(9_{435}) specific CTL was blocked at various Inhibitors/Target ratios by the following cold targets: o, .221A2.1 pulsed with HER-2(9_{435}); ▲, .221A2.1 pulsed with irrelevant A2.1 binding peptide (HBc_{18-27}); ●, .221A2.1 without peptide.*

In addition to the class I epitopes described above, a promiscuous MHC class II epitope was defined for HER-2/neu using the algorithm tables published by Southwood et al. [58, 72]. The epitope identified is HER-2_{883} (KVPIKWMALESILRRRF). It is important to show that these peptides represent true T cell epitopes that are relevant for the development of tumor immunotherapy. For these experiments autologous PBMCs or DCs were used as APCs and recombinant DNA derived intracellular domain or extracellular domain protein fragments of HER-2/neu were used as a source of antigen. The data in Fig. 4 show that four HER-2_{883}-reactive T cell lines proliferated well to HER-2/neu intracellular domain protein, which encompasses the HER-2_{883} peptide but not to HER-2/neu extracellular domain (ECD), which lacks HER-2_{883}..

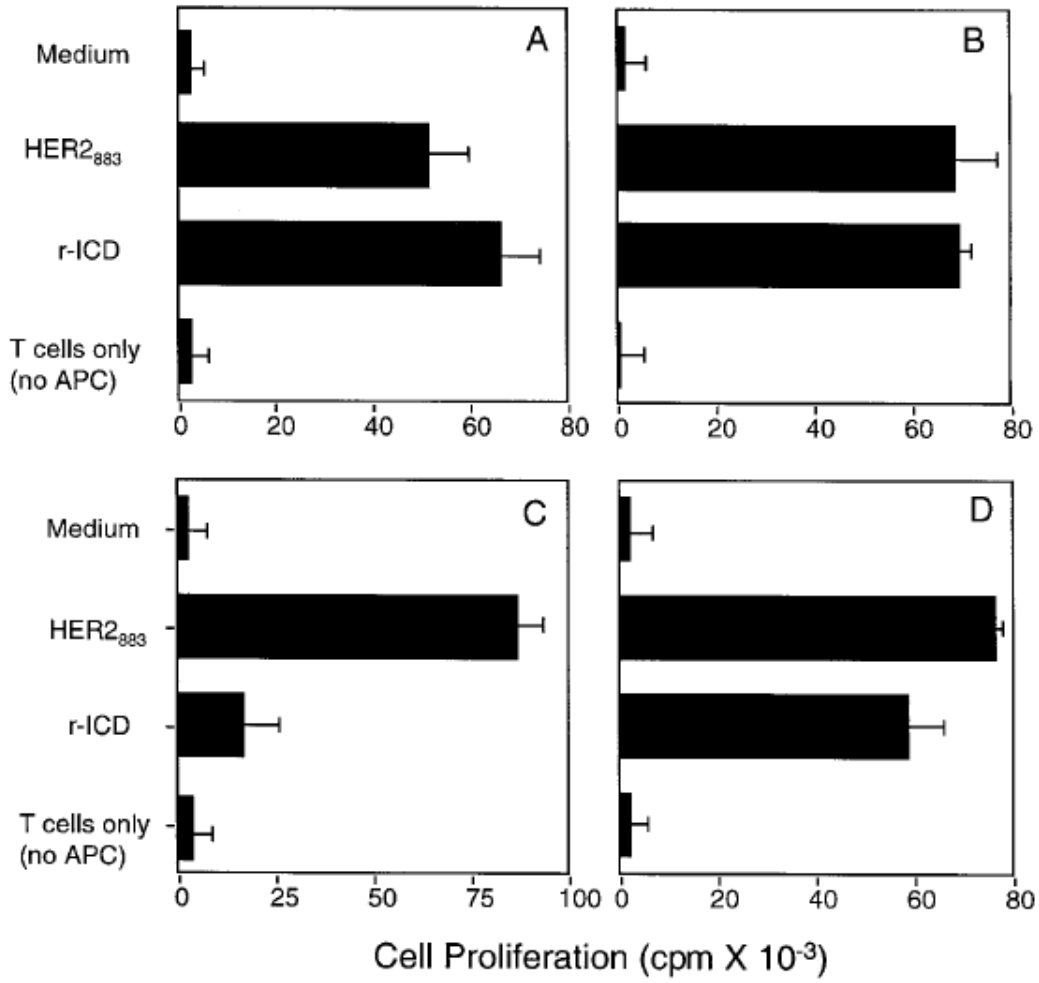

Figure 4. *HER-2_{883}-specific CD4+ T cells can recognize recombinant HER-2/neu intracellular domain (r-ICD) protein presented by autologous Dcs in the context of several HLA-DR alleles. The HER-2_{883}-reactive HTLs, TCL-7C (panel A, HLA-DR53 restricted), TCL-6D (panel B, HLA-DR4-restricted), a clone of TCL-1D (panel C, HLA-DR52-restricted), and TCL-1E (panel D. HLA-DR53 restricted), were tested for their capacity to proliferate to autologous DCs in the presence of HER-2_{883} peptide (2.5 mg/ml) or recombinant HER-2/neu recombinant ICD protein (10 mg/ml). No significant proliferative response was observed against HER-2/neu ECD protein (data not shown). Values shown are the means of triplicate determinations; bars, SD.*

1.9d Justification of vaccination strategy

1.9d.1 **Peptide dose** (1000 mcg): Over the last several years there has been extensive debate over the optimal dose of peptide in a variety of peptide immunization cancer clinical trials. Peptide doses have ranged from 50 mcg to 2500 mcg in various studies. Currently, the largest peptide vaccine clinical trial (E4697) utilizes a peptide dose of 1000 mcg. There are several published studies evaluating peptide vaccine dose-responses [66, 73], suggesting that 1000 mcg of peptide would be a reasonable vaccine dose for phase I/II clinical testing.

1.9d.2 **GM-CSF suspended in Montanide ISA 51 as a vaccine adjuvant.** The utility of GM-CSF suspended in montanide ISA 51 as an effective vaccine adjuvant has already been demonstrated in pre-clinical and clinical studies. Our own pre-clinical data (Fig 5) demonstrates a bell shaped dose-response curve for GM-CSF co-emulsified with 10

mcg of *ova* peptide in montanide ISA 51. Two weeks after immunization, the optimal dose of GM-CSF in the mouse model appears to be 100 mcg. In humans, Slingluff et al. demonstrated successful peptide immunization using 225 mcg of GM-CSF suspended in montanide ISA-51[67]. Up to 80% of treated patients demonstrated effective immunization with melanoma differentiation antigen peptides. Our clinical data using 10, 50, 75 and 100 mcg of GM-CSF suspended with peptides in Montanide ISA-51 failed to demonstrate effective generation of anti-peptide CTLs. In view of these data, we felt that it was reasonable to utilize the same dose of GM-CSF used by Slingluff [67] (225 mcg) with our current set of peptides. If successful, further studies will be performed attempting to generate a dose-response curve of GM-CSF and immunization efficacy similar to that of the mouse model.

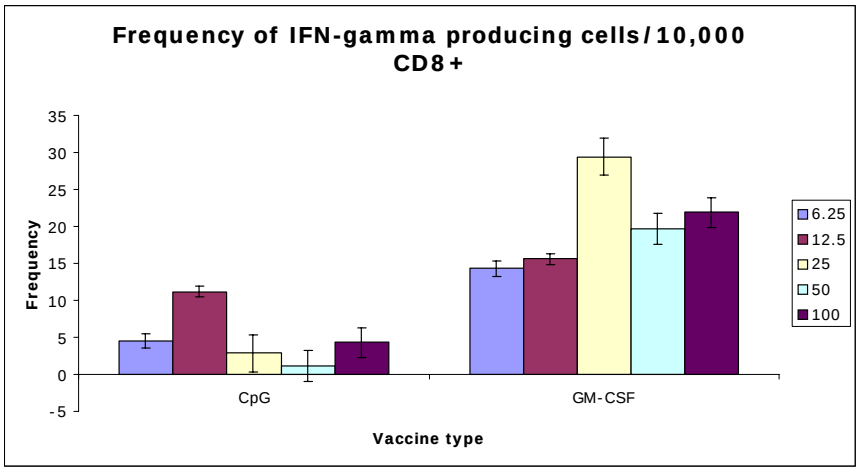

Fig. 5: C57BL6 mice (3 per group) were immunized with 10ug of ova peptide suspended in Montanide ISA51 and varying concentrations of CpG or GM-CSF .Represented are the frequencies of ova specific CTLs (IFN gamma ELISPOT) isolated from splenocytes on day 12 post immunization. Similar dose/response curves were observed in two other experiments.

1.9d.3 **CpG suspended in Montanide ISA 51 as vaccine adjuvant.** As described in section 15.7, the co-emulsification of peptide antigens with CpG and Montanide ISA-51 is an effective means of generation of peptide specific CTLs in a pre-clinical model. Our own data confirm these findings using non-transgenic mice immunized with ova peptide co-suspended with CpG in Montanide ISA 51 (Fig. 5). The dose of CpG used in the current study was empirically selected based on the results of a phase I clinical trial utilizing CpG (abbreviated as ISS in Fig. 6 legend) as an immune adjuvant for hepatitis B vaccine immunization in healthy volunteers. In this study, volunteers were immunized with an intramuscular injection of hepatitis B vaccine (20 mcg) mixed with CpG in one of the following amounts: 225 mcg, 650 mcg, 1000 mcg or 2250 mcg. A booster injection was administered 2 months later. Serologic data demonstrated (Fig 6) maximal immunization efficacy at CpG doses between 1000 and 2250 mcg. Based on these data suggesting a bell-shaped dose response curve for CpG (optimum may be between doses 1000 mcg and 2250 mcg) as well as our pre-clinical bell-shaped dose response curve, we elected to proceed with a CpG dose of 2000 mcg.

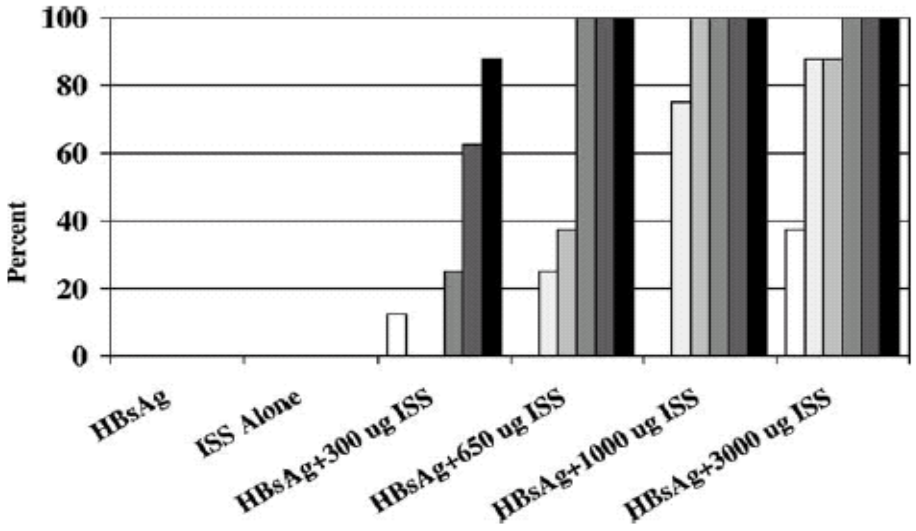

Figure 6: Proportion of participants achieving a protective antibody level (≥10mIU/mL) at various time points after immunization. Time points are (by increasing darkness of bar shade) 7 days after dose 1, 28 days after dose 1, 56 days after dose 1, 7 days after dose 2, 4 months after dose 2. CpG is designated as ISS.

The target population for this clinical trial, to whom the study findings will be generalized, are patients with a history of completely treated stage II or III breast adenocarcinoma that is MUC1 positive, currently off active therapy (with the exception of hormonal therapy) with no evidence of tumor relapse.

1.9e As of February 24, 2009, adverse event data are available for 4 patients randomized to Arm A, and 4 patients randomized to Arm B, and 5 patients randomized to Arm C. One patient on Arm A developed a grade 2 injection site reaction (ISR) during the first cycle of treatment and 2 patients on Arm B developed a grade 2 ISR during the third cycle of treatment. Three of the 5 patients randomized to Arm C also developed ISRs, namely, a grade 2 ISR during the first cycle of treatment which worsened to a grade 3 during the second cycle of treatment, a grade 2 ISR during the first and second cycles of treatment, and a grade 2 ISR during the third cycle of treatment. These ISRs were the only treatment-related toxicities reported. As the regimens containing CpG appear to induce a greater numbers of ISR, the dose of CpG will be lowered to 1 mg and all patients who develop a grade 2 ISR will discontinue study treatment.

2.0 Goals

2.1 Primary Goal

To determine the safety and immunization efficacy of MUC1 and HER-2/neu peptide vaccines combined with CpG, GM-CSF or both, as immune adjuvants suspended in Montanide ISA-51.

2.2 Secondary Goal

To describe the impact of immunization on clinical outcomes in patients with MUC1 positive breast cancer. Clinical outcomes of interest will include: (1) **disease-free survival** defined as the time from registration to the documentation of a first failure where a failure is the recurrence (REC) of breast cancer or a diagnosis of a second primary cancer (NEWP); and (2) **overall survival** defined as the time from registration to death due to any cause.

3.0 Patient Eligibility

3.1 Pre-registration – Inclusion Criterion

3.11 Central pathology review submission. This review for MUC1 positivity is mandatory prior to registration to confirm eligibility (see Section 17.0). **It should be initiated as soon as possible after pre-registration.**

3.2 Registration - Inclusion criteria

3.21 Age ≥18 years.

3.22 Completed "standard first line therapy ONLY" (including adjuvant therapy) for breast cancer, clinical stage II and III (≥3 months prior to registration) and currently with no evidence of disease. NOTE: Current use of "anti-estrogen" therapy is allowed. Patients with stage I breast cancer with "high-risk" features, including any of the following, are also eligible for enrollment if other entry criteria are met: HER2 over-expression or amplification, "triple-negative" (i.e., no expression of ER, PR, or over-expression of HER2 on routine immunohistochemical staining).

3.23 Histologically confirmed adenocarcinoma of the breast treated with surgery, adjuvant chemotherapy, and/or radiation therapy.

3.24 MUC1 positive breast cancer as determined by pre-registration central pathology review.

3.25 HLA-A2 positive.

3.26 The following laboratory values obtained ≤14 days prior to registration:
- Hemoglobin ≥8.0 g/dL
- Platelets ≥75,000/μL
- ANC ≥1,500/μL
- Creatinine ≤2 x ULN
- AST ≤2 x ULN

3.27 Capable of understanding the investigational nature, potential risks and benefits of the study and capable of providing valid informed consent.

3.28 Willingness to return to Mayo Clinic Rochester, Scottsdale, or Jacksonville for treatment and study-related follow up. Study treatment will be administered only at the Mayo Clinic site where the patient was enrolled. Post-treatment study follow-up is allowed at the other participating Mayo Clinic sites.

3.29a Willingness to provide the blood specimens and complete the imaging studies as required by the protocol.

Note: The goals of this study include assessment of the biologic effects on surrogate markers of the agent(s) being tested and are, therefore, contingent upon availability of the blood specimens and completion of the required imaging studies.

3.29b Negative serum pregnancy test done ≤7 days prior to registration, for women of childbearing potential only.

3.3 Registration - Exclusion criteria

3.31 ECOG performance status (PS) 3 or 4 (see Appendix I).

3.32 Uncontrolled infection.

3.33 Any of the following:
- Known HIV infection
- Other circumstances (i.e. concurrent use of systemic immunosuppressants and immunocompromising condition) that in the opinion of the physician renders the patient a poor candidate for this trial

3.34 Failure to fully recover from acute, reversible effects of prior breast cancer therapy regardless of interval since last treatment.

3.35 Any of the following:
- Pregnant women
- Nursing women unwilling to stop breast feeding
- Women of childbearing potential who are unwilling to employ adequate contraception (diaphragm, birth control pills, injections, intrauterine device [IUD], or abstinence, etc.)

NOTE: This study involves an investigational agent whose genotoxic,mutagenic and teratogenic effects on the developing fetus and newborn are unknown.

3.36 Other concurrent chemotherapy, immunotherapy, radiotherapy, or any ancillary therapy considered investigational (utilized for a non-FDA-approved indication and in the context of a research investigation).

3.37 Radiographic evidence of disease at the time of enrollment.

3.38 Any prior invasive malignancies ≤5 years (with the exception of curatively-treated basal cell or squamous cell carcinoma of the skin or carcinoma in situ of the cervix).

3.39 Primary surgery for breast cancer **beyond 3 years** at time of registration.

4.0 Test Schedule

Tests and procedures	Active Monitoring Phase				
	Pre-Reg	≤14 days prior to reg	Prior to each subsequent treatment (q 4 weeks)	At 4 weeks after last treatment	Observation q 3 months until disease recurrence or for maximum of 2 years following registration
Central pathology review (see Section 17.1) [5]	X				
History and assessment, wt, PS		X	X[R]	X	X
Height		X			
Hematology group: WBC, ANC, Hgb, PLT		X[R]	X[8]	X[R]	X
Chemistry group: total and direct bilirubin, AST, creatinine		X[R]	X[8]	X[R]	X
HLA class I and II typing [R]		At any time prior to reg			
Serum pregnancy test [1]		X			
Tumor typing [R]		At any time prior to reg			
Tumor evaluation by imaging study (x-ray, CT or PET)		X			X[2]
DTH skin testing (common recall antigens) [3, R]		X	Prior to cycle 6 only		
Research blood specimens [7] See section 14.0		X	X[4]		X[4]
Acute toxicity evaluation [6]			X	X	

1. For women of childbearing potential, must be obtained ≤7 days prior to registration.
2. Imaging will be performed per "standard of care" for patients and at the discretion of the treating physician
3. DTH skin testing will be performed using the same complement of antigens in routine use at the treatment site.
4. Research blood samples will be performed prior to registration, prior to cycles 3, 5 and 6 of therapy as well as every 3 months after conclusion of active therapy until 24 months following registration.
5. Tumor tissues will be stained for MUC1 and HER-2/neu mandatory central review after pre-registration but prior to registration.
6. Acute toxicity evaluations (physical exam and laboratory testing) will be performed for the purpose of evaluating potential immediate side effects of immunization.
7. Research blood specimens will be collected only if serum hemoglobin for the given collection is ≥10 g/dL. If hemoglobin is <10 g/dL, research blood samples will be postponed until the next study office visit.
8. Research funded prior to cycles 2 and 5.

R. Research Funded

5.0 Stratification Factors (*collected at registration*)

Her-2/neu status: Positive vs. negative

6.0 Registration/Randomization Procedures

6.1 Pre-Registration (Step 1)

6.11 To pre-register a patient, access the Mayo Clinic Cancer Center (MCCC) web page and enter the remote registration/randomization application. The remote registration/randomization application is available 24 hours a day, 7 days a week. Back up and/or system support contact information is available on the Web site. If unable to access the Web site, call the MCCC Registration Office at (507)-284-4130 between the hours of 8 a.m. and 4:30 p.m. Central Time (Monday through Friday).

The instructions for remote pre-registration are available on the MCCC web page (http://hsrwww.mayo.edu/ccs/training) and detail the process for completing and confirming patient pre-registration. Users should refer to the section titled "Pre-Registration Components" for details on how to pre-register a patient to a study. At the time of pre-registration the patient will receive a MCCC patient identification number. This number is to be used when submitting tissue or blood samples, if applicable for the study (See Sections 14.0 and/or 17.0). Patient pre-registration via the remote system can be confirmed in any of the following ways:

- Contact the MCCC Registration Office (507)-284-4130. If the patient was pre-registered, the Registration Office staff can access the information from the centralized database and confirm the pre-registration.
- Refer to "Instructions for Remote Registration" in section "Finding/Displaying Information about A Registered Subject."

6.12 Prior to accepting the registration/randomization, the remote registration/randomization application will verify the following:

- IRB approval at the registering institution
- Patient eligibility
- Existence of a signed consent form
- Existence of a signed authorization for use and disclosure of protected health information

6.2 Registration (Step 2)

6.21 To register a patient, access the Mayo Clinic Cancer Center (MCCC) web page and enter the remote registration/randomization application. The remote registration/randomization application is available 24 hours a day, 7 days a week. Back up and/or system support contact information is available on the Web site. If unable to access the Web site, call the MCCC Registration Office at (507) 284-2753 between the hours of 8 a.m. and 5:00 p.m. Central Time (Monday through Friday).

The instructions for remote registration are available on the MCCC web page (http://hsrwww.mayo.edu/ccs/training) and detail the process for completing and confirming patient registration. Prior to initiation of protocol treatment, this process must be completed in its entirety and a MCCC subject ID number must be available as noted in the instructions. It is the responsibility of the individual registering the patient to confirm the process has been successfully completed prior to release of the study agent. Patient registration via the remote system can be confirmed in any of the following ways:

- Contact the MCCC Registration Office (507) 284-2753. If the patient was fully registered, the Registration Office staff can access the information from the centralized database and confirm the registration.
- Refer to "Instructions for Remote Registration" in section "Finding/Displaying Information about A Registered Subject."

6.22 A mandatory translational research component is part of this study. The patient will be automatically registered onto this component (Section *14.0)*.

6.23 A signed HHS 310 form must be on file in the Registration Office before an investigator may register any patients. Ongoing approval documentation must be submitted (no less than annually) to the Registration Office.

6.24 Prior to accepting the registration/randomization, the remote registration/randomization application will verify the following:
- IRB approval at the registering institution
- Patient eligibility

6.25 Treatment on this protocol must commence at Mayo Clinic Rochester, Scottsdale or Jacksonville under the supervision of a medical oncologist or hematologist.

6.26 Treatment cannot begin prior to registration and must begin ≤7 days after registration.

6.27 Pretreatment tests/procedures must be completed within the guidelines specified on the test schedule.

6.28 All required baseline symptoms must be documented and graded.

6.29 Study drug availability checked.

7.0 Protocol Treatment

7.1 For the purposes of this trial, patients will be recruited from the breast cancer practice of the Mayo Clinic Cancer Center. Patients who are undergoing regular follow-up visits by Mayo Clinic oncologists, are interested in this study, and fulfill all eligibility criteria will be offered enrollment. The patients' primary physicians, co-investigators in this study, will have the opportunity to offer the study to interested patients during their regularly scheduled follow-up visits. It is not expected that recruitment or advertisement materials will be used.

The patients who are enrolled will be assigned a 'study number' which will be used for their identification, and that of their data, throughout their participation in the clinical trial.

The Informed Consent process will take place during the patient's regular follow-up visits with their oncologists, co-investigators in the clinical trial. The informed consent interview will begin as part of the patient's regular follow-up visit. At that time, interested patients will be given information about the study, and if interested, will also receive a copy of the Informed Consent document. Patients will have the opportunity to discuss the details of the study during this visit or, more likely, will be given the consent form and offered to review the document at home and schedule a follow-up visit if they are interested in taking part on the study. This way the patients will have a chance to investigate and discuss the study on their own. If interested, the patients will set-up a 2nd visit with their oncologists specifically for the purpose of deciding on study participation. At that visit, all issues of concern for the patient will be addressed, eligibility reviewed and, if appropriate, the Consent Form will be signed.

7.2 As part of the registration process described in Section 6.0, the Mayo Clinic Cancer Center (MCCC) Remote Registration application will assign patients to arms A through C.

7.3 Treatment Schedules:

Arm A

	Agent	Dose	Route	Rx Days	ReRx
Arm A	Montanide ISA-51	1.5 mL	subcutaneous injection in un-dissected LN region	Day 1 of Week 1	Q4 weeks (28-32 days) x 6 cycles
	MUC1 (STAPPVHNV)	1mg			
	HER-2 peptide 1 (ILHNGAYSL)	1mg			
	HER-2 peptide 2 (KVPIKWMALESILRRRF)	1mg			
	GM-CSF	0.225 mg			

Arm B

	Agent	Dose	Route	Rx Days	ReRx
Arm B	Montanide ISA-51	1.5 mL	subcutaneous injection in un-dissected LN region	Day 1 of Week 1	Q4 weeks (28-32 days) x 6 cycles
	MUC1 (STAPPVHNV)	1mg			
	HER-2 peptide-1 (ILHNGAYSL)	1mg			
	HER-2 peptide-2 (KVPIKWMALESILRRRF)	1mg			
	PF-3512676 (CPG7909)	1 mg			

Arm C

	Agent	Dose	Route	Rx Days	ReRx
Arm C	Montanide ISA-51	1.5 mL	subcutaneous injection in un-dissected LN region	Day 1 of Week 1	Q4 weeks (28-32 days) x 6 cycles
	MUC1 (STAPPVHNV)	1mg			
	HER-2 peptide-1 (ILHNGAYSL)	1mg			
	HER-2 peptide-2 (KVPIKWMALESILRRRF)	1mg			
	GM-CSF	0.225 mg			
	PF-3512676 (CPG7909)	1 mg			

7.4 Fifteen patients per arm (total of 45) will be randomly assigned to receive one of the three treatment schedules. Doses will not be escalated in any individual patient. It is not anticipated that there will be toxicity experienced with these regimens.

Vaccines will be administered as multiple (2-3) subcutaneous injections in regions of un-disturbed axillary or inguinal lymph nodes. Each vaccine cycle will be administered into a single lymph node draining area. Subsequent vaccination cycles will be administered to other (rotating) undisturbed lymph node drainage sites.

The main risks are those of an allergic reaction to the components of the peptide vaccine (local or systemic). To minimize risk, patients will be observed by a registered nurse for 30 minutes following each immunization. On-site physicians will be available in the unlikely event that complications do occur. Risks due to phlebotomy will be minimized by ensuring that all patients will undergo phlebotomy by certified phlebotomists. All patients will be provided detailed contact information so that they are able to contact their treating physicians/co-investigators if they experience problems (medical or otherwise) while undergoing therapy in this study.

There are no antidotes available for the peptide vaccines used in this protocol. If patients develop symptoms as a result of the vaccines (e.g. allergic reactions), those patients will be treated accordingly.

The benefit to patients who undergo treatment in this study is unknown.

As IND sponsor, the Principal Investigator will monitor the protocol in accordance with 21 CFR 312, as indicated in portions of section 4.0, the test schedule; section 10.0, the adverse event reporting; and section 15, the drug information.

8.0 Dosage Modification Based on Adverse Events - Adjustments are based on adverse events observed since the prior dose.

ALERT: *ADR reporting may be required for some adverse events (See Section 10)*

→ → *Use Common Terminology Criteria for Adverse Events (CTCAE) v3.0 unless otherwise specified* ← ←			
CTCAE CATEGORY	ADVERSE EVENT	AGENT	DOSAGE CHANGE OR OTHER ACTION
AT TIME OF RETREATMENT			
ALLERGY/ IMMUNOLOGY	≥Grade 2 allergic reaction/ hypersensitivity	Montanide GM-CSF CpG Peptides	Discontinue vaccinations indefinitely and begin observation.
	≥Grade 2 autoimmune reaction (excluding vitiligo)		Discontinue vaccinations indefinitely and begin observation.
Dermatology/Skin	≥Grade 2 injection site reaction		Discontinue vaccinations indefinitely and begin observation.
ALL OTHERS	≥Grade 3 Hematologic or ≥Grade 3 Nonhematologic (excluding alopecia) ≥Grade 2 neurologic		Discontinue vaccinations indefinitely and begin observation.

9.0 Ancillary Treatment/Supportive Care

9.1 Patients should receive blood product support, antibiotic treatment and treatment of other newly diagnosed or concurrent medical conditions.

9.2 Patients participating in this clinical trial are not to be considered for enrollment in any other study involving a pharmacologic agent (drugs, biologics, immunotherapy approaches, gene therapy) whether for symptom control or therapeutic intent.

10.0 Adverse Event (AE) Reporting and Monitoring

10.1 This study will utilize the Common Terminology Criteria for Adverse Events (CTCAE) v3.0 for adverse event monitoring and reporting. The CTCAE v3.0 can be downloaded from the CTEP home page (http://ctep.info.nih.gov/CTC3/ctc_ind_term.htm). All appropriate treatment areas should have access to a copy of the CTCAE v3.0.

10.11 Adverse event monitoring and reporting is a routine part of every clinical trial. First, identify and grade the severity of the event using the CTCAE. Next, determine whether the event is expected or unexpected (refer to Section 15.0 and/or product literature) and if the adverse event is related to the medical treatment or procedure (see Section 10.12). With this information, determine whether an adverse event should be reported as an expedited report (see Section 10.2) or as part of the routinely reported clinical data.

Expedited adverse event reporting requires submission of a written report, but may also involve telephone notifications. Telephone and written reports are to be completed within the timeframes specified in Section 10.2. All expedited adverse event reports should also be submitted to the local Institutional Review Board (IRB).

10.12 Assessment of Attribution

When assessing whether an adverse event is related to a medical treatment or procedure, the following attribution categories are utilized:

Definite - The adverse event *is clearly related* to the investigational agent(s).
Probable - The adverse event *is likely related* to the investigational agent(s).
Possible - The adverse event *may be related* to the investigational agent(s).
Unlikely - The adverse event *is doubtfully related* to the investigational agent(s).
Unrelated - The adverse event *is clearly NOT related* to the investigational agent(s)

10.2 Expedited Adverse Event Reporting Requirements

Phase I, II and III Studies (Investigational)

	Grade 4 or 5[1] Unexpected with Attribution of Possible, Probable, or Definite	Other Grade 4 or 5 or Any hospitalization during treatment[6]	Secondary AML/MDS[2]
Notify the Cancer Center IND Coordinator [3] within 24 hours	X		
Submit written report within 5 working days[4]	X		
NCI/CTEP Secondary AML/MDS Report Form within 15 working days[5]			X
Submit Grade 4 or 5 Non-AER Reportable Events/Hospitalization Form within 5 working days.[6]		**X[6]**	

1. Includes all deaths within 30 days of the last dose of investigational agent regardless of attribution or any death attributed to the agent(s) (possible, probable, or definite) regardless of timeframe.
2. Reporting for this AE required during or after treatment.
3. Notify the Cancer Center IND Coordinator (Mayo Clinic - Rochester) by telephone (507) 284-0938 and/or submit a written event summary via fax to (507) 538-7164.
4. Use *Adverse Event Expedited Report – Single Agent* or *Multiple Agents* report form. Submit to the Cancer Center IND Coordinator (Mayo Clinic - Rochester) and to the Cancer Center Protocol Development Coordinator (PDC) for IRB reporting. The IND Coordinator will review the event in consultation with the IND holder and report to the Food and Drug Administration (FDA) as warranted by the event and required by U.S. federal regulations.
5. Submit per form-specified instructions and provide copy to Cancer Center IND Coordinator for review and FDA reporting (as warranted by the event) and the Cancer Center PDC for IRB reporting.
6. In addition to standard reporting mechanism for this type of event, submit information to the Cancer Center IND Coordinator and Cancer Center PDC. These persons will facilitate FDA and IRB reporting, respectively, as warranted by the event. If Adverse Event Expedited Report – Single Agent or Multiple Agents report form was completed, this form does not need to be completed.

10.3 Adverse events to be graded at each evaluation and pretreatment symptoms/conditions to be evaluated at baseline per Common Terminology Criteria for Adverse Events (CTCAE) v3.0 grading unless otherwise stated in the table below:

CTCAE Category	Adverse event/Symptoms	Baseline	Each evaluation
Constitutional Symptoms	Fatigue (Asthenia, lethargy, malaise)	X	X
Dermatology/Skin	Injection site reaction		X
	Rash/desquamation	X	X
Pain	Musculoskeletal - *Select*s • Bone	X	X
	• Joint	X	X
	• Muscle	X	X

10.31 Submit via appropriate MCCC Case Report Forms (i.e., paper or electronic, as applicable) the following AEs experienced by a patient and not specified in Section 10.3:

10.311 Grade 2 AEs deemed *possibly, probably, or definitely* related to the study treatment or procedure.

10.312 Grade 3, 4, and 5 AEs and deaths within 30 days of the patient's last treatment, regardless of attribution to the study treatment or procedure, with the exception of signs or symptoms of definitely related to the patient's disease or disease progression.

10.313 Any death more than 30 days after the patient's last study treatment or procedure which is felt to be at least possibly treatment related must also be submitted as a Grade 5 AE, with a CTCAE type and attribution assigned.

10.32 Refer to the instructions in the electronic data entry screens regarding the submission of late occurring AEs following completion of the Active Monitoring Phase (i.e., compliance with Test Schedule in Section 4.0).

<u>The following</u> information is included at the request of the Department of Defense, a financial sponsor of the study.

"Major modifications to the research protocol and any modifications that could potentially increase risk to subjects must be submitted to the USAMRMC, Office of Research Protections (ORP), Human Research Protection Office (HRPO) for approval prior to implementation. All other amendments will be submitted with the continuing review report to the USAMRMC ORP HRPO for acceptance."

In addition, any reporting requirements within the protocol or protocol addendum that reference the HSRRB should be replaced with the reporting requirements outlined below.

9. Please note the following reporting obligations:

a. Major modifications to the research protocol and any modifications that could potentially increase risk to subjects must be submitted to the USAMRMC ORP HRPO for approval prior to implementation.

All other amendments must be submitted to the ORP HRPO for acceptance with the continuing review report.

b. All unanticipated problems involving risks to subjects or others, serious adverse events related to study participation, and deaths related to study participation must be reported promptly to the ORP HRPO.

c. Any deviation to the subject protocol that affects the safety or rights of the subject and/or integrity of the study data must be reported promptly to the ORP HRPO.

d. All modifications, deviations, unanticipated problems, adverse events, and deaths must also be reported at the time of continuing review of the protocol.

e. A copy of the continuing review report approved by the Mayo Clinic IRB should be submitted to the ORP HRPO as soon as possible after receipt of approval. It appears that the next continuing review is due no later than 13 October 2009.

f. In addition, the current version of the protocol and consent form (if applicable) should be submitted along with the continuing review report and the Mayo Clinic IRB approval notice for continuation of the protocol.

g. When available, the final study report submitted to the Mayo Clinic IRB, including a copy of any IRB acknowledgement documentation and any supporting documents, must be submitted to the ORP.

11.0 Treatment Evaluation

11.1 For the purposes of this study, patients should be re-evaluated every 4 weeks during immunizations (treatment) and every 12 weeks during follow-up.

11.2 At the time of reevaluation, patients will be classified in the following manner:

11.21 No evidence of disease (NED).

11.22 Breast cancer recurrence (PD). Local/regional breast cancer recurrence is defined as the development of tumor (except LCIS) in the ipsilateral breast (after lumpectomy); in the soft tissue/chest wall and/or skin of the ipsilateral chest wall; or tumor in the ipsilateral internal mammary, infraclavicular, or axillary nodes or soft tissue of ipsilateral axilla. Suspected tumor recurrence in the ipsilateral breast, chest wall structures or lower (level I ± II) axillary nodal areas must be confirmed by biopsy or cytology. Histologic or cytologic confirmation of tumor is recommended for internal mammary or infraclavicular/high axillary nodal recurrence. A distant recurrence is defined as development of tumor in areas other than the local/regional area that is documented by a positive cytology aspirate, biopsy, or imaging studies.

11.23 New primary (NEWP): A new primary is defined as the development of contralateral breast cancer or a second cancer other than squamous or basal cell carcinoma of the skin, carcinoma in situ of the cervix or LCIS of the breast that is histologically confirmed.

11.3 Further treatment after the documentation of a breast cancer recurrence or second primary cancer is left to the discretion of the treating physician.

12.0 Descriptive Factors: None.

13.0 Treatment/Follow–up Decision at Evaluation of Patient

13.1 Patients who have not recurred at time of their reassessment and have not experienced intolerable toxicity may continue protocol treatment at the same dose level for a maximum of 6 cycles or until progression of disease, a second primary or an intolerable adverse event occurs.

13.11 Patients who complete 6 cycles of treatment without disease recurrence, a second primary or intolerable toxicity will go to the observation phase of the study for a maximum of 2 years post randomization. Patients who develop recurrent disease during the observational phase will go to event monitoring phase for a maximum of 2 years post randomization.

13.2 Patients who develop progression of disease, a second primary or intolerable toxicity will be removed from protocol treatment and go to the observation phase of the study. Subsequent treatment is at the discretion of the treating physician.

13.3 Patients may refuse further protocol treatment at any time and go to the event-monitoring phase of the study.

13.4 If a patient is declared ineligible by the study team, on-study material, treatment evaluation forms, an End of Active Treatment/Cancel Notification Form must be submitted. No further follow-up after notification of ineligibility is required.

13.5 If a patient is declared a cancel by the study team before any study treatment is given, on-study material and End of Active Treatment/Cancel Notification Form must be submitted. No further follow-up is required.

13.6 If patient is found on central review to be MUC1 negative, the patient will be considered a cancel. The Pre-Registration Screening Failure Form must be submitted. No further data submission is necessary.

13.7 There will be no replacement of patients who discontinue or are removed from the protocol for any reason.

13.8 A patient is deemed a *cancel* if he/she is removed from study for any reason after pre-registration but prior to registration. The Pre-Registration Screening Failure Form must be submitted. No further data submission is necessary.

14.0 Correlative/Translational Studies

14.1 Description of Assays

Active vaccines for the immunotherapy of solid tumors have met with only limited success. It is our hypothesis that the causes of this failure are multifactorial and can be improved by the inclusion of stringent patient selection criteria, careful dose titration based on immunologic response monitoring, and correlation of immunologically based dosing parameters with clinical outcome. The following sections define the strategies that will be employed in this trial to evaluate immunologic response to MUC1, and HER-2 peptides.

14.11 Immune Responses to T Helper and CTL Epitopes

14.111 Elispot

Estimates of frequencies of peptide-specific, IFNγ- and IL-5-producing cytotoxic T lymphocytes and helper T lymphocytes will be obtained by ELISPOT assays following *in vitro* stimulation with peptide-sensitized stimulator cells [74, 75]. IL-5 production, rather than that of IL-4, will be assayed because of the increased signal:noise ratio [74]. $CD8^+$ and $CD4^+$ T cells will be positively selected by magnetic activated cell sorting (MACS, Miltenyi Biotech) from cryopreserved and thawed peripheral blood lymphocyte buffy coat. Antigen-presenting cells (APCs) will also be isolated from $CD4^-/CD8^-$ cell population by MACS (beads and reagents purchased from Miltenyi Biotech). $CD8^+$ and $CD4^+$ responder T cells will be stimulated with irradiated APCs pulsed with the target peptides used for vaccination. After 5 days of co-culture, the responding cells will be diluted, titrated, and re-stimulated with APCs pulsed with target peptides for 24 hours in 96 well microtiter ELISPOT plates coated with IFNγ- or IL-5-specific capture antibody (ELISPOT Kit purchased from MABTECH, Stockholm, Sweden). The target peptides for re-stimulation include the peptide used for primary stimulation (MUC1 and HER-2 peptides) and a negative control peptide (YIGEVLVSV). The wells are washed and treated with ALP-conjugated secondary antibody and cytokine-producing spots detected using appropriate substrate (all reagents are provided in the kit). After stopping the reaction, the developed microtiter plates are shipped to Zellnet Consulting in New York for evaluation of number of spot-producing cells for each responder cell titration. All analyses are performed by the consulting firm and data provided electronically to the investigator. The difference between the frequency of spot-producing cells obtained with the target peptides and control peptide will determine the frequency of peptide-specific, cytokine-producing $CD4^+$ or $CD8^+$ T cells.

14.112 Tetramers

The estimation of frequencies of CTLs that recognize specific peptides bound to class I molecules became increasingly easier and more quantifiable with the construction and application of class I tetramers [11, 76, 77]. Class I MHC tetramers are composed of a complex of four HLA MHC class I molecules each bound to the specific peptide and conjugated with a fluorescent protein (MHC Tetramer-Streptavidin-Phycoerythrin (SA-PE)). We will use MUC1 M1.1 peptide (STAPPVHNV) and HER-2/neu peptide 9_{435} (ILHNGAYSL). To detect epitope spreading, we will also use HER-2/neu $peptide_{369-377}$ (KIFGSLAFL). As a negative control, we will use the multi-allele negative tetramer from Beckman Coulter (T01044). For positive control we will use the HLA-A0201 CMV PP65 tetramer (NLVPMVATV) from Beckman Coulter (T01009). Tetramers of HLA-A2 molecules are commercially available (Beckman Coulter). On the day of staining, test PBLs are thawed, washed, and resuspended in the manufacturer's recommended staining buffer (PBS) at 1×10^6 cells/ml. Tetramers and any additional antibodies (such as anti-CD8 or anti-CD3 conjugated to a different fluor such as FITC) are added to the cell volumes and incubated for 30 min at room temperature. The cell suspension is then washed with PBS and resuspended in PBS with 0.5% formaldehyde (Fixative Reagent) and analyzed by flow cytometry with FACSCAN instrumentation and CellQuest software (BD Biosciences); a minimum of 5×10^5 cells/sample are analyzed for accurate estimation of $CD8^+$ CTLs with low frequencies. The analysis involves (1) gating on lymphocytes using

forward and side-scatter; (2) gating on FITC-positive PBLs that stain with anti-CD3 or anti-CD8, and (3) analyzing the gated cells for PE and FITC staining. The frequency of doubly stained cells ($tetramer^{+}/CD8^{+}$) will be estimated for each of three replicate tubes for calculation of the mean frequency ($\pm$sd).

14.12 Antigenic Profiling

14.121 Expression of Class I HLA Antigens on tumor tissue.

Initial entry criteria require HLA-A typing of peripheral blood with subsequent confirmation of HLA class I antigen expression on tumor cells by immunohistochemistry. One of the mechanisms by which tumors are postulated to evade the immune response is by down regulation of classical HLA molecules necessary for antigen presentation.

14.122 Tumor Expression of MUC1

Tumor blocks will be used to determine the levels of expression of MUC1 on breast cancer tumor cells obtained at the time of most recent surgical resection. MUC1 expression will be determined by positive staining with one of several antibodies to MUC1 (HMFG-2, BC-2, or B27.29). Negative controls will be incubated with PBS instead of monoclonal antibody. Staining of cytoplasm and plasma membrane will be evaluated. Cells will be considered positive when at least one of these components is stained. Antibody staining patterns will be scored in a semi quantitative manner from +1 to +3.

14.13 Sample Schedule

14.131 Blood

100 mL of blood (about 7 tablespoons) will be collected (heparin) prior to registration, prior to cycles 3, 5 and 7 of therapy as well as every 3 months after conclusion of active therapy until 24 months following registration. Prior to each study blood collection a complete blood count will be performed. If the serum hemoglobin is less than 10.0, the study sample will not be collected. Study sample collection will be postponed for the next study visit.

14.132 Tumor

Tumor blocks will be collected from the patient's most recent surgery prior to study registration. Sections from the tumor blocks will be stained for MUC1. Any/all remaining tissue samples will be returned to the clinical file. Any/all excess samples will be destroyed.

14.14 Sample Preparation

14.141 Blood

Peripheral blood lymphocytes (PBLs) are enriched by flotation over Ficoll-Hypaque and frozen in aliquots in 10% DMSO for storage at -150^{o}C.

Percentages of $CD4^+$ and $CD8^+$ T cells, B cells, monocytes, and dendritic cells are estimated by flow cytometry with a panel of specific monoclonal antibodies. In addition, proliferation assays (3H-thymidine uptake) are performed to estimate T cell responses to polyclonal stimulus (phytohemagglutinin), target antigens (MUC1 and HER-2/neu) and a recall antigen (tetanus toxoid). These two sets of experiments are important for estimating the representation of individual lymphoid populations and evaluating overall T cell responsiveness. $CD8^+$ (CTLs) and $CD4^+$ (HTLs) are positively purified from cryopreserved and thawed PBLs by magnetic bead separation (Miltenyi Biotek). Additionally, serum will be collected and stored from each of these samples. Cells will then be frozen and stored at -150^o for future use.

14.3 Delayed-type hypersensitivity (DTH) skin testing

Skin testing (baseline - prior to registration) will be coordinated at each participating site. A typical panel includes candida, mumps, PPD, and trichophyton. Other antigens may be substituted in the event of antigen unavailability. Patients will return for 1-2 follow-up measurements consistent with site procedures.

15.0 Drug Information

15.1 MUC-1 (STAPPVHNV) - *Investigational supply*

15.11 Other Names: epithelial membrane antigen (EMA), polymorphic epithelial antigen (PEM), DF3 antigen, Ca1, MAM-6, H23

15.12 Formulation and Storage: MUC-1 will be provided as a powder in a glass vial with a Teflon coated stopper. Each vial will contain 1 mg of peptide. The product is frozen at -20^{o}C until use.

15.13 Drug Procurement and Accountability: to be purchased from Clinalfa

15.2 HER-2 Peptide-1 (ILHNGAYSL) - *Investigational supply*

15.21 Other Names: erbB2, neu

15.22 Formulation and Storage: HER-2 Peptide-1 will be provided as a powder in a glass vial with a Teflon coated stopper. Each vial will contain 1 mg of peptide. The product is frozen at –20^{o}C until use.

15.23 Drug Procurement and Accountability: purchased from Clinalfa

15.3 HER-2 Peptide-2 (KVPIKWMALESILRRRF) - *Investigational supply*

15.31 Other Names: erbB2, neu

15.32 Formulation and Storage: HER-2 Peptide 2 will be provided as a powder in a glass vial with a Teflon coated stopper. Each vial will contain 1 mg of peptide. The product is frozen at –20^{o}C until use.

15.33 Drug Procurement and Accountability: purchased from Clinalfa

15.4 Montanide ISA-51 Adjuvant [MONTAN] - *Investigational supply*

15.41 Formulation and Storage

Montanide ISA-51 or Montanide ISA-51 VG is an oil-based adjuvant product similar to Incomplete Freund's Adjuvant. When mixed with a water-based solution at a 1:1 w/w ratio, it forms a water-in-oil emulsion. It consists of highly purified oil, Drakol VR, and a surfactant, mannide oleate. Montanide ISA-51 is manufactured by Seppic, Inc., and is provided in amber glass ampoules or vials containing 3 mL of the solution. Montanide ISA-51 or Montanide ISA-51 VG will be purchased from Seppic Inc.

15.42 Mode of Action

Acts to enhance immune response to vaccination; the precise mode of action is unknown.

15.43 Storage and Stability

The solution is stored at controlled room temperature. Exposure to cold temperatures may result in a clouded solution, which should be discarded. An expiration date is printed on the ampoule label.

15.44 Compatibilities/Incompatibilities

The oil may break down the rubber tip of the plunger on syringes; it is advisable to use a different syringe for each ampoule or vial. Do not allow the Montanide ISA-51 to be in direct contact with the rubber tip of the plunger for more time than is necessary to withdraw the solution and inject it into the peptide vial. Fresh syringes will be needed to withdraw the emulsified vaccine from the vaccine vial. Once the emulsion is made, there is less interaction of the oil directly with the rubber tip of the plunger.

15.45 Drug Procurement and Accountability

Montanide ISA-51 will be purchased from Seppic Inc. using study grant funds.

15.5 GM-CSF (sargramostim, Leukine®)

15.51 Preparation and Storage

Liquid sargramostim (used in this study) is available in vials containing 500 mcg/mL (2.8×10^6 IU/mL) sargramostim. LEUKINE liquid should be refrigerated at 2-8°C (36-46°F). Do not freeze or shake. Do not use beyond the expiration date printed on the vial.

15.52 Known Potential Toxicities

Fever, chills, asthenia, malaise, numbness, increased sensitivity to touch, loss of balance, dizziness, rash, peripheral edema, dyspnea, headache, pericardial effusion, bone pain, arthralgia, nausea, vomiting, loss of appetite, developing or worsening of kidney or liver problems, difficulty breathing, shortness of breath, redness of the skin, facial flushing, rapid or irregular heartbeat or other heart problems, low blood pressure, myalgia, and serious allergic reactions such as a severe asthmas attack.

15.53 Drug Procurement:

Leukine 500 mcg vials are available commercially. Drug will be purchased for this project using study grant funds. Patients will not be charged for the GM-CSF.

15.6 CpG-7909 (PF-3512676, Pfizer Pharmaceuticals, Inc)

15.61 Preparation and Storage: PF-3512676 (Injection) is formulated as a sterile phosphate buffered saline solution suitable for parenteral administration. This sterile and pyrogen-free solution contains no preservatives; vials are intended for single entry to prevent contamination. The drug product is packaged in clear, type I USP glass vials with Teflon-coated stopper closures and flip-caps. The drug product should be stored under refrigeration (2 to 8^{o}C). Each vial provides 15mg/mL (1.2mL fill volume).

15.62 Known potential toxicities: The list of reported serious adverse events with the use of CpG-7909 demonstrates the following toxicities:

15.621 **Related**: reactive follicular lymphatic hyperplasia.

15.622 **Possibly Related**: anemia, superior vena cava syndrome, dyspnea, malignant ascites, post-operative bleeding, hepatic failure, renal failure, post-operative wound infection, GI hemorrhage, prolonged coagulation time, bacteriemia, ureteric obstruction, congestive heart failure, DVT, vomiting, dehydration, vein compression, hydronephrosis, urinary retention, proctalgia, hypercalcemia, pleural effusion, subacute inflammatory demyelinating polyneuropathy, pelvic inflammatory disease, unstable angina, myocardial infarction, atrial fibrillation and grand mal seizures.

15.63 Drug Procurement: will be provided free of charge by Pfizer Pharmaceuticals, Inc.

15.7 Vaccine Preparation Instructions

15.71 General Vaccine Preparation Information

Emulsify the peptide(s)/GM-CSF and/or CpG mixture with Montanide ISA-51. Prepare the vials as directed for each group below. Because neither the peptide solution nor the Montanide ISA-51 contains preservatives or bacteriostatics, the prepared peptide vaccines should be administered as soon as possible.

15.711 Arm A

Remove one vial of Montanide ISA-51 or Montanide ISA-51 VG from the study supply. Remove one vial each of MUC1, HER-2 peptide 1, and HER-2 peptide 2 from the freezer and allow them to reach room temperature. Remove a vial of liquid GM-CSF (500 mcg/mL) from the refrigerator and allow to reach room temperature. Withdraw 0.5 mL (250 mcg) of GM-CSF and add to one of the peptide vials. Add 0.5 mL of Sterile Water for Injection to a second peptide vial and 0.5 mL of Sterile Water for Injection to a the third peptide vial. Swirl the vials to dissolve the powder in each vial. Use a 5-6 mL latex-free or glass syringe to withdraw the entire solution from each vial. Attach a stopcock to the syringe. The stopcock should have the off-lever pointed toward the male connector. Use a second 5-6 mL latex-free or glass syringe to withdraw 1.5

mL from the Montanide vial. Attach this syringe to the stopcock. Inject the peptide solution into the syringe containing the Montanide. Continue injecting the mixture back and forth between the two syringes for approximately 5 minutes. Test the emulsion by adding a drop to the surface of chilled sterile water. If the drop disperses over the surface of the water, continue mixing and re-test. This test may be repeated twice. Load two 3 mL syringes with equal volumes of this emulsion prior to use. The nurse will administer the vaccine mixture to the patient as soon as possible.

Arm B

Remove one vial of Montanide ISA-51 or Montanide ISA-51 VG from the study supply. Remove one vial each of MUC1, HER-2 peptide 1, and HER-2 peptide 2 from the freezer and allow them to reach room temperature. Remove a vial of liquid CpG-7909 (PF-3512676, 15mg/mL) from the refrigerator and allow to reach room temperature. Withdraw 0.14 mL of CpG-7909 (approximately 2.1 mg) and add to one of the peptide vials. Add 0.35 mL sterile water to the same vial. Add 0.5 mL of Sterile Water for Injection to a second peptide vial and 0.5 mL of Sterile Water for Injection to the third peptide vial. Swirl the vials to dissolve the powder in each vial. Use a 5-6 mL latex-free or glass syringe to withdraw the intire solution from easch vial. Attach a stopcock to the syringe. The stopcock should have the off-lever pointed toward the male connector. Use a second 5-6 mL latex-free or glass syringe to withdraw 1.5 mL from the Montanide vial Attach this syringe to the stopcock. Inject the peptide solution into the syringe containing the Montanide. Continue injecting the mixture back and forth between the two syringes for approximately 5 minutes. Test the emulsion by adding a drop to the surface of chilled sterile water. If the drop disperses over the surface of the water, continue mixing and re-test. This test may be repeated twice. Load two 3 mL syringes with equal volumes of this emulsion prior to use. The nurse will administer the vaccine mixture to the patient as soon as possible.

Arm C

Remove one vial of Montanide ISA-51 or Montanide ISA-51 VG from the study supply. Remove one vial each of MUC1, HER-2 peptide 1, and HER-2 peptide 2 from the freezer and allow them to reach room temperature. Remove a vial of liquid GM-CSF (500 mcg/mL) from the refrigerator and allow it to reach room temperature. Remove a vial of liquid CpG-7909 (PF-3512676 15mg/mL) from the refrigerator and allow it to reach room temperature. Withdraw 0.14mL of CpG-7909 (approximately 2.1 mg) and add to one of the peptide vials. Add 0.35 mL sterile water to the same vial. Add 0.4 mL (225 mcg) of GM-CSF to a second peptide vial.

Add 0.5 mL of Sterile Water for Injection to the third peptide vial. Swirl the vials to dissolve the powder in each vial. Use a 5-6 mL latex-free or glass syringe to withdraw the entire solution from each vial. Attach a stopcock to the syringe. The stopcock should have the off-lever pointed toward the male connector. Use a second 5-6 mL latex-free or glass syringe to withdraw 1.5 mL from the Montanide vial Attach this syringe to the stopcock. Inject the peptide solution into the syringe containing the Montanide. Continue injecting the mixture back and forth between the two

syringes for approximately 5 minutes. Test the emulsion by adding a drop to the surface of chilled sterile water. If the drop disperses over the surface of the water, continue mixing and re-test. This test may be repeated twice. Load two 3 mL syringes with equal volumes of this emulsion prior to use. The nurse will administer the vaccine mixture to the patient as soon as possible.

15.8 Vaccine Administration Information

15.81 Dose Specifics

Each peptide vaccine will consist of a total volume of approximately 2 - 3 mL, containing the correct dose of the peptide(s), and/or GM-CSF and/or CpG. Be sure to confirm the proper cohort and dose level before preparing the product.

15.82 Administration

Vaccinations will be given subcutaneously on day 1 of each treatment cycle. Due to the large volume, each peptide vaccine is administered in 2 shots in a contiguous location in the vicinity of one of the major nodal basins. This basin must not have been dissected.

15.9 Vaccine Side Effects:

15.91 Because of the low dose of GM-CSF used and the slow release nature of the vaccine emulsion, side effects normally seen with systemic treatment doses of GM-CSF should not play a factor in this vaccination treatment. Expected side effects are related to the peptides and Montanide ISA-51. It is possible that the GM-CSF and CpG-7909 may potentiate the reaction seen at the injection site.

15.92 Dermatology/Skin: Injection site reaction, rare granuloma formation, possible development or worsening of pre-existing vitiligo, rash.

15.93 Hepatic: transient rises in liver transaminases.

15.94 Constitutional: Low-grade fever.

16.0 Statistical Considerations and Methodology

16.1 Study goals:

- **Primary goal**: to determine the safety and immunization efficacy of MUC1 and HER-2/neu peptide vaccines combined with CpG, GM-CSF or both, as immune adjuvants suspended in Montanide ISA-51.

- **Secondary goal**: to describe the impact of immunization on clinical outcomes in patients with MUC1 positive breast cancer.

16.2 The study design chosen for this proposal is a stratified randomized design.

16.21 Patients randomized prior to the implementation of Addendum 1
Toxicities will be carefully monitored and accrual will be suspended if 2 or more of the first six patients experience a grade 4 hematologic toxicity lasting for 5 or more days. In

the event of at least two patients experiencing immunologic toxicity ≥ grade 2 or any toxicity ≥ grade 3 accrual will be temporarily suspended for the given treatment arm.

16.22 Patients randomized after the implementation of Addendum 1

Toxicities will be carefully monitored and accrual will be suspended if 2 or more of the first six patients experience a grade 4 hematologic toxicity lasting for 5 or more days. In the event of at least two patients experiencing immunologic toxicity ≥ grade 2 or any toxicity ≥ grade 3 accrual will be temporarily suspended for the given treatment arm.

16.2 Accrual: Fifteen eligible patients with MUC1/HER-2 positive breast cancer and no evidence of disease will be randomized to each of the 3 treatment schedules. We anticipate 20% of the patients who pre-register to this study will be found not to have MUC-1 positive disease and 5% of the patients who do have MUC-1 positive disease will either cancel participation prior to starting treatment or will be found to be ineligible. As such, we anticipate preregistering 58 patient to obtain 45 eligible patients who will sign a consent form and start study treatment.

Patients will be assigned to treatment using a dynamic allocation procedure that balances the marginal distribution of type of dominant disease between treatments. The expected accrual rate for this study is approximately 15-20 patients per year at Mayo Clinic Rochester, 5-7 patients per year at Mayo Clinic Arizona and 5-7 patients per year at Mayo Clinic Florida. Enrollment is expected to extend approximately 2.5 years.

16.3 Study Endpoints:

16.41 Primary Endpoints

16.411 The immunologic parameters of interest are: (1) the percentage of CD4+ T cells, CD8+ T cells, B cells, monocytes, and dendritic cells in a patient's peripheral blood sample as estimated by flow cytometry with a panel of monoclonal antibodies and (2) the frequency of both peptide-specific IFN-gamma producing T cells and peptide-specific IL-5 producing T cells estimated by ELISPOT assays following *in vitro* stimulation with peptide-sensitized stimulator cells for the MUC1 and HER-2 peptides.

16.412 The number and severity of hematologic and non-hematologic toxicities reported using the NCI-CTC version 3.0 criteria

16.42 Secondary Endpoints

16.421 Disease-free survival is defined as the time from registration to the documentation of a first failure where a failure is the recurrence (REC) of breast cancer or a diagnosis of a second primary cancer (NEWP).

16.422 Overall survival is defined as the time from registration to death due to any cause.

16.43 Immunologic Parameters

16.431 All eligible patients who have completed one cycle of treatment are evaluable for the analysis of the immunologic parameters.

16.432 For each of the immunologic parameters, a plot of the parameter level against time will be constructed such that each patient is represented by a line connecting that patient's data points. These plots will enable visual assessment of patterns of change and variability within a parameter as well as a visual assessment of whether the immunologic parameters peak or fall at similar time points.

16.433 Also, for each of the immunologic parameters, a plot of the percent change from pre-treatment levels against time will be constructed such that each patient is represented by a line connecting that patient's data points. These plots will enable visual assessment of time trends within a parameter controlling for pretreatment levels.

16.44 Adverse Events

16.441 All eligible patients who received at least one vaccination are evaluable for toxicity.

16.442 The frequency of those hematologic and non-hematologic toxicities considered at least possibly related to treatment will be tabulated by severity.

16.443 The circumstances surrounding any treatment-related death will be reported.

16.444 As this is a pilot study, no formal hypothesis tests comparing treatment schedules are planned. An immunization strategy will be considered for further testing if at least 70% patients treated with that strategy had a ≥2-fold increase in the percentage of vaccine-peptide specific CD8+ T cells during the course of treatment, with tolerable toxicity.

16.445 The principal investigator and study statistician will review the study every 3 months to identify potential accrual, toxicity, or endpoint problems. In addition, this study will be monitored by the Cancer Center Data Safety Monitoring Board. All patient related clinical data will be entered and maintained online, with reports generated as needed to comply with reporting guidelines.

16.446 It should be noted that representatives of the U.S. Army Medical Research and Merial Command are eligible to review research records as a part of their responsibility to protect human subjects in research.

16.447 If the protocol requires any modifications, deviations or termination prior to completion, all administrative activities will comply with the Protocol Review and Monitoring System of the Mayo Clinic Comprehensive Cancer Center. In addition, all local IRB communications, including deviations from protocol, will be forwarded to the Department of Defense HSRRB, upon local approval.

16.45 Inclusion of Minorities

This study will be available to all eligible patients, regardless of race or ethnic group. There is no information currently available regarding differential agent effects in subjects defined by gender, race, or ethnicity. The planned analyses will, as always,

look for differences in treatment effect based on racial groupings. The sample sizes of this pilot study, however, are not sufficient to provide power for such subset analyses.

To predict the characteristics of patients likely to enroll in this trial we have reviewed registration to (non-North American Breast Cancer Intergroup) NCCTG breast cancer clinical trials by race. This revealed that roughly 3% of patients registered into cancer trials during the past five years could be classified as minorities, which would suggest that only 1 or 2 patients in the study sample are expected to be classified as minorities. This small sample precludes the possibility of a separate subset analysis beyond simple inspection of results for the 1 or 2 minority patients.

17.0 Pathology Considerations for Pre-registration Central Pathology Review

17.1 There will be a central pre-registration review of MUC-1 expression.

17.11 The following materials are to be submitted.

- Central Testing of MUC1 Expression Form
- Surgical Pathology and Operative Report
- One H&E and 6 unstained slides

Slides should be placed in appropriate slide container and labeled with the protocol number, study patient number, and patient initials. Slides will be stained in Dr. Sandra Gendler's lab. All samples should be submitted to:

Cathy S. Madsen
Senior Research Technologist for Dr. Sandra Gendler
Mayo Clinic Scottsdale
Johnson Research Building SCJ 2-221
13400 E. Shea Blvd.
Scottsdale AZ 85259

Notify Cathy S. Madsen by phone (79)2-6064, or e-mail (cathy.madsen@mayo.edu) that samples have been shipped.

The slides will be logged and forwarded to Dr. Ann McCullough in Scottsdale for central pre-registration review of MUC1 expression.

Slides and correlating paperwork will be returned to Cathy Madsen for Dr. Gendler's lab.

1 8.0 Records and Data Entry Procedures

18.1 Data Entry Timetable

Forms	Active-Monitoring Phase (Compliance with Test Schedule)				Event-Monitoring Phase [1] (Completion of Active-Monitoring Phase)				At Each Occurrence			
		Initial material	Follow-up material									
	Pre-Reg	≤2 weeks after registration	At each evaluation	At end of treatment	q.3 months until PD	At PD	After PD q.3 mos.	Death	ADR/ AER	New Primary	Grade 4 or 5 Non-AER Reportable Events/ Hospitalization	Late Adverse Event
On-Study Form		X										
Blood Specimen Submission Form [2]		X	X									
Pathology Materials (see Section 17.0)	X											
Pre-reg Screening Failure Form [8]	X											
Baseline Adverse Events Form		X										
Measurement Form		X	X	X								
Evaluation/Treatment Form			X[7]	X								
Evaluation/Observation Form			X[5]									
DTH Laboratory Form [3]		X	X									
Interval Laboratory Form [4]		X	X	X								
Adverse Event Form			X	X								
End of Active Treatment/ Cancel Notification Form		X[6]		X								
Event Monitoring Form				X	X	X	X	X		X		X
Concurrent Treatment Form		X	X	X								
ADR/AER (See Section 10)									X			
Secondary AML/MDS Report Form (See Section 10)									X			
Grade 4 or 5 Non-AER Reportable Events/Hospitalization Form (See Section 10.0)											X	

1. If a patient is still alive 2 years after registration, no further follow-up is required.
2. Research blood samples will be performed prior to registration, prior to cycles 3, 5, and 7 of therapy as well as every 3 months after conclusion of active therapy until 24 months following registration.
3. At baseline and prior to cycle 6 only.
4. At baseline, prior to each subsequent treatment and at 4 weeks after last treatment.
5. Complete at each evaluation during Observation (see Section 4.0).
6. Submit if withdrawal/refusal prior to beginning protocol therapy occurs.
7. Complete at each evaluation during Active Treatment (see Section 4.0).
8. Complete only if patient is NOT registered after he/she is pre-registered

19.0 Budget Considerations

19.1 Costs charged to patient: routine clinical care.

19.2 Tests and procedures to be research funded: HLA typing, tumor typing. DTH testing and serum pregnancy tests. Funding will be provided by the Department of Defense (DOD).

20.0 References

1. Morton, D.L., E.C. Hsueh, R. Essner, L.J. Foshag, S.J. O'Day, A. Bilchik, R.K. Gupta, D.S. Hoon, M. Ravindranath, J.A. Nizze, G. Gammon, L.A. Wanek, H.J. Wang, and R.M. Elashoff, Prolonged survival of patients receiving active immunotherapy with Canvaxin therapeutic polyvalent vaccine after complete resection of melanoma metastatic to regional lymph nodes. (2002) Ann Surg. 236:438-48; discussion 448-9.

2. Apostolopoulos, V., G.A. Pietersz, and I.F. McKenzie, MUC1 and breast cancer. (1999) Curr Opin Mol Ther. 1:98-103.

3. Disis, M.L., T.A. Gooley, K. Rinn, D. Davis, M. Piepkorn, M.A. Cheever, K.L. Knutson, and K. Schiffman, Generation of T-cell immunity to the HER-2/neu protein after active immunization with HER-2/neu peptide-based vaccines. (2002) J Clin Oncol. 20:2624-32.

4. Chomez, P., O. De Backer, M. Bertrand, E. De Plaen, T. Boon, and S. Lucas, An overview of the MAGE gene family with the identification of all human members of the family. (2001) Cancer Res. 61:5544-51.

5. Schlom, J., J. Kantor, S. Abrams, K.Y. Tsang, D. Panicali, and J.M. Hamilton, Strategies for the development of recombinant vaccines for the immunotherapy of breast cancer. (1996) Breast Cancer Res Treat. 38:27-39.

6. Townsend, A. and H. Bodmer, Antigen recognition by class I-restricted T lymphocytes. (1989) Annu Rev Immunol. 7:601-24.

7. Tsai, V., I. Kawashima, E. Keogh, K. Daly, A. Sette, and E. Celis, In vitro immunization and expansion of antigen-specific cytotoxic T lymphocytes for adoptive immunotherapy using peptide-pulsed dendritic cells. (1998) Crit Rev Immunol. 18:65-75.

8. Tsai, V., S. Southwood, J. Sidney, K. Sakaguchi, Y. Kawakami, E. Appella, A. Sette, and E. Celis, Identification of subdominant CTL epitopes of the GP100 melanoma-associated tumor antigen by primary in vitro immunization with peptide-pulsed dendritic cells. (1997) J Immunol. 158:1796-802.

9. Nestle, F.O., S. Alijagic, M. Gilliet, Y. Sun, S. Grabbe, R. Dummer, G. Burg, and D. Schadendorf, Vaccination of melanoma patients with peptide- or tumor lysate-pulsed dendritic cells. (1998) Nat Med. 4:328-32.

10. Cerundolo, V., Use of major histocompatibility complex class I tetramers to monitor tumor-specific cytotoxic T lymphocyte response in melanoma patients. (2000) Cancer Chemother Pharmacol. 46 Suppl:S83-5.

11. Altman, J.D., P.A. Moss, P.J. Goulder, D.H. Barouch, M.G. McHeyzer-Williams, J.I. Bell, A.J. McMichael, and M.M. Davis, Phenotypic analysis of antigen-specific T lymphocytes. (1996) Science. 274:94-6.

12. Amoscato, A.A., D.A. Prenovitz, and M.T. Lotze, Rapid extracellular degradation of synthetic class I peptides by human dendritic cells. (1998) J Immunol. 161:4023-32.

13. Nair, S.K., D. Snyder, B.T. Rouse, and E. Gilboa, Regression of tumors in mice vaccinated with professional antigen-presenting cells pulsed with tumor extracts. (1997) Int J Cancer. 70:706-15.

14. Zotter, S., P.C. Hageman, A. Lossnitzer, W.J. Mooi, and J. Hilgers, Tissue and tumor distribution of human polymorphic epithelial mucin. (1988) Cancer Reviews. 11-12:55-101.

15. Girling, A., J. Bartkova, J. Burchell, S. Gendler, C. Gillet, and J. Taylor-Papadimitriou, A core protein epitope of the polymorphic epithelial mucin detected by the monoclonal antibody SM-3 is selectively exposed in a range of primary carcinomas. (1989) Int J Cancer. 43:1072-1076.

16. Croce, M.V., M.T. Isla-Larrain, C.E. Rua, M.E. Rabassa, S.J. Gendler, and A. Segal-Eiras, Patterns of MUC1 tissue expression defined by an anti-MUC1 cytoplasmic tail monoclonal antibody in breast cancer. (2003) J Histochem Cytochem. 51:781-8.

17. Treon, S.P., J.A. Mollick, M. Urashima, G. Teoh, D. Chauhan, A. Ogata, N. Raje, J.H.M. Hilgers, L. Nadler, A.R. Belch, L.M. Pilarski, and K.C. Anderson, MUC1 core protein is expressed on multiple myeloma cells and is induced by dexamethasone. (1999) Blood. 93:1287-1298.

18. Brossart, P., A. Schneider, P. Dill, T. Schammann, F. Grunebach, S. Wirths, L. Kanz, H.J. Buhring, and W. Brugger, The epithelial tumor antigen MUC1 is expressed in hematological malignancies and is recognized by MUC1-specific cytotoxic T-lymphocytes. (2001) Cancer Res. 61:6846-50.

19. Gendler, S.J., MUC1, the renaissance molecule. (2001) J Mammary Gland Biol Neoplasia. 6:339-53.

20. Barnd, D.L., M.S. Lan, R.S. Metzgar, and O.J. Finn, Specific, major histocompatibility complex-unrestricted recognition of tumor-associated mucins by human cytotoxic T cells. (1989) Proc Natl Acad Sci U S A. 86:7159-63.

21. Finn, O.J., K.R. Jerome, R.A. Henderson, G. Pecher, N. Domenech, J. Magarian-Blander, and S.M. Barratt-Boyes, MUC-1 epithelial tumor mucin-based immunity and cancer vaccines. (1995) Immunological Reviews. 145:61-89.

22. Takahashi, T., Y. Makiguchi, Y. Hinoda, H. Kakiuchi, N. Nakagawa, K. Imai, and A. Yachi, Expression of MUC1 on myeloma cells and induction of HLA-unrestricted CTL against MUC1 from a multiple myeloma patient. (1994) J Immunol. 153:2102-9.

23. Noto, H., T. Takahashi, Y. Makiguchi, T. Hayashi, Y. Hinoda, and K. Imai, Cytotoxic T lymphocytes derived from bone marrow mononuclear cells of multiple myeloma patients recognize an underglycosylated form of MUC1 mucin. (1997) Int Immunol. 9:791-8.

24. Domenech, N., R.A. Henderson, and O.J. Finn, Identification of an HLA-A11-restricted epitope from the tandem repeat domain of the epithelial tumor antigen mucin. (1995) J Immunol. 155:4766-74.

25. Agrawal, B., M.A. Reddish, and B.M. Longenecker, In vitro induction of MUC-1 peptide-specific type 1 T lymphocyte and cytotoxic T lymphocyte responses from healthy multiparous donors. (1996) J Immunol. 157:2089-95.

26. Apostolopoulos, V., J.S. Haurum, and I.F.C. McKenzie, Muc1 Peptide Epitopes Associated With Five Different H-2 Class I Molecules. (1997) Eur J Immunol. 27:2579-2587.

27. Apostolopoulos, V., V. Karanikas, J.S. Haurum, and I.F. McKenzie, Induction of HLA-A2-restricted CTLs to the mucin 1 human breast cancer antigen. (1997) J Immunol. 159:5211-8.

28. Reddish, M., G.D. MacLean, R.R. Koganty, J. Kan-Mitchell, V. Jones, M.S. Mitchell, and B.M. Longenecker, Anti-MUC1 class I restricted CTLs in metastatic breast cancer patients immunized with a synthetic MUC1 peptide. (1998) Int J Cancer. 76:817-23.

29. Mukherjee, P., A.R. Ginardi, C.S. Madsen, C.J. Sterner, M.C. Adriance, M.J. Tevethia, and S.J. Gendler, Mice with spontaneous pancreatic cancer naturally develop MUC1-specific CTLs that eradicate tumors when adoptively transferred. (2000) J Immunol. 165:3451-3460.

30. Mukherjee, P., C.S. Madsen, A.R. Ginardi, T.L. Tinder, F. Jacobs, J. Parker, B. Agrawal, B.M. Longenecker, and S.J. Gendler, Mucin 1-specific immunotherapy in a mouse model of spontaneous breast cancer. (2003) J Immunother. 26:47-62.

31. Mukherjee, P., A.R. Ginardi, T.L. Tinder, C.J. Sterner, and S.J. Gendler, MUC1-specific CTLs eradicate tumors when adoptively transferred in vivo. (2001) Clin Can Res. 7:848s-855s.

32. Mukherjee, P., A.R. Ginardi, C.S. Madsen, T.L. Tinder, F. Jacobs, J. Parker, B. Agrawal, B.M. Longenecker, and S.J. Gendler, MUC1-specific CTLs are non-functional within a pancreatic tumor microenvironment. (2003) Glycoconj J. 18:931-942.

33. Brossart, P., K.S. Heinrich, G. Stuhler, L. Behnke, V.L. Reichardt, S. Stevanovic, A. Muhm, H.G. Rammensee, L. Kanz, and W. Brugger, Identification of HLA-A2-restricted T-cell epitopes derived from the MUC1 tumor antigen for broadly applicable vaccine therapies. (1999) Blood. 93:4309-17.

34. Slamon, D.J., W. Godolphin, L.A. Jones, J.A. Holt, S.G. Wong, D.E. Keith, W.J. Levin, S.G. Stuart, J. Udove, A. Ullrich, and et al., Studies of the HER-2/neu proto-oncogene in human breast and ovarian cancer. (1989) Science. 244:707-12.

35. Yokota, J., T. Yamamoto, K. Toyoshima, M. Terada, T. Sugimura, H. Battifora, and M.J. Cline, Amplification of c-erbB-2 oncogene in human adenocarcinomas in vivo. (1986) Lancet. 1:765-7.

36. Clark, G.M. and W.L. McGuire, Follow-up study of HER-2/neu amplification in primary breast cancer. (1991) Cancer Res. 51:944-8.

37. Revillion, F., J. Bonneterre, and J.P. Peyrat, ERBB2 oncogene in human breast cancer and its clinical significance. (1998) Eur J Cancer. 34:791-808.

38. Disis, M.L., K.L. Knutson, K. Schiffman, K. Rinn, and D.G. McNeel, Pre-existent immunity to the HER-2/neu oncogenic protein in patients with HER-2/neu overexpressing breast and ovarian cancer. (2000) Breast Cancer Res Treat. 62:245-52.

39. Disis, M.L., S.M. Pupa, J.R. Gralow, R. Dittadi, S. Menard, and M.A. Cheever, High-Titer Her-2/Neu Protein-Specific Antibody Can Be Detected In Patients With Early-Stage Breast Cancer. (1997) Journal of Clinical Oncology. 15:3363-3367.

40. Kawashima, I., S.J. Hudson, V. Tsai, S. Southwood, K. Takesako, E. Appella, A. Sette, and E. Celis, The multi-epitope approach for immunotherapy for cancer: identification of several CTL epitopes from various tumor-associated antigens expressed on solid epithelial tumors. (1998) Hum Immunol. 59:1-14.

41. Vanderlugt, C.L. and S.D. Miller, Epitope spreading in immune-mediated diseases: implications for immunotherapy. (2002) Nat Rev Immunol. 2:85-95.

42. Butterfield, L.H., A. Ribas, V.B. Dissette, S.N. Amarnani, H.T. Vu, D. Oseguera, H.J. Wang, R.M. Elashoff, W.H. McBride, B. Mukherji, A.J. Cochran, J.A. Glaspy, and J.S. Economou, Determinant spreading associated with clinical response in dendritic cell-based immunotherapy for malignant melanoma. (2003) Clin Cancer Res. 9:998-1008.

43. McRae, B.L., C.L. Vanderlugt, M.C. Dal Canto, and S.D. Miller, Functional evidence for epitope spreading in the relapsing pathology of experimental autoimmune encephalomyelitis. (1995) J Exp Med. 182:75-85.

44. Vanderlugt, C.L., K.L. Neville, K.M. Nikcevich, T.N. Eagar, J.A. Bluestone, and S.D. Miller, Pathologic role and temporal appearance of newly emerging autoepitopes in relapsing experimental autoimmune encephalomyelitis. (2000) J Immunol. 164:670-8.

45. Swain, S.L., Regulation of the generation and maintenance of T-cell memory: a direct, default pathway from effectors to memory cells. (2003) Microbes Infect. 5:213-9.

46. Schoenberger, S.P., R.E. Toes, E.I. van der Voort, R. Offringa, and C.J. Melief, T-cell help for cytotoxic T lymphocytes is mediated by CD40-CD40L interactions. (1998) Nature. 393:480-3.

47. Ridge, J.P., F. Di Rosa, and P. Matzinger, A conditioned dendritic cell can be a temporal bridge between a CD4+ T- helper and a T-killer cell [see comments]. (1998) Nature. 393:474-8.

48. Bennett, S.R., F.R. Carbone, F. Karamalis, R.A. Flavell, J.F. Miller, and W.R. Heath, Help for cytotoxic-T-cell responses is mediated by CD40 signalling. (1998) Nature. 393:478-80.

49. Riddell, S.R., K.S. Watanabe, J.M. Goodrich, C.R. Li, M.E. Agha, and P.D. Greenberg, Restoration of viral immunity in immunodeficient humans by the adoptive transfer of T cell clones. (1992) Science. 257:238-41.

50. Heslop, H.E., C.Y. Ng, C. Li, C.A. Smith, S.K. Loftin, R.A. Krance, M.K. Brenner, and C.M. Rooney, Long-term restoration of immunity against Epstein-Barr virus infection by adoptive transfer of gene-modified virus-specific T lymphocytes. (1996) Nat Med. 2:551-5.

51. Mailliard, R.B., S. Egawa, Q. Cai, A. Kalinska, S.N. Bykovskaya, M.T. Lotze, M.L. Kapsenberg, W.J. Storkus, and P. Kalinski, Complementary dendritic cell-activating function of CD8+ and CD4+ T cells: helper role of CD8+ T cells in the development of T helper type 1 responses. (2002) J Exp Med. 195:473-83.

52. Disis, M.L., E. Calenoff, G. McLaughlin, A.E. Murphy, W. Chen, B. Groner, M. Jeschke, N. Lydon, E. McGlynn, R.B. Livingston, and et al., Existent T-cell and antibody immunity to HER-2/neu protein in patients with breast cancer. (1994) Cancer Res. 54:16-20.

53. Disis, M.L., H. Bernhard, F.M. Shiota, S.L. Hand, J.R. Gralow, E.S. Huseby, S. Gillis, and M.A. Cheever, Granulocyte-macrophage colony-stimulating factor: an effective adjuvant for protein and peptide-based vaccines. (1996) Blood. 88:202-10.

54. Cheever, M.A., M.L. Disis, H. Bernhard, J.R. Gralow, S.L. Hand, E.S. Huseby, H.L. Qin, M. Takahashi, and W. Chen, Immunity to oncogenic proteins. (1995) Immunol Rev. 145:33-59.

55. Disis, M.L. and M.A. Cheever, HER-2/neu protein: a target for antigen-specific immunotherapy of human cancer. (1997) Adv Cancer Res. 71:343-71.

56. Tuttle, T.M., B.W. Anderson, W.E. Thompson, J.E. Lee, A. Sahin, T.L. Smith, K.H. Grabstein, J.T. Wharton, C.G. Ioannides, and J.L. Murray, Proliferative and cytokine responses to class II HER-2/neu-associated peptides in breast cancer patients. (1998) Clin Cancer Res. 4:2015-24.

57. Fisk, B., J.M. Hudson, J. Kavanagh, J.T. Wharton, J.L. Murray, C.G. Ioannides, and A.P. Kudelka, Existent proliferative responses of peripheral blood mononuclear cells from healthy donors and ovarian cancer patients to HER-2 peptides. (1997) Anticancer Res. 17:45-53.

58. Kobayashi, H., M. Wood, Y. Song, E. Appella, and E. Celis, Defining promiscuous MHC class II helper T-cell epitopes for the HER2/neu tumor antigen. (2000) Cancer Res. 60:5228-36.

59. Jones, T., A. Stern, and R. Lin, Potential role of granulocyte-macrophage colony-stimulating factor as vaccine adjuvant. (1994) Eur J Clin Microbiol Infect Dis. 13:S47-53.

60. Jager, E., M. Ringhoffer, H.P. Dienes, M. Arand, J. Karbach, D. Jager, C. Ilsemann, M. Hagedorn, F. Oesch, and A. Knuth, Granulocyte-macrophage-colony-stimulating factor enhances immune responses to melanoma-associated peptides in vivo. (1996) Int J Cancer. 67:54-62.

61. Fagerberg, J., Granulocyte-macrophage colony-stimulating factor as an adjuvant in tumor immunotherapy. (1996) Med Oncol. 13:155-60.

62. Carlsson, T. and J. Struve, Granulocyte-macrophage colony-stimulating factor given as an adjuvant to persons not responding to hepatitis B vaccine [letter]. (1997) Infection. 25:129.

63. Pardoll, D.M., Paracrine cytokine adjuvants in cancer immunotherapy. (1995) Annu Rev Immunol. 13:399-415.

64. Golumbek, P.T., R. Azhari, E.M. Jaffee, H.I. Levitsky, A. Lazenby, K. Leong, and D.M. Pardoll, Controlled release, biodegradable cytokine depots: a new approach in cancer vaccine design. (1993) Cancer Res. 53:5841-4.

65. Kawakami, Y., P.F. Robbins, X. Wang, J.P. Tupesis, M.R. Parkhurst, X. Kang, K. Sakaguchi, E. Appella, and S.A. Rosenberg, Identification of new melanoma epitopes on melanosomal proteins recognized by tumor infiltrating T lymphocytes restricted by HLA-A1, -A2, and -A3 alleles. (1998) J Immunol. 161:6985-92.

66. Salgaller, M.L., F.M. Marincola, J.N. Cormier, and S.A. Rosenberg, Immunization against epitopes in the human melanoma antigen gp100 following patient immunization with synthetic peptides. (1996) Cancer Res. 56:4749-57.

67. Slingluff, C.L., Jr., G.R. Petroni, G.V. Yamshchikov, D.L. Barnd, S. Eastham, H. Galavotti, J.W. Patterson, D.H. Deacon, S. Hibbitts, D. Teates, P.Y. Neese, W.W. Grosh, K.A. Chianese-Bullock, E.M. Woodson, C.J. Wiernasz, P. Merrill, J. Gibson, M. Ross, and V.H. Engelhard, Clinical and immunologic results of a randomized phase II trial of vaccination using four melanoma peptides either administered in granulocyte-macrophage colony-stimulating factor in adjuvant or pulsed on dendritic cells. (2003) J Clin Oncol. 21:4016-26.

68. Miconnet, I., S. Koenig, D. Speiser, A. Krieg, P. Guillaume, J.C. Cerottini, and P. Romero, CpG are efficient adjuvants for specific CTL induction against tumor antigen-derived peptide. (2002) J Immunol. 168:1212-8.

69. Maletto, B., A. Ropolo, V. Moron, and M.C. Pistoresi-Palencia, CpG-DNA stimulates cellular and humoral immunity and promotes Th1 differentiation in aged BALB/c mice. (2002) J Leukoc Biol. 72:447-54.

70. Sa, H., B.R. Mei, Y.H. Wang, and D.J. Qian, [Diagnostic value of integral of dorsal acoustic scattering for acute viral myocarditis]. (2003) Zhonghua Er Ke Za Zhi. 41:228-9.

71. Celis, E., V. Tsai, C. Crimi, R. DeMars, P.A. Wentworth, R.W. Chesnut, H.M. Grey, A. Sette, and H.M. Serra, Induction of anti-tumor cytotoxic T lymphocytes in normal humans using primary cultures and synthetic peptide epitopes. (1994) Proc Natl Acad Sci U S A. 91:2105-9.

72. Southwood, S., J. Sidney, A. Kondo, M.F. del Guercio, E. Appella, S. Hoffman, R.T. Kubo, R.W. Chesnut, H.M. Grey, and A. Sette, Several common HLA-DR types share largely overlapping peptide binding repertoires. (1998) J Immunol. 160:3363-73.

73. Ramanathan, R.K., K.M. Lee, J. McKolanis, E. Hitbold, W. Schraut, A.J. Moser, E. Warnick, T. Whiteside, J. Osborne, H. Kim, R. Day, M. Troetschel, and O.J. Finn, Phase I study of a MUC1 vaccine composed of different doses of MUC1 peptide with SB-AS2 adjuvant in resected and locally advanced pancreatic cancer. (2005) Cancer Immunol Immunother. 54:254-64.

74. Bennouna, J., A. Hildesheim, K. Chikamatsu, W. Gooding, W.J. Storkus, and T.L. Whiteside, Application of IL-5 ELISPOT assays to quantification of antigen-specific T helper responses. (2002) J Immunol Methods. 261:145-56.

75. Jager, E., Y. Nagata, S. Gnjatic, H. Wada, E. Stockert, J. Karbach, P.R. Dunbar, S.Y. Lee, A. Jungbluth, D. Jager, M. Arand, G. Ritter, V. Cerundolo, B. Dupont, Y.T. Chen, L.J. Old, and A. Knuth, Monitoring CD8 T cell responses to NY-ESO-1: correlation of humoral and cellular immune responses. (2000) Proc Natl Acad Sci U S A. 97:4760-5.

76. McMichael, A.J. and C.A. O'Callaghan, A new look at T cells. (1998) J Exp Med. 187:1367-71.

77. Speiser, D.E., M.J. Pittet, P. Guillaume, N. Lubenow, E. Hoffman, J.C. Cerottini, and P. Romero, Ex vivo analysis of human antigen-specific CD8+ T-cell responses: quality assessment of fluorescent HLA-A2 multimer and interferon-gamma ELISPOT assays for patient immune monitoring. (2004) J Immunother. 27:298-308.

Appendix I

ECOG PERFORMANCE STATUS

Grade	
0	Fully active, able to carry on all pre-disease activities without restriction (Karnofsky 90-100).
1	Restricted in physically strenuous activity but ambulatory and able to carry out work of a light or sedentary nature, e.g., light housework, office work (Karnofsky 70-80).
2	Ambulatory and capable of all self-care, but unable to carry out any work activities. Up and about more than 50 percent of waking hours (Karnofsky 50-60).
3	Capable of only limited self-care, confined to bed or chair 50 percent or more of waking hours (Karnofsky 30-40).
4	Completely disabled. Cannot carry on any self-care. Totally confined to bed or chair (Karnofsky 10-20).
5	Dead

Appendix II

Site Injection Record

Protocol #: _____ Patient #: _____ Patient Initials: ___ ___ ___
F M L

Please indicate on the diagrams below all sites of vaccine injection (circle).

Date of determination: __ __ / __ __ / __ __
M D Y

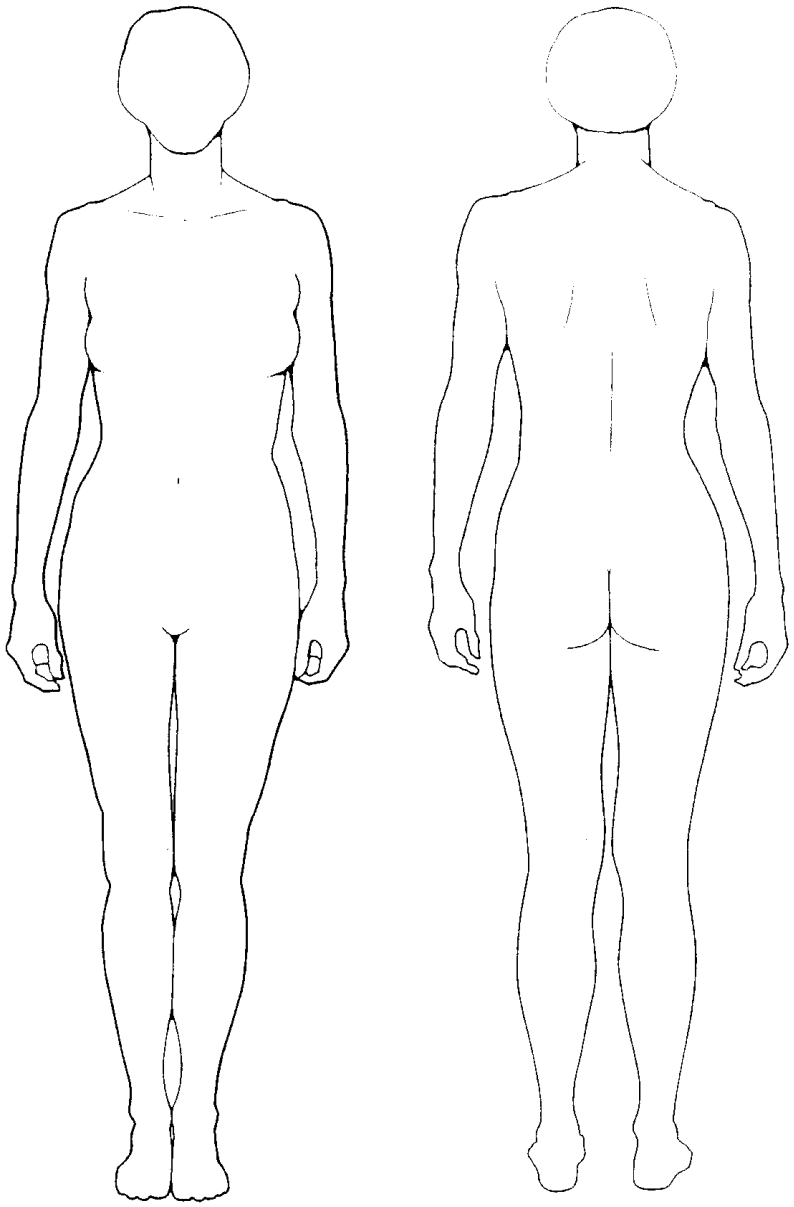

Anterior

Posterior